May 10, 2013

Comanche Peak Nuclear Power Plant, Units 3 & 4
COL Application

Part 2

FSAR Revision 3

Update Tracking Report

Revision 1

(Update Tracking Report – file 1/4)

File 2/4 Figures 2.5.2-201 through 2.5.2-220

File 3/4 Figures 2.5.2-221 through 2.5.2-240

File 4/4 Figures 2.5.2-241 through 2.5.2-259 and new figures 2.5.2-260 through 2.5.20277

Revision History

Revision	Date	Update Description
-	6/28/2012	COLA Revision 3 Transmittal See Luminant Letter no. TXNB-12023 Date 6/28/2012
-	05/16/2012	Updated Chapters: Ch. 8, 13 See Luminant Letter no. TXNB-12013 Date 05/16/2012 Incorporated responses to following RAIs No. 249, 255
-	05/31/2012	Updated Chapters: Ch. 9, 14, 19 See Luminant Letter no. TXNB-12016 Date 05/31/2012 Incorporated responses to following RAIs No. 248, 251
-	6/13/2012	Updated Chapters: Ch. 3, 6, 9 See Luminant Letter no. TXNB-12021 Date 6/13/2012 Incorporated responses to following RAIs No. 52 Supplemental 01, 240 Supplemental 01, 244 Supplemental 01
-	6/21/2012	Updated Chapters: Ch. 3, 9, 14 See Luminant Letter no. TXNB-12022 Date 6/21/2012 Incorporated responses to following RAIs No. 254, 257
-	7/20/2012	Updated Chapters: Ch. 14 See Luminant Letter no. TXNB-12026 Date 7/20/2012

		Incorporated responses to following RAIs No. 256
-	7/24/2012	Updated Chapters: Ch. 13 See Luminant Letter no. TXNB-12027 Date 7/24/2012 Incorporated responses to following RAIs No. 261
-	8/29/2012	Updated Chapters: Ch. 9 See Luminant Letter no. TXNB-12030 Date 8/29/2012 Incorporated responses to following RAIs No. 243 S01
-	9/10/2012	Updated Chapters: Ch. 3, 9, 14 See Luminant Letter no. TXNB-12031 Date 9/10/2012 Incorporated responses to following RAIs No. 251 S01, 252 S01
-	9/14/2012	Updated Chapters: Ch. 1, 2, 3, 8, 9, 11, 19 See Luminant Letter no. TXNB-12032 Date 9/14/2012 Incorporated responses to following RAIs No. 250
-	9/24/2012	Updated Chapters: Ch. 3, 9, 14 See Luminant Letter no. TXNB-12034 Date 9/24/2012 Incorporated responses to following RAIs No. 254 S01, 257 S01
-	9/26/2012	Updated Chapters: Ch. 1, 3 See Luminant Letter no. TXNB-12035 Date 9/26/2012 Incorporated responses to following RAIs No. 262
-	11/12/2012	Updated Chapters: Ch. 9, 14 See Luminant Letter no. TXNB-12036 Date 11/12/2012 Incorporated responses to following RAIs No. 252 S02, 254 S02, 257 S02
-	12/03/2012	Updated Chapters: Ch. 1, 9, 14

		See Luminant Letter no. TXNB-12041 Date 12/03/2012 Incorporated responses to following RAIs No. 251 S02
-	12/06/2012	Updated Chapters: Ch. 9, 10, 11, 12 See Luminant Letter no. TXNB-12042 Date 12/06/2012 Incorporated responses to following RAIs No. 135 S04
-	12/18/2012	Updated Chapters: Ch. 9 See Luminant Letter no. TXNB-12043 Date 12/18/2012 Incorporated responses to following RAIs No. 266
-	12/18/2012	Updated Chapters: Ch. 19 See Luminant Letter no. TXNB-12043 Date 12/18/2012 Incorporated responses to following RAIs No. 267
-	12/18/2012	Updated Chapters: Ch. 19 See Luminant Letter no. TXNB-12043 Date 12/18/2012 Incorporated responses to following RAIs No. 264
-	12/18/2012	Updated Chapters: Ch. 1, 19 See Luminant Letter no. TXNB-12043 Date 12/18/2012 Incorporated responses to following RAIs No. 268
-	12/18/2012	Updated Chapters: Ch. 3, 9 See Luminant Letter no. TXNB-12043 Date 12/18/2012 Incorporated responses to following RAIs No. 265
-	01/17/2013	Updated Chapters: Ch. 1, 6 See Luminant Letter no. TXNB-13001 Date 01/17/2013 Incorporated responses to following RAIs No. 271

-	03/04/2013	Updated Chapters: Ch. 1, 6 See Luminant Letter no. TXNB-13005 Date 03/04/2013 Incorporated responses to following RAIs No. 272
-	03/04/2013	Updated Chapters: Ch. 9 See Luminant Letter no. TXNB-13006 Date 03/04/2013 Incorporated responses to following RAIs No. 243 S02
-	03/04/2013	Updated Chapters: Ch. 8 See Luminant Letter no. TXNB-13007 Date 03/04/2013 Incorporated responses to following RAIs No. 9 S03
0	2/26/2013	Updated Chapters: Ch 1, 2, 3, 8, 9, 12
-	04/29/2013	Updated Chapters: Ch. 2 See Luminant Letter no. TXNB-13013 Date 04/29/2013 Incorporated responses to following RAIs No. 147 S01, 147 S04
1	05/10/2013	Updated Chapters: Ch 2, 6, 8, 9, 19

Chapter 1

Chapter 1 Tracking Report Revision List

Change ID No.	Section	FSAR Rev. 3 Page	Reason for change	Change Summary	Rev. of FSAR T/R
RCOL2_03.03.02-9	Table 1.8-201 (Sheets 4, 6, 10, 21 of 71) Table 1.9-201 (Sheet 12 of 12) Table 1.9-206 (Sheet 1 of 2)	1.8-15 1.8-17 1.8-21 1.8-32 1.9-15 1.9-24 [1.9-25]	Response to RAI No. 250 Luminant Letter no.TXNB-12032 Date 09/14/2012	Revised to incorporate RG 1.221.	-
RCOL2_03.06.01-1	Table 1.8-201 (Sheets 7, 8 of 71)	1.8-18 1.8-19	Response to RAI No. 262 Luminant Letter no.TXNB-12035 Date 9/26/2012	Revised COL 3.6(1) and COL 3.6(4).	-
RCOL2_09.02.01-9 S02	Table 1.8-201 (Sheet 39 of 71)	1.8-50	2nd Supplemental Response to RAI No. 251 Luminant Letter no.TXNB-12041 Date 12/03/2012	Change the wording to address the need of COL evaluation for a void detection system.	-
RCOL2_19-24	Table 1.8-201 (Sheets 68, 70, 71 [68, 70, 72] of 71 [72])	1.8-79, 1.8-81, 1.8-82 [1.8-79, 1.8-81, 1.8-83]	Response to RAI No. 268 Luminant Letter no.TXNB-12043 Date 12/18/2012	Clarified resolution of combined license items on site specific information.	-
RCOL2_19-25	Table 1.8-201 (Sheet 70 [71] of 71 [72])	1.8-81 [1.8-82]	Response to RAI No. 268 Luminant Letter no.TXNB-12043 Date 12/18/2012	Included updated FSAR reference locations.	-

Change ID No.	Section	FSAR Rev. 3 Page	Reason for change	Change Summary	Rev. of FSAR T/R
RCOL2_06.02.02-5	Table 1.8-201 (Sheet 26 of 71[72])	1.8-37	Response to RAI No. 271 Luminant Letter no.TXNB-13001 Date 01/17/2013	Added FSAR Location and Resolution Category for COL Item 6.2(6).	-
RCOL2_06.02.02-6	Table 1.8-201 (Sheet 26 of 71 [72])	1.8-37	Response to RAI No. 272 Luminant Letter no.TXNB-13005 Date 03/04/2013	COL Item 6.2(5) location made more specific (Section 6.2.2.3 to Section 6.2.2.3.2)	-
CTS-01506	Figure 1.2-1R	1.2-5 1.2-6	Consistency with DCD as described in Letter. TXNB-12033 (ML12268A413) and TXNB-12038 (ML12334A026)	Figure was updated to reflect standard plant and site-specific layout	0
CTS-01506	Figure 1.2-201	1.2-8	Consistency with DCD as described in Letter. TXNB-12033 (ML12268A413) and TXNB-12038 (ML12334A026)	Figure was updated to reflect standard plant and site-specific layout and general arrangement design changes.	0
CTS-01507	Figure 1.2-202	1.2-9	Design change as described in Letter TXNB-12033 (ML12268A413)	Figure was revised to reflect the integration of the north portions of the ESWPT into the south side of the UHSRS	0
CTS-01507	Figures 1.2-203 through 1.2-210	1.2-10 through 1.2-17	Design change as described in Letter TXNB-12033 (ML12268A413), TXNB-12038 (ML12334A026), and TXNB-12030 (ML12243A456)	Figures were revised to reflect: Integration of the north portions of the ESWPT into the south side of the UHSRS. Integration of adjacent UHSRS (C and D) and (A	0

Change ID No.	Section	FSAR Rev. 3 Page	Reason for change	Change Summary	Rev. of FSAR T/R
				and B) on a single foundation. ESW Pump House layout changes described in responses to RAIs 243 S01 and 254 S03. Addition of an ESW Pipe Removal Shaft to the ESWPT Segment integrated to UHSRS C and D	

*Page numbers for the attached marked-up pages may differ from the revision 3 page numbers due to text additions and deletions. When the page numbers for the attached pages do differ, the page number for the attached page is shown in brackets.

Chapter 2

Chapter 2 Tracking Report Revision List

Change ID No.	Section	FSAR Rev. 3 Page	Reason for change	Change Summary	Rev. of FSAR T/R
RCOL2_03.03.02-9	Table 2.0-1R (Sheet[s] 1, [2] of 13) 2.3.1.2.2 2.3.2.3	2.0-2 [2.0-2, 2.0-3] 2.3-13 2.3-37	Response to RAI No. 250 Luminant Letter no.TXNB-12032 Date 09/14/2012	Revised to incorporate RG 1.221.	-
CTS-01514	Table 2.0-1R (Sheets 3, 4,5,6 of 13)	2.0-4 2.0-5 2.0-6 2.0-7	Consistency with DCD as described in Letter. TXNB-12033 (ML12268A413)	Updated to reflect revised X/Q values.	0
CTS-01514	Table 2.3-338 (Sheets 1,3 of 3)	2.3-244 2.3-246	Consistency with DCD as described in Letter. TXNB-12033 (ML12268A413)	Updated to reflect revised source and receptor locations.	0
CTS-01514	Table 2.3-339 (Sheet 1 of 2)	2.3-247	Consistency with DCD as described in Letter. TXNB-12033 (ML12268A413)	Updated to reflect revised X/Q values.	0
CTS-01513	Figure 2.1-201 2.3-380	- -	Consistency with DCD as described in Letter. TXNB-12033 (ML12268A413)	Updated to reflect standard plant and site-specific layout.	0
RCOL2_02.04.12-9 S04	Acronyms and Abbreviations	2-lxi 2-lxv 2-lxvi	4th Supplemental Response to RAI No. 147 Luminant Letter no.TXNB-13013 Date 4/29/2013	Section was revised to reflect new acronyms and abbreviations used in the groundwater elevation and pathways analysis description.	-

Change ID No.	Section	FSAR Rev. 3 Page	Reason for change	Change Summary	Rev. of FSAR T/R
RCOL2_02.04.12-9 S04	Table 2.0-1R (Sheet 8 of 13)	2.0-9	4th Supplemental Response to RAI No. 147 Luminant Letter no.TXNB-13013 Date 4/29/2013	Table updated to describe site-specific groundwater levels.	-
RCOL2_02.04.12-9 S04	2.4.12.3 2.4.12.3.1 2.4.12.3.1.1 2.4.12.3.1.1.1 (New Subsection) 2.4.12.3.1.1.2 (New Subsection) 2.4.12.3.1.1.3 (New Subsection) 2.4.12.5	2.4-78 2.4-79 2.4-79 through 2.4-82 2.4-82 through 2.4-85 2.4-85 2.4-86 through 2.4-88	4th Supplemental Response to RAI No. 147 Luminant Letter no.TXNB-13013 Date 4/29/2013	Section was revised to reflect updates to the maximum groundwater elevation and pathways.	-
RCOL2_02.04.12-9 S04	Table 2.4.12-208 (Sheets 1, 2 of 2)	2.4-230 2.4-231	4th Supplemental Response to RAI No. 147 Luminant Letter no.TXNB-13013 Date 4/29/2013	Table was revised to reflect updates to the groundwater monitoring wells installation details.	-
RCOL2_02.04.12-9 S04	Table 2.4.12-211	2.4-239	4th Supplemental Response to RAI No. 147 Luminant Letter no.TXNB-13013 Date 4/29/2013	Table was revised to reflect updatedresults of the groundwater pathways analysis.	-

Change ID No.	Section	FSAR Rev. 3 Page	Reason for change	Change Summary	Rev. of FSAR T/R
RCOL2_02.04.12-9 S04	Figure 2.4.12-212	-	4th Supplemental Response to RAI No. 147 Luminant Letter no.TXNB-13013 Date 4/29/2013	Figure was revised to reflect updated results of the groundwater pathways analysis.	-
RCOL2_02.04.12-9 S04	Figure 2.4.12-213	-	4th Supplemental Response to RAI No. 147 Luminant Letter no.TXNB-13013 Date 4/29/2013	Figure was revised to reflect updated results of the groundwater pathways analysis.	-
RCOL2_02.04.12-9 S04	Figure 2.4.12-214	-	4th Supplemental Response to RAI No. 147 Luminant Letter no.TXNB-13013 Date 4/29/2013	Figure was revised to reflect updated vertical release pathway.	-
RCOL2_02.04.12-9 S04	Figure 2.4.12-215	-	4th Supplemental Response to RAI No. 147 Luminant Letter no.TXNB-13013 Date 4/29/2013	Figure was updated to show comparisonbetween pre and post construction surface topography.	-
RCOL2_02.04.12-9 S04	Figure 2.4.12-216	-	4th Supplemental Response to RAI No. 147 Luminant Letter no.TXNB-13013 Date 4/29/2013	Figure was added to show cut and engineered fill buildup areas.	-
RCOL2_02.04.12-9 S04	Figure 2.4.12-217	-	4th Supplemental Response to RAI No. 147 Luminant Letter no.TXNB-13013 Date 4/29/2013	Figure was updated to reflect the updated post-construction groundwater conceptual model.	-

Change ID No.	Section	FSAR Rev. 3 Page	Reason for change	Change Summary	Rev. of FSAR T/R
RCOL2_02.04.12-9 S04	Figure 2.4.12-218	-	4th Supplemental Response to RAI No. 147 Luminant Letter no.TXNB-13013 Date 4/29/2013	Figure was added showing post-construction surface topography.	-
RCOL2_02.04.12-9 S04	Figure 2.4.12-219 (Sheets 1, 2 of 2)	-	4th Supplemental Response to RAI No. 147 Luminant Letter no.TXNB-13013 Date 4/29/2013	Figure was added to show MODFLOW model grid.	-
RCOL2_02.04.12-9 S04	Figure 2.4.12-220	-	4th Supplemental Response to RAI No. 147 Luminant Letter no.TXNB-13013 Date 4/29/2013	Figure was added to reflect results of the groundwater pathways analysis.	-
RCOL2_02.04.12-12 S01	Acronyms and Abbreviations	2-lxvi	Supplemental Response to RAI No. 147 Luminant Letter no.TXNB-13013 Date 4/29/2013	Section was revised to reflect new acronyms and abbreviations used in the groundwater elevation and pathways analysis description.	-
RCOL2_02.04.12-12 S01	2.4.12.2.4 2.4.12.5	2.4-73 through 2.4-76 2.4-86	Supplemental Response to RAI No. 147 Luminant Letter no.TXNB-13013 Date 4/29/2013	Sections were updated to reflect updated groundwater well monitoring results.	-
RCOL2_02.04.12-12 S01	Table 2.4.12-209 (Sheets 1 through 3 of 3)	2.4-232 through 2.4-234	Supplemental Response to RAI No. 147 Luminant Letter no.TXNB-13013 Date 4/29/2013	Table was revised to reflect updatedgroundwater monitoring results.	-

Change ID No.	Section	FSAR Rev. 3 Page	Reason for change	Change Summary	Rev. of FSAR T/R
RCOL2_02.04.12-12 S01	Table 2.4.12-213 (New Table)	2.4-240	Supplemental Response to RAI No. 147 Luminant Letter no.TXNB-13013 Date 4/29/2013	Table was added to show average rate of rise in non-equilibrium groundwater monitoring wells.	-
RCOL2_02.04.12-12 S01	Figure 2.4.12-208	-	Supplemental Response to RAI No. 147 Luminant Letter no.TXNB-13013 Date 4/29/2013	Figure was update to reflect new site layout and plot plan.	-
RCOL2_02.04.12-12 S01	Figure 2.4.12-209 (Sheets 1 through 20 of 20)	-	Supplemental Response to RAI No. 147 Luminant Letter no.TXNB-13013 Date 4/29/2013	Figure was updated to reflect latest groundwater monitoring results (adding 40 more sheets)	-
RCOL2_02.04.12-12 S01	Figure 2.4.12-210 (Sheets 1 through 4 of 4)	-	Supplemental Response to RAI No. 147 Luminant Letter no.TXNB-13013 Date 4/29/2013	Figure was updated to reflect new site layout and plot plan and updated groundwater monitoring results (adding 2 more sheets)	-
CTS-01521	Table 2.0-1R (Sheet 9 of 13 [10 of 13])	2.0-10 [2.0-11]	To reflect plant layout changes and inclusion of EPRI-CEUS Seismic Catalog, as described in both the Luminant ISCP Letter ML12268A41 and Fukushima RAI 261 response ML12207A599.	Updated table entry to reflect revisions to Section 2.5	1

Change ID No.	Section	FSAR Rev. 3 Page	Reason for change	Change Summary	Rev. of FSAR T/R
CTS-01521	2.5.1	2.5-2	To reflect plant layout changes and inclusion of EPRI-CEUS Seismic Catalog, as described in both the Luminant ISCP Letter ML12268A41 and Fukushima RAI 261 response ML12207A599.	Section was revised due to CEUS and CPNPP layout update.	1
CTS-01521	2.5.1.1.4	2.5-16	To reflect plant layout changes and inclusion of EPRI-CEUS Seismic Catalog, as described in both the Luminant ISCP Letter ML12268A41 and Fukushima RAI 261 response ML12207A599.	Section was revised due to CEUS and CPNPP layout update.	1
CTS-01521	2.5.1.1.4.2	2.5-20 [2.5-21]	To reflect plant layout changes and inclusion of EPRI-CEUS Seismic Catalog, as described in both the Luminant ISCP Letter ML12268A41 and Fukushima RAI 261 response ML12207A599.	Section was revised due to CEUS and CPNPP layout update.	1

Change ID No.	Section	FSAR Rev. 3 Page	Reason for change	Change Summary	Rev. of FSAR T/R
CTS-01521	2.5.1.1.4.2.3	2.5-23	To reflect plant layout changes and inclusion of EPRI-CEUS Seismic Catalog, as described in both the Luminant ISCP Letter ML12268A41 and Fukushima RAI 261 response ML12207A599.	Section was revised due to CEUS and CPNPP layout update.	1
CTS-01521	2.5.1.1.4.3	2.5-23 [2.5-24]	To reflect plant layout changes and inclusion of EPRI-CEUS Seismic Catalog, as described in both the Luminant ISCP Letter ML12268A41 and Fukushima RAI 261 response ML12207A599.	Section was revised due to CEUS and CPNPP layout update.	1
CTS-01521	2.5.1.1.4.3.4.2	2.5-28 through 2.5-29	To reflect plant layout changes and inclusion of EPRI-CEUS Seismic Catalog, as described in both the Luminant ISCP Letter ML12268A41 and Fukushima RAI 261 response ML12207A599.	Section was revised due to CEUS and CPNPP layout update.	1

Change ID No.	Section	FSAR Rev. 3 Page	Reason for change	Change Summary	Rev. of FSAR T/R
CTS-01521	2.5.1.1.4.3.6	2.5-30	To reflect plant layout changes and inclusion of EPRI-CEUS Seismic Catalog, as described in both the Luminant ISCP Letter ML12268A41 and Fukushima RAI 261 response ML12207A599.	Section was revised due to CEUS and CPNPP layout update.	1
CTS-01521	2.5.1.1.4.3.6.1	2.5-30 [2.5-31]	To reflect plant layout changes and inclusion of EPRI-CEUS Seismic Catalog, as described in both the Luminant ISCP Letter ML12268A41 and Fukushima RAI 261 response ML12207A599.	Section was revised due to CEUS and CPNPP layout update.	1
CTS-01521	2.5.1.1.4.3.6.1.1 through 2.5.1.1.4.3.6.1.2	2.5-31 through 2.5-40	To reflect plant layout changes and inclusion of EPRI-CEUS Seismic Catalog, as described in both the Luminant ISCP Letter ML12268A41 and Fukushima RAI 261 response ML12207A599.	Section was revised due to CEUS and CPNPP layout update.	1

Change ID No.	Section	FSAR Rev. 3 Page	Reason for change	Change Summary	Rev. of FSAR T/R
CTS-01521	2.5.1.1.4.3.6.2	2.5-40 through 2.5-41	To reflect plant layout changes and inclusion of EPRI-CEUS Seismic Catalog, as described in both the Luminant ISCP Letter ML12268A41 and Fukushima RAI 261 response ML12207A599.	Section was revised due to CEUS and CPNPP layout update.	1
CTS-01521	2.5.1.1.4.3.7	2.5-41	To reflect plant layout changes and inclusion of EPRI-CEUS Seismic Catalog, as described in both the Luminant ISCP Letter ML12268A41 and Fukushima RAI 261 response ML12207A599.	Section was revised due to CEUS and CPNPP layout update.	1
CTS-01521	2.5.1.1.4.3.7.1	2.5-41 through 2.5-42 [2.5-43]	To reflect plant layout changes and inclusion of EPRI-CEUS Seismic Catalog, as described in both the Luminant ISCP Letter ML12268A41 and Fukushima RAI 261 response ML12207A599.	Section was revised due to CEUS and CPNPP layout update.	1

Change ID No.	Section	FSAR Rev. 3 Page	Reason for change	Change Summary	Rev. of FSAR T/R
CTS-01521	2.5.1.1.4.3.7.2	2.5-43	To reflect plant layout changes and inclusion of EPRI-CEUS Seismic Catalog, as described in both the Luminant ISCP Letter ML12268A41 and Fukushima RAI 261 response ML12207A599.	Section was revised due to CEUS and CPNPP layout update.	1
CTS-01521	2.5.1.1.4.3.7.3	2.5-43 through 2.5-44 [2.5-45]	To reflect plant layout changes and inclusion of EPRI-CEUS Seismic Catalog, as described in both the Luminant ISCP Letter ML12268A41 and Fukushima RAI 261 response ML12207A599.	Section was revised due to CEUS and CPNPP layout update.	1
CTS-01521	2.5.1.2.5.1	2.5-55 [2.5-56]	To reflect plant layout changes and inclusion of EPRI-CEUS Seismic Catalog, as described in both the Luminant ISCP Letter ML12268A41 and Fukushima RAI 261 response ML12207A599.	Section was revised due to CEUS and CPNPP layout update.	1

Change ID No.	Section	FSAR Rev. 3 Page	Reason for change	Change Summary	Rev. of FSAR T/R
CTS-01521	2.5.1.2.5.2	2.5-56	To reflect plant layout changes and inclusion of EPRI-CEUS Seismic Catalog, as described in both the Luminant ISCP Letter ML12268A41 and Fukushima RAI 261 response ML12207A599.	Section was revised due to CEUS and CPNPP layout update.	1
CTS-01521	2.5.1.2.5.6	2.5-58 [2.5-59]	To reflect plant layout changes and inclusion of EPRI-CEUS Seismic Catalog, as described in both the Luminant ISCP Letter ML12268A41 and Fukushima RAI 261 response ML12207A599.	Section was revised due to CEUS and CPNPP layout update.	1
CTS-01521	2.5.1.2.5.10.1	2.5-60 [2.5-61]	To reflect plant layout changes and inclusion of EPRI-CEUS Seismic Catalog, as described in both the Luminant ISCP Letter ML12268A41 and Fukushima RAI 261 response ML12207A599.	Section was revised due to CEUS and CPNPP layout update.	1

Change ID No.	Section	FSAR Rev. 3 Page	Reason for change	Change Summary	Rev. of FSAR T/R
CTS-01521	2.5.1.2.5.10.2.3	2.5-64 [2.5-65]	To reflect plant layout changes and inclusion of EPRI-CEUS Seismic Catalog, as described in both the Luminant ISCP Letter ML12268A41 and Fukushima RAI 261 response ML12207A599.	Section was revised due to CEUS and CPNPP layout update.	1
CTS-01521	2.5.1.2.5.10.3	2.5-64 [2.5-65]	To reflect plant layout changes and inclusion of EPRI-CEUS Seismic Catalog, as described in both the Luminant ISCP Letter ML12268A41 and Fukushima RAI 261 response ML12207A599.	Section was revised due to CEUS and CPNPP layout update.	1
CTS-01521	Figure 2.5.1-213	-	To reflect plant layout changes and inclusion of EPRI-CEUS Seismic Catalog, as described in both the Luminant ISCP Letter ML12268A41 and Fukushima RAI 261 response ML12207A599.	Figure was revised due to CEUS and CPNPP layout update.	1

Change ID No.	Section	FSAR Rev. 3 Page	Reason for change	Change Summary	Rev. of FSAR T/R
CTS-01521	Figure 2.5.1-215	-	To reflect plant layout changes and inclusion of EPRI-CEUS Seismic Catalog, as described in both the Luminant ISCP Letter ML12268A41 and Fukushima RAI 261 response ML12207A599.	Figure was revised due to CEUS and CPNPP layout update.	1
CTS-01521	Figure 2.5.1-230	-	To reflect plant layout changes and inclusion of EPRI-CEUS Seismic Catalog, as described in both the Luminant ISCP Letter ML12268A41 and Fukushima RAI 261 response ML12207A599.	Figure was revised due to CEUS and CPNPP layout update.	1
CTS-01521	2.5.2	2.5-66	To reflect plant layout changes and inclusion of EPRI-CEUS Seismic Catalog, as described in both the Luminant ISCP Letter ML12268A41 and Fukushima RAI 261 response ML12207A599.	Section was revised due to CEUS and CPNPP layout update.	1

Change ID No.	Section	FSAR Rev. 3 Page	Reason for change	Change Summary	Rev. of FSAR T/R
CTS-01521	2.5.2	2.5-67 [2.5-68]	To reflect plant layout changes and inclusion of EPRI-CEUS Seismic Catalog, as described in both the Luminant ISCP Letter ML12268A41 and Fukushima RAI 261 response ML12207A599.	Section was revised due to CEUS and CPNPP layout update.	1
CTS-01521	2.5.2.1	2.5-68	To reflect plant layout changes and inclusion of EPRI-CEUS Seismic Catalog, as described in both the Luminant ISCP Letter ML12268A41 and Fukushima RAI 261 response ML12207A599.	Section was revised due to CEUS and CPNPP layout update.	1
CTS-01521	2.5.2.1.1	2.5-68 2.5-69	To reflect plant layout changes and inclusion of EPRI-CEUS Seismic Catalog, as described in both the Luminant ISCP Letter ML12268A41 and Fukushima RAI 261 response ML12207A599.	Section was revised due to CEUS and CPNPP layout update.	1

Change ID No.	Section	FSAR Rev. 3 Page	Reason for change	Change Summary	Rev. of FSAR T/R
CTS-01521	2.5.2.1.2	2.5-69 through 2.5-71 [2.5-72 through 2.5-74]	To reflect plant layout changes and inclusion of EPRI-CEUS Seismic Catalog, as described in both the Luminant ISCP Letter ML12268A41 and Fukushima RAI 261 response ML12207A599.	Section was revised due to CEUS and CPNPP layout update.	1
CTS-01521	2.5.2.1.3	2.5-71 [2.5-74]	To reflect plant layout changes and inclusion of EPRI-CEUS Seismic Catalog, as described in both the Luminant ISCP Letter ML12268A41 and Fukushima RAI 261 response ML12207A599.	Section was revised due to CEUS and CPNPP layout update.	1
CTS-01521	2.5.2.1.3.1	2.5-72 2.5-73 [2.5-74 through 2.5-77]	To reflect plant layout changes and inclusion of EPRI-CEUS Seismic Catalog, as described in both the Luminant ISCP Letter ML12268A41 and Fukushima RAI 261 response ML12207A599.	Section was revised due to CEUS and CPNPP layout update.	1

Change ID No.	Section	FSAR Rev. 3 Page	Reason for change	Change Summary	Rev. of FSAR T/R
CTS-01521	2.5.2.1.3.2	2.5-73 through 2.5-75 [2.5-77 through 2.5-80]	To reflect plant layout changes and inclusion of EPRI-CEUS Seismic Catalog, as described in both the Luminant ISCP Letter ML12268A41 and Fukushima RAI 261 response ML12207A599.	Section was revised due to CEUS and CPNPP layout update.	1
CTS-01521	2.5.2.2	2.5-75 through 2.5-77 [2.5-80 through 2.5-82]	To reflect plant layout changes and inclusion of EPRI-CEUS Seismic Catalog, as described in both the Luminant ISCP Letter ML12268A41 and Fukushima RAI 261 response ML12207A599.	Section was revised due to CEUS and CPNPP layout update.	1
CTS-01521	2.5.2.2.1	2.5-77, 2.5-78 [2.5-82 through 2.5-84]	To reflect plant layout changes and inclusion of EPRI-CEUS Seismic Catalog, as described in both the Luminant ISCP Letter ML12268A41 and Fukushima RAI 261 response ML12207A599.	Section was revised due to CEUS and CPNPP layout update.	1

Change ID No.	Section	FSAR Rev. 3 Page	Reason for change	Change Summary	Rev. of FSAR T/R
CTS-01521	2.5.2.2.1.1	2.5-78, 2.5-79 [2.5-84 through 2.5-85]	To reflect plant layout changes and inclusion of EPRI-CEUS Seismic Catalog, as described in both the Luminant ISCP Letter ML12268A41 and Fukushima RAI 261 response ML12207A599.	Section was revised due to CEUS and CPNPP layout update.	1
CTS-01521	2.5.2.2.1.2	2.5-79, 2.5-80 [2.5-85 through 2.5-87]	To reflect plant layout changes and inclusion of EPRI-CEUS Seismic Catalog, as described in both the Luminant ISCP Letter ML12268A41 and Fukushima RAI 261 response ML12207A599.	Section was revised due to CEUS and CPNPP layout update.	1
CTS-01521	2.5.2.2.1.3	2.5-80 2.5-81 [2.5-87 2.5-88]	To reflect plant layout changes and inclusion of EPRI-CEUS Seismic Catalog, as described in both the Luminant ISCP Letter ML12268A41 and Fukushima RAI 261 response ML12207A599.	Section was revised due to CEUS and CPNPP layout update.	1

Change ID No.	Section	FSAR Rev. 3 Page	Reason for change	Change Summary	Rev. of FSAR T/R
CTS-01521	2.5.2.2.1.4 through 2.5.2.2.2.6	2.5-81 through 2.5-84 [2.5-88 through 2.5-99]	To reflect plant layout changes and inclusion of EPRI-CEUS Seismic Catalog, as described in both the Luminant ISCP Letter ML12268A41 and Fukushima RAI 261 response ML12207A599.	Section was revised due to CEUS and CPNPP layout update.	1
CTS-01521	2.5.2.3	2.5-93 2.5-94 [2.5-99 through 2.5-101]	To reflect plant layout changes and inclusion of EPRI-CEUS Seismic Catalog, as described in both the Luminant ISCP Letter ML12268A41 and Fukushima RAI 261 response ML12207A599.	Section was revised due to CEUS and CPNPP layout update.	1
CTS-01521	2.5.2.4	2.5-94 [2.5-101]	To reflect plant layout changes and inclusion of EPRI-CEUS Seismic Catalog, as described in both the Luminant ISCP Letter ML12268A41 and Fukushima RAI 261 response ML12207A599.	Section was revised due to CEUS and CPNPP layout update.	1

Change ID No.	Section	FSAR Rev. 3 Page	Reason for change	Change Summary	Rev. of FSAR T/R
CTS-01521	2.5.2.4.1	2.5-94, 2.5-95 [2.5-101 through 2.5-102]	To reflect plant layout changes and inclusion of EPRI-CEUS Seismic Catalog, as described in both the Luminant ISCP Letter ML12268A41 and Fukushima RAI 261 response ML12207A599.	Section was revised due to CEUS and CPNPP layout update.	1
CTS-01521	2.5.2.4.2	2.5-95, 2.5-96 [2.5-102 2.5-103]	To reflect plant layout changes and inclusion of EPRI-CEUS Seismic Catalog, as described in both the Luminant ISCP Letter ML12268A41 and Fukushima RAI 261 response ML12207A599.	Section was revised due to CEUS and CPNPP layout update.	1
CTS-01521	2.5.2.4.2.1	2.5-96, 2.5-97 [2.5-103 through 2.5-104]	To reflect plant layout changes and inclusion of EPRI-CEUS Seismic Catalog, as described in both the Luminant ISCP Letter ML12268A41 and Fukushima RAI 261 response ML12207A599.	Section was revised due to CEUS and CPNPP layout update.	1

Change ID No.	Section	FSAR Rev. 3 Page	Reason for change	Change Summary	Rev. of FSAR T/R
CTS-01521	2.5.2.4.2.2	2.5-97 [2.5-105 2.5-105]	To reflect plant layout changes and inclusion of EPRI-CEUS Seismic Catalog, as described in both the Luminant ISCP Letter ML12268A41 and Fukushima RAI 261 response ML12207A599.	Section was revised due to CEUS and CPNPP layout update.	1
CTS-01521	2.5.2.4.2.2.1 through 2.5.2.4.2.3.4	2.5-97 through 2.5-113 [2.5-106 through 2.5-121]	To reflect plant layout changes and inclusion of EPRI-CEUS Seismic Catalog, as described in both the Luminant ISCP Letter ML12268A41 and Fukushima RAI 261 response ML12207A599.	Section was revised due to CEUS and CPNPP layout update.	1
CTS-01521	2.5.2.4.3	2.5-113, 2.5-114 [2.5-122 2.5-123]	To reflect plant layout changes and inclusion of EPRI-CEUS Seismic Catalog, as described in both the Luminant ISCP Letter ML12268A41 and Fukushima RAI 261 response ML12207A599.	Section was revised due to CEUS and CPNPP layout update.	1

Change ID No.	Section	FSAR Rev. 3 Page	Reason for change	Change Summary	Rev. of FSAR T/R
CTS-01521	2.5.2.4.4	2.5-114 through 2.5-117 [2.5-123 through 2.5-127]	To reflect plant layout changes and inclusion of EPRI-CEUS Seismic Catalog, as described in both the Luminant ISCP Letter ML12268A41 and Fukushima RAI 261 response ML12207A599.	Section was revised due to CEUS and CPNPP layout update.	1
CTS-01521	2.5.2.5	2.5-117, 2.5-118 [2.5-127, 2.5-128]	To reflect plant layout changes and inclusion of EPRI-CEUS Seismic Catalog, as described in both the Luminant ISCP Letter ML12268A41 and Fukushima RAI 261 response ML12207A599.	Section was revised due to CEUS and CPNPP layout update.	1
CTS-01521	2.5.2.5.1	2.5-118, 2.5-119 [2.5-128 and 2.5-129]	To reflect plant layout changes and inclusion of EPRI-CEUS Seismic Catalog, as described in both the Luminant ISCP Letter ML12268A41 and Fukushima RAI 261 response ML12207A599.	Section was revised due to CEUS and CPNPP layout update.	1

Change ID No.	Section	FSAR Rev. 3 Page	Reason for change	Change Summary	Rev. of FSAR T/R
CTS-01521	2.5.2.5.2.1	2.5-119, 2.5-120 [2.5-129 through 2.5-131]	To reflect plant layout changes and inclusion of EPRI-CEUS Seismic Catalog, as described in both the Luminant ISCP Letter ML12268A41 and Fukushima RAI 261 response ML12207A599.	Section was revised due to CEUS and CPNPP layout update.	1
CTS-01521	2.5.2.5.2.2	2.5-121 [2.5-131]	To reflect plant layout changes and inclusion of EPRI-CEUS Seismic Catalog, as described in both the Luminant ISCP Letter ML12268A41 and Fukushima RAI 261 response ML12207A599.	Section was revised due to CEUS and CPNPP layout update.	1
CTS-01521	2.5.2.5.2.3	2.5-121 through 2.5-123 [2.5-132 through 2.5-134]	To reflect plant layout changes and inclusion of EPRI-CEUS Seismic Catalog, as described in both the Luminant ISCP Letter ML12268A41 and Fukushima RAI 261 response ML12207A599.	Section was revised due to CEUS and CPNPP layout update.	1

Change ID No.	Section	FSAR Rev. 3 Page	Reason for change	Change Summary	Rev. of FSAR T/R
CTS-01521	2.5.2.6.1	2.5-123 2.5-124 [2.5-134, 2.5-135]	To reflect plant layout changes and inclusion of EPRI-CEUS Seismic Catalog, as described in both the Luminant ISCP Letter ML12268A41 and Fukushima RAI 261 response ML12207A599.	Section was revised due to CEUS and CPNPP layout update.	1
CTS-01521	2.5.2.6.1.1	2.5-124 Through 2.5-126 [2.5-135 through 2.5-137]	To reflect plant layout changes and inclusion of EPRI-CEUS Seismic Catalog, as described in both the Luminant ISCP Letter ML12268A41 and Fukushima RAI 261 response ML12207A599.	Section was revised due to CEUS and CPNPP layout update.	1
CTS-01521	2.5.2.6.1.2	2.5-126 [2.5-138]	To reflect plant layout changes and inclusion of EPRI-CEUS Seismic Catalog, as described in both the Luminant ISCP Letter ML12268A41 and Fukushima RAI 261 response ML12207A599.	Section was revised due to CEUS and CPNPP layout update.	1

Change ID No.	Section	FSAR Rev. 3 Page	Reason for change	Change Summary	Rev. of FSAR T/R
CTS-01521	2.5.2.6.2	2.5-127 through 2.5-129 [2.5-139 through 2.5-142]	To reflect plant layout changes and inclusion of EPRI-CEUS Seismic Catalog, as described in both the Luminant ISCP Letter ML12268A41 and Fukushima RAI 261 response ML12207A599.	Section was revised due to CEUS and CPNPP layout update.	1
CTS-01521	2.5.2.6.2 (New Subsection 2.5.2.6.3)	2.5-129 [2.5-143 through 2.5-144]	To reflect plant layout changes and inclusion of EPRI-CEUS Seismic Catalog, as described in both the Luminant ISCP Letter ML12268A41 and Fukushima RAI 261 response ML12207A599.	Section was revised due to CEUS and CPNPP layout update.	1
CTS-01521	2.5.3.1	2.5-130 2.5-131 [2.5-145] 2.5-146]	To reflect plant layout changes and inclusion of EPRI-CEUS Seismic Catalog, as described in both the Luminant ISCP Letter ML12268A41 and Fukushima RAI 261 response ML12207A599.	Section was revised due to CEUS and CPNPP layout update.	1

Change ID No.	Section	FSAR Rev. 3 Page	Reason for change	Change Summary	Rev. of FSAR T/R
CTS-01521	2.5.3.2	2.5-131 Through 2.5-131 [2.5-146 2.5-147]	To reflect plant layout changes and inclusion of EPRI-CEUS Seismic Catalog, as described in both the Luminant ISCP Letter ML12268A41 and Fukushima RAI 261 response ML12207A599.	Section was revised due to CEUS and CPNPP layout update.	1
CTS-01521	2.5.3.3	2.5-134 [2.5-149]	To reflect plant layout changes and inclusion of EPRI-CEUS Seismic Catalog, as described in both the Luminant ISCP Letter ML12268A41 and Fukushima RAI 261 response ML12207A599.	Section was revised due to CEUS and CPNPP layout update.	1
CTS-01521	2.5.7	2.4-242 2.5-246 2.5-249 Through 2.5-252 2.5-255 2.5-256 2.5-259 [2.5-257 2.5-261, 2.5-264 through 2.5-267, 2.5-270 2.5-271, 2.5-274, 2.5-275]	To reflect plant layout changes and inclusion of EPRI-CEUS Seismic Catalog, as described in both the Luminant ISCP Letter ML12268A41 and Fukushima RAI 261 response ML12207A599.	Section was revised to remove unused references and due to CEUS and CPNPP layout update.	1

Change ID No.	Section	FSAR Rev. 3 Page	Reason for change	Change Summary	Rev. of FSAR T/R
CTS-01521	Table 2.5.2-201	2.5-299 through 2.5-304 [2.5-315 through 2.5-324]	To reflect plant layout changes and inclusion of EPRI-CEUS Seismic Catalog, as described in both the Luminant ISCP Letter ML12268A41 and Fukushima RAI 261 response ML12207A599.	Table was revised due to CEUS and CPNPP layout update.	1
CTS-01521	Table 2.5.2-202	2.5-305 2.5-306 [2.5-325 through 2.5-328]	To reflect plant layout changes and inclusion of EPRI-CEUS Seismic Catalog, as described in both the Luminant ISCP Letter ML12268A41 and Fukushima RAI 261 response ML12207A599.	Table was revised due to CEUS and CPNPP layout update.	1
CTS-01521	Table 2.5.2-203	2.5-307 2.5-308 [2.5-329 through 2.5-332]	To reflect plant layout changes and inclusion of EPRI-CEUS Seismic Catalog, as described in both the Luminant ISCP Letter ML12268A41 and Fukushima RAI 261 response ML12207A599.	Table was revised due to CEUS and CPNPP layout update.	1

Change ID No.	Section	FSAR Rev. 3 Page	Reason for change	Change Summary	Rev. of FSAR T/R
CTS-01521	Table 2.5.2-204	2.5-309 [2.5-333 through 2.5-334]	To reflect plant layout changes and inclusion of EPRI-CEUS Seismic Catalog, as described in both the Luminant ISCP Letter ML12268A41 and Fukushima RAI 261 response ML12207A599.	Table was revised due to CEUS and CPNPP layout update.	1
CTS-01521	Table 2.5.2-205	2.5-310 [2.5-335 through 2.5-336]	To reflect plant layout changes and inclusion of EPRI-CEUS Seismic Catalog, as described in both the Luminant ISCP Letter ML12268A41 and Fukushima RAI 261 response ML12207A599.	Table was revised due to CEUS and CPNPP layout update.	1
CTS-01521	Table 2.5.2-206	2.5-311 [2.5-337 through 2.5-338]	To reflect plant layout changes and inclusion of EPRI-CEUS Seismic Catalog, as described in both the Luminant ISCP Letter ML12268A41 and Fukushima RAI 261 response ML12207A599.	Table was revised due to CEUS and CPNPP layout update.	1

Change ID No.	Section	FSAR Rev. 3 Page	Reason for change	Change Summary	Rev. of FSAR T/R
CTS-01521	Table 2.5.2-207	2.5-312 2.5-313 [2.5-339 through 2.5-341]	To reflect plant layout changes and inclusion of EPRI-CEUS Seismic Catalog, as described in both the Luminant ISCP Letter ML12268A41 and Fukushima RAI 261 response ML12207A599.	Table was revised due to CEUS and CPNPP layout update.	1
CTS-01521	Table 2.5.2-208	2.5-314 [2.5-342 through 2.5-343]	To reflect plant layout changes and inclusion of EPRI-CEUS Seismic Catalog, as described in both the Luminant ISCP Letter ML12268A41 and Fukushima RAI 261 response ML12207A599.	Table was revised due to CEUS and CPNPP layout update.	1
CTS-01521	Table 2.5.2-209	2.5-315 [2.5-344 through 2.5-345]	To reflect plant layout changes and inclusion of EPRI-CEUS Seismic Catalog, as described in both the Luminant ISCP Letter ML12268A41 and Fukushima RAI 261 response ML12207A599.	Table was revised due to CEUS and CPNPP layout update.	1

Change ID No.	Section	FSAR Rev. 3 Page	Reason for change	Change Summary	Rev. of FSAR T/R
CTS-01521	Table 2.5.2-210	2.5-316 [2.5-346 through 2.5-347]	To reflect plant layout changes and inclusion of EPRI-CEUS Seismic Catalog, as described in both the Luminant ISCP Letter ML12268A41 and Fukushima RAI 261 response ML12207A599.	Table was revised due to CEUS and CPNPP layout update.	1
CTS-01521	Table 2.5.2-211	2.5-317 [2.5-348]	To reflect plant layout changes and inclusion of EPRI-CEUS Seismic Catalog, as described in both the Luminant ISCP Letter ML12268A41 and Fukushima RAI 261 response ML12207A599.	Table was revised due to CEUS and CPNPP layout update.	1
CTS-01521	Table 2.5.2-212	2.5-318 [2.5-349 through 2.5-355]	To reflect plant layout changes and inclusion of EPRI-CEUS Seismic Catalog, as described in both the Luminant ISCP Letter ML12268A41 and Fukushima RAI 261 response ML12207A599.	Table was revised due to CEUS and CPNPP layout update.	1

Change ID No.	Section	FSAR Rev. 3 Page	Reason for change	Change Summary	Rev. of FSAR T/R
CTS-01521	Table 2.5.2-213	2.5-319 [2.5-356 through 2.5-357]	To reflect plant layout changes and inclusion of EPRI-CEUS Seismic Catalog, as described in both the Luminant ISCP Letter ML12268A41 and Fukushima RAI 261 response ML12207A599.	Table was revised due to CEUS and CPNPP layout update.	1
CTS-01521	Table 2.5.2-214	2.5-320 2.5-321 [2.5-358 through 2.5-361]	To reflect plant layout changes and inclusion of EPRI-CEUS Seismic Catalog, as described in both the Luminant ISCP Letter ML12268A41 and Fukushima RAI 261 response ML12207A599.	Table was revised due to CEUS and CPNPP layout update.	1
CTS-01521	Table 2.5.2-215	2.5-322 2.5-323 [2.5-362 through 2.5-365]	To reflect plant layout changes and inclusion of EPRI-CEUS Seismic Catalog, as described in both the Luminant ISCP Letter ML12268A41 and Fukushima RAI 261 response ML12207A599.	Table was revised due to CEUS and CPNPP layout update.	1

Change ID No.	Section	FSAR Rev. 3 Page	Reason for change	Change Summary	Rev. of FSAR T/R
CTS-01521	Table 2.5.2-216	2.5-324 [2.5-366 through 2.5-368]	To reflect plant layout changes and inclusion of EPRI-CEUS Seismic Catalog, as described in both the Luminant ISCP Letter ML12268A41 and Fukushima RAI 261 response ML12207A599.	Table was revised due to CEUS and CPNPP layout update.	1
CTS-01521	Table 2.5.2-217	2.5-325 [2.5-369 through 2.5-371]	To reflect plant layout changes and inclusion of EPRI-CEUS Seismic Catalog, as described in both the Luminant ISCP Letter ML12268A41 and Fukushima RAI 261 response ML12207A599.	Table was revised due to CEUS and CPNPP layout update.	1
CTS-01521	Table 2.5.2-218	2.5-326 [2.5-372 through 2.5-374]	To reflect plant layout changes and inclusion of EPRI-CEUS Seismic Catalog, as described in both the Luminant ISCP Letter ML12268A41 and Fukushima RAI 261 response ML12207A599.	Table was revised due to CEUS and CPNPP layout update.	1

Change ID No.	Section	FSAR Rev. 3 Page	Reason for change	Change Summary	Rev. of FSAR T/R
CTS-01521	Table 2.5.2-219	2.5-327 [2.5-375 through 2.5-377]	To reflect plant layout changes and inclusion of EPRI-CEUS Seismic Catalog, as described in both the Luminant ISCP Letter ML12268A41 and Fukushima RAI 261 response ML12207A599.	Table was revised due to CEUS and CPNPP layout update.	1
CTS-01521	Table 2.5.2-220	2.5-328 [2.5-378]	To reflect plant layout changes and inclusion of EPRI-CEUS Seismic Catalog, as described in both the Luminant ISCP Letter ML12268A41 and Fukushima RAI 261 response ML12207A599.	Table was revised due to CEUS and CPNPP layout update.	1
CTS-01521	Table 2.5.2-221	2.5-329 [2.5-379 through 2.5-381]	To reflect plant layout changes and inclusion of EPRI-CEUS Seismic Catalog, as described in both the Luminant ISCP Letter ML12268A41 and Fukushima RAI 261 response ML12207A599.	Table was revised due to CEUS and CPNPP layout update.	1

Change ID No.	Section	FSAR Rev. 3 Page	Reason for change	Change Summary	Rev. of FSAR T/R
CTS-01521	Table 2.5.2-222	2.5-330 [2.5-382]	To reflect plant layout changes and inclusion of EPRI-CEUS Seismic Catalog, as described in both the Luminant ISCP Letter ML12268A41 and Fukushima RAI 261 response ML12207A599.	Table was revised due to CEUS and CPNPP layout update.	1
CTS-01521	Table 2.5.2-223	2.5-331 [2.5-383 through 2.5-385]	To reflect plant layout changes and inclusion of EPRI-CEUS Seismic Catalog, as described in both the Luminant ISCP Letter ML12268A41 and Fukushima RAI 261 response ML12207A599.	Table was revised due to CEUS and CPNPP layout update.	1
CTS-01521	Tables 2.5.2-224 through 2.5.2-237	2.5-332 through 2.5-351 [2.5-386 through 2.5-405]	To reflect plant layout changes and inclusion of EPRI-CEUS Seismic Catalog, as described in both the Luminant ISCP Letter ML12268A41 and Fukushima RAI 261 response ML12207A599.	Tables were deleted due to CEUS and CPNPP layout update.	1

Change ID No.	Section	FSAR Rev. 3 Page	Reason for change	Change Summary	Rev. of FSAR T/R
CTS-01521	Figures 2.5.2-201 through 259 New Figures 2.5.2-260 through 277 Figures are located in UTR files 2, 3, and 4 of 4.	-	To reflect plant layout changes and inclusion of EPRI-CEUS Seismic Catalog, as described in both the Luminant ISCP Letter ML12268A41 and Fukushima RAI 261 response ML12207A599.	Figures were revised due to CEUS and CPNPP layout update.	1

*Page numbers for the attached marked-up pages may differ from the revision 3 page numbers due to text additions and deletions. When the page numbers for the attached pages do differ, the page number for the attached page is shown in brackets.

Table 2.0-1R (Sheet 10 of 13)
Key Site Parameters

	SSE (certified seismic design) horizontal ground response spectra	Regulatory Guide (RG) 1.60, enhanced spectra in high frequency range (see Figure 3.7.1-1)	~~The minimum DCD spectrum envelops all four FIRS, down to frequencies of 0.5 Hz. Values of the horizontal 10^{-5} UHRS and FIRS are shown in Table 2.5.2-229 for the seven spectral frequencies.~~ The DCD spectrum envelopes all FIRS down to frequencies of 0.5 Hz. Values of the horizontal 10^{-4} mean UHRS, 10^{-5} mean UHRS (both at GMRS/FIRS1/FIRS2 control elevations), and GMRS/FIRS1/FIRS2 are in Table 2.5.2-220 for seven spectral frequencies. Values for remaining FIRS are in Table 2.5.2-222. CTS-01521
	SSE (certified seismic design) vertical ground response spectra	RG 1.60, enhanced spectra in high frequency range (see Figure 3.7.1-2)	For vertical FIRS motions, the same considerations used for the GMRS were used for the FIRS. That is, as a conservative assumption the V/H ratio for the FIRS spectra is assumed to be equal to the V/H ratio from RG 1.60.
	Potential for surface tectonic deformation at site	None within the exclusion area boundary	No potential tectonic surface deformation has been identified at the site.
CP COL 2.5(1)	Subsurface stability – minimum allowable static bearing capacity	15,000 lb/ft^2	The minimum allowable bearing capacity of the foundation bearing stratum meets or exceeds the DCD requirement
	Subsurface stability – minimum allowable dynamic bearing capacity, normal conditions plus SSE	60,000 lb/ft^2	The minimum allowable dynamic bearing capacity of the foundation bearing stratum meets or exceeds the DCD requirement
	Subsurface stability – minimum shear wave velocity at SSE input at ground surface	1000 ft/s	The site stratigraphy has a measured velocity in excess of 1000 ft/sec

2.5.1 Basic Geologic and Seismic Information

CP COL 2.5(1) Replace the content of DCD Subsection 2.5.1 with the following.

This subsection presents information on the geological, seismological, and geotechnical engineering properties of CPNPP Units 3 and 4.

CP COL 2.5(1) RG 1.208 provides guidance for the recommended level of investigation at different distances from a proposed site for a nuclear facility.

- The site region is that area within 200 miles (mi) of the site.
- The site vicinity is that area within 25 mi of the site.
- The site area is that area within 5 mi of the site.
- The site location is that area within 0.6 mi of the site.

These terms–site region, site vicinity, site area, and site–are used in Subsections 2.5.1, 2.5.2, 2.5.3, 2.5.4 and 2.5.5 to describe these specific areas of investigation and are not applicable to other subsections of the FSAR.

The geological and seismological information presented in this subsection was developed from a review of previous reports prepared for CPNPP Units 1 and 2, published geologic literature, interpretation of aerial photography, subsurface investigations, geological mapping, and aerial reconnaissance conducted to support this CPNPP Units 3 and 4 application. Previous site-specific reports reviewed include the CPNPP Units 1 and 2 FSAR (Reference 2.5-201). A review of published geologic literature was used to supplement and update the existing geological and seismological information.

This subsection of the CPNPP Units 3 and 4 FSAR is intended to demonstrate compliance with the requirements of 10 CFR 100 “Reactor Site Criteria,” Section 100.23(c). The results of detailed, site-specific investigations to define the geologic and geotechnical conditions are presented in the following subsections. Results of these investigations are used to demonstrate the subsurface conditions for site response as well as static and dynamic geotechnical performance. The presented analysis and conclusions were developed by the following:

- ~~William Lettis & Associates~~Fugro Consultants, Inc. - Overall technical responsibility for Subsections 2.5.1, 2.5.2, 2.5.3, 2.5.4 and 2.5.5 including geotechnical analysis and reporting, site response, and Probabilistic Seismic Hazard Analysis (PSHA). CTS-01521
- ~~Fugro West Inc. - Geotechnical analysis and laboratory testing.~~
- ~~Risk Engineering Inc. - Site Response and Probabilistic Seismic Hazard Analysis (PSHA).~~

A series of isolated magnetic dipoles is associated with the gravity gradient and maximum that marks the edge of the Laurentian craton and the interior-zone gravity maximum. In contrast to the western and northwestern portions of the site region, the magnetic signature to the southeast is characterized by magnetic anomalies exhibiting relatively low values and subdued gradients. This response is due to the relatively thick blanket of nonmagnetic sedimentary material associated with the Gulf of Mexico Coastal Plain that serves to attenuate the underlying magnetic sources.

In concert with the regional gravity field, the features in the regional magnetic field can be attributed to development of the Laurentian Margin, the Ouachita orogeny, or development of the Gulf of Mexico. The location of the Meers fault, the only capable tectonic source recognized in the site region, is marked by the presence of a steep magnetic gradient (Figure 2.5.1-206) along its southeastern extension. However, this signature is the result of the juxtaposition of material of different magnetic susceptibilities during Late Paleozoic thrusting and not an expression of the recent kinematic history of the fault (Reference 2.5-223).

2.5.1.1.4 Regional Tectonic Setting

The CPNPP Units 3 and 4 site region is located within the Central and Eastern United States (CEUS), a stable continental region characterized by low rates of crustal deformation and no active plate boundary conditions. ~~In 1986, the Electric Power Research Institute (EPRI) developed a seismic source model~~In 2012, the CEUS Seismic Source Characterization for Nuclear Facilities Project (CEUS SSC) released an updated regional seismic source characterization model for the CEUS, which was developed using the Senior Seismic Hazard Analysis Committee (SSHAC) Level 3 assessment process based on NUREG/CR-6372 (Reference 2.5-292). The CEUS SSC model is based on historical seismicity extending through the end of the 2008 calendar year and it replaces the earlier Electric Power Research Institute Seismicity Owners Group (EPRI-SOG) (Reference 2.5-369) CEUS seismic source model. In addition to relying on an updated seismicity catalog, the CEUS SSC model also provides a full assessment and rigorous treatment of uncertainties, and it embraces a suite of various technical interpretations for the CEUS that included the CPNPP Units 3 and 4 region (~~Reference 2.5-369~~Reference 2.5-486). ~~This seismic source model was developed using the interpretations provided by six independent Earth Science Teams (ESTs) and aimed to reflect the general state of knowledge of the earth science community as of 1986.~~ The source models developed ~~by the ESTs~~for the CEUS SSC combined tectonic setting and rates and distribution of historical seismicity; the models are summarized in Subsection 2.5.2.2. The following subsection summarizes the current state of knowledge of the tectonic setting and tectonic structures in the CPNPP site region, with a focus on ~~post-1986~~ geologic, seismologic, or geophysical information that is relevant to assessing potential for seismic activity in the region through the end of the 2008 calendar year. CTS-01521 CTS-01521 CTS-01521

The other Cenozoic tectonic event of interest to the site is the development of the Rio Grande Rift system in New Mexico and westernmost Texas and the Basin and Range Province farther west. These features are outside of the site region, but their Miocene development led to broad epeirogenic uplift and erosion of the Paleocene and Upper Cretaceous strata in central Texas. The resulting flexure of the lithosphere occurs along a northeast-southwest-trending line between the uplifted Edwards Plateau of central Texas (on which the CPNPP is sited) and the down-to-the-southeast warped coastal plain to the southeast. The northeast-southwest-trending Balcones and Luling-Mexia-Talco fault zones are spatially associated with this hingeline and geomorphic transition from the Edwards Plateau to the interior zone of the Gulf Coastal Plain (Reference 2.5-237). These fault zones were active in the Late Oligocene or Early Miocene (Reference 2.5-237), and were probably driven by the crustal flexure and tilting associated with sedimentary loading of the Gulf of Mexico Basin. The tectonic activity of the CPNPP site region since the Miocene has been minimal. The site region has predominately undergone local erosion and deposition along rivers and drainages while transporting sediments shed from the Rockies and the Appalachians south to depocenters in the Gulf of Mexico.

2.5.1.1.4.2 Tectonic Stress

Three types of forces are generally responsible for the stress in the lithosphere:

a. Gravitational body forces or buoyancy forces, such as the ridge-push force resulting from hot, positively buoyant young oceanic lithosphere near the ridge against the older, colder, less buoyant lithosphere away from the ridge (Dahlen, Reference 2.5-238). This force is transmitted by the elastic strength of the lithosphere into the continental interior.

b. Shear and compressive stresses transmitted across plate boundaries (such as strike-slip faults or subduction zones).

c. Shear tractions acting on the base of the lithosphere from relative flow of the underlying asthenospheric mantle.

~~Earth science teams (ESTs) that participated in the EPRI (Reference 2.5-369) evaluation of intra-plate stress found that tectonic stress in the CEUS region is primarily characterized by northeast-southwest-directed horizontal compression. In general, the ESTs concluded that the most likely source of tectonic stress in the mid-continent region was ridge-push force associated with the Mid-Atlantic Ridge, transmitted to the interior of the North American Plate by the elastic strength of the lithosphere. Other potential forces acting on the North American Plate were judged to be less significant in contributing to the magnitude and orientation of the maximum compressive principal stress.~~ CTS-01521

~~In general, the ESTs focused on evaluating the state of stress in the mid-continent and Atlantic seaboard regions, for which stress indicator data were relatively abundant. Fewer stress indicator data were available for the Gulf of Mexico, Gulf~~

~~Coastal Plain, and Western Great Plains, and thus these areas received less scrutiny in the EPRI (Reference 2.5-369) studies. Notably, the Dames & Moore, Law Engineering, and Bechtel ESTs observed that the orientation of maximum horizontal compression in the Gulf Coastal Plain and west Texas may be perturbed from the regional northeast-southwest orientation that characterizes much of the CEUS.~~ CTS-01521

~~Since 1986, a~~An international effort to collate and evaluate stress indicator data culminated in publication of a ~~new~~ World Stress Map in 1989 (References 2.5-239 and 2.5-240) that has been periodically updated (Reference 2.5-241). Plate-scale trends in the orientations of principal stresses were assessed qualitatively based on the analysis of high-quality data (Reference 2.5-242) and previous delineations of regional stress provinces were refined. Statistical analyses of stress indicators confirmed that the trajectory of the maximum compressive principal stress is uniform across broad continental regions at a high level of confidence (Reference 2.5-243). In particular, the northeast-southwest orientation of principal stress in the CEUS ~~inferred by the EPRI ESTs~~ is statistically robust and is consistent with the theoretical orientation of compressive forces acting on the North American Plate from the Mid-Atlantic Ridge (Reference 2.5-242). CTS-01521

According to the continental U.S. stress map of Zoback and Zoback (Reference 2.5-239), the site is located in the Mid-Plate Stress province, a large area of the CEUS that displays a consistent northeast-southwest maximum compressive stress orientation (Figure 2.5.1-209). Portions of the site region are also in the Southern Great Plains Stress province, which is characterized by a northeast-southwest-oriented extensional stress regime, and the Gulf Coast Stress province, which is characterized by northeast-southwest to north-northeast to south-southwest horizontal tension (Reference 2.5-239).

2.5.1.1.4.2.1 Mid-Plate Stress Province

The Mid-Plate Stress province characterizes most of the CEUS (Figure 2.5.1-209). This province may exhibit reverse or strike-slip faulting under east-northeast- to west-southwest- to northwest-southeast-oriented compressive stress. This region extends from an approximately north-south-oriented line through Texas, Colorado, Wyoming, and Montana east all the way to the Atlantic Margin and potentially into the Atlantic Ocean Basin (Reference 2.5-239). Within this province, the orientation of maximum compressive stress is generally parallel to plate velocity direction (Reference 2.5-240). Richardson and Reding (Reference 2.5-244) were able to reproduce the northeast-southwest orientation of principal stress in CEUS with numerical models that assume horizontal shear tractions acting on the base of the North American Plate from the underlying asthenospheric mantle. Humphreys and Coblentz (Reference 2.5-245) concluded that a dominant control on the northeast-southwest orientation of the maximum compressive principal stress in the CEUS is ridge-push force from the Atlantic Ocean Basin.

correlation is valid in Texas, then the boundary between the Mid-Plate and Southern Great Plains Stress provinces probably is located near the eastern foot of the mountains in West Texas, west of the site.

2.5.1.1.4.2.3 Gulf Coast Stress Province

The southeastern portion of the site region is in, or adjacent to, the Gulf Coast Stress province. This province generally coincides with the belts of growth faults in the coastal regions of Texas, Louisiana, Mississippi, Alabama, and northwestern Florida. The Gulf Coast Stress province is characterized by north-south-directed tensile stress (Reference 2.5-239) and is spatially associated with down-to-the-Gulf extension and slumping of the Coastal Plain stratigraphic section. Because these strata are deforming above subhorizontal detachment faults and/or large bodies of Jurassic salt, gravitational tensile stress driving growth faulting is confined to the sedimentary section, and thus decoupled mechanically from the state of stress in the underlying crystalline basement.

The state of stress in the crystalline basement underlying the Coast Plain strata is very poorly constrained (Reference 2.5-244) and may be affected by flexural loading of the lithosphere due to rapid and voluminous sedimentation in the Gulf of Mexico during the Pleistocene. Detailed numerical modeling of flexural deformation associated with sedimentary loading in the Gulf by Nunn (Reference 2.5-246) suggested that large bending stresses may be present in the crust and systematically vary from north-south tension in the Coastal Plain, to north-south compression in an approximately 62-mi-wide zone in the northern offshore region directly adjacent to the coast, to north-south tension at distances of greater than 62 mi from the coast.

CTS-01521

To summarize, research on the state of stress in the CEUS~~continental U.S. since the publication of the EPRI (1986) studies~~ has confirmed observations that stress~~ in the CEUS~~ is characterized by relatively uniform northeast-southwest compression, and that this regional trend may be perturbed at distances beyond 150 mi from the CPNPP Units 3 and 4 site due to the influence of buoyancy forces in the uplifted Cordillera to the west, and flexure of the crust due to sedimentary loading of the Gulf of Mexico to the southeast. ~~Very few new data have been reported since the EPRI (Reference 2.5-369) study to better determine the orientations and relative magnitudes of the principal stresses in the site region. Given that the current interpretation of the orientation of principal stress is similar to that adopted in EPRI (Reference 2.5-369), a new evaluation of the seismic potential of tectonic features based on a favorable or unfavorable orientation to the stress field would yield similar results. Thus, t~~There is no significant change in the understanding of the static stress in the site region~~ since the publication of the EPRI source models in 1986~~, and there are no significant implications for existing characterizations of potential activity of tectonic structures.

CTS-01521

2.5.1.1.4.3 Principal Tectonic Features

The tectonic features within the site region are discussed below, categorized by their age of movement or activity. Generally, these features were most recently active in either the Late Paleozoic (associated with the Ouachita orogeny) or Mesozoic to Eocene (related to the opening of the Gulf of Mexico). Specifically, workers have found evidence for only one tectonically capable fault or feature within the 200-mi radius, the Meers fault. The seismic hazard from all tectonic features incorporated in the CEUS SSC (Reference 2.5-486) were included in calculating the seismic hazard at the site. Two of those features outside of the 200-mi radius are discussed which contribute to the hazard at the site: the Cheraw fault and the New Madrid fault system~~Given the low seismic hazard associated with the majority of features within the 200-mi radius, 3 features outside of this radius are discussed which contribute to the hazard at the site: the Rio Grande Rift, the Cheraw fault, and the New Madrid seismic zone~~. CTS-01521

2.5.1.1.4.3.1 Late Proterozoic Tectonic Features

The oldest outcropping rocks in Texas occur in part in the Llano Uplift in south-central Texas (Figures 2.5.1-202 and 2.5.1-207), 90 mi south-southwest of the site. Ultramafic to amphibolitic metamorphic rocks and plutons record Mesoproterozoic high-grade metamorphism and deformation as part of the Grenville orogeny (References 2.5-247 and 2.5-248). This deformation primarily comprises broad folds and thrusts within the metamorphic units and resulted from a north-directed collision of a continental block with the southern margin of North America during the formation of Rodinia, likely between ~1300 and 1080 Ma (References 2.5-228 and 2.5-248). The Mesoproterozoic rocks are surrounded by Cambrian-Mississippian marine strata that were deposited during the Early Paleozoic rifting and ocean development that preceded the Late Paleozoic Ouachita orogeny (Reference 2.5-249). The current map pattern of the Llano Uplift is dominated by northeast-trending exposures of normal to oblique faults that have Late Paleozoic ages (Reference 2.5-249). These faults originated during the Ouachita orogeny and exhumed the Llano basement rocks to temperatures of less than 120 °C in the Late Permian (Reference 2.5-250). This thermal history indicates that the Llano Uplift experienced little uplift since the Permian. The Mesoproterozoic basement and Paleozoic marine strata are then overlain by nearly flat-lying Lower Cretaceous shallow marine deposits that also limit the deformation in the Llano Uplift to pre-Cretaceous (Reference 2.5-249).

2.5.1.1.4.3.2 Early Paleozoic Tectonic Features

There are few exposures of faults that accommodated the Cambrian rifting of Laurentia. The most abundant evidence for this extension is recorded by the sedimentary sequences deposited during and after extension--the Southern Oklahoma Aulacogen, located 100 mi north of the site (Figure 2.5.1-208). Normal faults and fault-bounded basins associated with Late Proterozoic to Early Paleozoic rifting of Laurentia are inferred from geophysical surveys to lie beneath overthrust rocks of the Late Paleozoic Ouachita orogenic belt and Mesozoic to

above the Pennsylvanian Ouachita thrust belt, and comprises the northern and western margins of the East Texas Basin (Reference 2.5-262). The Luling fault zone is southeast of the Balcones fault zone and comprises a series of north-side-down normal faults including the Staples, Larremore, Lytton Springs, Luling, Darst Creek, Salt Flat, Somerset, and Alta Vista faults (Reference 2.5-266). The Mexia fault zone is over 500 mi long (Reference 2.5-266). The Mexia-Talco fault zone is a graben system coincident with the updip extent of subsurface Middle Jurassic Louann salt, and was active from the Jurassic to Eocene based upon the ages of the oldest and youngest strata offset by this fault system (Reference 2.5-262).

The Mt. Enterprise-Elkhart graben fault system is a zone of normal faults that obliquely crosses the southeastern margin of the East Texas Basin and extends eastward to the western flank of the Sabine Uplift (References 2.5-228 and 2.5-262). The Mt. Enterprise-Elkhart graben fault system strikes east-northeast and extends for a total distance of 90 mi from south of Carthage, Texas, to the Trinity River near Palestine, Texas (Figure 2.5.1-210). At its closest point, the Mt. Enterprise-Elkhart graben fault system is about 129 mi southeast of the site. Like the Luling-Mexia-Talco fault zone, the Mt. Enterprise-Elkhart graben fault system is characterized by a structurally complex series of grabens that are interpreted to root in Middle Jurassic Louann salt (References 2.5-262 and 2.5-267). The Mt. Enterprise-Elkhart graben faults were primarily active in Late Jurassic-Early Cretaceous time and the youngest rocks they offset are Eocene in age (References 2.5-228 and 2.5-262). No data have been published to support an interpretation that the Mt. Enterprise-Elkhart graben fault system is a capable tectonic structure. It should be noted, however, that the CPNPP FSAR for Units 1 and 2 described the most recent movement to be Eocene or younger on the Mt. Enterprise-Elkhart graben fault system. ~~In publications that predate the 1986 EPRI studies, l~~Lines of evidence indicating potential Quaternary motion and active creep along the Mt. Enterprise-Elkhart graben fault system include the following: CTS-01521

- Three faults at the western end of the Mt. Enterprise-Elkhart graben fault system in the Trinity River Valley near Palestine, Texas, displace Late Quaternary deposits overlying Eocene Claiborne strata (Reference 2.5-268; Figure 2.5.1-210). Maximum normal displacement of the Eocene strata on the fault at this site is 46 inches (in), with maximum offset of the overlying Quaternary gravels of 26 in. On the basis of an estimated age of 37 thousand years (ka) for the Late Quaternary gravels (Reference 2.5-258), the implied average, Late Quaternary separation rate across the fault is about 0.02 mm/yr.

- Geodetic leveling data showing a relative movement of 130 mm across the geographic center of the Mt. Enterprise-Elkhart graben fault system between 1920 and the mid 1950s, with a down-to-the-south displacement across the southern margin (Reference 2.5-268). If this motion is due to slip on normal faults, then the average vertical separation rate is 4.3 mm/yr.

- Historical and instrumentally located seismicity is spatially associated with the Mt. Enterprise-Elkhart graben fault system, including the 1891 Rusk earthquake (maximum Modified Mercalli Intensity [MMI] VI: magnitude (unspecified scale) 4.0 and location estimated from felt effects); four earthquakes in 1957 (maximum intensity III to V; magnitudes (unspecified scale) 3.0 to 4.7 and locations estimated from felt effects); and the 1981 Center (m_b 3.0) and Jacksonville (m_b 3.2) earthquakes (References 2.5-269 and 2.5-270). Locations and estimated magnitudes are further discussed in Subsection 2.5.2.1.

As discussed in Subsection 2.5.1.1.4.3.3, seismic reflection data suggest that the Mt. Enterprise-Elkhart graben fault system is rooted in the Jurassic Louann salt at maximum depths of 4.5 to 6 km (References 2.5-262 and 2.5-267). This suggests that movement of salt at depth may drive observed Late Quaternary displacement and contemporary creep across the Mt. Enterprise-Elkhart graben fault system and that the fault is not accommodating tectonic deformation and thus is not an independent source of moderate to large earthquakes. ~~Presumably, this was the evaluation of the EPRI ESTs, who had access to the pre-1986 literature on the Mt. Enterprise-Elkhart graben fault system and did not specifically characterize it as a Quaternary tectonic fault and potentially capable structure. However,~~ Ewing (Reference 2.5-228) ~~commented in a post-EPRI publication that~~states "... surface strata are displaced and seismicity suggests continuing deformation. . ." on the Mt. Enterprise-Elkhart graben fault system. CTS-01521

On the basis of a review of ~~post-EPRI~~ scientific literature, no new data have been published to support an interpretation that the Mt. Enterprise-Elkhart graben fault system is a capable tectonic structure. Recent reviews of suspected Quaternary tectonic features in the CEUS by Crone and Wheeler (Reference 2.5-271) and Wheeler (Reference 2.5-272) did not identify or discuss the Mt. Enterprise-Elkhart graben fault system as a potential tectonic fault. Because of the unverified statement that the western end of the Mt. Enterprise-Elkhart graben fault system could potentially be seismogenic (Reference 2.5-268), William Lettis & Associates, Inc., conducted a field reconnaissance study. This study did not find evidence to support post-Eocene tectonic activity on the Mt. Enterprise-Elkhart graben fault system. The documented association of the Mt. Enterprise-Elkhart graben fault system with Jurassic salt deposits and the high rate of active creep measured by geodetic methods both support the interpretation that Quaternary activity of the Mt. Enterprise-Elkhart graben fault system is related to salt migration at depth. The separation rate of 4.3 mm/yr implied by the geodetic data is highly anomalous for a fault located in a stable continental block; if tectonic, deformation rates and fault slip rates of about 4 to 5 mm/yr are more characteristic of those associated with an active plate boundary. There is broad consensus within the informed geosciences community that the Grand Prairie of Texas is not part of an active plate boundary. The high geodetic deformation rates, if accurate, are most simply explained by movement at depth and do not reflect whole-crustal strain. In conclusion, there is no new information bearing on the Quaternary activity of the Mt. Enterprise-Elkhart graben fault system faults requiring a revision of the EPRI seismic source characterization of this region. CTS-01521

2.5.1.1.4.3.5 Tertiary Tectonic Features

South and east of the Llano Uplift, the Balcones fault zone is a series of faults that generally strike north to northeast and dip 45 to 85° southeast, with down-dip fault striae indicating normal sense of displacement (References 2.5-266 and 2.5-273). The fault zone is approximately 75 mi east of the site and the throw on the faults varies from 500 to 1200 ft (Figure 2.5.1-210, Reference 2.5-266). The fault zone has resulted in a series of fault-line scarps between Uvaled and Georgetown, Texas, known as the Balcones Escarpment (Reference 2.5-273). The Balcones fault zone includes multiple fault blocks (2 to 7 mi wide) bounded by the en échelon normal faults, each with 100 to 850 ft throws, northwest-dipping antithetic faults, and relay ramps between the en échelon fault (Reference 2.5-273).

Initial movement on the Balcones fault zone may have occurred in the Mesozoic, because Late Cretaceous volcanic rocks of the Balcones igneous province generally are exposed along the trend of the fault zones, and in some cases volcanic centers are aligned along the faults (Reference 2.5-228). The youngest rocks cut by the faults are Eocene, though a lack of Oligocene to Miocene deposits adjacent to the structure has been interpreted as evidence for post-Eocene movement (Reference 2.5-266). Collins (Reference 2.5-274) stated that most of the displacement on the Balcones fault zone occurred in Late Oligocene and Early Miocene, but did not provide a basis for this assessment.

The fault zone is associated with the southeast-facing Balcones Escarpment, a prominent geomorphic feature in central Texas (Reference 2.5-275). The Balcones Escarpment is a fault-line scarp produced by differential erosion of these units (Reference 2.5-276). Rocks exposed on the upthrown side of the fault zone are dominantly Lower Cretaceous, erosion-resistant carbonates, whereas strata on the downthrown side are less resistant, Upper Cretaceous chalk and mudstone.

2.5.1.1.4.3.6 Quaternary Tectonic Features Within the Site Region

The site region is part of a tectonically stable continental margin. ~~No capable tectonic faults were identified within the CPNPP Units 1 and 2 site region during the 1986 EPRI studies, and the CPNPP FSAR for Units 1 and 2 concluded that there were no capable tectonic faults within the site region.~~ The Great Plains region, in general, and the CPNPP Units 3 and 4 site region, in particular, is characterized by very low rates of background seismicity (Subsection 2.5.2.1). Within the site region, only the Meers fault has been identified as demonstrating evidence for Quaternary activity. However, a nearby fault bounding a Late Paleozoic Uplift, the Criner fault, has been speculated to have Quaternary activity because of its proximity to the Meers. Therefore, we also discuss this feature, concluded to be a Late Paleozoic thrust with a fault-line scarp, in detail below. Both the Meers fault and Criner fault are included within the CEUS SSC (Reference 2.5-486).

CTS-01521

CTS-01521

2.5.1.1.4.3.6.1 Meers Fault

Quaternary activity on the Meers fault was not recognized until the early 1980s (References 2.5-277 and 2.5-278) after completion of the FSAR for CPNPP Units 1 and 2. ~~Following from these studies, the Meers fault~~ As such, the Meers fault has been included within the CEUS SSC and is the only capable fault within the CPNPP Units 3 and 4 site region. ~~, and t~~The Meers fault should be characterized as a seismic source for CPNPP Units 3 and 4. The seismic source characterization of the Meers fault used for CPNPP Units 3 and 4 is presented in Subsection 2.5.2.4.2.3.2. CTS-01521

This ~~source characterization is developed following the Senior Seismic Hazard Analysis Committee (SSHAC) guidelines for a SSHAC level 2 study described in NUREG/CR-6372. Following the guidance of NUREG/CR-6372, this~~ characterization of the Meers fault represents the legitimate range of technically supportable interpretations of the seismic capability of the Meers fault among the informed technical community. This characterization is based on the existing literature of the Meers fault and on the elicitation of expert opinion. A summary of these opinions and a review of the existing literature used in the Meers source characterization is reviewed below. CTS-01521

The Meers fault is the southern boundary of the Frontal Wichita fault system in southern Oklahoma and is approximately 180 mi from the site (Figures 2.5.1-207 and 2.5.1-210). The history of the Meers fault, like the majority of the Frontal Wichita fault system, largely reflects the history of rifting and orogenesis in southern Oklahoma (see discussion in Subsection 2.5.1.1.4.1.1, Southern Oklahoma Aulacogen and Wichita uplift). The Meers fault may have initiated as a rift-bounding normal fault during the formation of the Southern Oklahoma Aulacogen (Reference 2.5-223). During the Permian, the Meers fault accommodated some contraction associated with the closing of the Atlantic Ocean and the Ouachita orogeny that led to the formation of the Wichita Uplift (References 2.5-223, 2.5-279, 2.5-280, 2.5-281 and 2.5-282). Slip on the Meers fault during this time was characterized by up-to-the-north motion on a southward dipping fault with an unknown component of left-lateral slip. Ultimately approximately 7.5 mi of vertical offset is thought to have occurred across the Frontal Wichita system, and roughly 1.2 mi was accommodated on the Meers fault (References 2.5-223, 2.5-280, and 2.5-281).

Since formation of the Wichita Uplift, the Meers fault has been reactivated at least twice: first during the Late Permian, and most recently during the Late Holocene. During the known reactivations, the sense of vertical slip on the Meers fault reversed from north-side-down to south-side-down. The change in sense of slip during the Permian reactivation was determined from observations of sedimentary material eroded off of the northern, upthrown side of the fault and deposited on the southern, downthrown side of the fault (References 2.5-281 and 2.5-282). The second known reactivation of the Meers fault began sometime in the Quaternary with the most recent slip in the Late Holocene (References 2.5-223, 2.5-281, 2.5-283, 2.5-284 and 2.5-285).

The trace of the Meers fault is easily identified on aerial photographs for a total distance of approximately 23 mi as a south-down topographic escarpment (Figure 2.5.1-211). The scarp over much of this extent has been visited by various researchers, and is thought to be related to Holocene rupture along the Meers fault (References 2.5-277, 2.5-278, 2.5-281, 2.5-284, 2.5-285 and 2.5-286).

CTS-01521

2.5.1.1.4.3.6.1.1 ~~Existing Literature~~

~~The modern state of knowledge regarding the Quaternary activity of the Meers fault is primarily based on four sets of studies: the studies of Ramelli and others (References 2.5-271 and 2.5-286); the studies of Madole (References 2.5-283 and 2.5-287); the study of Crone and Luza (Reference 2.5-284); and the studies of Swan and others (References 2.5-277 and 2.5-285). These studies are summarized in Table 2.5.1-202. Other studies of the Meers fault have been conducted (References 2.5-223, 2.5-288 and 2.5-289), but these studies do not significantly add to the modern state of knowledge of the Meers fault as a potential seismic source. The seismic source characterization of the Meers fault developed in Subsection 2.5.2.4.2.3.2 is based on the first four studies. A summary of each of these four Meers fault studies is presented in Table 2.5.1-202.~~

2.5.1.1.4.3.6.1.1.1 ~~Meers Fault Studies of Ramelli and Others~~

~~The major contribution of the studies of Ramelli and others (References 2.5-281 and 2.5-286) to investigations of the Quaternary activity of the Meers fault was to acquire and analyze low sun-angle aerial photography and to extend the mapped length of the Meers fault an additional 6.8 mi (11 km) to the southwest, for a total length of approximately 23 mi (37 km) (Figure 2.5.1-211).~~

~~The southeast extension of the scarp identified by Ramelli, et al. (Reference 2.5-286) and further discussed by Ramelli and Slemmons (Reference 2.5-281) is described as more subtle and discontinuous than the originally identified 16-mi-long scarp. Ramelli and Slemmons (Reference 2.5-281) argue that the southeastern continuation of the scarp shares the same history of events on the Meers fault due to its alignment with the original scarp, the consistent down-to-south separation across the scarp, its proximity to the original scarp, and the presence of a small drainage aligned parallel to the scarp and across the pattern of local drainage networks. However, Ramelli and Slemmons (Reference 2.5-281) also acknowledge uncertainty in the structural relationship between the northwest and southeast scarps due to a left step in the scarp near the junction of the two scrap strands and the absence of a scarp across East Cache Creek (Figure 2.5.1-211). In addition, field evaluation of the southeast extension of the scarp has not been possible because the scarp traverses onto the Fort Sill Military Reservation (References 2.5-278, 2.5-281 and 2.5-286).~~

~~The studies of Ramelli, et al. (Reference 2.5-286) and Ramelli and Slemmons (Reference 2.5-281) also discuss:~~

- ~~Estimates of vertical separation and left lateral offsets across the fault (16 ft and 33 to 66 ft, respectively);~~ CTS-01521

- ~~Magnitude estimates of earthquakes that caused the scarp (Ms 6.75 to 7.25);~~

- ~~Fault dip (sub-vertical to vertical); and~~

- ~~Dating of the last surface rupturing event (within the last several thousand years).~~

~~All of these characteristics of the fault are more thoroughly investigated in studies that post-date the work of Ramelli, et al. (Reference 2.5-286) and Ramelli and Slemmons (Reference 2.5-281).~~

2.5.1.1.4.3.6.1.1.2 ~~Meers Fault Studies of Madole~~

~~The studies of Madole (References 2.5-283 and 2.5-287) used radiocarbon dating of organic material to constrain the timing of well-defined movement along the Meers fault. Madole mapped alluvial stratigraphy at two sites along the fault (Canyon Creek and Browns Creek; Figure 2.5.1-211) and used radiocarbon dates determined from deposits distal to the fault trace (tens to hundreds of ft from downthrown side of the fault) to estimate depositional ages of the pre-faulting, fault-related, and post-faulting alluvial units.~~

~~The two key sedimentary units used by Madole's study are the Browns Creek alluvium, the youngest faulted unit, and the East Cache alluvium, the oldest unfaulted unit. Madole reported three ages for the Browns Creek alluvium taken from clay and humus layers (9,880 ± 160 and 12,240 ± 240 C-14 years B.P.) and snail shells (13,670 ± 120 C-14 years B.P.) (Table 2.5.1-201) that suggest deposition of the unit began around 13,000 B.P. in C-14 years. Madole presented four ages from the East Cache Creek Alluvium taken from clay and humus layers (310 ± 150 and 470 ± 150 C-14 years B.P.) and charcoal fragments (70 ± 150 and 600 ± 50 C-14 years B.P.). Madole concluded that the unit was deposited after 800 years B.P. and before 100 years B.P.~~

~~Madole (Reference 2.5-283) also constrained the age of deposition of alluvial fans derived from the Meers fault scarp. At the Canyon Creek site, Madole reported a C-14 age (1,280 ± 140 years B.P.) (Table 2.5.1-202) from charcoal buried by scarp-derived alluvial fan deposits that he interprets as providing a maximum age of faulting. Madole (Reference 2.5-283) concluded that this date combined with the C-14 ages of the East Cache Creek alluvium at this site (600 ± 50 years B.P.) bounds the age of faulting at Canyon Creek. At the Browns Creek site, Madole reported two C-14 ages (1,740 ± 140 years B.P. and 1,360 ± 100 years B.P.) (Table 2.5.1-201) from a clay and humus layer buried by the fault-related fan. Again, Madole (Reference 2.5-283) concluded that these ages combined with the C-14 ages of the East Cache Creek alluvium at this site (70 ± 150 years B.P., 310 ± 150 years B.P., and 470 ± 150 years) constrains the age of faulting at Browns~~

~~Creek. Overall, Madole (Reference 2.5-283) concluded that the 1,280 ± 140 C-14 years age from the Canyon Creek site is the best estimate for the time of faulting.~~ CTS-01521

2.5.1.1.4.3.6.1.1.3 ~~Meers Fault Studies of Crone and Luza~~

~~Crone and Luza (Reference 2.5-284) and Luza, et al. (Reference 2.5-290) completed two fault-perpendicular trenches at the Canyon Creek site, four fault-parallel trenches at the ponded alluvium site, and several excavations of the fault scarp near the ponded alluvium site to investigate the paleoseismic history of the Meers fault (Figure 2.5.1-211). The ponded alluvium site was used to estimate the ratio of lateral to vertical offset along the fault, and the excavations were used to estimate the number of Holocene events. Here we discuss their results as presented in the Crone and Luza (Reference 2.5-284) publication. The best constraints on the timing of faulting came from the Canyon Creek trenches.~~

~~Canyon Creek Site~~

~~Trench 1 of Crone and Luza (Reference 2.5-284) was excavated across the fault in the Holocene Browns Creek alluvium. In the trench, Browns Creek alluvium overlies Permian Henessey Shale. Crone and Luza (Reference 2.5-284) also suggested that the stratigraphic relations show evidence of only one surface faulting event.~~

~~Crone and Luza (Reference 2.5-284) used two radiocarbon dates to constrain the timing of faulting in the trench. One age (1570 cal. years B.P.) (Table 2.5.1-201) was taken from soil humus interpreted to have fallen into a crevice caused by surface faulting. The second age (1646 cal. years B.P.) (Table 2.5.1-201) was taken from soil humus deposited at the base of the scarp shortly after faulting. Crone and Luza (Reference 2.5-284) interpreted these ages as maximum ages for faulting because they are determined using soil humus likely to have long-lived organic components that predate soil deposition. Crone and Luza (Reference 2.5-284) corrected for this long-lived C-14 component of the soil by subtracting 300 years (their estimate of the Average Mean Residence Time, AMRT) from the calibrated radiocarbon ages to give estimates of scarp formation. As such, they interpreted the samples from this trench to indicate scarp formation between 1,200 to 1,300 years B.P.~~

~~Trench 2 of Crone and Luza (Reference 2.5-284) was excavated across the scarp in Middle Pleistocene Porter Hill alluvium. Overlying the Porter Hill alluvium, on the downthrown side, were scarp-derived deposits. The Hennessey Shale bedrock was only encountered on the upthrown side of the fault. A stratigraphic offset of 10 to 11 ft was observed in the trench, and Crone and Luza (Reference 2.5-284) interpreted stratigraphic relationships within the trench as providing evidence of only one episode of faulting. Crone and Luza (Reference 2.5-284) also indicated that the amount of offset observed in the Porter Hill alluvium in the trench is roughly equivalent to the offset observed in the younger Browns Creek alluvium in trench 1. Crone and Luza (Reference 2.5-284) interpreted this observation as indicating that there has not been any substantial vertical~~

movement other than that observed in trench 1 since deposition of the Porter Hill Alluvium. CTS-01521

Crone and Luza (Reference 2.5-284) used one radiocarbon date to constrain the timing of faulting in trench 2. An age of 1290 calendar years B.P. was determined for a soil 7 to 10 ft (2 to 3 m) downslope of the scarp that was buried by scarp-derived colluvium (Table 2.5.1-201). Given this stratigraphic relation and the distance from the scarp, Crone and Luza (Reference 2.5-284) interpreted this as a minimum age for the time of faulting.

Ponded Alluvium Site

The ponded alluvium site of Crone and Luza (Reference 2.5-284, Figure 2.5.1-211) consists of a southwest-facing fault scarp cutting across three northeast-draining gullies. Alluvium from the gullies ponded against the scarp, creating a well-preserved history of Holocene faulting. At the site, Crone and Luza (Reference 2.5-284) excavated two pairs of fault-parallel trenches and several soil pits across the scarp.

Each pair of the fault-parallel trenches was excavated with one trench on each side of the fault, and each pair exposed a bedrock paleo-channel and a stratigraphy consisting of ponded alluvium and fault-related alluvium and colluvium. Crone and Luza (Reference 2.5-284) obtained radiocarbon ages from three different horizons at the easternmost set of trenches: (1) a non-fault-related, pebbly silt alluvial deposit (1816 cal. years) from near the base of the trench, (2) a silt layer interpreted as a ponded alluvium deposited immediately after the initial scarp formation (1539 cal. years), and (3) a sample 12 in stratigraphically higher in a similar silt layer (1354 cal. years) (Table 2.5.1-201). Crone and Luza (Reference 2.5-284) report that after correcting 300 years for the AMRT, the oldest two ages bracket formation of the scarp. At the western set of trenches, Crone and Luza (Reference 2.5-284) determined only one radiocarbon age (1606 cal. years), and they believe the sample contained pre- and post-faulting organic material. As such, they do not believe the age provides a reliable constraint on scarp formation.

Crone and Luza (Reference 2.5-284) also used the bedrock gullies in the two pairs of trenches to estimate the amount of lateral and vertical offset across the Meers fault. For each pair of trenches, they determined the position of the channel thalweg and estimated the offset accounting for channel gradient and potential variations in channel orientation. In the westernmost pair of trenches, they estimated a vertical separation of 4.9 ft and a left-lateral separation of 16 ft. In the easternmost pair of trenches, they estimated a vertical separation of at least 6.9 ft and left-lateral separation of 11 to 17 ft.

Crone and Luza (Reference 2.5-284) also excavated several soil pits across the fault scarp to constrain the number of scarp-forming faulting events. Crone and Luza (Reference 2.5-284) reported that stratigraphic relations within the pits provide evidence of one to two faulting events. However, Crone and Luza

(Reference 2.5-284) preferred the single event interpretation due to the evidence in the Canyon Creek trenches of only one event. CTS-01521

Summary

In summarizing their results, Crone and Luza (Reference 2.5-284) stated their best estimate for the age of the Meers fault scarp as 1200 to 1300 years B.P. They also estimated that the magnitude of the event that caused the scarp was approximately Ms 7 or Mw greater than 7.

2.5.1.1.4.3.6.1.1.4 Meers Fault Studies of Swan and Others

Geomatrix Consultants undertook a detailed study of the Meers fault in the late 1980s funded by the U. S. Nuclear Regulatory Commission (Reference 2.5-291). The study resulted in two reports: a contribution to a proceedings volume for a NRC meeting (Reference 2.5-277), and a draft report to the NRC (Reference 2.5-285). These reports present the same material with the draft report providing the greatest level of detail.

The Swan, et al. (Reference 2.5-285) study consisted of numerous trenches, soil pits, hand auger samples, surveys of offset features, and over 30 radiocarbon dates (all of which were converted to calibrated ages and deemed not needing an AMRT correction). With respect to the Meers fault, the study focused on four sites (Figure 2.5.1-211): the valley site, the NW ponded alluvium site, the SE ponded alluvium site (the same location as the ponded alluvium site of Crone and Luza (Reference 2.5-284), and the Canyon Creek site (the same location as the Canyon Creek site of Crone and Luza (Reference 2.5-284) and Madole (Reference 2.5-283).

Valley Site

The valley site of Swan, et al. (Reference 2.5-285; Figure 2.5.1-211) is characterized by a 4.9-ft high scarp in Holocene valley fill deposits. At this site Swan, et al. (Reference 2.5-285) reported that the Browns Creek alluvium is faulted, the scarp-derived colluvium is faulted, and the stratigraphically highest alluvium is unfaulted. They interpreted these observations as documenting two surface-rupturing events: (1) an older event that faulted the Browns Creek alluvium, formed a scarp, and created the scarp-derived colluvium; and (2) a younger event that faulted the initial scarp-derived colluvium. Swan, et al. (Reference 2.5-285) presented calibrated radiocarbon dates that constrain event timing as follows (Table 2.5.1-201) (Figure 2.5.1-212):

- An age of 2918 years B.P. (sample PITT-0373) from the uppermost section of the Browns Creek alluvium is a maximum age for the oldest event;
- Two ages from the base and middle of the scarp-derived colluvium (1942 and 1610 years B.P. for samples PITT-0370 and PITT-0369) provide minimum ages for the oldest event and maximum ages for the youngest

event; and

CTS-01521

- Four ages from the post faulting colluvium and alluvium (1296, 1296, 777, and 777 years BP for samples PITT-0372, PITT-0375, PITT-0368, and AA-4093, respectively) constrain the minimum age of the youngest event.

Swan, et al. (Reference 2.5-285) measured a stratigraphic separation of 12 ± 2 ft (3.6 ± 0.6 m) associated with the fault. Lateral offset at the site was not as well constrained, but Swan, et al. (Reference 2.5-285) estimated an approximate left lateral offset of 30 ± 7 ft (9 ± 2 m).

NW Ponded Alluvium Site

The NW ponded alluvium site of Swan, et al. (Reference 2.5-285; Figure 2.5.1-211) is characterized by Holocene alluvial and colluvial sediments ponded behind the Meers scarp. At this site, Swan, et al. (Reference 2.5-285) excavated seven trenches and found Late Quaternary deposits from a paleo-channel overlying Post Oak Conglomerate.

From oldest to youngest Swan, et al. (Reference 2.5-285) reported the two stratigraphically highest units as: (1) faulted colluvium; and (2) unfaulted ponded alluvial deposits and colluvium. Swan, et al. (Reference 2.5-285) concluded that these units document two surface rupturing events: (1) an older event that led to the formation of the deeper colluvium, and (2) a younger event that faulted the deeper colluvium and led to the deposition of the ponded alluvium and unfaulted colluvium. Swan, et al. (Reference 2.5-285) also presented calibrated radiocarbon dates from these units to constrain the timing of faulting as follows (Table 2.5.1-201) (Figure 2.5.1-212):

- An age of 1912 years B.P. (sample PITT-0378) from the middle of the deeper, faulted colluvium interpreted as a minimum age for the oldest faulting event;

- An age of 1484 years B.P. (sample PITT-0379) from the top of the deeper, faulted colluvium interpreted as a maximum age for the youngest faulting event; and

- Two ages from the base of the unfaulted ponded alluvium (1238 and 1265 years B.P. for samples PITT-0380 and PITT-0381) interpreted as minimum ages for the youngest faulting event.

The buried channel exposed in the trenches also provided Swan, et al. (Reference 2.5-285) with a channel thalweg with which they estimated fault offset. Their best estimates of lateral and vertical offset were 10 ± 3.3 ft of left lateral offset and 7.9 ± 1 ft of vertical offset.

CTS-01521

~~SE Ponded Alluvium Site~~

~~The SE ponded alluvium site of Swan, et al. (Reference 2.5-285) is at the same location as the ponded alluvium site of Crone and Luza (Reference 2.5-284; Figure 2.5.1-211). At the site, the stratigraphy of the site is equivalent to that at the NW ponded alluvium site: Post Oak Conglomerate bedrock is overlain by Late Quaternary alluvial and colluvial deposits (Reference 2.5-285).~~

~~Swan, et al. (Reference 2.5-285) reported the three stratigraphically highest units, from oldest to youngest, as: (1) a faulted, silty and clayey alluvium likely deposited in a paleo-channel that was cut by the fault, (2) faulted ponded alluvium and colluvium, and (3) a stratigraphically distinct, unfaulted second set of ponded alluvium and colluvium deposits. Swan, et al. (Reference 2.5-285) interpreted these relations as documenting two surface rupturing events: (1) an older event that cut the paleo-channel deposits and led to the formation of the deeper, ponded alluvium and fault-derived colluvium, and (2) a younger event that faulted the deeper, ponded alluvium and colluvium and led to the deposition of the stratigraphically higher ponded alluvium and fault-derived colluvium. Swan, et al. (Reference 2.5-285) also presented calibrated radiocarbon dates to constrain the event ages (Table 2.5.1-201) (Figure 2.5.1-212):~~

- ~~Two ages of 6836 and 5943 calibrated years B.P. (samples PITT-0476 and PITT-0475, respectively) from the deep paleo-channel alluvium were interpreted as chronologically high maximum ages for the oldest event;~~
- ~~An age of 3397 calibrated years B.P. (sample PITT-0477) from the middle of the deeper, faulted colluvium was interpreted as a maximum age for the oldest event;~~
- ~~An age of 2093 calibrated years B.P. (sample PITT-0478) from the base of the deeper, faulted ponded alluvium was interpreted as a minimum age for the oldest event;~~
- ~~An age of 1669 calibrated years B.P. (sample PITT-0479) from the middle of the deeper, faulted ponded alluvium was interpreted as a maximum age for the youngest event;~~
- ~~Two ages of 1336 and 1167 calibrated years B.P. (samples PITT-0481 and PITT-0489, respectively) from the base of the unfaulted ponded alluvium were interpreted as minimum ages for the youngest event;~~
- ~~An age of 1053 calibrated years B.P. (sample PITT-0480) from the middle of the unfaulted, colluvium was interpreted as a minimum age for the youngest event; and~~
- ~~An age of 684 calibrated years B.P. (sample PITT-0482) from the middle of the unfaulted, ponded alluvium was interpreted as a minimum age for the youngest event.~~

CTS-01521

~~The trenches also exposed two channel thalwegs that Swan, et al. (Reference 2.5-285) used to estimate fault displacement. Their best estimates of lateral and vertical offset from the thalwegs are 11 ± 3.3 ft of left-lateral offset and 8.9 m ± 3.3 ft of vertical offset for the upper thalweg and 12 ± 3.3 ft of left-lateral offset and 8.9 ± 2 ft of vertical offset for the lower thalweg. Finally, Swan, et al. (Reference 2.5-285) also conducted several surveys of ridge crest offset at the site and found that additional Quaternary events besides the two Holocene events are required to generate the observed ridge crest offsets.~~

~~Canyon Creek Site~~

~~Swan, et al. (Reference 2.5-285) visited the same Canyon Creek site as Crone and Luza (Reference 2.5-284, Figure 2.5.1-211) to survey the vertical separation of the Holocene Browns Creek alluvium and Pleistocene Porter Hill alluvium. Swan, et al. (Reference 2.5-285) conducted two scarp-perpendicular surveys of terrace elevations, nine test pits, and three hand-auger boreholes. They reported that the vertical separation at the contact of Browns Creek alluvium and bedrock is 17 ± 5.3 ft and that the vertical separation at the contact of Porter Hill alluvium and underlying bedrock is 17 ± 3.9 ft. Swan, et al. (Reference 2.5-285) interpreted the similarity in offset between the two bedrock contacts as an indication that there has been no faulting between the deposition of the Porter Hill and Browns Creek alluvium. To temporally constrain this period of fault inactivity, Swan, et al. (Reference 2.5-285) correlated the soil development of the Porter Hill alluvium to a soil at a distant site that overlies a 560,000-year-old ash deposit. From this correlation Swan, et al. (Reference 2.5-285) estimated that the Porter Hill alluvium was deposited around 200,000 to 500,000 years ago and that this time period reflects the minimum period of inactivity between earthquake clusters. This time period is consistent with Madole's conclusion that the Porter Hill alluvium was deposited in the Middle Pleistocene (Reference 2.5-287).~~

2.5.1.1.4.3.6.1.2 ~~Meers Fault Expert Opinions~~

~~As part of the SSHAC level 2 process (Reference 2.5-292), a group of experts was queried to further assess and document the range of opinions within the informed technical community with respect to the seismic characterization of the Meers fault. The experts consulted were:~~

- ~~Keith Kelson, a Principal Geologist with William Lettis & Associates, Inc;~~
- ~~Kathryn Hanson, a Principal Geologist with Geomatrix Consultants;~~
- ~~Dr. Frank Swan, a Principal Geologist with Geomatrix Consultants;~~
- ~~Dr. Anthony Crone, Senior Research Geologist with the USGS;~~
- ~~Alan Ramelli, Research Engineering Geologist with the Nevada Bureau of Mines and Geology; and~~

- ~~Dr. Ken Luza, Engineering Geologist, Oklahoma Geological Survey.~~ CTS-01521

~~Each of the experts were asked the following questions:~~

- ~~Is the Meers fault active?~~
- ~~Can the Meers fault be adequately represented as a line source?~~
- ~~What is your estimate of Mmax for the Meers fault?~~
- ~~What approach would you use to estimate Mmax?~~
- ~~What recurrence model would you use to parameterize the Meers fault?~~
- ~~If clustered, is the fault currently in a cluster?~~
- ~~What data would you use to determine the recurrence rate?~~

~~A summary of the responses from each expert is presented in Table 2.5.1-203. In general, the opinions of the experts are consistent with the published work summarized in Subsection 2.5.1.1.4.3.6.1.1.1.~~

~~In summary, the results of the SSHAC level 2 study were incorporated into a new seismic source characterization for the Meers fault. The seismic source characterization of the Meers fault used for CPNPP Units 3 and 4 is presented in Subsection 2.5.2.4.2.3..~~

2.5.1.1.4.3.6.2 Criner Fault

The Criner fault is exposed in southern Oklahoma and coincident with the northern edge of the Wichita Uplift. The Criner fault strikes N45°W and produces a southwest-facing escarpment, similar to the expression of the Meers fault about 120 km along strike to the northwest. The escarpment is 12 km long and 0.5 to 2 m high. Given the evidence for Quaternary activity along the Meers fault (References 2.5-283, 2.5-284, 2.5-286, and 2.5-293) workers have speculated that the Criner may also have been active in the Quaternary.

~~In 1986, none of the EPRI ESTs recognized the Criner fault as a structure with Quaternary earthquake hazard potential (Reference 2.5-369). Preliminary s~~Studies by Geomatrix Consultants, however, had indicated that the Criner fault displaces Middle to Late Pleistocene fluvial deposits adjacent to Hickory Creek in Love County (Reference 2.5-277). Following the submission to the NRC of the CPNPP Units 1 and 2 FSAR and communication with Geomatrix Consultants, a field party, including workers from EPRI, the NRC, Geomatrix Consultants, and the Oklahoma State Geological Survey, conducted a geological reconnaissance of the Criner fault in 1989 (NUREG-0797, CPNPP SSER 23, 1990). This study concluded that the escarpment was either (1) a fault-line scarp resulting from differential erosion of units juxtaposed along the fault in the Late Paleozoic or (2) a CTS-01521

fault-line scarp with a 10- to 20-cm free face resulting from Late Quaternary displacement. The team was denied access to the key exposure along Hickory Creek and determined that there was insufficient evidence available to prove or disprove the capability of the Criner fault. Therefore, the team conservatively concluded that if the Criner fault was capable, it would have a length and surface displacement less than that of the Meers fault (NUREG-0797, CPNPP SSER 23, 1990).

Since these studies, new work has indicated that the Criner fault is less of a hazard than conservatively estimated in the late 1980s. In 1996, Williamson (Reference 2.5-294) conducted a thorough hand-excavation of the exposures along Hickory Creek. The resulting thesis concluded that only Pennsylvanian units were faulted along Hickory Creek in the same location cited by Geomatrix Consultants, and this faulting was overlapped by Quaternary alluvial units composed of sand, clay, and gravel (Reference 2.5-294). Furthermore, Williamson (Reference 2.5-294) pointed out that the scarp is restricted to the area where the resistant Ordovician limestone is adjacent to the fault and interpreted the scarp as a fault-line scarp. In addition, follow-up studies conducted by Geomatrix Consultants have suggested that displacement along the scarp may be related to Late Pleistocene landslides (Reference 2.5-295). Geomatrix Consultants reported that small alluvial fans overlap the fault and that the fault could not be seen cutting units younger than Paleozoic (Reference 2.5-285).

Based on a review of post-EPRI scientific and industry literature, it is concluded that there is no conclusive evidence of the fault yielding Quaternary tectonic slip (e.g., CPNPP SER Suppl. 23; References 2.5-236 and 2.5-272). Because of the proximity of this structure to the CPNPP Units 3 and 4 site, William Lettis & Associates, Inc., conducted a field reconnaissance study along the escarpment in Love and Carter counties, Oklahoma. This study also found no evidence to support Quaternary tectonic activity on the Criner fault. In conclusion, the newest information bearing on the Quaternary activity of the Criner fault indicates that fault is not capable and should not be included ~~in the EPRI seismic source characterization~~as a refinement to the CEUS SSC of this region. CTS-01521

2.5.1.1.4.3.7 Quaternary Tectonic Features Beyond the Site Region

In addition to the Quaternary tectonic features within the site region discussed above, all tectonic structures incorporated in the CEUS SSC were included in evaluating the hazard of the CPNPP Units 3 and 4 site. Two of the repeated large magnitude earthquakes (RLMEs) in the CEUS SSC: the Cheraw fault and the New Madrid Fault System (NMFS), are discussed below.~~three structures play significant roles in the hazard of the CPNPP Units 3 and 4 site, but are outside of the 200 mi radius (Figure 2.5.1-213). These features, the Rio Grande Rift, the Cheraw fault, and New Madrid fault zone, are discussed below.~~ CTS-01521

2.5.1.1.4.3.7.1 ~~Rio Grande Rift~~

~~The Rio Grande Rift (RGR) is a north-south-trending continental rift system that is recognized to extend from central Colorado through New Mexico, Texas, and into northern Mexico (Reference 2.5-296, 2.5-297, 2.5-298, 2.5-299, 2.5-300, and 2.5-301; Figure 2.5.1-213). At the time of the CPNPP Units 1 and 2 FSAR, relatively little was known about the seismogenic potential of faults within the RGR. However, more recent research has documented previously unrecognized Late Quaternary fault activity within the RGR (References 2.5-302, 2.5-303, 2.5-304, 2.5-305, 2.5-306, 2.5-307, 2.5-308, and 2.5-309). These studies indicate that the RGR is a zone of distinct and elevated tectonic activity relative to other regions at a similar distance from CPNPP Units 3 and 4. On the basis of these observations, the tectonic features of the RGR are relevant to CPNPP Units 3 and 4, despite the greater than 400 mi distance between the RGR and the site, because the faults of the RGR are some of the closest capable tectonic features.~~ CTS-01521

~~The RGR is commonly thought to have developed in two main stages. The first stage, from approximately 30 to 20 Ma, involved low-angle normal faulting and basaltic volcanism. The second stage, from approximately 10 to 3 Ma, involved high-angle normal faulting that cut across and overprinted the earlier faulting and more expansive basaltic volcanism (Reference 2.5-310). The precise cause of the rifting during these two phases of activity is debated, but it is generally thought that a combination of elevated lithospheric temperatures and east-west tensional stress caused by plate interactions in western North America led to the thinning of the lithosphere and thus the associated faulting and volcanism (Reference 2.5-310, 2.5-311, and 2.5-312). Despite the cessation of large-scale RGR formation, numerous faults within the RGR have been active within the Quaternary (References 2.5-302, 2.5-303, 2.5-304, 2.5-305, 2.5-306, 2.5-307, and 2.5-309).~~

~~Presently, the RGR is characterized by north-trending grabens centered on a broad topographic high, elevated heat flow, and a tensile stress regime (References 2.5-296, 2.5-300, 2.5-310, and 2.5-313). The east-west extent of the RGR surficial expression (e.g., faults and elevated topography) occupies a narrower region than the lithospheric structure of the RGR (region of tensile stress, thinned crust, elevated mantle, gravity anomaly) (References 2.5-241, 2.5-245, 2.5-300, 2.5-314, and 2.5-315). This observation suggests that the processes driving the Quaternary seismic activity observed within the RGR also extend beyond the region of the surficial expression of the rift (Reference 2.5-316).~~

~~An example of this phenomenon is the April 14, 1995, Alpine earthquake in West Texas discussed in Subsection 2.5.2.1.3.1 that occurred significantly eastward of the nearest RGR fault. The focal mechanism for this event shows that the earthquake was a normal faulting event with the minimum compressive stress (tensile stress) oriented north-northeast and the maximum horizontal stress oriented east-west (Reference 2.5-317). This event and others with similar focal mechanisms have been interpreted as reflecting the interaction of the topographically high RGR with relatively stable and low-lying Great Plains further east (References 2.5-318 and 2.5-319). Essentially, the RGR region is characterized by large gradients in gravitational potential energy caused by a~~

~~combination of excess topography and variations in lithospheric density. These potential energy gradients create a tensile stresses regime at the eastern edge of the RGR, with the maximum horizontal compressive stress generally oriented east–west. These tensile stresses partially drive deformation within and well eastward of the physiographic RGR (References 2.5-245 and 2.5-220) as evident with the 1995 Alpine earthquake.~~ CTS-01521

~~Quaternary faulting within the RGR has been reported in numerous studies that are well summarized and documented in the USGS Quaternary Fault and Fold Database of the United States (Reference 2.5-308). Summaries of these faults are not presented here due to the large number of faults. However, some of these faults have been studied in enough detail to generate complete seismic source characterizations, and these faults are included in the 2002 USGS National Seismic Hazard Maps (Reference 2.5-321). The seismic source characterizations of these faults are discussed in detail in Subsection 2.5.2.4.2.3.3.~~

2.5.1.1.4.3.7.2 Cheraw Fault

The Cheraw fault is located in southeastern Colorado over 500 mi from the site (Figure 2.5.1-213). The potential for Quaternary events on the fault was first noted by Scott (Reference 2.5-322) and three Late Quaternary events were dated by Crone, et al. (Reference 2.5-323). The fault is included in this discussion because, despite its great distance from the site, it is one of the closest capable faults to the site. The Cheraw fault is structurally positioned above and between the Las Animas Arch, an approximately 200-mi-long arch in Precambrian crystalline rocks, and the Denver Basin, a complementary basement low to the northwest of the arch (References 2.5-324 and 2.5-325). Offset across the fault is concordant with the offset in the basement surface between the arch and basin, down to the northwest, but the fault is not observed to offset the basement surface (Reference 2.5-324). Fault offsets across buried bedrock horizons are on the order of tens to hundreds of ft, and fault offsets of Quaternary deposits are only 20~~3~~ to 26 ft (References 2.5-323 and 2.5-326). These observations suggest that the fault has not had a long history of movement (millions of years). CTS-01521

The surface trace of the fault has been mapped for approximately 28~~7~~ mi, but in many places the fault is mapped as approximately located, inferred, or concealed. Where observed, the fault displaces Early Pleistocene piedmont surfaces, and in trenches the fault is observed to displace Late Pleistocene deposits (References 2.5-325 and 2.5-326). A trenching study by Crone, et al. (Reference 2.5-323) found evidence for three surface-rupturing events at approximately 8, 12, and 20 to 25 ka. Prior to these three events, Crone, et al. (Reference 2.5-323) hypothesize that the fault was inactive since approximately 100 ka based on the presence of a filled paleo-stream channel. These observations suggest that the fault may have a clustered earthquake behavior (Reference 2.5-326). Based on these studies, the Cheraw fault is characterized as an RLME fault within the CEUS SSC (Reference 2.5-486). CTS-01521 CTS-01521

2.5.1.1.4.3.7.3 New Madrid Fault System~~Seismic Zone~~

The ~~New Madrid Seismic Zone (~~NMFS~~Z)~~ extends from southeastern Missouri to southwestern Tennessee and is located approximately 500 mi northeast of the site (Figure 2.5.1-213). ~~The NMSZ~~It lies within the Reelfoot rift and is defined by post-Eocene to Quaternary faulting with previous older seismic activity. Given its significant distance from the site, the NMFS~~NMSZ~~ did not contribute to the seismic hazard calculated ~~by the Electric Power Research Institute Seismicity Owners Group (EPRI SOG)~~ for CPNPP Units 1 and 2 (Reference 2.5-327). However, the NMFS~~NMSZ~~ needs to be reconsidered for CPNPP Units 3 and 4 because several more recent studies provide significant new information regarding characterization of the seismic capability of the NMFS~~NMSZ~~. CTS-01521 CTS-01521 CTS-01521 CTS-01521

The NMFS~~NMSZ~~ is approximately 125 mi long and 25 mi wide. ~~Research conducted since the EPRI SOG study has~~Researchers have identified three distinct fault segments embedded within the seismic zone, consisting of a southern northeast-trending dextral slip fault, a middle northwest-trending reverse fault, and a northern northeast-trending dextral strike-slip fault (Reference 2.5-271). In the current east-northeast to west-southwest directed regional stress field, Precambrian and Late Cretaceous age extensional structures of the Reelfoot rift appear to have been reactivated as right-lateral strike-slip and reverse faults.

The NMFS~~NMSZ~~ produced a series of historical, large-magnitude earthquakes between December 1811 and February 1812 (Reference 2.5-328). The December 16, 1811, earthquake is associated with strike-slip fault displacement along the southern part of the NMFS~~NMSZ~~. Johnston (Reference 2.5-329) estimates a magnitude of Mw 8.1 $\pm$ 0.31 for the 16 December 1811 event. However, Hough, et al. (Reference 2.5-328) re-evaluated the isoseismal data for the region and conclude that the December 16 event had a magnitude of Mw 7.2 to 7.3. Bakun and Hopper (Reference 2.5-330) similarly concluded this event had a magnitude of Mw 7.2. CTS-01521 CTS-01521

The February 7, 1812, New Madrid earthquake is associated with reverse fault displacement along the middle part of the NMFS~~NMSZ~~ (Reference 2.5-331). This earthquake most likely occurred along the northwest-striking Reelfoot fault that extends approximately 43 mi from northwestern Tennessee to southeastern Missouri. The Reelfoot fault is a northeast-dipping, southwest-vergent reverse fault. The Reelfoot fault does not extend updip to the earth's surface, but a topographic scarp has developed above the buried tip of the fault as a result of fault-propagation folding (References 2.5-332, 2.5-333, and 2.5-334). Johnston (Reference 2.5-329) estimated a magnitude of Mw 8.0 ± 0.33 for the 7 February 1812 event. However, Hough, et al. (Reference 2.5-328) re-evaluated the isoseismal data for the region and concluded that the February 7 event had a magnitude of Mw 7.4 to 7.5. More recently, Bakun and Hopper (Reference 2.5-330) estimated a similar magnitude of Mw 7.4. CTS-01521

The January 23, 1812, earthquake is associated with strike-slip fault displacement on the ~~East Prairie fault~~northern seismicity arm of the NMFS (New Madrid North Segment) along the northern part of the NMFS~~NMSZ~~. Johnston (Reference 2.5- CTS-01521

329) estimates a magnitude of Mw 7.8 ± 0.33 for the January 23, 1812, event. Hough, et al. (Reference 2.5-328), however, re-evaluated the isoseismal data for the region and concluded that the January 23, 1812, event had a magnitude of Mw 7.1. More recently, Bakun and Hopper (Reference 2.5-330) estimated a similar magnitude of Mw 7.1. ~~The upper bound Mmax values used in the EPRI SOG study (References 2.5-369 and 2.5-335) for the NMSZ range from m_b 7.2 to 7.9, generally consistent with the revised magnitudes for the three events reviewed here.~~ CTS-01521

Because there is very little surface expression of faults within the NMFS~~NMSZ~~, earthquake recurrence estimates are based largely on dates of paleoliquefaction and offset geological features. The most recent summaries of paleoseismologic data (References 2.5-336, 2.5-337, and 2.5-338) suggest a mean recurrence time of 500 years, which was used in the 2002 USGS model (Reference 2.5-321). This recurrence interval is half of the 1,000-year recurrence interval used in the 1996 USGS hazard model (Reference 2.5-339)~~, and an order of magnitude less than the seismicity based recurrence estimates used in the EPRI SOG study (Reference 2.5-369 and 2.5-240)~~. CTS-01521

The seismic source characterization for the NMFS is based on CEUS SSC (Reference 2.5-486). ~~The NMSZ studies described above that post-date the EPRI SOG study require an updated NMSZ source model for CPNPP Units 3 and 4 because the studies provided revised estimates of the source geometry, maximum magnitudes, and recurrence intervals compared to those of the EPRI SOG study (References 2.5-221 and 2.5-239). The updated source model used for CPNPP Units 3 and 4 is described in Subsection 2.5.2.4.3.~~

2.5.1.2 Site Geology

This subsection discusses details about the site area and site, geologic history, physiography, stratigraphy, lithologies, and geologic structure.

2.5.1.2.1 Site Physiography and Topography

This subsection discusses the physiography, geologic history, stratigraphy, and tectonic setting within a 5- and 0.6-mi radius of the site.

Topographic maps of the site area (5-mi radius) and site (0.6-mi radius) are shown in Figures 2.5.1-214 and 2.5.1-215, respectively. The site area is almost completely contained within the Grand Prairie physiographic province, which is underlain by flat-lying Lower Cretaceous limestones and shales with intervening sandstone units that mark transgressive events. The limestone–shale sequences are variably resistant to erosion with the harder, more resistant limestone units forming steeper slopes than the less resistant shale units. This results in the stair-step topographic expression characteristic of this region.

The major drainage is the Brazos River, which is expressed as several incised meander loops in eastern portions of the site area (Cox Bend) and beyond.

geotechnical exploration program discussed in Subsection 2.5.4. The following engineering geology aspects were identified as pertinent to the site.

2.5.1.2.5.1 Dynamic Behavior During Past Earthquakes

The CPNPP site is located in a tectonically stable region as indicated by the compilation of earthquake activity for the region, as discussed in Subsection 2.5.2.1, and a thorough study of the regional geologic history, presented in Subsection 2.5.1.1.2. Subsection 2.5.2.1.1 discusses historic earthquake activity in the region surrounding the CPNPP site. Subsection 2.5.2.3 documents that no evidence for correlating earthquake activity of E_{mb} > 3.0 to any known seismic sources exists within 90 mi of the site. Although the region is not well instrumented to measure small-magnitude earthquakes, a screening of the region within the 200-mi area surrounding the site shows, a total of 31 events occurred between January 1, 2009 and December 31, 2011. Moment magnitudes (Mw) ranged from 2.9 to 4.3. See Section 2.5.2.1 for further discussion~~no seismic activity, as discussed in Subsection 2.5.2.1~~. CTS-01521

Field reconnaissance of the region and immediate site area indicates no evidence of seismic activity, either recent or historic. Field reconnaissance, other than that conducted on the site location, consisted of visiting publicly accessible locations in the site area and immediately surrounding vicinity (Figure 2.5.1-231 and 2.5.1-232). Generally, all publicly accessible locations in and around the site area were visited in order to verify the accuracy of the site area map, to search for signs of deformation (faulting or folding) in bedrock and surficial outcrops, and to search for paleoliquefaction features. Minor flexures, limited in both vertical and lateral extent (less than 3 ft and 40 ft, respectively) have been noted in surrounding exposures of the Glen Rose Formation. However the limited extent and lack of evidence of offset or brittle deformation indicate that these flexures may be related to non-tectonic factors such as differential consolidation, or dissolution of underlying sediments. This interpretation is strengthened by the observation that underlying beds do not mimic the structure in the case of the fold in the Glen Rose Formation. A review of the core that was obtained from the borings drilled as part of the site geotechnical investigation (discussed in Subsection 2.5.4) shows no evidence for brittle or ductile deformation that can be related to seismic activity.

2.5.1.2.5.2 Zones of Weathering, Alteration or Structural Weakness

The area for CPNPP Units 3 and 4 is cut to a yard grade of elevation 822 ft msl and all weathered materials are to be removed, as discussed in Subsection 2.5.4.5.1. All Category 1 structures are founded directly on a thick (average 65 ft), laterally extensive, limestone unit within the Glen Rose Formation, at an elevation of approximately 779 ft msl to 782 ft msl~~at about elevation 782 ft msl~~. Subsection 2.5.4 discusses these conditions, including the static and dynamic properties of this and other subsurface layers. Site reconnaissance of exposures surrounding the site, a review of aerial photography, and examination of borings drilled as part of the geotechnical investigation showed no zones of enhanced weathering or structural weakness such as fractures or joints. Also, petrographic analysis of CTS-01521

2.5.1.2.5.6 Reservoir Effects

No adverse effects due to the construction of man-made reservoirs in the CPNPP area, including SCR, Lake Granbury, and Lake Whitney, have been noted (Figure 2.5.1-218). The SCR is located immediately to the north of the CPNPP Units 3 and 4 site. Groundwater conditions are discussed in Subsection 2.4.12.

No reservoir-induced earthquakes have been noted since the construction of SCR and other large reservoirs in the site area. This absence may be attributed to the low hydraulic conductivity of the subsurface materials as well as to lack of faults or planes of weakness that may respond to increased pore fluid pressure from the downward migration of water from the reservoirs.

The pool elevation of SCR is 775 ft msl. The excavation for CPNPP Units 3 and 4 extends to approximately elevation 7798~~82~~ ft msl to facilitate removal of a shale layer, so that the Category 1 structures are directly founded on a limestone layer or fill concrete, at an elevation between 779 ft msl and 782 ft msl~~at elevation 782 ft msl~~, as discussed in Subsection 2.5.4. There are two areas of undocumented artificial fill near the CPNPP Units 3 and 4 area, as shown on (Figure 2.5.1-218). Groundwater within these fill areas is in communication and hydrostatic equilibrium with SCR, as indicated from monitoring wells. No Category 1 or critical structures are located over these areas. CTS-01521 CTS-01521

2.5.1.2.5.7 Slope Stability

Slope stability is not considered a hazard to the site. The nearest slopes exist immediately north of the CPNPP Units 3 and 4 area along the SCR. These slopes will be re-graded as part of the general site grading plan. A detailed discussion of the slope stability analysis is presented in Subsection 2.5.5.

2.5.1.2.5.8 Unrelieved Residual Stresses in Bedrock

The regional tectonic setting, discussed in Subsection 2.5.1.1.4, indicates that no active tectonics exist in the region surrounding the CPNPP site. No active faults are noted within 25 mi of the CPNPP site, and the overlying Cretaceous section truncates several nonactive Paleozoic faults, which indicates that no reactivation has occurred in the past 65 million years. Subsection 2.5.1.2.5.10 discusses issues related to potential reactivation of faults due to man-induced activities.

2.5.1.2.5.9 Geologically Hazardous Materials

No geologically hazardous materials, such as expansive soils or reactive minerals (e.g., gypsum or anhydrite) of appreciable amounts, exist within 25 mi of the site and, thus, are not considered a hazard.

the discussion. ~~In the following discussion, fluid injection and extraction activities may apply to various techniques and activities and are specified as required for the discussion.~~ CTS-01521

2.5.1.2.5.10.1.1 Potential Hazards Related to Hydraulic Fracturing

The potential hazards related to hydraulic fracturing for gas production include changes to the rock properties and induced seismicity. These issues are discussed below and are determined not to present a hazard to the CPNPP site.

2.5.1.2.5.10.1.2 Changes to Rock Properties Related to Hydraulic Fracturing

Because of the low porosity of the Barnett Shale, enhanced production techniques are required to achieve enough gas production to make the process economically feasible. Thus, hydraulic fracturing is commonly employed. Hydraulic fracturing involves injecting fluid into the gas-bearing strata to induce fractures that allow the gas to flow more easily to the production well. These induced fractures are on the order of 0.1 to 0.25 in thick and are filled with sand or other high-permeability materials (called proppant) so that they remain open and can conduct the gas to the well.

A hydraulic fracture is idealized as a single vertical plane of hundreds to a few thousand ft in total length, hundreds of ft in height, and a fraction of an inch in width. The actual size of a hydraulic fracture will largely depend on the amount of fluid and sand injected, the permeability of the formation, and the variation of the minimum horizontal stress over depth (which determines whether or not the fracture is contained in height growth). Hydraulic-fracture diagnostic data from microseismic monitoring in the Barnett Shale suggests that hydraulic fracture growth is more complex than this simple idealization, with multiple strands forming as the propagating hydraulic fracture interacts with pre-existing natural fractures (Reference 2.5-348). Although there is no direct observation of subsurface hydraulic fracture geometry for the Barnett Shale, it is presumed that the created fractures approximate an orthogonal grid-like pattern (References 2.5-349 and 2.5-350), with minimum spacing on the order of 50 ft between fracture zones (which may be narrow vertical corridors of closely spaced fractures).

Rock fractures generally reduce the wave propagation velocities of rock (Reference 2.5-351). Leucci and De Giorgi (Reference 2.5-352) showed that for a fracture spacing of about 0.5 m and high-frequency waves (> 1 kHz), the shear wave velocity was reduced by about 30 percent for a sedimentary rock specimen under atmospheric pressure. Fratta and Santamarina (Reference 2.5-353) provide a relationship (Backus' average) that predicts the wave velocity of fractured rock (with the fractures filled with a material distinct from the intact rock) based on the characteristics of the rock and fracture infill material ratio. The velocity of the fractured rock is a function of the fracture ratio (equal to the fracture thickness / spacing between fractures), the velocity of the intact rock, the velocity of the fracture infill material, and the density of the intact rock and fracture infill material.

was reported as V (Reference 2.5-359). It is important to note that the injection rates at Cogdell are an order of magnitude greater than the rates injected at Rocky Mountain Arsenal, yet the induced rate of seismicity and the size of events were considerably smaller.

Water injection may be used for secondary oil recovery (waterflooding) or waste disposal. Because of its large extent, the Ellenburger Limestone, which is stratigraphically below the Barnett Shale, is a prime target for injection in the Fort Worth Basin. Such injection may increase fluid pressure in the subsurface, reducing the effective stress on faults and promoting slip. As mentioned above, there are documented examples of injection-induced seismicity. However, Davis and Pennington (Reference 2.5-269) find that even though modeling suggests that reported injection pressures in oil and gas fields under water injection in Texas should cause fault slip, only one field (Cogdell) was known to have seismic activity. Their conclusion to explain the apparent discrepancy between predicted fault failure and known seismicity was that much of the failure actually may be aseismic. In addition to changing the stress state, the injected fluid is suspected to weaken the faults to such an extent that they creep to relieve shear stress.

The mechanism for induced seismicity due to fluid extraction is not immediately known because the removal of fluid decreases pore pressures and increases effective stresses, a change that is generally expected to stabilize faults because it restrains slip (Reference 2.5-361). However, it is expected that poro-elastic changes in the in situ stress state are the causal mechanism for induced seismicity due to fluid extraction (References 2.5-361 and 2.5-364). The most notable location of seismicity induced by gas or oil extraction is the Lacq gas field in France, which experienced 44 earthquakes with $M_l > 3$ and 4 events with $M_l > 4$ over a twenty year period (References 2.5-365 and 2.5-366).

Some earthquakes in south-central Texas have been related to local gas and/or oil extraction. The largest of these earthquakes was the April 9, 1993, m_bLg 4.3 event that occurred 50 mi south of San Antonio, with reported MMIs as high as VI (Reference 2.5-367). The most significant damage occurred at the Warren Petroleum Plant, and included cracking of reinforced concrete foundation blocks, failure of one pipe connection, damage to steel bolts, and horizontal movement on the order of an inch. Frohlich and Davis (Reference 2.5-359) estimate that of the 130 earthquakes that have occurred over the last 150 years in Texas and have been felt by residents, only 22 were induced by gas or oil production. Additionally, it is important to note that there has been significant gas and oil production within the state of Texas over the last century, including within the Fort Worth Basin, yet the seismicity rate remains relatively low. In particular, the Texas seismicity catalog generated by ~~William Lettis & Associates, Inc.,~~Fugro Consultants, Inc. for the time period 1627 to 2011~~06~~ shows no earthquakes ~~greater than m_b 3 within the Fort Worth Basin~~with Mw greater than 5.0 within the Fort Worth Basin. All events had an Mw of less than 3.2. Subsection 2.5.2 contains a discussion on seismic activity in the region and the development of an earthquake catalog update.~~)~~ CTS-01521 CTS-01521

2.5.1.2.5.10.3 Probabilistic Seismic Hazard Analysis ~~(PSHA)~~ Considerations for Induced Seismicity

CTS-01521

Current procedures used to perform PSHA for nuclear facilities incorporate background seismicity zones (Reference 2.5-335). The earthquake recurrence models for these background seismicity zones are derived from the observed earthquakes with ~~body wave magnitudes (m_b) greater than 3.0~~Mw greater than 2.9. However, the minimum Mw~~m_b~~ magnitude that is considered to be of engineering significance is 5.0, and smaller magnitudes are not considered in the PSHA analysis to derive design ground motions.

CTS-01521

It is very uncommon for induced earthquakes to exceed Mw~~m_b~~ 5.0. However, some of the earthquakes induced by injection at the Rocky Mountain Arsenal were larger than 5.0, so it is important to consider what characteristics might be favorable to generating earthquakes larger than 5.0. In the case of the Rocky Mountain Arsenal, injection took place in naturally fractured, otherwise non-porous, Precambrian crystalline rock (Reference 2.5-368). In such a situation, where there is little to no pressure diffusion into the pore space, injected fluid would be confined strictly to flow within the natural fractures, and thus could reduce effective stresses over very large fractures areas. Larger magnitude earthquakes require large slip areas, so injection into naturally fractured crystalline rock might reasonably be expected to result in larger induced earthquake magnitudes. Although the Barnett Shale and the Ellenburger Limestone of the Fort Worth Basin are competent sedimentary rocks, the crystalline rocks of Colorado are much stronger and allow for greater build-up of stress that can cause larger earthquakes. Finally, Gibbs, et al. (Reference 2.5-363) suggest that the Rocky Mountain Arsenal injection was releasing built-up tectonic stress locked in the rock. Because the Denver area is one of more recent tectonic activity (the Laramide orogeny, ended about 25 million years ago, and ongoing post-Laramide Uplift) than the Fort Worth Basin (last major tectonic event was the Ouachita orogeny, which ended about 300 million years ago), the shear stress magnitudes and active tectonic strain rates are expected to be larger in Colorado than in North Texas, and consequently this may limit potential earthquake magnitude.

CTS-01521

On the basis of information collected, it appears that any earthquake induced by gas production or fluid injection in the Fort Worth Basin would not be larger than Mw~~m_b~~ 5.0. Therefore, the enhanced seismicity that potentially would be induced would not need to be taken into account in the PSHA.

CTS-01521

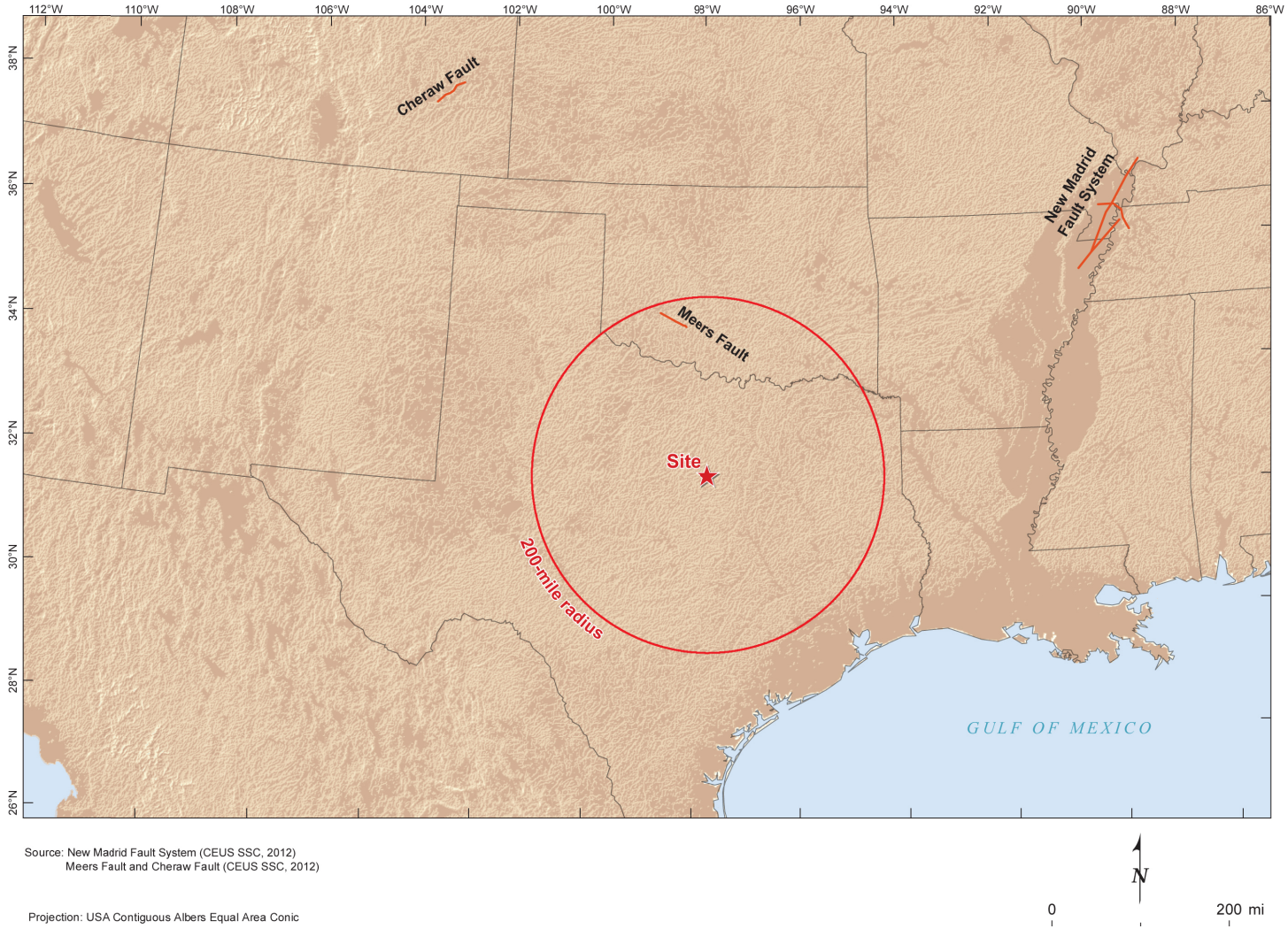

Figure 2.5.1-213 Significant Quaternary Features Outside of the Site Region

CTS-01521

Figure 2.5.1-215 0.6 Mile Topographic Map

CTS-01521

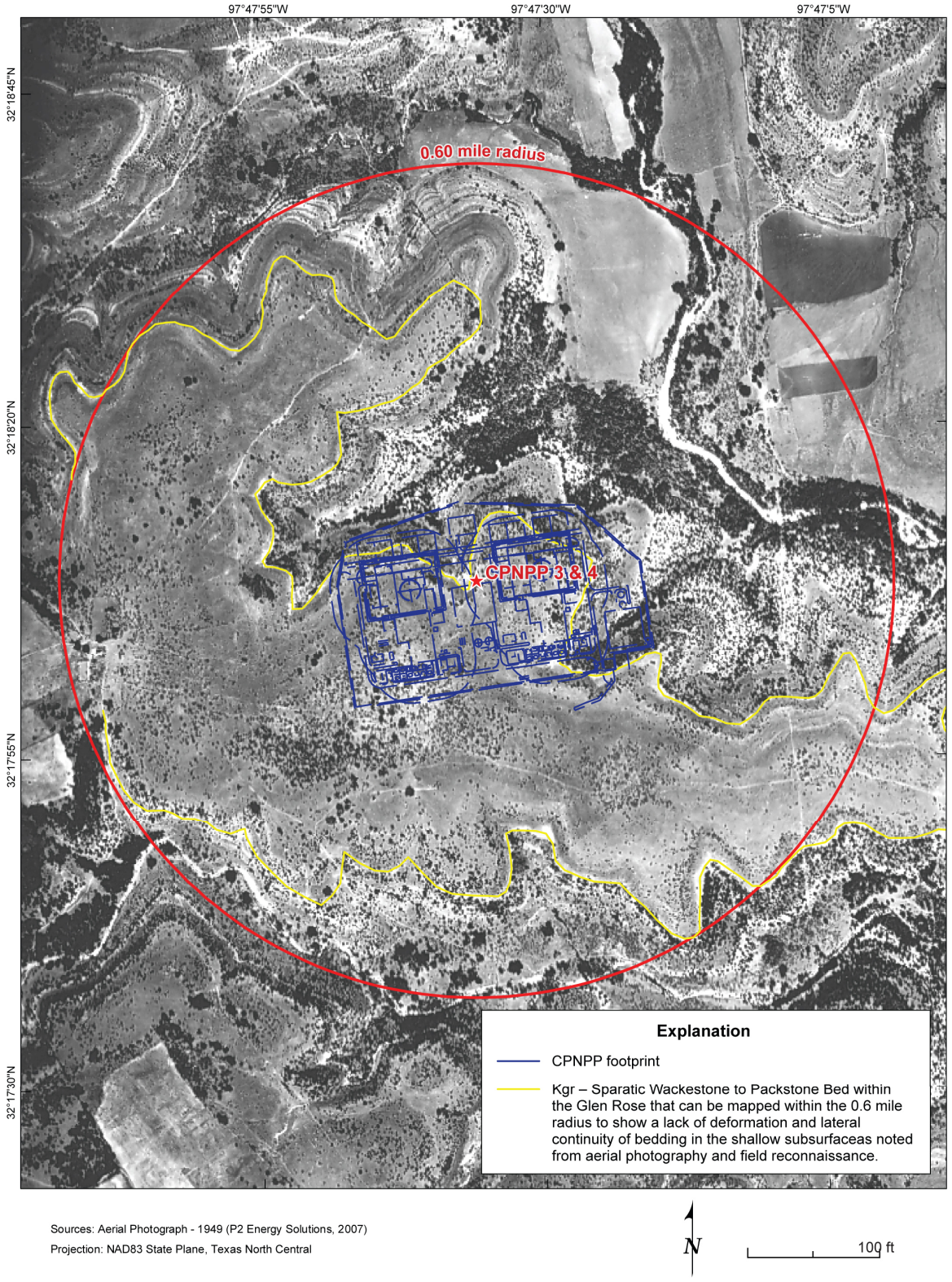

Figure 2.5.1-230 1949 Historical Photograph

2.5.2 Vibratory Ground Motion

CP SUP2.5(2) Add the following after the content of DCD Section 2.5.2.

This subsection provides a detailed description of vibratory ground motion assessments, specifically the criteria and methodology for establishing the Ground Motion Response Spectra (GMRS) and Foundation Input Response Spectra (FIRS) for the Comanche Peak Nuclear Power Plant Units 3 and 4 (CPNPP Units 3 and 4). It includes the information needed to address DCD COL Item 2.5(1), which is incorporated by reference with the following variances and supplements. The development of the GMRS for CPNPP Units 3 and 4 follows a methodology consistent with the approach recommended in Regulatory Guide (RG) 1.208 and, therefore, satisfies the requirements set forth in Section 100.23, "Geologic and Seismic Siting Criteria," of Title 10, Part 100, of the Code of Federal Regulations (10 CFR 100), "Reactor Site Criteria." This subsection begins with a review of the approach outlined in RG 1.208 and is followed by these subsections: CTS-01521

- Seismicity (Subsection 2.5.2.1)
- Geologic and Tectonic Characteristics of the Site and Region (Subsection 2.5.2.2)
- Correlation of Earthquake Activity with Seismic Sources (Subsection 2.5.2.3)
- PSHA and Controlling Earthquake (Subsection 2.5.2.4)
- Seismic Wave Transmission Characteristics of the Site (Subsection 2.5.2.5)
- Ground Motion and Site Response Analysis (Subsection 2.5.2.6).

RG 1.208 provides guidance on methods acceptable by the Nuclear Regulatory Commission (Reference 2.5-369) for satisfying the requirements of developing the site-specific GMRS, which in turn represents the first step in developing the Safe Shutdown Earthquake (SSE) ground motion levels as a characterization of the seismic hazard at CPNPP Units 3 and 4. The process outlined in RG 1.208 for determining the GMRS includes:

- The geological, geophysical, seismological, and geotechnical investigations of the site and site region, including the identification of seismic sources significant to seismic hazard at the site.
- The procedures for performing a Probabilistic Seismic Hazard Analysis (PSHA) and deaggregating mean hazard.
- Characterization of the seismic wave transmission characteristics of the site.

- Development of the performance-based site-specific earthquake ground motion.

RG 1.208 states that an acceptable starting point for developing probabilistic seismic hazards calculations for a Combined Operating License (COL) is a PSHA model that has been reviewed and accepted by the NRC. ~~This COL application uses the accepted PSHA model developed by the Electric Power Research Institute Seismicity Owners Group (EPRI SOG) in the 1980s (Reference 2.5-369) as the starting point for determining the GMRS for CPNPP Units 3 and 4. The EPRI SOG PSHA model (Reference 2.5-369) was developed as part of a comprehensive study of seismic hazard at nuclear power plants in the Central and Eastern United States (CEUS). The study involved a comprehensive compilation of geological, geophysical, and seismological data for the CEUS that was used by six independent and multi-disciplinary Earth Science Teams (ESTs) of experts in geology, seismology, and geophysics to develop seismic source characterizations for the CEUS that explicitly incorporated uncertainty in source geometry, earthquake recurrence, and earthquake magnitude. The seismic sources developed in the EPRI SOG model were then used in a PSHA of the ground motions at nuclear power plants in the United States (U.S.) (Reference 2.5-370). This COL application uses the seismicity, seismic source models, ground motion equations, and PSHA methodology of the EPRI SOG study (References 2.5-369 and 2.5-370) as a starting point for the PSHA at CPNPP Units 3 and 4. A more detailed discussion of the suitability of the EPRI SOG seismic sources is presented in Subsection 2.5.2.2.1.~~This COL application uses the new seismic source characterization (SSC) model for Central and Eastern United States (CEUS) (Reference 2.5-486) as the starting point for determining the GMRS for CPNPP Units 3 and 4. The CEUS SSC model replaces the PSHA model developed by the Electric Power Research Institute Seismicity Owners Group (EPRI-SOG) (Reference 2.5-369) and was developed using a Senior Seismic Hazard Analysis Committee (SSHAC) Level 3 assessment process based on NUREG/CR-6372 (Reference 2.5-292). The CEUS SSC model is based on historical seismicity extending through the end of the 2008 calendar year, provides a full assessment and rigorous treatment of uncertainties, and embraces a suite of various technical interpretations.This COL application uses the seismic source characterization and ground motion characterization of the CEUS SSC model (Reference 2.5-486) as a starting point for the PSHA at CPNPP Units 3 and 4. A more detailed discussion of the suitability of the CEUS SSC seismic sources is presented in Subsection 2.5.2.2.1. CTS-01521

Following the guidance of RG 1.208, a comprehensive review of new geological, geophysical, and seismological data developed following the ~~EPRI SOG~~CEUS SSC study was conducted to determine the need for updating the ~~EPRI SOG~~CEUS SSC source models for CPNPP Units 3 and 4. Post-~~EPRI SOG~~CEUS SSC site and regional geologic and geophysical data are discussed in Subsection 2.5.1, and post-~~EPRI SOG~~CEUS SSC site and regional seismological data are presented in Subsection 2.5.2.1. ~~Additionally, post-EPRI SOG seismic source characterizations for sources relevant to CPNPP Units 3 and 4 are reviewed in Subsection 2.5.2.2.2. This information is reviewed to update some EPRI SOG~~ CTS-01521

~~source zones and develop new source characterizations for CPNPP Units 3 and 4 in Subsection 2.5.2.4.2. Only those new source characterizations determined through a screening study to be significant to hazard at CPNPP Units 3 and 4 are included in the final calculation for the GMRS. Subsection 2.5.2.5 also describes the use of updated ground motion equations and the use of Cumulative Absolute Velocity (CAV) filtering to limit the effects of low-magnitude, non-damaging earthquakes on the GMRS.~~ CTS-01521

Also following guidance provided in RG 1.208, the horizontal GMRS developed in Subsection 2.5.2.6 was calculated using a performance-based, risk-consistent method based on the ASCE/SEI Standard 43-05, Seismic Design Criteria for Structures, Systems, and Components in Nuclear Facilities (Reference 2.5-371) that takes into account soil amplification factors determined using Approach 3 of NUREG/CR-6769 and soil properties presented in Subsection 2.5.2.5. The method specifies the level of conservatism and rigor in the seismic design process such that the performance of structures, systems, and components of the plant achieve a uniform seismic safety performance. Subsection 2.5.2.6 also describes the development of the vertical GMRS through the scaling of the horizontal GMRS by frequency-dependent vertical-to-horizontal response spectra and describes development of the FIRS for the four elevations at which seismic category I structures at CPNPP Units 3 and 4 will be founded.

2.5.2.1 Seismicity

CP COL 2.5(1) Replace the content of DCD Subsection 2.5.2.1 with the following.

The ~~EPRI SOG~~CEUS SSC PSHA methodology used as the basis for determining the GMRS at CPNPP Units 3 and 4 primarily relies on the analysis of historical seismicity within the CEUS to estimate seismicity rate and relative magnitude recurrence parameters (i.e., activity rates and Gutenberg-Richter b-values) for seismic sources defined by ~~each of the ESTs~~the CEUS SSC Project (~~Reference 2.5-369~~Reference 2.5-486). As part of the ~~EPRI SOG~~CEUS SSC study, a seismicity catalog was developed for the entire CEUS SSC Study Region spanning the years ~~1627~~1568 through the ~~beginning of 1985~~end of the 2008 calendar year. The resultant catalog is briefly reviewed in Subsection 2.5.2.1.1. As part of evaluating the impact of post-~~EPRI SOG~~CEUS SSC information on seismic source characterizations relevant to CPNPP Units 3 and 4, an updated seismicity catalog was developed through the end of the 2011 calendar year, that extends beyond the site region. Subsection 2.5.2.1.2 describes the development of this catalog. The seismicity catalog used for CPNPP Units 3 and 4 is the combination of the original ~~EPRI SOG~~CEUS SSC catalog and the updated catalog developed here. Recent and historical earthquakes with the potential to affect CPNPP Units 3 and 4 are discussed in Subsection 2.5.2.1.3. CTS-01521 CTS-01521 CTS-01521 CTS-01521

2.5.2.1.1 Seismicity Catalog Used in ~~EPRI SOG~~the CEUS SSC Seismic Hazard Analysis

CTS-01521

~~The seismicity catalog used in the EPRI SOG study (Reference 2.5-370) extends from the Rocky Mountain front to beyond the Atlantic coastline and from the U.S.-Canada border to the Gulf of Mexico, well beyond the extent of the CPNPP Units 3 and 4 site region. The EPRI SOG study spent considerable effort in ensuring that the catalog is complete throughout the historical record to the time of the catalog compilation (early 1985) in that all instrumental earthquakes and significant historical earthquakes were included (References 2.5-369 and 2.5-370). In addition, all duplicate events were removed from the catalog, all non-earthquakes (e.g., explosions) were removed from the catalog, only main events of earthquake clusters were included in the catalog, and all event magnitudes were converted to a uniform estimate (Emb) of body wave magnitude (m_b).~~The seismicity catalog used in the CEUS SSC (Reference 2.5-486) extends from longitude approximately coincident with the Rocky Mountain foothills (105°W) on the west to 200 miles (322 km) offshore of the Atlantic coastline on the east. The northern boundary extends a minimum of 200 miles (322 km) north of the US-Canadian border and the southern boundary extends a minimum of 200 miles (322 km) into the Gulf of Mexico. The CEUS SSC expended considerable effort ensuring that the catalog is complete throughout the historical record to the time of the catalog compilation (end of the 2008 calendar year) in that all instrumental earthquakes and significant historical earthquakes were included. In addition, assessment of a uniform size measure was applied to each earthquake where only main events of earthquake clusters were included in the catalog (i.e., the catalog was declustered), and completeness of the catalog was assessed based on location, time, and earthquake size.

Given the characteristics of the seismicity catalog developed for the ~~EPRI SOG~~CEUS SSC study (~~References 2.5-369 and 2.5-370~~Reference 2.5-486), the ~~EPRI SOG~~CEUS SSC catalog meets the requirement of RG 1.206 that a COL applicant shall "provide a complete list of all historically reported earthquakes that could have reasonably affected the region surrounding the site, including all earthquakes of modified ~~Mercalli intensity~~MMI (RG 1.208) greater than or equal to IV or of m_b greater than or equal to 3.0 that have been reported within 200 mi of the site" up until ~~1985~~2008. In the current study, moment magnitudes (Mw) greater than or equal to 2.9 have been considered for consistency with the CEUS SSC.

CTS-01521

CTS-01521

2.5.2.1.2 Updated Seismicity Catalog

The updated seismicity catalog for the years ~~1985~~2009 to 20~~06~~11 is developed to:

CTS-01521

- Satisfy the requirements of RG 1.206 regarding the reporting of earthquakes within 200 mi of the site, and
- Assist in the evaluation of the existing ~~EPRI SOG~~CEUS SSC source model to adequately describe seismic hazard at CPNPP Units 3 and 4.

CTS-01521

~~Spatially, the updated catalog extends over an update region defined as the area from 28° to 38° north latitude and 93° to 104° west longitude. Figure 2.5.2-201 shows the site, the site region, the extent of the updated catalog, earthquakes from the final updated catalog, and earthquakes from the EPRI SOG catalog.~~The catalog update was initially performed for the entire CEUS SSC Study Region as defined in Reference 2.5-486 and later filtered for the limit of regional seismicity. The CEUS SSC Study Region is geographically defined by the window encompassed by 22.5° to 51° north latitude and 62.5° to 105.25° west longitude. The limit of regional seismicity is defined as the area from 28° to 38° north latitude and 93° to 104° west longitude. Figure 2.5.2-201 shows the site, site region, and catalog for the limit of updated seismicity for the CPNPP Units 3 and 4. CTS-01521

~~The updated catalog is based on a compilation of the following catalogs:~~

~~Advanced National Seismic System (ANSS) Catalog~~

~~The ANSS catalog was searched on February 9, 2007, for all earthquakes within the update region occurring between January 1, 1985, and December 12, 2006, resulting in a catalog of 231 events (Reference 2.5-372). The ANSS catalog is used as the base catalog for the CPNPP catalog update.~~

~~National Earthquake Information Center (NEIC) Catalog~~

~~The NEIC Preliminary Determination of Epicenters (PDE) catalog was searched on March 16, 2007, for all earthquakes within the update region occurring between January 1, 1985, and December 12, 2006, resulting in a catalog of 217 events (Reference 2.5-373). The NEIC catalog is used to supplement the ANSS catalog.~~

~~Oklahoma Geological Survey (OGS) Catalog~~

~~The OGS (Reference 2.5-374) operates ten seismograph stations in the state of Oklahoma and develops a local catalog with lower event detection thresholds than catalogs generated from regional seismograph networks. The OGS archives the local catalog as separate annual files online at the Oklahoma Geological Survey Observatory (http://www.okgeosurvey1.gov/level2/okeqcat.index.html). Twenty-two annual files covering the years 1985 through 2006 were downloaded from the site on March 13, 2007, resulting in a combined 1327 events (Reference 2.5-374). The compiled OGS catalog is used to supplement the ANSS catalog in Oklahoma.~~

~~New Mexico Institute of Mining and Technology (NMT) Catalog~~

~~The NMT Seismological Observatory operates 17 seismograph stations in the state of New Mexico, some of which provide coverage of eastern New Mexico and west Texas. The NMT catalog is archived online and contains 768 events between 1985 and 1998 (Reference 2.5-375). The NMT catalog is used to supplement the ANSS catalog in west Texas.~~

~~Center for Earthquake Research and Information (CERI) Catalog~~ CTS-01521

~~The CERI (Reference 2.5-376) at the University of Memphis was searched on March 14, 2007, for all earthquakes within the update region occurring between January 1, 1985, and December 12, 2006, resulting in a catalog of 20 events (Reference 2.5-376). The CERI earthquake catalog is used to supplement the ANSS catalog.~~The primary earthquake catalogs chosen to update the CEUS SSC and Regional Seismicity catalogs are the USGS National Earthquake Information Center (NEIC) and the Advanced National Seismic System (ANSS). These catalogs are compilations of earthquakes from regional seismograph networks. The ANSS composite catalog is created by merging the master earthquake catalogs from contributing ANSS institutions and removing duplicate solutions for the same event. This catalog covers the time period from 1898 to the present. The NEIC catalog is a compilation of worldwide earthquakes from 2100 B.C. to the present. The catalog source for the earthquakes in the CEUS SSC comes from the NEIC Preliminary Determination of Epicenters (PDE) catalog.

The Center for Earthquake Research and Information (CERI), the Oklahoma Geological Survey (OGS), and the New Mexico Tech Seismological Observatory (NMT) regional networks are also used to supplement this information.

NEIC Catalog

The NEIC PDE catalog (Reference 2.5-373) was searched on August 28, 2012, for all records in the CEUS SSC geographic window, resulting in 1,183 events from January 1, 2009 through December 31, 2011.

ANSS Catalog

The ANSS catalog (Reference 2.5-372) was searched on August 28, 2012 for all records in the CEUS SSC geographic window, resulting in 3,643 events from January 1, 2009 through December 31, 2011. The ANSS catalog is used to supplement the national catalog, but the NEIC catalog takes precedence over ANSS.

CERI Catalog

The CERI earthquake catalog (Reference 2.5-376) was searched on August 28, 2012, for all records in the CEUS SSC geographic window, resulting in 2,397 events from January 1, 2009 through December 31, 2011. The CERI catalog is used to supplement the NEIC and ANSS catalogs.

OGS Catalog

The OGS (Reference 2.5-374) operates ten seismograph stations in the state of Oklahoma and provides a lower event detection threshold than the regional catalogs. The OGS archives the local catalog as separate annual files online at the Oklahoma Geological Survey Observatory and the Leonard Geophysical

Observatory. Four catalogs covering the years 2009 through 2011 were downloaded from the sites on August 28, 2012, resulting in a combined 2,554 events. The compiled OGS catalog is used to supplement the national catalogs in Oklahoma. CTS-01521

NMT Catalog

The NMT Seismological Observatory operates 17 seismograph stations in the state of New Mexico, some of which provide coverage of eastern New Mexico and west Texas. The NMT catalog (Reference 2.5-375) was downloaded on August 28, 2012 for the years of 2010 and 2011.No data is available for 2009. The first catalog for 2010 contained 325 events, while the second catalog for 2011 contained 694 events (Reference 2.5-375).The NMT catalog is used to supplement the national catalogs in west Texas.

The above catalogs are compiled into a single catalog, and the ~~updated catalog for CPNPP Units 3 and 4~~CEUS SSC seismicity catalog update is derived from this compiled catalog through the following steps:

- ~~Duplicates in the catalog are removed by comparing origin time and location. For duplicate events, the event record from the source with the largest magnitude estimate is kept to ensure conservatism in earthquake magnitude reporting.~~ CTS-01521

- Earthquakes occurring outside the specified time period (January 1, ~~1985~~2009, and December 31, 20~~06~~11) are excluded. CTS-01521

- Earthquakes occurring outside the ~~update region~~CEUS SSC geographic window are excluded.

- ~~Best estimate body wave magnitudes (Emb) are determined for all events following the EPRI SOG methodology (References 2.5-340 and 2.5-335). Within this methodology, reported m_b magnitudes for earthquakes are taken as equivalent to Emb magnitudes and, for other reported magnitudes, Emb magnitudes are determined using the relationships presented in Table 4-1 of EPRI (Reference 2.5-340):~~

  ~~$Emb = 0.253 + 0.907 \cdot M_d$ Equation 1~~
  ~~$Emb = 0.655 + 0.812 \cdot M_L$ Equation 2~~
  ~~$Emb = 2.302 + 0.618 \cdot M_S$ Equation 3~~

  ~~where M_d is duration or coda magnitude, M_L is local magnitude, and M_s is surface-wave magnitude. For these events the final Emb magnitude for an event is taken as the largest estimated Emb magnitude.~~Earthquakes of unknown magnitude are removed, blanks in data are marked as unknown, and magnitude types are replaced according to key files for each network.

- Best estimate of moment magnitudes (Mw) are determined for all events following the CEUS SSC methodology. Mw magnitudes are determined using the relationships presented in Table 3-3 of the CEUS SSC report (Reference 2.5-486). CTS-01521

- All events with ~~Emb~~Mw less than ~~3.0~~2.9 are excluded from the catalog, and

- ~~Uniform m_b magnitudes (Rmb) are determined for all events for use in estimating seismicity parameters as outlined in the EPRI SOG methodology (References 2.5-340 and 2.5-335). Rmb is calculated using Equation 4-2 from EPRI (Reference 2.5-340):~~ CTS-01521

  ~~$Rmb = Emb + (1/2) \cdot \ln(10) \cdot b \cdot Smb^2$ Equation 4~~

  ~~where Smb is the standard deviation of m_b. Values of Smb are estimated from the original EPRI SOG catalog.~~Earthquakes outside the CEUS SSC Study Region boundary and exact duplicates or eminent dependent events are removed.

The update of the regional seismicity catalog for CPNPP Units 3 and 4 includes the following steps:

- The CEUS SSC seismicity catalog update, with magnitudes Mw higher or equal to 2.9, is filtered for events within the limit of regional seismicity encompassed by 28° to 38° north latitude and 93° to 104° west longitude as shown in Figure 2.5.2-201.

- The catalog is declustered to remove dependent events and establish the regional seismicity catalog update using the magnitude-time and magnitude-distance windows methodology described in Reference 2.5-487. In the declustering, regional networks were given priority over national networks within their Authoritative Regions according to the ANSS provisions (Reference 2.5-372). Additionally, national networks were given priority over regional networks when events were outside the regional networks or when the magnitude reported by the national NEIC network was higher than the magnitude reported by the regional networks. Preference was given to the NEIC catalog over the ANSS catalog.

~~Table 2.5.2-201 presents the 97 events of the updated catalog for CPNPP Units 3 and 4. This updated catalog is used in conjunction with the EPRI SOG catalog to determine seismicity parameters following the EPRI SOG methodology (References 2.5-369 and 2.5-370). It should be noted that the updated catalog does vary from the EPRI SOG catalog in that the updated catalog has not been declustered to remove dependent events. Therefore, seismicity rates determined using the updated catalog may be higher (i.e., more conservative) than if the catalog had been declustered. The combination of the updated catalog and the~~

~~original EPRI SOG catalog present a complete description of mainshock seismicity for CPNPP Units 3 and 4 through December 31, 2006.~~Table 2.5.2-201 presents the 73 events of the regional seismicity catalog update for CPNPP Units 3 and 4,from January 1, 2009 through December 31, 2011. The observed recurrence parameters from a combined catalog of the regional seismicity catalog update and the CEUS SSC catalog (Reference 2.5-486) is estimated within the limit of regional seismicity. The estimated seismicity rates show that there is no need to update the CEUS SSC Model regional earthquake recurrence parameters as discussed in Subsection 2.5.2.4.2.1. CTS-01521

2.5.2.1.3 Recent Earthquakes and Historical Seismicity

The updated seismicity catalog described in Subsection 2.5.2.1.2 and the original ~~EPRI SOG~~CEUS SSC seismicity catalog described in Subsection 2.5.2.1.1 are shown in Figure 2.5.2-201~~ and Figure 2.5.2-202, respectively~~. ~~These~~This figure~~s~~ show~~s~~ that there is no significant difference in the spatial pattern of seismicity within the update region between the ~~EPRI SOG~~CEUS SSC catalog and the updated catalog. Subsection 2.5.2.4.2.1 provides a quantitative comparison of seismicity rates and shows that there is also no significant difference between the two catalogs. As noted in the ~~EPRI SOG~~CEUS SSC study, the most seismically active region within the extent of Figure 2.5.2-201 is the ~~New Madrid Seismic Zone (NMSZ)~~NMFS ~~in the northeast section of the figure,~~ well outside of the CPNPP Units 3 and 4 site region. ~~Seismicity within the NMSZ is discussed in more detail in Subsection 2.5.2.4.2.3.1 and in Subsection 2.5.1.1.4.3.7.3.~~ Within the site region, the largest concentration of earthquakes occurs in Oklahoma and along the trend of the Southern Oklahoma Aulacogen (OKA, Figure~~s~~ 2.5.2-20~~8~~5 and~~through~~ ~~Figure~~ 2.5.2-20~~2~~8). ~~The association of seismicity with the Southern Oklahoma Aulacogen is discussed in more detail in Subsection 2.5.2.3. No earthquakes with Emb > 3.0 have occurred within 50 mi of the site (Figure 2.5.2-202).~~ CTS-01521 CTS-01521 CTS-01521

Also, there is no evidence of historical or modern earthquakes causing earthquake-induced geologic failure within the site region. The Holocene Meers fault scarp, discussed in Subsection 2.5.1.1.4.3.6.1~~.1~~, is the only fault with ~~paleoseismic~~tectonic geomorphic evidence of earthquake-induced geologic failure within the site region. CTS-01521

2.5.2.1.3.1 Recent Earthquakes

~~No significant earthquakes, defined as earthquakes with an impact on the seismic hazard at CPNPP Units 3 and 4 or seismic source characterization of sources relevant to CPNPP Units 3 and 4, have occurred within the site region since the end date of the EPRI SOG seismicity catalog (i.e., post 1984). For example, the largest post 1984 earthquake within the site region is the September 6, 1997, Emb 4.5 earthquake in south central Oklahoma, approximately 180 mi from CPNPP Units 3 and 4. However, four earthquakes have occurred outside of the site region with relevance to seismic hazard at CPNPP Units 3 and 4 and seismic source characterizations for CPNPP Units 3 and 4. Two of these earthquakes, the~~ CTS-01521

CTS-01521

~~January 2, 1992, Emb 5.0 in southeast New Mexico and the April 14, 1995, Emb 5.7 Alpine earthquake in west Texas (Figure 2.5.2-201), are documented within the updated seismicity catalog (see Subsection 2.5.2.1.2). The other two events, the February 10, 2006, Ms 5.3 and September 10, 2006 earthquakes in the Gulf of Mexico (Reference 2.5-377), are well outside the update region (Figure 2.5.2-205) and are not in the updated catalog. Each of these events is discussed below.~~

~~January 2, 1992, Emb 5.0 Rattlesnake Canyon, New Mexico~~

~~The January 2, 1992, Emb 5.0 earthquake near Rattlesnake Canyon, New Mexico (Table 2.5.2-201) was felt over an area of approximately 440,000 km^2 and had a maximum Modified Mercalli Intensity of V (Reference 2.5-378). CPNPP Units 3 and 4 are outside of the felt area as defined by Frohlich and Davis (Reference 2.5-378), and no damage was reported from this earthquake within the felt area (Reference 2.5-378). A focal mechanism of the event determined by Sanford, et al. (Reference 2.5-379) shows that the event was characterized by thrust motion with an east-west compression axis. The event occurred within the central basin platform of the Permian basin, a region of active hydrocarbon exploration. Exploration within the basin produces some seismicity, but it is unknown if this earthquake is of tectonic or man-induced origin (References 2.5-379 and 2.5-380).~~

~~April 14, 1995, Emb 5.7 Alpine, Texas~~

~~The April 14, 1995, Emb 5.7 earthquake near Alpine, Texas, (Table 2.5.2-201) was felt over an area of approximately 760,000 km^2 and had a maximum intensity of MMI VI (Reference 2.5-378). CPNPP Units 3 and 4 are within the MMI I to III intensity isoseismal region defined by Frohlich and Davis (Reference 2.5-378). Near the epicenter, reported damage includes broken gas mains, cracked walls, and broken windows (Reference 2.5-378). Frolich and Davis (Reference 2.5-378) report that the earthquake was felt in Dallas, Texas, only in high-rise buildings. No known felt reports come from the region immediately surrounding CPNPP Units 3 and 4. A focal mechanism of the event determined by the Global Centroid Moment Tensor Project shows that the event was an earthquake with normal faulting motion with a tensile axis oriented approximately north-northeast (Reference 2.5-317). The event occurred along the eastern boundary of the Rio Grande Rift (RGR) (Reference 2.5-318), an extensional tectonic province characterized by active seismicity related to normal faulting (see discussion in Subsection 2.5.1.1.4.3.7.1). Research has shown that the RGR influences the upper crustal state of stress well eastward of the topographically defined RGR (see discussion in Subsection 2.5.1.1.4.3.7.1). Partly based on these observations, some researchers believe that this earthquake is related to RGR tectonics. For the CPNPP Units 3 and 4 PSHA, this earthquake is interpreted as related to RGR tectonics.~~

~~February 10, 2006, Ms 5.3 Green Canyon, Gulf of Mexico~~

~~The February 10, 2006, Ms 5.3 event in the Gulf of Mexico is well outside the update region (Reference 2.5-377) and is not in the updated catalog. The event was felt in coastal Louisiana, Texas, and Florida and had a maximum intensity of MMI III (Reference 2.5-381). The earthquake occurred along the Sigsbee escarpment off Louisiana. Nettles (Reference 2.5-382) has interpreted this event as a gravity-driven landslide based on the lack of high-frequency energy in the waveforms, slow rise time, preliminary focal mechanism determinations, and the location of the event on the Sigsbee escarpment. Preliminary conclusions of Dellinger, et al. (Reference 2.5-383) also support this interpretation, but Dellinger, et al. (Reference 2.5-383) admit that neither a consensus nor conclusive interpretation of the event mechanism has been determined. The implication of the "landslide" interpretation is that large mass sliding events along the Sigsbee escarpment may be detectable on local and regional seismic networks. However, no other earthquakes within the Gulf of Mexico have been attributed to this mechanism, and other independent researchers have not confirmed the landslide mechanism for the February 10 event.~~ CTS-01521

~~September 10, 2006 Mw 5.8, Gulf of Mexico~~

~~The September 10, 2006, Mw 5.8 event in the Gulf of Mexico is well outside the update region (Reference 2.5-478) and is not in the updated catalog. However, this event is one of the largest in the Gulf of Mexico and was considered during the investigations for the CPNPP Units 3 and 4 site (see Subsection 2.5.2.4.2.2). The event occurred within the oceanic crust within the eastern Gulf of Mexico. The focal mechanism for the earthquake indicates a reverse sense of motion, and the earthquake depth is reported as 13 to 19 miles (22 to 31 km) (Reference 2.5-478). The Mw 5.8 magnitude for this earthquake is equivalent to Emb 6.1 (see Subsection 2.5.2.1.2 for relationships used in magnitude conversions).~~Four large significant earthquakes, defined as earthquakes with an impact on the seismic hazard or the seismic source characterization at CPNPP Units 3 and 4, have occurred within the limit of regional seismicity. Three of these earthquakes were included in the CEUS SSC catalog and are discussed in Subsection 2.5.2.1.3.2 below. The most recent significant event, the November 6, 2011 Mw 5.6 earthquake in Oklahoma, was located approximately 230 miles (370 km) from CPNPP Units 3 and 4 (Table 2.5.2-201)and is discussed here.

November 6, 2011, Mw 5.6, Oklahoma

The November 6, 2011, Mw 5.6 event occurred approximately 31 mi (50 km) east of Oklahoma City, Oklahoma and 230 miles (370 km) from CPNPP Units 3 and 4. The event occurred within the limit of updated seismicity and is included in the regional seismicity catalog update (Table 2.5.2-201). The earthquake had a maximum median intensity of MMI between VI and VII, and was felt as far away as Idaho Falls, ID (1,556km from epicenter). Focal mechanism solutions provided by the USGS are consistent with predominantly strike-slip to oblique-slip movement on a northwest- or northeast-oriented nodal plane. The hypocenter depth was reported by the USGS at 3,1 miles (5 km), though ancillary data associated with various focal mechanism solutions for this event list it as deep as

7.2 miles (12.1 km). The 5.6 moment magnitude value for this earthquake was reported by NEIC. CTS-01521

2.5.2.1.3.2 Historical Earthquakes

~~No additional significant historical earthquakes, defined as earthquakes having an impact on the seismic hazard at CPNPP Units 3 and 4 or seismic source characterization for CPNPP Units 3 and 4, other than those reported in the EPRI SOG seismicity catalog have been reported since publication of the EPRI SOG study (References 2.5-369 and 2.5-370). Below is a review of historical earthquakes that are thought to have had significant felt effects within the region immediately surrounding CPNPP Units 3 and 4 (Figure 2.5.2-201). Magnitudes reported below are Emb magnitudes from the EPRI SOG catalog (References 2.5-369 and 2.5-370).~~ CTS-01521

Three large significant earthquakes, defined as earthquakes with an impact on the seismic hazard or the seismic source characterization at CPNPP Units 3 and 4, are reported in the CEUS SSC seismicity catalog that occurred within the limit of regional seismicity. These earthquakes correspond to the October 22, 1882, Mw 5.5 in Oklahoma, the July 30, 1925, Mw 5.2 in Texas, and the April 9, 1952, Mw 5.3 in Oklahoma. Each of these events and its magnitude from the CEUS SSC catalog update is discussed below.

October 22, 1882, Mw 5.5 Fort Gibson, Oklahoma

The October 22, 1882, Mw 5.5 earthquake with probable epicenter in Oklahoma was felt in an area of about 375,000 square km as reported by the USGS. A maximum MMI of VIII was documented for this event near Fort Gibson, Indian Territory. Frohlich and Davis (Reference 2.5-378) present an isoseismal map of the Fort Gibson earthquake as having intensities of MMI I to III within the region surrounding CPNPP Units 3 and 4, but they also state that Dallas newspapers at the time reported felt effects at more proximal cities but not in Dallas. Since Dallas is closer to the epicenter than is CPNPP Units 3 and 4, it is reasonable to assume that intensities at CPNPP Units 3 and 4 were very low if at all detectable. This is discussed in CPNPP Units 1 and 2 FSAR (Reference 2.5-201) Subsection 2.5.2.1.1.

July 30, 1925, Mw 5.2, Texas

The July 30, 1925, Mw 5.2 earthquake occurred northeast of Amarillo, Texas, was felt in an area of about 520,000 square miles, and produced an MMI of V-VI near the epicenter (Reference 2.5-488).

April 9, 1952, Mw 5.3, Oklahoma

The April 9, 1952, Mw 5.3 earthquake occurred near El Reno, Oklahoma, was felt in an area of 362,600 square km, and produced an MMI of VII-IX near the epicenter. Frohlich and Davis present an isoseismal map for the El Reno earthquake as having an MMI from I to III near CPNPP Units 3 and 4. The closest felt reports to CPNPP Units 3 and 4 summarized by Frohlich and Davis

(Reference 2.5-378) include swaying in the upper floors of buildings in Austin, Abilene, and Wichita Falls. This event is also discussed in the FSAR for CPNPP Units 1 and 2 (Reference 2.5-201) where the event is reported as having intensities of MMI I to III for Dallas and Fort Worth. CTS-01521

Below is a review of historical earthquakes that are thought to have had significant felt events within the region immediately surrounding CPNPP Units 3 and 4 (Figure 2.5.2-201). Magnitudes reported below are taken from the CEUS SSC catalog update.

1811 to 1812 ~~Emb~~Mw 7.~~0~~2 to 7.~~4~~8 New Madrid, Missouri

Frohlich and Davis (Reference 2.5-378) note that there were no reliable earthquake accounts in Texas prior to 1847, but they mention that the series of New Madrid, Missouri, earthquakes between 1811 and 1812 (December 16, 1811, ~~Emb~~Mw 7.2; December 16, 1811, ~~Emb~~Mw 7.~~0~~6; January 23, 1812, ~~Emb~~Mw 7.~~1~~5; February 7, 1812, ~~Emb~~Mw 7.~~4~~8) ~~event~~ would have been felt in Texas, assuming isoseismal intensities from the earthquakes are roughly symmetrical about the epicentral area. Frohlich and Davis ~~(Reference 2.5-378)~~ reproduce a figure of Carlson (Reference 2.5-384) that estimates the intensity in the region of CPNPP Units 3 and 4 from the events as MMI IV to V. CTS-01521 CTS-01521

~~October 22, 1882, Emb 5.4 Fort Gibson, Oklahoma~~ CTS-01521

~~Frohlich and Davis (Reference 2.5-378) present an isoseismal map of the October 22, 1882, Fort Gibson earthquake as having intensities of MMI I to III within the region surrounding CPNPP Units 3 and 4, but they also state that Dallas newspapers at the time reported felt effects at more proximal cities but not in Dallas. Since Dallas is closer to the epicenter than is CPNPP Units 3 and 4, it is reasonable to assume that intensities at CPNPP Units 3 and 4 were very low if at all detectable. This is discussed in the FSAR for CPNPP Units 1 and 2 (Reference 2.5-201).~~

August 16, 1931, ~~Emb~~Mw 5.~~8~~5 Valentine, Texas

Frohlich and Davis (Reference 2.5-378) report that the August 16, 1931, ~~Emb~~Mw 5.~~8~~5 earthquake in Valentine, Texas, was felt as far east as Waco, Dallas, San Antonio, and Houston. Felt reports that Frohlich and Davis ~~(Reference 2.5-378)~~ compiled suggest intensities within the region surrounding CPNPP Units 3 and 4 of approximately MMI III to IV. Doser (Reference 2.5-303) determined a normal faulting mechanism with extension oriented northwest-southeast for the event and attribute the event to rupture along the Mayfield fault, a range-bounding fault within the Basin and Range physiographic province (Reference 2.5-385). This event is also discussed in the FSAR for CPNPP Units 1 and 2 (Reference 2.5-201) where it is reported as having an intensity of MMI II to III at the site. The measured intensity range (MMI II to III) is more precise than the felt intensity range (MMI III to IV) from the historical record.

~~April 9, 1952, Emb 4.9 El Reno, Oklahoma~~ CTS-01521

~~Frohlich and Davis (Reference 2.5-378) present an isoseismal map for the April 9, 1952, Emb 4.9 El Reno earthquake as having intensities of MMI I to III near CPNPP Units 3 and 4. The closest felt reports to CPNPP Units 3 and 4 summarized by Frohlich and Davis (Reference 2.5-378) include swaying in the upper floors of buildings in Austin, Abilene, and Wichita Falls. This event is also discussed in the FSAR for CPNPP Units 1 and 2 (Reference 2.5-201) where the event is reported as having intensities of MMI I to III for Dallas and Fort Worth.~~

January 2, 1992, Mw 4.7 Rattlesnake Canyon, New Mexico

The January 2, 1992, Mw 4.7 earthquake near Rattlesnake Canyon, New Mexico was felt over an area of approximately 440,000 square km and had a maximum MMI of V. CPNPP Units 3 and 4 are located outside of the felt area defined by Frohlich and Davis and no damage was reported from this earthquake within the felt area (Reference 2.5-378). A focal mechanism of the event determined by Sanford, et al. (Reference 2.5-379) shows that the event was characterized by thrust motion with an east-west compression axis. The event occurred within the central basin platform of the Permian basin, a region of active hydrocarbon exploration. Exploration within the basin produces some seismicity, but it is unknown if this earthquake is of tectonic or man-induced origin (References 2.5-379 and 2.5-380).

April 14, 1995, Mw 5.6, Alpine, Texas

The April 14, 1995, Mw 5.6 earthquake near Alpine, Texas, was felt over an area of approximately 760,000 square km and had a maximum MMI of VI. CPNPP Units 3 and 4 are located within the MMI I to III intensity isoseismal region defined by Frohlich and Davis (Reference 2.5-378).Near the epicenter, reported damage includes broken gas mains, cracked walls, and broken windows.Frolich and Davis (Reference 2.5-378) report that the earthquake was felt in Dallas, Texas, only in high-rise buildings. No known felt reports come from the region immediately surrounding CPNPP Units 3 and 4. A focal mechanism of the event determined by the Global Centroid Moment Tensor Project shows that the event was an earthquake with normal faulting motion with a tensile axis oriented approximately north-northeast (Reference 2.5-317).

February 10, 2006, Mw 4.85 Green Canyon, Gulf of Mexico

The February 10, 2006, Mw 4.85 event in the Gulf of Mexico is well outside the update region (Reference 2.5-377) and is not in the CEUS SSC seismicity updated catalog. The event was felt in coastal Louisiana, Texas, and Florida and had a maximum intensity of MMI III (Reference 2.5-381). The earthquake occurred along the Sigsbee escarpment off the coast of Louisiana. Nettles (Reference 2.5-382) has interpreted this event as a gravity-driven landslide based on the lack of high-frequency energy in the waveforms, slow rise time, preliminary focal mechanism determinations, and the location of the event on the Sigsbee

escarpment. Preliminary conclusions of Dellinger, et al. (Reference 2.5-383) also support this interpretation, but Dellinger,et al. admit that neither a consensus nor conclusive interpretation of the event mechanism has been determined. The implication of the "landslide" interpretation is that large mass sliding events along the Sigsbee escarpment may be detectable on local and regional seismic networks. However, no other earthquakes within the Gulf of Mexico have been attributed to this mechanism and other independent researchers have not confirmed the landslide mechanism for the February 10, 2006 event. CTS-01521

September 10, 2006, Mw 5.8, Gulf of Mexico

The September 10, 2006, Mw 5.8 event in the Gulf of Mexico is well outside the limit of updated seismicity and is not in the updated catalog.The event occurred within the oceanic crust within the eastern Gulf of Mexico. The focal mechanism for the earthquake indicates a reverse sense of motion, and the earthquake depth is reported as 13 to 19 miles (22 to 31 km) (Reference 2.5-478).

2.5.2.2 Geologic and Tectonic Characteristics of the Site and Region

CP COL 2.5(1) Replace the content of DCD Subsection 2.5.2.2 with the following.

Guidance from the NRC regarding seismic source characterizations is presented in RG 1.208. This guidance states that:

> "…PSHA should be conducted with up-to-date interpretations of earthquake sources, earthquake recurrence, and strong ground motion estimation" (page 3, RG 1.208).

The issued guidance also states that

> "… seismic sources and data accepted by the NRC in past licensing decisions may be used as a starting point (for the PSHA)" (page 14, RG 1.208).

Acceptable starting-point source zone characterizations identified within RG 1.208 include the Lawrence Livermore National Lab study presented in NUREG/CR-5250 and the EPRI-SOG study (References 2.5-369, 2.5-370, and 2.5-335). CTS-01521 These are now considered obsolete and have been replaced with the CEUS SSC (Reference 2.5-486). As part of the acceptance of these studies, RG 1.208 requires that site-specific geological, geophysical, and seismological studies be conducted to determine if the~~se~~ accepted source model~~s~~ adequately describes CTS-01521 the seismic hazard for the site of interest given any new data developed since acceptance of the original models. The regulatory guidance explicitly states that:

> "The results of these investigations will also be used to assess whether new data and their interpretation are consistent with the information used in recent probabilistic seismic hazard studies accepted by NRC staff. If new data, such as new seismic sources and new ground motion

attenuation relationships, are consistent with the existing earth science database, updating or modification of the information used in the site-specific hazard analysis is not required. It will be necessary to update seismic sources and ground motion attenuation relationships for sites where there is significant new information provided by the site investigation" (page C-1, RG 1.208).

CTS-01521

~~For the case of new information requiring updated source characterizations, RG 1.208 requires that the development of updated source characterizations conform to the guidance presented in NUREG/CR-6372.~~

~~NUREG/CR-6372, prepared by a Senior Seismic Hazard Analysis Committee (SSHAC), provides recommendations on the development of PSHA studies for nuclear facilities. A primary recommendation of the SSHAC is that for a given technical issue (i.e., source zone characterization),~~

> ~~"The following should be sought … (1) a representation of the legitimate range of technically supportable interpretations among the entire informed technical community…" (page xv, NUREG/CR-6372).~~

~~The SSHAC outlines four levels of study for developing the range of interpretations with the choice of level depending on the complexity of the issue to be addressed. The four levels, Level 1 through 4, are distinguished by the increasing levels of sophistication, resources, and participation by technical experts.~~

For CPNPP Units 3 and 4, the CEUS SSC is used as the base source model for determining the GMRS and FIRS (Reference 2.5-486). The CEUS SSC is chosen based on RG 1.208 that explicitly identifies the source characterizations as an acceptable base model and the availability of detailed documentation describing the CEUS SSC (Reference 2.5-486). The CEUS SSC replaces the now obsolete Lawrence Livermore National Lab study presented in NUREG/CR-5250 and the EPRI-SOG study (References 2.5-369, 2.5-370, and 2.5-335). In addition, the CEUS SSC methodology and resultant source characterizations (Reference 2.5-486) are consistent with a high level SSHAC study (Level 3), and the final aggregate source characterizations were developed to:

> "…provide high levels of confidence that the data, models, and methods of the larger technical community have been considered and the center, body, and range oftechnically defensible interpretations have been included" (Executive Summary page 1xxxv, Reference 2.5-486).

~~For CPNPP Units 3 and 4, the EPRI SOG source characterizations are used as the base source models for determining the GMRS (Reference 2.5-369). The EPRI SOG model is chosen based on RG 1.208 that explicitly identifies the source characterizations as an acceptable base model and the availability of detailed documentation describing the EPRI SOG model (References 2.5-369, 2.5-370, and 2.5-335). However, another supporting reason for using the EPRI~~

~~SOG model is that the EPRI SOG methodology and resultant source characterizations (Reference 2.5-369) are consistent with a high level SSHAC study (Level 3 to 4), and the final aggregate source characterizations were developed to:~~

> ~~"… reflect the range of current thinking on the causes of earthquakes in the eastern United States" (report summary page 1, Reference 2.5-369).~~

CTS-01521

As required by RG 1.208, site and regional data collected for CPNPP Units 3 and 4 presented in Subsection 2.5.1 and Subsection 2.5.2.1 have been reviewed to:

> "…determine whether there are any new data or interpretations that are not adequately incorporated into the existing PSHA databases" (page 11, RG 1.208).

As required by the regulatory guidance, if significant new data or interpretations are found they require update of the ~~EPRI SOG~~CEUS SSC source characterizations. ~~Particular attention was paid to this review of new data collected for CPNPP Units 3 and 4 because of the time elapsed since development of the EPRI SOG source characterizations. The source characterizations of the Dames & Moore (zone 20) and Law Engineering (zone 124) ESTs were subject to additional scrutiny because their respective source models generated the highest and lowest hazard estimates for CPNPP Units 3 and 4, respectively.~~ From this review, it has been determined no new data exist requiring alteration of the ~~EPRI SOG~~CEUS SSC source characterizations for CPNPP Units 3 and 4~~, with the exception of those updates presented in Subsection 2.5.2.4.2. The only significant update is that for the Meers fault, and, as described in Subsection 2.5.2.4.2.3.2, this update is developed following SSHAC guidelines.~~

CTS-01521

The following subsections present the seismic source characterizations from the ~~EPRI SOG~~CEUS SSC model (~~Reference 2.5-369~~Reference 2.5-486) that are within the site region. ~~Following those descriptions, a summary of seismic sources used in more recent seismic hazard studies relevant to CPNPP Units 3 and 4 are presented. Source characterizations developed since the EPRI SOG study commonly use moment magnitude (Mw) to describe earthquake magnitude whereas the EPRI SOG study used body wave magnitude (m_b). To allow comparisons between these magnitudes, both m_b and Mw magnitudes are reported below. To convert between the two magnitude scales, the arithmetic mean of the magnitude conversions reported in Atkinson and Boore (Reference 2.5-386), Frankel, et al. (Reference 2.5-339), and EPRI (Reference 2.5-387) are used.~~

CTS-01521

2.5.2.2.1 Summary of ~~EPRI SOG~~CEUS SSC Source Model

~~The EPRI SOG study completed during the 1980s (References 2.5-369, 2.5-370, and 2.5-335) captured uncertainty in seismic source characterizations for the CEUS through the elicitation of six independent ESTs to develop source models of~~

~~the CEUS. The six teams (Bechtel Group, Dames & Moore, Law Engineering, Rondout Associates, Weston Geophysical Corporation, and Woodward Clyde Consultants) independently evaluated the same database of geologic, geophysical, and seismological observations to develop seismic sources for the CEUS. The teams began by developing criteria for assessing the seismogenic activity of a tectonic feature (e.g., spatial association with large- or small-magnitude earthquakes, evidence of geologically recent slip, orientation relative to the regional stress regime). The ESTs then used the common database to identify potentially seismogenic tectonic features and used their individual criteria to determine the probability of seismogenic activity for these features. Each EST then defined seismic sources from the tectonic features and characterized the sources using the EPRI-SOG PSHA methodology (References 2.5-369 and 2.5-335) within which each source is characterized by the following: probability of activity, maximum earthquake magnitude (Mmax) distribution, alternative source geometries, source interdependencies, and smoothing parameters for use in determining seismicity recurrence parameters.~~ CTS-01521

~~Each EST team provided detailed documentation of their seismic hazard assessments and source characterizations in separate volumes of the EPRI-SOG study (Reference 2.5-369). However, for implementing the EST source zones into the EPRI-SOG PSHA model, some simplifications were made to the original source characterizations, as documented in the EQHAZARD Primer (Reference 2.5-335). These simplifications primarily reduced unneeded complexity in Mmax distributions. The EQHAZARD Primer (Reference 2.5-335) is the primary source of zone characterizations presented below.~~

~~Table 2.5.2-202 through Table 2.5.2-207 summarize the source zone characterizations for sources within 200 mi of CPNPP Units 3 and 4. The contributing sources are shown in Figure 2.5.2-203 through Figure 2.5.2-208 and indicated in Tables 2.5.2-202 through 2.5.2-207. These contributing sources were selected from the larger group by excluding all sources that contribute to less than 1% of the hazard at the site, as determined in a screening evaluation that used the updated source characterizations described in Subsection 2.5.2.4.2 and the updated ground motion equations described in Subsection 2.5.2.4.3. These contributing source zones are the starting point for the PSHA at CPNPP Units 3 and 4. Also shown in Figure 2.5.2-203 through Figure 2.5.2-208 are earthquakes from the combined catalog for CPNPP Units 3 and 4 (see Subsection 2.5.2.1) for earthquakes with Emb > 3.0.~~

~~In Subsection 2.5.2.2.1.1 through Subsection 2.5.2.2.1.6, the contributing source zones for each EST are briefly discussed. More detailed information on each source zone is provided in the EST volumes of the EPRI-SOG documentation (Reference 2.5-369).~~The Central and Eastern United States Seismic Source Characterization for Nuclear Facilities (CEUS SSC) Project was published in 2012(Reference 2.5-486). This report provides a regional seismic source model for use in PSHAs for nuclear facilities. The study was developed using a Senior Seismic Hazard Analysis Committee (SSHAC) Level 3 assessment process based on NUREG/CR-6372 (Reference 2.5-292). This report replaces the Electric

Power Research Institute-Seismicity Owners Group (EPRI-SOG) model (Reference 2.5-369). Seismic hazard calculations performed for the CPNPP Units 3 and4, use the CEUS SSC model for the full CEUS SSC Study Region presented in Appendix H of the CEUS SSC Report (Reference 2.5-486). CTS-01521

The CEUS SSC model is made up of two types of seismic sources. The first type of seismic sources (distributed seismicity sources) uses the recorded history of seismicity to model the frequency and spatial distribution of moderate to large earthquakes (M>5). The background distributed seismicity sources are made up of Mmax and Seismotectonic zones. The second type of seismic source uses the paleo-earthquake record to model the frequency and spatial distribution of repeated large magnitude earthquakes (RLMEs) at specific locations. The master logic tree for the CEUS SSC model, showing the division of the Mmax, Seismotectonic, and RLME sources can be found in Figure H-2-1 of HID in the CEUS SSC Report (Reference 2.5-486).

2.5.2.2.1.1 ~~Sources Identified by Bechtel Group~~Mmax Sources

~~Five source zones from the Bechtel Group EST contribute to hazard at CPNPP Units 3 and 4 (Table 2.5.2-202) (Figure 2.5.2-203) (References 2.5-369, 2.5-370, and 2.5-335): Texas Platform (zone BZ2), Ouachita (zone 38), Oklahoma Aulacogen (zone 39), North Great Plains (zone BZ3), and Combination (zone C04). Bechtel defined four additional zones that extended to within the site region that do not contribute to hazard (Table 2.5.2-202) (References 2.5-369, 2.5-370, and 2.5-335): Meers Fault (zone 40), El Reno (zone 65), Gulf Coast (zone BZ1), and S.E. Oklahoma (zone 55). Following is a brief discussion of the seismic source zones that contribute to hazard:~~

~~Texas Platform (zone BZ2)~~

~~The Texas Platform source zone is a large background source zone extending from eastern New Mexico into Texas (Figure 2.5.2-203). The zone is characterized by an upper-bound Mmax of m_b 6.6 (Table 2.5.2-202). CPNPP Units 3 and 4 are contained within the zone.~~

~~Ouachita (zone 38)~~

~~The Ouachita source zone extends from Arkansas into east Texas (Figure 2.5.2-203) and was defined to encompass the extent of the Ouachita fold belt within this region. The zone is characterized by an upper-bound Mmax of m_b 6.6 (Table 2.5.2-202). The closest approach of the zone to CPNPP Units 3 and 4 is 125 mi.~~

~~Oklahoma Aulacogen (zone 39)~~

~~The Oklahoma Aulacogen source zone was drawn to encompass the Oklahoma Aulacogen in Texas, Oklahoma, and New Mexico (Figure 2.5.2-203). The zone is characterized by an upper-bound Mmax of m_b 6.6 (Table 2.5.2-202). The closest approach of the zone to CPNPP Units 3 and 4 is 89 mi.~~

~~North Great Plains (zone BZ3)~~

CTS-01521

~~The North Great Plains source zone is a large background zone extending over much of the central U.S. and into southern Canada (Figure 2.5.2-203). The zone is characterized by an upper bound Mmax of m_b 6.6 (Table 2.5.2-202). The closest approach of the zone to CPNPP Units 3 and 4 is 89 mi.~~

~~Combination (zone C04)~~

~~Combination (zone C04) is comprised of the Oklahoma Aulacogen (zone 39) and Ouachita (zone 38) source zones. The zone is characterized by an upper bound Mmax of m_b 6.6 (Table 2.5.2-202). The closest approach of the zone to CPNPP Units 3 and 4 is 89 mi.~~The Study Region, which includes the whole study region of the CEUS SSC (Figure 2.5.2-202)can be treated as a single background source. However, it can also be divided into multiple sources when there are zones of different Mmax distributions. These additional background sources are called Mmax zones. These zones are further divided into Mesozoic and Non Mesozoic zones, and can also be divided on whether the boundary between the Mesozoic and Non Mesozoic zones is narrow or wide (Figures 2.5.2-203 and 2.5.2-204). A list of the Mmax zones is included in Table 2.5.2-202. Each Mmax source has a unique geometry, seismogenic crustal thickness distribution, characteristic magnitude distribution, and seismicity rates. The logic tree for the Mmax zones branch of the CEUS SSC master logic tree can be found in Figure H-3-1 of HID in the CEUS SSC Report (Reference 2.5-486).

2.5.2.2.1.2 ~~Sources Identified by Dames & Moore~~Seismotectonic Sources

~~Seven source zones from the Dames & Moore Group EST contribute to hazard at CPNPP Units 3 and 4 (Table 2.5.2-203) (Figure 2.5.2-204) (References 2.5-369, 2.5-370, and 2.5-335): Southern Coastal Margin (zone 20), Ouachitas Fold Belt (zone 25), Kink in Ouachita Fold Belt (zone 25a), Southern Oklahoma Aulacogen (zone 28), Default for Southern Oklahoma (zone 28b), New Mexico (zone 67) and Combinzation (zone C08). Dames & Moore defined four additional zones that extend to within the site region that do not contribute to hazard (Table 2.5.2-203) (References 2.5-369, 2.5-370, and 2.5-335): B-W-M Fault (zone 29), A/W Uplift (zone 30), Ardmore Basin (zone 32) and Anadarko Basin (zone 33). Following is a brief discussion of the seismic source zones that contributed to hazard at CPNPP Units 1 and 2 and are used in the PSHA for CPNPP Units 3 and 4:~~

~~Southern Coastal Margin (zone 20)~~

~~The South Coastal Margin source zone is a large regional zone that extends from the continental shelf off eastern Florida, along the Texas coastal plain, and into Mexico (Figure 2.5.2-204). Dames & Moore designed the zone to largely parallel the southern rifted margin of North America, and they state that they have no tectonic basis with which to define the seismic potential of the zone. The zone is~~

characterized by an upper bound Mmax of m_b 7.2 (Table 2.5.2-203). The closest approach of the zone to CPNPP Units 3 and 4 is 83 mi. CTS-01521

Ouachitas Fold Belt (zone 25)

The Ouachitas Fold Belt source zone encompasses the Ouachita orogenic front extending from Arkansas through Oklahoma, Texas, and into eastern Mexico (Figure 2.5.2-204). The zone is characterized by an upper bound Mmax of m_b 7.2 (Table 2.5.2-203). The closest approach of the zone to CPNPP Units 3 and 4 is 26 mi.

Kink in Ouachita Fold Belt (zone 25a)

The Kink in Ouachita Fold Belt source zone is an alternative interpretation of the Ouachitas Fold Belt (zone) representing the opinion of the Dames & Moore EST that seismicity within the fold belt may be preferentially associated with a kink in the fold belt located at the Texas-Oklahoma border (Figure 2.5.2-204). The zone is characterized by an upper bound Mmax of m_b 7.2 (Table 2.5.2-203). The closest approach of the zone to CPNPP Units 3 and 4 is 75 mi.

Southern Oklahoma Aulacogen (zone 28)

The Southern Oklahoma Aulacogen source zone extends along the Texas-Oklahoma border into the Texas panhandle (Figure 2.5.2-204). The source was defined to encompass the Southern Oklahoma Aulacogen. The zone is characterized by an upper bound Mmax of m_b 7.2 (Table 2.5.2-203). The closest approach of the zone to CPNPP Units 3 and 4 is 91 mi.

Default for Southern Oklahoma (zone 28b)

The Default for Southern Oklahoma Aulacogen source zone extends along the Texas-Oklahoma border into the Texas panhandle (Figure 2.5.2-204). The source is a default source zone used to represent the seismic activity of the Southern Oklahoma Aulacogen in conjunction with the Southern Oklahoma Aulacogen (zone 28) source zone. The zone is characterized by an upper bound Mmax of m_b 7.2 (Table 2.5.2-203). The closest approach of the zone to CPNPP Units 3 and 4 is 70 mi.

New Mexico (zone 67)

The New Mexico source zone extends from Texas into New Mexico and part of northern Mexico (Figure 2.5.2-204). Dames & Moore describe the boundaries of the zone as being defined largely on the basis of the extent of arches and basins formed during the Paleozoic (Reference 2.5-369). The zone is characterized by an upper bound Mmax of m_b 7.2 (Table 2.5.2-203). CPNPP Units 3 and 4 are located within this source zone.

~~Combination (zone C08)~~

CTS-01521

~~The Combination source zone (zone C08) is comprised of the Ouachitas Fold Belt (zone 25) and the Kink in Ouachitas Fold Belt (zone 25A) source zones (Figure 2.5.2-204). The zone is characterized by an upper-bound Mmax of m_b 7.2 (Table 2.5.2-203). The closest approach of the zone to CPNPP Units 3 and 4 is 26 miles.~~Similar to Mmax zones, the Study Region can be divided into a number of sources based on seismotectonic features (Figures 2.5.2-205 through 2.5.2-208). Also similar to Mmax zones, Seismotectonic sources can further be divided based on wide and narrow interpretations of source boundaries and whether or not certain sources are included in parts of other sources. A list of the Seismotectonic zones is included in Table 2.5.2-202. Each Seismotectonic source has a unique geometry, seismogenic crustal thickness distribution, characteristic magnitude distribution, and seismicity rates.The logic tree for the Seismotectonic zones branch of the CEUS SSC master logic tree can be found in Figures H-4-1(a) and H-4-1(b) of HID in the CEUS SSC Report (Reference 2.5-486).

2.5.2.2.1.3 ~~Sources Identified by Law Engineering~~Repeated Large Magnitude Earthquake Sources

~~Two source zones from the Law Engineering EST contribute to hazard at CPNPP Units 3 and 4 (Table 2.5.2-204) (Figure 2.5.2-205) (References 2.5-369, 2.5-370, and 2.5-335): New Mexico-Texas Block (zone 124) and Oklahoma Aulacogen-Arbuckle-Wichita Rift (zone 26). Law Engineering defined three additional zones that extend to within the site region that do not contribute to hazard (Table 2.5.2-204) (References 2.5-369, 2.5-370, and 2.5-335): Eastern Mid-Continent (zone 119), Western Mid-Continent (zone 120) and South Coastal Block (zone 126). Following is a brief discussion of the seismic source zones that contribute to hazard:~~

~~New Mexico-Texas Block (zone 124)~~

~~The New Mexico-Texas Block source zone is a large areal source defined by the boundaries of the Southern Oklahoma Aulacogen, the Ouachita gravity high, and the magnetic trend of the Rio Grande Rift-Colorado Front Ranges (Reference 2.5-369). This zone encompasses the majority of Texas, excluding the Gulf Costal Plain, and extends into eastern New Mexico (Figure 2.5.2-205). The zone is characterized by an upper-bound Mmax of m_b 5.8 (Table 2.5.2-204). CPNPP Units 3 and 4 are located within this source zone.~~

~~Oklahoma Aulacogen-Arbuckle-Wichita Rift (zone 26)~~

~~The Oklahoma Aulacogen-Arbuckle-Wichita Rift source zone overlaps the Texas-Oklahoma border and extends into the Texas panhandle and New Mexico (Figure 2.5.2-205). The source zone geometry was defined to encompass the extent of the Southern Oklahoma Aulacogen. The zone is characterized by an upper-bound Mmax of m_b 6.8 (Table 2.5.2-204). The closest approach of the zone to CPNPP Units 3 and 4 is 93 mi.~~RLME sources are additional seismic sources

that are superimposed on the Mmax and Seismotectonic sources. A list of the RLME sources is included in Table 2.5.2-202. Each RLME source has a unique geometry and/or faulting style, seismogenic crustal thickness distribution, characteristic magnitude distribution, and seismicity rates. The logic tree for the RLME zones branch of the CEUS SSC master logic tree can be found in Figure H-5-1of HID in the CEUS SSC Report (Reference 2.5-486). CTS-01521

2.5.2.2.1.4 ~~Sources Identified by Rondout Associates~~

~~Four source zones from the Rondout Associates EST that contribute to hazard at CPNPP Units 3 and 4 (Table 2.5.2 205) (Figure 2.5.2 206) (References 2.5 369, 2.5 370, and 2.5 335): Southern Oklahoma Aulacogen Ouachita Mountains (zone 16), Nemaha Anadark (zone 23), Gulf Coast to Bahamas Fracture Zone (zone 51) and Grenville Crust (zone C02). Rondout Associates defined one additional zone that extends to within the site region that does not contribute to hazard (Table 2.5.2 205) (References 2.5 369, 2.5 370, and 2.5 335): Pre Grenville Precambrian Craton (zone 52). Following is a brief discussion of the seismic source zones that contributed to hazard:~~

~~Southern Oklahoma Aulacogen Ouachita Mountains (zone 16)~~

~~The Southern Oklahoma Aulacogen Ouachita Mountains source zone extends from Arkansas into Texas and Oklahoma along the Texas Oklahoma border (Figure 2.5.2 206). The zone geometry was defined to encompass the Oklahoma Aulacogen (Reference 2.5 369). The zone is characterized by an upper bound Mmax of m_b 6.8 (Table 2.5.2 205). The closest approach of the zone to CPNPP Units 3 and 4 is 80 mi.~~

~~Grenville Crust (zone G02)~~

~~The Grenville Crust source zone is a set of discrete source zones that extend across the eastern and southern margin of the U.S. (Figure 2.5.2 206). The closest portion of the source zone to CPNPP Units 3 and 4 encompasses central and eastern Texas. The source zone is a background source representing all of the Grenville age crust that is not contained within a source zone based on the presence of tectonic features (Reference 2.5 369). The zone is characterized by an upper bound Mmax of m_b 5.8 (Table 2.5.2 205). CPNPP Units 3 and 4 are located within this source zone.~~

~~Nemaha Anadark (zone 23)~~

~~The Nemaha Anadark source zone is an elongated zone extending from southern to northern Oklahoma (Figure 2.5.2 206). The zone geometry was defined to encompass the intersection of possible extensions of the Humboldt fault zone and the Nemaha anticline (Reference 2.5 369). The zone is characterized by an upper bound Mmax of m_b 7.0 (Table 2.5.2 205). The closest approach of the zone to CPNPP Units 3 and 4 is 140 miles.~~

~~Gulf Coast to Bahamas Fracture (zone 51)~~

CTS-01521

~~The Gulf Coast to Bahamas Fracture source zone is a large background source zone extending from the coastal plains of the Gulf of Mexico into the central Gulf of Mexico (Figure 2.5.2-206). The zone geometry was defined to represent the Paleozoic crust of the Gulf of Mexico region as distinct from that of the Appalachians (Reference 2.5-369). The zone is characterized by an upper-bound Mmax of m_b 5.8 (Table 2.5.2-205). The closest approach of the zone to CPNPP Units 3 and 4 is 57 miles.~~

2.5.2.2.1.5 ~~Sources Identified by Weston Geophysical Corporation~~

~~Four source zones from the Weston Geophysical Corporation EST contribute to hazard at CPNPP Units 3 and 4 (Table 2.5.2-207) (Figure 2.5.2-208) (References 2.5-369, 2.5-370, and 2.5-335): Southwest (zone 109), Combination (zone C31), Ancestral Rockies (zone 36) and Gulf Coast (zone 107). Weston Geophysical Corporation defined one additional zone that extends to within the site region that does not contribute to hazard (References 2.5-369, 2.5-370, and 2.5-335): Delaware Basin (zone 37). Following is a brief discussion of the seismic source zones that contributed to hazard:~~

~~Southwest (zone 109)~~

~~The Southwest source zone is a large background source that extends over much of Texas, New Mexico, Colorado, and Wyoming (Figure 2.5.2-207). The zone is characterized by an upper-bound Mmax of m_b 6.6 (Table 2.5.2-206). CPNPP Units 3 and 4 are located within this zone.~~

~~Combination (zone C31)~~

~~The Combination (zone C31) source zone is an alternative geometry for the Southwest (zone 109) background zone that excludes the Delaware Basin in west Texas (Figure 2.5.2-207). The zone is characterized by an upper-bound Mmax of m_b 6.6 (Table 2.5.2-206). CPNPP Units 3 and 4 are located within this zone.~~

~~Ancestral Rockies (zone 36)~~

~~The Ancestral Rockies source zone extends from Arkansas, through the majority of Oklahoma, and into the Texas panhandle (Figure 2.5.2-207). The geometry of this zone was defined to encompass the extent of the Southern Oklahoma Aulacogen and associated tectonic features. The zone is characterized by an upper-bound Mmax of m_b 6.0 (Table 2.5.2-206). The closest extent of this zone to CPNPP Units 3 and 4 is 79 mi.~~

~~Gulf Coast (zone 107)~~

CTS-01521

~~The Gulf Coast source zone is a large background source zone extending from the coastal plains of the Gulf of Mexico into the central Gulf of Mexico (Figure 2.5.2-207). The zone geometry encompasses regions for which no other source zones were defined (Reference 2.5-369). The zone is characterized by an upper bound Mmax of m_b 6.0 (Table 2.5.2-206). The closest approach of the zone to CPNPP Units 3 and 4 is 79 miles.~~

2.5.2.2.1.6 ~~Sources Identified by Woodward-Clyde Consultants~~

~~Four source zones from the Woodward-Clyde Consultants EST contributed to hazard at CPNPP Units 3 and 4 (Table 2.5.2-207) (Figure 2.5.2-208) (References 2.5-369, 2.5-370, and 2.5-335): Central U.S. Background (zone BG44), Southern Oklahoma Aulacogen (zone 46), Alternate Configuration of Southern Oklahoma Aulacogen (46a) and Southern Oklahoma Gravity Anomaly (zone 48). Woodward-Clyde Consultants defined two additional zones that extend to within the site region that do not contribute to hazard at CPNPP Units 1 and 2 (Table 2.5.2-207) (References 2.5-369, 2.5-370, and 2.5-335): Meers Fault (zone 49) and Eastern Oklahoma Seismic Zone (zone 52). Following is a brief discussion of the seismic source zones that contribute to hazard:~~

~~Central US Background (zone BG44)~~

~~The Central US Background (zone BG44) is a large areal background source centered on CPNPP Units 1 and 2. The zone is a quadrilateral shape with sides approximately 6° long, in both longitude and latitude (Figure 2.5.2-208). The zone is characterized by an upper bound Mmax of m_b 6.5 (Table 2.5.2-207). CPNPP Units 3 and 4 are in this zone.~~

~~Southern Oklahoma Aulacogen (zone 46)~~

~~The Southern Oklahoma Aulacogen source zone extends from south central Oklahoma along the Oklahoma-Texas border into the Texas panhandle (Figure 2.5.2-208). The zone geometry is defined to encompass the extent of the Southern Oklahoma Aulacogen. The zone is characterized by an upper bound Mmax of m_b 7.2 (Table 2.5.2-207). The closest approach of the zone to CPNPP Units 3 and 4 is 100 mi.~~

~~Alternate Configuration for Southern Oklahoma Aulacogen (zone 46A)~~

~~The Alternate Configuration for Southern Oklahoma Aulacogen source zone is an alternative geometry for the Southern Oklahoma Aulacogen (zone 46) source zone that extends further to the northeast into New Mexico. The zone is characterized by an upper bound Mmax of m_b 7.2 (Table 2.5.2-207). The closest approach of the zone to CPNPP Units 3 and 4 is 100 mi.~~

~~Southern Oklahoma Gravity Anomaly (zone 48)~~

CTS-01521

~~The Southern Oklahoma Gravity Anomaly source zone is a northwest trending, elongated zone that extends from northern Texas into southern Oklahoma. (Figure 2.5.2-208). The zone geometry was defined to encompass the Bouguer gravity low north of the Oklahoma aulacogen (References 2.5-369). The zone is characterized by an upper bound Mmax of m_b 7.1 (Table 2.5.2-207). The closest approach of the zone to CPNPP Units 3 and 4 is 131 miles.~~

2.5.2.2.2 ~~Post-EPRI-SOG Source Characterization Studies~~

~~Since publication of the EPRI-SOG seismic source characterizations for the CEUS in 1986 (Reference 2.5-369), there have been several regional-scale source characterization studies within the CPNPP Units 3 and 4 site region. These studies include:~~

- ~~A Lawrence Livermore National Laboratory (LLNL) report on the seismic hazard characterization of nuclear power plants in CEUS (NUREG/CR-5250, Vol. 1 and Vol. 5);~~
- ~~A draft report prepared by Geomatrix Consultants for the U.S. Bureau of Reclamation detailing the seismotectonics of the Wichita Uplift and Oklahoma Aulacogen region (Reference 2.5-388);~~
- ~~A draft report prepared by Geomatrix Consultants for the NRC on the Quaternary activity of the Meers fault (Reference 2.5-389);~~
- ~~A U.S. Bureau of Reclamation PSHA study for dams in Oklahoma (Reference 2.5-390);~~
- ~~A LLNL PSHA study for the Pantex nuclear weapon support facility outside Amarillo, TX (Reference 2.5-391); and~~
- ~~The United States Geological Survey (USGS) National Seismic Hazard Map program source characterizations used in developing the USGS National Seismic Hazard Maps (References 2.5-339, 2.5-392, and 2.5-321).~~

~~The source characterizations used within these studies relevant to the characterization of seismic sources for CPNPP Units 3 and 4 are briefly summarized below. Source characterizations from these studies that were developed using post-EPRI-SOG research will be considered as possible revisions or additions to the EPRI-SOG model that must be considered to meet the guidelines of RG 1.208.~~

2.5.2.2.2.1 ~~Lawrence Livermore National Laboratory 1989 Study~~

~~In 1988 LLNL completed a PSHA study, for the NRC, for nuclear power plants within the CEUS that was similar to the EPRI-SOG study (NUREG/CR-5250, Vol. 1). The LLNL study developed a PSHA methodology that included source~~

CTS-01521

characterizations and ground motion equations for the CEUS provided by independent experts. Hazard at a particular site was calculated for the source model defined by each expert using each of the ground motion relationships, and the final hazard at the site was the aggregate of all source models and ground motion relationships. As stated in RG 1.208, the resultant PSHA model is accepted by the NRC for use in determining the GMRS for modern COL applications if modifications are made to account for advances in ground motion equations and source characterizations.

The source characterizations of the 1989 LLNL study were developed by eleven independent experts resulting in eleven different source models (NUREG/CR-5250, Vol. 1). The source models were developed by the experts using geologic and geophysical data the experts compiled themselves, though at later stages of the study seismicity catalogs were provided to the experts for use with their discretion. The source models were revised through a series of feedback loops with the project organizers at LNLL that provided clarification of the project methodology and preliminary results for the source models. The final source models presented in the 1989 report volume (NUREG/CR-5250, Vol. 1) are defined by their source zone geometry, type of recurrence relationship, Mmax, and seismicity recurrence parameters, all provided by the individual experts.

The results of the 1989 LLNL study identified which source zones each expert considers the most significant contributors to hazard at CPNPP Units 1 and 2 (NUREG/CR-5250, Vol. 5). In general, these significant contributors include source zones characterizing the New Madrid region, the Oklahoma Aulacogen and Wichita Uplift, the Ouachita fold belt, and large background zones. The parameterizations of these source zones for each expert is described in Bernreuter, et al. (NUREG/CR-5250, Vol. 1) and is briefly summarized below:

- New Madrid: Probability of activity (Pa) is 1.0 for all experts' characterizations, and Mmax varies between m_b 7.0 and 8.0, depending on expert;
- Oklahoma Aulacogen and Wichita Uplift: Pa varies between 0.7 and 1.0, and Mmax varies between m_b 5.8 and 7.5, depending on expert;
- Ouachita fold belt: Pa varies between 0.6 and 0.7, and Mmax varies between m_b 5.4 and 6.3, depending on expert; and
- Background zones: Pa varies between 0.7 and 1.0, and Mmax varies between m_b 4.8 and 7.5, depending on expert.

An update to the 1989 LLNL study was completed in 1994 with the publication of NUREG-1488. The focus of this study was to reduce the uncertainty in ground motion estimates, and this was accomplished in part by having the experts reevaluate the uncertainty they reported in seismicity parameters. There were no significant changes to the above characterizations.

~~The geometry and seismicity parameters of these source zones identified as being significant to the hazard are broadly consistent with the EPRI SOG source zones used as the basis for the PSHA at CPNPP Units 3 and 4 (Table 2.5.2-202 through Table 2.5.2-207; Figure 2.5.2-203 through Figure 2.5.2-208). The source zones of the LLNL study do not present any new information that requires consideration for CPNPP Units 3 and 4.~~ CTS-01521

2.5.2.2.2.2 ~~Draft Report to the Bureau of Reclamation on the Wichita Uplift Region~~

~~In 1990 Geomatrix Consultants provided the U.S. Bureau of Reclamation with a draft report describing the results of a study on the seismotectonics of the Oklahoma-Wichita Uplift region in southern Oklahoma and northern Texas (Reference 2.5-388). The southernmost extent of the study region is approximately 50 mi north of CPNPP Units 3 and 4. The study evaluated faults, tectonic structures, and historical seismicity within the region to estimate the potential seismic hazard at seven dams in Oklahoma and northern Texas. Of the faults and tectonic structures investigated, only two features were determined to have potential Quaternary activity: the Meers and Criner faults. Seismic source characterizations for the Meers and Criner faults, as well as two areal source zonations, were developed as a final product of the study with the general characteristics as follows:~~

- ~~Meers fault: Mmax of Ms 6.75 to 7.25 (m_b 6.5 to 6.8) with a return period on the order of 2000 to 3000 years;~~
- ~~Criner fault: Mmax of Ms 6.5 to 7.0 (m_b 6.3 to 6.6) with a return period on the order of 2000 to 3000 years; and~~
- ~~Source zones: two separate source zonations with three and four areal source zones, respectively. The source zone geometries, based on seismicity and tectonic structure, encompassed the region of the Southern Oklahoma Aulacogen in Oklahoma and Texas. Seismicity parameters were determined individually for each zone, and the Mmax for all zones was Ms 6.5 (m_b 6.3).~~

~~The areal sources defined by Geomatrix Consultants (Reference 2.5-388) are broadly consistent with the EPRI SOG source zones used as the basis for the PSHA at CPNPP Units 3 and 4 (Table 2.5.2-202 through Table 2.5.2-207; Figure 2.5.2-203 through Figure 2.5.2-208), and do not present any new information that requires consideration for CPNPP Units 3 and 4. However, the characterization of the Meers and Criner faults by Geomatrix Consultants (Reference 2.5-388) is based on information published after the EPRI SOG study (Reference 2.5-369), and these fault source characterizations do require consideration for CPNPP Units 3 and 4. A summary of the information published since the EPRI SOG study (Reference 2.5-369) on the Meers and Criner faults is presented in Subsections 2.5.1.1.4.3.6.1.2 and 2.5.1.1.4.3.6.2. Information presented in those subsections identifies the Criner fault as not capable and the Meers fault as capable. The~~

~~updated source characterization of the Meers fault used in this study is presented in Subsection 2.5.2.4.2.3.2.~~ CTS-01521

2.5.2.2.2.3 ~~Draft Report (Quaternary faulting) to the NRC on the Wichita Uplift Region~~

~~In 1993 Swan, et al. (Reference 2.5-389) provided the NRC with a draft report describing the results of a study investigating Quaternary faulting along the Wichita fault system. Much of the work for the study was done in conjunction with the work described in the Geomatrix Consultants draft report to the U.S. Bureau of Reclamation (Reference 2.5-388) described in Subsection 2.5.2.2.2.2. Therefore, the conclusions of the reports are largely the same, and the Meers and Criner faults are identified as the only potentially capable faults along the Wichita Uplift. As discussed in Subsection 2.5.2.2.2.2, the conclusions of the Swan, et al. (Reference 2.5-389) study require that the Meers and Criner faults be evaluated as potential seismic sources for CPNPP Units 3 and 4. A summary of the evaluation of the capability of the faults based on information published since the EPRI SOG study (Reference 2.5-369) is presented in Subsections 2.5.1.1.4.3.6.1.1 and 2.5.1.1.4.3.6.2. In Subsection 2.5.1.1.4.3.6.2 it is determined that the Criner fault is not a capable fault and that the Meers fault is a capable fault. The updated source characterization of the Meers fault used in this study is presented in Subsection 2.5.2.4.2.3.2.~~

2.5.2.2.2.4 ~~Bureau of Reclamation PSHA Study of Dams in Oklahoma and Texas~~

~~In 1997 LaForge (Reference 2.5-390) conducted a PSHA study for seven dams in Oklahoma. The closest extent of the study area to CPNPP Units 3 and 4 is approximately 110 mi. For the study he defined three areal source zones and one fault source, the Meers fault. The areal source zones were limited in extent to Oklahoma and were defined based on spatial seismicity patterns. LaForge (Reference 2.5-390) estimated Mmax values between Mw 6.0 and 6.5 (m_b 6.3 to 6.6) for the zones from Mmax estimates from geographically similar source zones in the EPRI SOG (Reference 2.5-369) and 1989 LLNL (NUREG/CR-5250, Vol. 1) studies for the NRC. LaForge (Reference 2.5-390) characterized the Meers fault as capable of Mw 7.0 (m_b 6.9) earthquakes with a return period of 5000 years based on the results of Swan, et al. (Reference 2.5-389). Despite the proximity of the Criner fault to the dams analyzed in this study and the identification of the Criner fault by Swan, et al. (Reference 2.5-389) as a potentially active feature, LaForge (Reference 2.5-390) explicitly excludes the fault as a source based on work post dating the Swan, et al. (Reference 2.5-389) study that characterizes the fault as inactive. A summary of this work is presented in Subsection 2.5.1.1.4.3.6.1.2.~~

~~The areal sources defined by LaForge (Reference 2.5-390) are broadly consistent with the EPRI SOG source zones used as the basis for the PSHA at CPNPP Units 3 and 4 (Table 2.5.2-202 through Table 2.5.2-207; Figure 2.5.2-203 through Figure 2.5.2-208). These source zones do not present any new information that~~

requires consideration for CPNPP Units 3 and 4. As discussed in Subsection 2.5.2.2.2.2, the Meers fault characterization used in this report requires that it be evaluated as a potential seismic source for CPNPP Units 3 and 4. A summary of this evaluation based on information published since the EPRI SOG study (Reference 2.5-369) is presented in Subsection 2.5.1.1.4.3.6.1.1. The updated source characterization of the Meers fault used in this study is presented in Subsection 2.5.2.4.2.3.2. CTS-01521

2.5.2.2.2.5 LLNL PSHA for Pantex Nuclear Weapons Support Facility

In 1998 Savy, et al. (Reference 2.5-391) with LLNL conducted a PSHA of the Pantex nuclear weapons support facility in Amarillo, Texas, approximately 300 mi to the northeast of CPNPP Units 3 and 4. The study region was a 10° x 10° quadrilateral centered on the Pantex site that includes eastern Colorado and New Mexico, Oklahoma, Kansas, and the majority of Texas. Within this region Savy, et al. (Reference 2.5-391) defined five areal source zones and fourteen faults largely based on the results of previous seismic source characterization studies. These sources are summarized as follows:

Background Zones

Savy, et al. (Reference 2.5-391) defined three background source zones (the Rocky Mountain, craton, and extended margin zones) based on zones of the same name used in the 1996 USGS National Seismic Hazard Maps (Reference 2.5-339). Savy, et al. (Reference 2.5-391) defined an additional zone to represent the Rio Grande Rift (RGR) in Texas, New Mexico, and southern Colorado. Seismicity rates for these zones are spatially uniform and were developed primarily using rates from the 1996 USGS model (Reference 2.5-339) and regional seismicity catalogs described within Savy, et al. (Reference 2.5-391). Upper- and lower-bound Mmax values for the zones were defined as: craton Mw 6.0 and 6.75 (m_b 6.3 and 6.76); extended margin Mw 6.75 and 7.8 (m_b 6.76 and 7.4); RGR Mw 6.3 and 7.0 (m_b 6.5 and 6.9); Rocky Mountain Mw 6.0 and 6.75 (m_b 6.3 and 6.76).

Amarillo-Wichita Uplift Zone

Savy, et al. (Reference 2.5-391) defined an areal source zone representing the Amarillo-Wichita Uplift and Southern Oklahoma Aulacogen based on their opinion that the zone is capable of elevated rates of seismicity relative to surrounding areas. Savy, et al. (Reference 2.5-391) report that the geometry of the zone is defined by the bounding faults of the Uplift. Seismicity parameters are uniform within the zone and determined from observed seismicity. Savy, et al. (Reference 2.5-391) state that the zone is characterized to represent seismicity of magnitudes less than the characteristic magnitude of the Meers fault, and as such the zone has lower- and upper-bound Mmax of Mw 6.0 and 7.0 (m_b 6.3 and 6.9).

Spatially Variable Seismicity Parameter Zones

CTS-01521

~~Savy, et al. (Reference 2.5-391) also defined an approximately 50 mi x 50 mi (80 km x 80 km) region around the site where seismicity parameters varied over 6.2 mi x 6.2 mi (10 km x 10 km) cells based on seismicity parameters from the 1996 USGS National Seismic Hazard Maps (Reference 2.5-339). Upper- and lower bound Mmax values within the zones are Mw 6.0 and 6.75 (m_b 6.3 and 6.76).~~

~~Meers Fault~~

~~Savy, et al. (Reference 2.5-391) defined a discrete fault source for the Meers fault based on the work of Swan, et al. (Reference 2.5-389) and Crone and Luza (Reference 2.5-284) (see Subsection 2.5.1.1.4.3.6.1.1). Based on this work, Savy, et al. (Reference 2.5-391) use a characteristic earthquake model to represent the Meers fault with lower- and upper bound magnitudes of Mw 6.75 and 7.25 and best estimate, upper bound, and lower bound return periods of 1150 years, 500,000 years, and 700 years, respectively. Savy, et al. (Reference 2.5-391) also include an alternative source model of the Meers fault that allows for the rupture to occur along an extension of the Meers fault extending the entire length of their Amarillo-Wichita Uplift zone. This alternative Meers fault source is meant to represent the possibility of Meers-like ruptures within the Southern Oklahoma Aulacogen on faults that do not yet have recognized Quaternary events. Savy, et al. (Reference 2.5-391) use a characteristic earthquake model to represent the Meers extension with lower- and upper bound magnitudes of Mw 7.25 and 7.75 (m_b 7.1 and 7.4) and best estimate, upper bound, and lower bound return periods of 500,000 years, 1,000,000 years, and 200,000 years, respectively.~~

~~Cheraw Fault~~

~~Savy, et al. (Reference 2.5-391) defined a discrete fault source for the Cheraw fault in southeast Colorado based on the work of Crone, et al. (Reference 2.5-323) (see discussion in Subsection 2.5.1.1.4.3.7.2). Savy, et al. (Reference 2.5-391) use a characteristic earthquake model to represent the Meers extension with lower- and upper bound magnitudes of Mw 6.75 and 7.25 (m_b 6.76 and 7.1) and best estimate, upper bound, and lower bound return periods of 6500 years, 500,000 years, and 3600 years, respectively.~~

~~Rio Grande Rift Faults~~

~~Savy, et al. (Reference 2.5-391) defined 14 discrete fault sources for faults within the central and eastern RGR based on a study evaluating seismic hazard at Los Alamos National Laboratory (Reference 2.5-309). Mmax and recurrence rates for the faults are based on the results of the Los Alamos report (Reference 2.5-309) and the 1996 USGS National Seismic Hazard Maps (Reference 2.5-339). The best-estimate return periods for Mw 6 (m_b 6.3) events vary between 1200 years and 10,000 years, depending on the fault, and the best-estimate characteristic magnitude varies between Mw 6.7 and 7.5 (m_b 6.7 and 7.2), depending on the fault.~~

CTS-01521

~~The areal source zones defined within the LLNL Pantex report (Reference 2.5-391) are broadly consistent with the EPRI SOG source zones used as the basis for the PSHA at CPNPP Units 3 and 4 (Table 2.5.2-202 through Table 2.5.2-207; Figure 2.5.2-203 through Figure 2.5.2-208). For example, the LLNL zones were defined to represent tectonic features similar to those identified by many of the ESTs, and the seismicity parameters for those zones were determined from regional catalogs of seismicity. Two aspects of the areal zones that are noticeably different are:~~

- ~~Mmax values for the LLNL extended margin source zone are generally higher than Mmax values for corresponding zones from the EPRI SOG model (Table 2.5.2-202 through Table 2.5.2-207; Figure 2.5.2-203 through Figure 2.5.2-208); and~~

- ~~The RGR is characterized as a seismic source in the LLNL study and is not included by most ESTs in the EPRI SOG study (Reference 2.5-369).~~

~~The Mmax value for the extended margin used is based on the USGS National Seismic Hazard Maps evaluation of Mmax values. As discussed in Subsection 2.5.2.2.2.6, the USGS characterization of CEUS seismic sources allows for large earthquakes (Mw > 7.5) within the entire region of extended crust with the goal of developing a source model capable of explaining the 1886 Mw 7.3 (m_b 7.1) Charleston earthquake (Reference 2.5-321).~~

~~During development of the EPRI SOG model, the ESTs were aware of the 1886 Mw 7.3 (m_b 7.1) Charleston earthquake and chose to limit the possible region where earthquakes this large could occur to the Charleston area and not allow the Mmax associated with this event to extend out to the extended margin of the Texas coastal plain. The use of a larger Mmax within the USGS model, and thus the LLNL Pantex model, primarily reflects different interpretations and opinions of the seismogenic potential of the Texas coastal plain and not new post EPRI SOG information on the seismogenic potential of the coastal plain. As such, the high Mmax value for the USGS extended margin source zones do not necessitate the revision of Mmax values for correlative source zones in the EPRI SOG model.~~

~~The inclusion of the RGR in the LLNL source zones and not in the EPRI SOG source descriptions reflects the CEUS focus of the EPRI SOG study and the lack of information regarding the seismic potential of RGR related faults at the time of the EPRI SOG study. The post EPRI SOG information on the seismic potential for the RGR on which these source zones are based requires an evaluation for CPNPP Units 3 and 4. New information on the activity of RGR faults, presented in Subsection 2.5.1.1.4.3.7.1, is used to develop preliminary source characterizations of RGR faults (see Subsection 2.5.2.4.2.3.3) used in a screening study for seismic sources at CPNPP Units 3 and 4 (see Subsection 2.5.2.4.2.3.3.1).~~

~~The fault sources described in the Pantex report also require consideration for CPNPP Units 3 and 4. The need to consider an update to the Meers fault and~~

~~RGR faults was previously mentioned. In addition to these faults, post EPRI SOG studies of the Cheraw fault have noted three surface rupturing events in the past 25,000 years (References 2.5-323 and 2.5-326). The results of these studies are presented in Subsection 2.5.1.1.4.3.7.2 and are used to develop a preliminary source characterization of the Cheraw faults used in a screening study for seismic sources at CPNPP Units 3 and 4 (see Subsection 2.5.2.4.2.3.4).~~ CTS-01521

2.5.2.2.2.6 ~~USGS National Seismic Hazard Maps~~

~~As part of the USGS National Seismic Hazard Mapping program, seismic hazard maps for the conterminous U.S. were produced in 1996 (Reference 2.5-339) and updated in 2002 (Reference 2.5-321) using source characterizations developed by the USGS. The USGS does not use a formal expert elicitation process and does not explicitly attempt to represent the full range of uncertainty in source characterizations. However, the source models are developed from published literature, and working groups are held to discuss source characterizations. Therefore, the USGS source characterizations can be viewed as good representations of the modern interpretation of seismic hazard posed by a given source. Aspects of the USGS source characterizations based on the 2002 model (Reference 2.5-321) relevant to CPNPP Units 3 and 4 are discussed below. It should be noted that preliminary updated source characterizations for a 2007 version of the hazard maps were released for public comment during the CPNPP Units 3 and 4 project (Reference 2.5-392). The updated characterizations provide minor changes to some of the source characterizations relevant to CPNPP Units 3 and 4, but these changes do not impact any conclusions reached regarding source models for CPNPP Units 3 and 4.~~

~~In contrast to the EPRI SOG model (Reference 2.5-369) that incorporates many background zones and local sources, the USGS source model for the CEUS includes a small number of large areal source zones and discrete sources. Within the CPNPP Units 3 and 4 site region there are two areal source zones (the extended crust and craton) and one fault source (the Meers fault). In addition to these sources, the Cheraw fault, RGR faults, and New Madrid seismic zone are additional sources within the 2002 USGS model that are potentially pertinent to hazard calculations for CPNPP Units 3 and 4.~~

~~In the 2002 USGS model, the craton zone is characterized by an Mmax of Mw 7.0 (m_b 6.9) and the extended crust is characterized by an Mmax of Mw 7.5 (m_b 7.2) (Reference 2.5-321). In both zones seismicity recurrence parameters are determined from observed seismicity. As discussed in Subsection 2.5.2.2.2.5 with respect to the LLNL Pantex plant PSHA, Mmax values for the extended margin source zone are generally higher than Mmax values for corresponding zones in the EPRI SOG model (Table 2.5.2-202 through Table 2.5.2-207; Figure 2.5.2-203 through Figure 2.5.2-208). However, this contrast in Mmax does not necessitate updating the EPRI SOG Mmax values because it is not based on post EPRI SOG information.~~

~~The Meers and Cheraw fault source characterizations in the USGS 2002 model (Reference 2.5-339) are based on information that post dates the EPRI SOG study (References 2.5-389, 2.5-284, and 2.5-323, for example). As discussed above with respect to other post EPRI SOG source characterizations, the Meers and Cheraw faults need to be reevaluated for CPNPP Units 3 and 4 based on the post EPRI SOG source characterizations. The post EPRI SOG information from which these characterizations are derived is reviewed in Subsection 2.5.1.1.4.3.6, and the source characterizations that are developed using this information are presented in Subsection 2.5.2.4.2.3.~~ CTS-01521

~~The 2002 USGS models (Reference 2.5-321) characterize the NMSZ using a characteristic earthquake model with Mmax values and weights of Mw 7.3 (0.15), 7.5 (0.2), 7.7 (0.5), and 8.0 (0.15) (m_b 7.1, 7.2, 7.3, and 7.5, respectively). The mean recurrence interval for characteristic earthquakes is defined as 500 years. As with the Meers and Cheraw faults, the USGS characterization of the NMSZ is based on post EPRI SOG research (References 2.5-393, 2.5-330, 2.5-336, and 2.5-329, for example), so the source characterization of the NMSZ needs to be reevaluated for CPNPP Units 3 and 4. The post EPRI SOG information on which these characterizations are based is summarized in Subsection 2.5.1.1.4.3.7.3, and the source characterizations that are developed using this information are presented in Subsection 2.5.2.4.2.3.1.~~

~~The 2002 USGS model (Reference 2.5-321) also includes 41 RGR faults. These faults are characterized using both characteristic earthquake and exponential recurrence models. Characteristic earthquake magnitudes for the faults vary between Mw 6.2 and 7.5 (m_b 6.4 and 7.2), and return periods vary between 4000 and 190,000 years. The source characterizations of the RGR faults used by the USGS are largely based on post EPRI SOG research (References 2.5-339 and 2.5-321) and, as discussed in Subsection 2.5.2.2.2.5, the EPRI SOG ESTs generally did not include the RGR in their source characterizations. Therefore, RGR sources are evaluated as potential seismogenic sources for CPNPP Units 3 and 4. Background information on RGR faults sources is presented in Subsection 2.5.1.1.4.3.7.1, and the source characterizations that are developed using this information are presented in Subsection 2.5.2.4.2.3.~~

2.5.2.3 Correlation of Earthquake Activity with Seismic Sources

CP COL 2.5(1) Replace the content of DCD Subsection 2.5.2.3 with the following.

As discussed in Subsection 2.5.2.2.1, ~~ESTs within the EPRI SOG project used the spatial distribution of seismicity to subdivide the CEUS into seismic source zones (Reference 2.5-369)~~, the CEUS SSC (Reference 2.5-486) provided a regional seismic source model for use in probabilistic seismic hazard analysis. The seismicity catalog used ~~by the ESTs~~ was the ~~EPRI SOG~~CEUS SSC catalog described in Subsection 2.5.2.1.1. An updated catalog was developed for use in the CPNPP Units 3 and 4 study (see discussion in Subsection 2.5.2.1.2), and the two catalogs can be compared to assess any changes in the patterns of seismicity or if there exists any correlation between geologic structures and seismicity not CTS-01521

identified within the ~~EPRI SOG study~~CEUS SSC (~~Reference 2.5-369~~Reference 2.5-486). Comparison of the catalogs yields the following conclusions: CTS-01521

- ~~The updated seismicity catalog does not show any earthquakes of Emb ³ 3.0 within approximately 90 mi of the site. Accordingly, there are no earthquakes of Emb ³ 3.0 within 90 mi of the site that can be associated with a known geologic structure (Figure 2.5.2-201 and Figure 2.5.2-202);~~ The regional updated seismicity catalog shows six earthquakes within approximately 90 miles of the site that have Mw values ≥ 2.9, but < 3.2 (Table 2.5.2-201).These small magnitude events are essentially located with the Fort Worth basin and are relatively shallow. The USGS Quaternary Fault and Fold database (Reference 2.5-308) does not have any identified structural features in the vicinity of these earthquake epicenters. Also, the Fort Worth basin and underlying Barnett shale have been heavily explored over the past decade (References 2.5-343, 2.5-347, 2.5-348, 2.5-349, 2.5-350, and 3.5-355). Therefore, it is reasonable to associate these events with the extraction of oil and gas in the area.

- The updated seismicity catalog does show a concentration of seismicity in the ~~Southern~~ Oklahoma Aulacogen that has a spatial pattern consistent with the pattern observed in the ~~EPRI SOG~~CEUS SSC catalog (Figure 2.5.2-201 and Figure 2.5.2-208). In particular, there is a west-northwest band of seismicity extending from Arkansas, through southern Oklahoma, and into the Texas panhandle. This correlation and pattern was noted by the ~~ESTs during the EPRI SOG study~~CEUS SSC study members (~~Reference 2.5-369~~Reference 2.5-486); CTS-01521 CTS-01521

- The updated seismicity catalog does not show a pattern of seismicity different from that of the ~~EPRI SOG~~CEUS SSC catalog that would suggest a new seismic source in addition to those included in the ~~EPRI SOG~~CEUS SSC characterizations (Figure 2.5.2-201); CTS-01521

- The updated seismicity catalog does show a similar spatial distribution of earthquakes to that of the ~~EPRI SOG~~CEUS SSC catalog, suggesting that no significant revisions to the geometry of seismic sources defined in the ~~EPRI SOG~~CEUS SSC characterization is required (Figure 2.5.2-201); and CTS-01521 CTS-01521

- ~~The updated catalog contains two earthquakes that are larger in magnitude than some of the lower bound Mmax values used by ESTs to characterize source zones within which these earthquakes occurred. These earthquakes are the April 14, 1995, earthquake and the January 2, 1992, earthquake (Figure 2.5.2-203 through Figure 2.5.2-208). In addition, the February 10, 2006, earthquake (not in the updated catalog but discussed in Subsection 2.5.2.1.3.1) also has a larger magnitude than the source zone that contains it (Figure 2.5.2-204). Two of these events require revisions to Mmax values for some EPRI SOG source zones (see discussion in Subsection 2.5.2.4.2.2), and the other partially motivates the development of a source zone used in a screening study for CPNPP Units~~

~~3 and 4 (see discussion in Subsection 2.5.2.4.2.3.3).~~The updated CEUS SSC seismicity catalog (Subsection 2.5.2.1.2) has no events with magnitude larger than the minimum Mmax magnitude of any of the CEUS SSC background source zones in the CEUS SSC Model included in Appendix H of the CEUS SSC Project (Reference 2.5-486). Therefore, the Mmax values for the CEUS SSC model do not need to be revised, as described in Subsection 2.5.2.4.2.2. CTS-01521

2.5.2.4 Probabilistic Seismic Hazard Analysis and Controlling Earthquake

CP COL 2.5(1) Replace the content of DCD Subsection 2.5.2.4 with the following.

Subsection 2.5.2.4 describes the Probabilistic Seismic Hazard Analysis (PSHA) conducted for the Comanche Peak nuclear site. Subsection 2.5.2.4.1 discusses the basis for the PSHA, which is the ~~1989 EPRI study~~CEUS SSC (~~Reference 2.5-370~~Reference 2.5-486). This follows the procedures recommended in Regulatory Guide 1.208. ~~Next, Subsection 2.5.2.4.2 presents investigations that were undertaken to revise seismic sources in the EPRI study. These investigations include updates to the seismicity catalog of historical earthquakes, updates to maximum magnitudes assigned to seismic sources in the 1989 EPRI study, and new seismic sources that were identified for inclusion in the seismic hazard calculations.~~Subsection 2.5.2.4.2 presents the evaluation of potential revisions to the CEUS SSC (Reference 2.5-486). Subsection 2.5.2.4.3 discusses new ground motion equations that were used to update the seismic hazard calculations. Subsection 2.5.2.4.4 presents the results of these revisions to the PSHA in the form of hard rock uniform hazard response spectra (UHRS) and deaggregation analyses. Next, Subsection 2.5.2.5 presents seismic wave transmission characteristics of the site. Finally, Subsection 2.5.2.6 presents horizontal and vertical ground motion response spectra (GMRS) and FIRS for various elevations. CTS-01521

2.5.2.4.1 ~~1989 EPRI SOG~~CEUS SSC Probabilistic Seismic Hazard Analysis CTS-01521

The starting point for probabilistic seismic hazard calculations is the ~~EPRI SOG study that was fully documented in 1989~~CEUS SSC (~~Reference 2.5-370~~Reference 2.5-486). This follows the recommendation of Regulatory Guide 1.208 (Reference 2.5-369). ~~An underlying principle of the EPRI SOG study is that expert opinion on alternative, competing models of earthquake occurrence (size, location, and rates of occurrence) and of ground motion amplitude and its variability should be used to weight alternative hypotheses.~~ Interpretations of seismic sources and seismicity parameters were made in the CEUS SSC based on the seismic source characterizations summarized in Subsection 2.5.2.2.1.~~EPRI SOG study using the six ESTs discussed in Subsection 2.5.2.2.1: Bechtel Corporation, Dames & Moore, Law Engineering, Rondout Associates, Weston Geophysical Corporation, and Woodward-Clyde Consultants.~~ CTS-01521

~~Seismic hazard at a site for each team's interpretation is calculated separately, and combined results are determined by weighting each team equally. The result is a family of weighted seismic hazard curves from which composite hazard curves, including the mean and fractile seismic hazard, can be derived.~~Seismic hazard at a site is calculated using the seismic source characterization and ground motion characterization from which hazard curves, including mean and fractile seismic hazard, can be derived.The seismic hazard was calculated using the full CEUS SSC covering the full CEUS SSC Study Region (Reference 2.5-486). CTS-01521

~~The initial task in this COLA is to replicate the seismic hazard calculated for CPNPP Units 1 and 2 using the assumptions on seismic sources and ground motion equations developed in the EPRI SOG study. This task is undertaken to ensure that seismic sources are modeled correctly for this COLA and that the software being used (Risk Engineering, Inc.'s FRISK88 software) can accurately reproduce the EPRI SOG results.~~The primary task is to update the seismic hazard calculated for CPNPP Units 3 and 4 using the seismic source characterization developed in the CEUS SSC (Reference 2.5-486) and EPRI ground-motion characterization (GMC) model (Reference 2.5-401) with aleatory uncertainties from Reference 2.5-403.

~~Comparisons of hazards calculated from the EPRI SOG study with those calculated here are shown in Tables 2.5.2-208 and 2.5.2-209, for peak ground acceleration (PGA) and 1-Hz spectral velocity, respectively. For hazards (annual frequencies of exceedance) in the range of 10^{-4} to 10^{-5} (the first two rows of numbers in each table), differences in mean hazard are less than 10%, with the 2007 calculations for this COLA showing higher (more conservative) hazards than the EPRI SOG results. For the median and 0.85 fractile, and for higher amplitudes (lower hazards), the differences are larger, with the 2007 results generally showing larger hazards than the EPRI SOG results. These differences are of less concern, because only mean hazards in the range of 10^{-4} to 10^{-5} are used to develop spectra recommended for seismic design.~~

~~The conclusion from these comparisons is that the EPRI SOG hazard calculations can be reproduced within about 10% accuracy, and estimates are conservative, for mean hazards at ground motion levels corresponding to hazard levels used to recommend design spectra. For other hazards (corresponding to higher ground motions and to median and 0.85 fractile hazards), the 2007 calculations for this COLA are less consistent but are generally conservative (indicate higher hazard). This comparison validates the FRISK88 code, the representation of EPRI SOG seismic sources, the EPRI SOG source combinations, and the EPRI SOG attenuation equations.~~

2.5.2.4.2 Potential Revisions to ~~1989 EPRI SOG~~CEUS SSC Probabilistic Seismic Hazard Analysis

Several types of new information on the sources of earthquakes may require changes in inputs to PSHA, resulting in changes in the level of seismic hazard at

the CPNPP Units 3 and 4 site compared to what would be calculated based on the ~~EPRI SOG~~CEUS SSC evaluation. Seismic source characterization data and information that could affect the calculated level of seismic hazard include: CTS-01521

- Effects caused by an updated earthquake catalog and resulting changes in the characterization of the rate of earthquake occurrence as a function of magnitude for one or more seismic sources (Subsection 2.5.2.4.2.1). CTS-01521
- Identification of possible new seismic sources in the site vicinity. None were identified for the current study.
- Changes in the characterization of the maximum magnitude for seismic sources (Subsection 2.5.2.4.2.2). CTS-01521
- ~~Changes to models used to estimate strong ground shaking and its variability in the central and eastern US.~~

Possible changes to seismic hazard caused by changes in these areas are addressed in the following subsections.

2.5.2.4.2.1 Updated Seismicity Catalog

Subsection 2.5.2.1.2 describes the development of an updated earthquake catalog. This updated catalog documents additional earthquakes through 20~~06~~11 that have occurred after the earthquake compilation for the ~~EPRI SOG study~~CEUS SSC project (which went through ~~1984~~2008). The impact of the new catalog information is investigated by examining the effect of the new earthquake data on earthquake recurrence estimates within a several-hundred-kilometer region around the CPNPP Units 3 and 4 site. CTS-01521

The effect of the updated earthquake catalog on earthquake occurrence rates in the local region around the CPNPP Units 3 and 4 site is assessed by computing observed and predicted equivalent earthquake counts using the same methodology adopted in the CEUS SSC (Reference 2.5-486) for the limit of updated seismicity, which is encompassed by the area between 28° to 38° north latitude and 93° to 104° west longitude.~~earthquake recurrence parameters for two test areas shown in Figure 2.5.2-209. Test Area 1 consisted of a rectangular area encompassing seismicity in the vicinity of the site, with dimensions 4° latitude by 5.5° longitude. These dimensions are chosen to encompass historical seismicity in the vicinity of the site, and because local events within 100 km of the site generally dominate the hazard (with the exception of the New Madrid seismic zone, which is treated separately) (see Subsection 2.5.2.4.4). Test Area 2 consists of a region north of the site encompassing historical earthquakes in north Texas and Oklahoma, which shows higher historical seismicity than the region surrounding the CPNPP Units 3 and 4 site.~~ CTS-01521

~~For both test areas, the truncated exponential recurrence model is fit to historical seismicity data using the EPRI EQPARAM program, which uses the maximum~~

~~likelihood technique. Earthquake recurrence parameters are computed first using the original EPRI catalog and periods of completeness, and then using the updated catalog and extending the periods of completeness to 2006, assuming that the probability of detection for all magnitudes is unity for the time period 1985 to 2006. The resulting earthquake recurrence rates are compared in Figure 2.5.2-210 for Test Area 1 and in Figure 2.5.2-211 for Test Area 2. Both figures show that the extended earthquake catalog results in earthquake recurrence rates that are lower than rates from the original earthquake catalog.~~ CTS-01521

~~On the basis of the comparison shown in Figures 2.5.2-210 and 2.5.2-211, it is concluded that the earthquake occurrence rate parameters developed in the EPRI-SOG study for seismic sources are conservative estimates of what would be calculated if the extended catalog were to be used to recalculate earthquake occurrence rates. As a result of this conclusion, the original EPRI-SOG earthquake rate parameters are used for EPRI-SOG seismic sources to make hazard estimates for the CPNPP Units 3 and 4 site. Treatment of earthquake rate parameters for other seismic sources, specifically the New Madrid seismic source, is addressed in Subsection 2.5.2.4.4 below.~~To estimate the observed recurrence within the limit of updated seismicity, it is necessary to use a combined catalog of the CEUS SSC Catalog (Reference 2.5-486) and the regional seismicity catalog update from 2009 through 2011 developed in Subsection 2.5.2.1.2. The observed recurrence is estimated using the methodology in the CEUS SSC that uses the summation of the equivalent earthquake counts for each of the specified magnitude bins, after applying corresponding weights related to magnitude weighting cases per Chapter 5 of the CEUS SSC Report.The CEUS SSC catalog already provides information on the equivalent earthquake counts for each event. The equivalent earthquake counts for the updated seismicity catalog from 2009 through 2011 are estimated using Eq. 3.3.1-12 in the CEUS SSC.The value of equivalent earthquake counts is calculated as a function of the standard deviation of the moment magnitude and the magnitude type using Table 3.3-1 in the CEUS SSC. The resulting observed earthquake counts for the CEUS SSC seismicity catalog update are presented in Figure 2.5.2-209. The observed earthquake counts in Figure 2.5.2-209 are compared to the predicted "modeled" earthquake counts.The predicted earthquake values are based on summing up the total events within the specified region after applying corresponding weights related to magnitude weighting cases, the corresponding contributing background sources per Chapter 5 of the CEUS SSC Project, and accounting for the corresponding completeness times for the corresponding completeness regions for each magnitude bin/magnitude weighting case. The full catalog includes three years past the catalog in the CEUS SSC and was considered complete for those three years. Hence the completeness times had three added to them. Figure 2.5.2-209 shows that the modeled earthquake recurrence parameters regionally were sufficient and that there is no need to update the earthquake recurrence parameters. In addition, there is no need to update the individual seismotectonic sources, since the most significant recent earthquake event (November 7, 2011, Mw 5.6 event in Oklahoma) is approximately 230 mi (370 km) from the CPNPP Units 3 and 4 site. This event was already included in the regional comparison above.

2.5.2.4.2.2 New Maximum Magnitude Information

CTS-01521

~~Geologic and seismological data published since the EPRI-SOG study for the site region and more distal areas are summarized and discussed in Subsection 2.5.1 and Subsection 2.5.2.1.2. A review of these data has shown that there is no basis for updating the Mmax distributions of the EPRI-SOG source zones used for the PSHA at CPNPP Units 3 and 4 (Table 2.5.2-202 through 2.5.2-207), with the exception of Dames & Moore's South Coastal Margin (zone 20) and Law Engineering's New Mexico-Texas Block (zone 124). The basis for these updates is that earthquakes have occurred since the EPRI-SOG study (see discussion in Subsection 2.5.2.1 and Subsection 2.5.2.3) within these source zones that have magnitudes greater than the lower-bound Mmax magnitudes for these zones. The update to the Mmax values for these source zones consists of raising the lower-bound Mmax value for the two zones and is discussed in the following subsections.~~

~~In addition to these two earthquakes, another earthquake, the April 14, 1995, event, occurred within several source zones with lower-bound Mmax values less than the magnitude of the earthquake. This occurrence could be interpreted as justification for updating the Mmax of these EPRI-SOG source zones. However, accounting for the seismotectonic environment and seismic hazard potential reflected by this earthquake is best done through the addition of a new source zone for CPNPP Units 3 and 4. This event, the potentially affected source zones, and development of the new source zone are described in Subsection 2.5.1.1.4.3.7.1 and Subsection 2.5.2.4.2.3.3.~~The value of the highest magnitude in each of the CEUS SSC background source zones was compared to the corresponding lowest magnitude value included in the Mmax distribution as included in Appendix H of Reference 2.5-486, to identify the need to update the Mmax distributions of any of the CEUS SSC background source zones.

After assembling the updated CEUS SSC seismicity catalog from the various sources developed in Subsection 2.5.2.1.2, events outside the CEUS SSC Study Region were removed from the seismicity catalog and the magnitudes of the remaining events were then converted to moment magnitudes (Mw). The magnitude conversion was performed using the methodology described in the CEUS SSC Project (Reference 2.5-486). Figure 2.5.2-202 provides the resultant updated CEUS SSC seismicity catalog developed for the CEUS SSC Study Region.The remaining events were sorted within each of the CEUS SSC background source zones (Figures 2.5.2-203 through 2.5.2-208). The event generating the Mmax value in each of the CEUS SSC source zones was identified and declustered by comparing the event to all the other events in the zone using the magnitude-time and magnitude-distance windows methodology described in Reference 2.5-487.The largest magnitude event in each zone was then compared to the lower-bound Mmax for the source zones containing the earthquake and comparisons are presented in Table 2.5.2-203. No earthquakes in the updated CEUS SSC seismicity catalog within any of the source zones exceeds the lower-bound Mmax as presented in the CEUS SSC (Reference 2.5-486).

CTS-01521

2.5.2.4.2.2.1 ~~Mmax Update for Dames & Moore South Coastal Margin~~

~~The Dames & Moore South Coastal Margin (zone 20) is characterized by a Mmax distribution of m_b 5.3 (0.8) and m_b 7.2 (0.2), with weights shown in parentheses (Table 2.5.2-210). On February 10, 2006, an earthquake of magnitude Ms 5.3 (References 2.5-377 and 2.5-381) occurred within this source zone (Figure 2.5.2-204). The earthquake occurred within a region of the Gulf of Mexico with relatively poor seismograph station coverage. However, at the time of the event an ocean-bottom seismometer array was deployed near the earthquake allowing for a relatively good determination of the earthquake epicenter. The earthquake occurred well outside the extent of the updated catalog, so an Emb magnitude for the event is not listed in Table 2.5.2-201, but an Emb magnitude of 5.5 is calculated for the event using the relationship between Ms and Emb reported in Table 4-1 of EPRI (Reference 2.5-340) as described in Subsection 2.5.2.1.2. Since the Emb 5.5 magnitude is greater than the lower bound m_b 5.3 magnitude of the zone, the Mmax distribution for the zone needs to be updated.~~

~~The methodology used by Dames & Moore in determining the Mmax distribution for the South Coastal Margin source zone is not explicitly stated in the EPRI SOG documentation (References 2.5-369 and 2.5-335). Given the lack of a documented methodology, an updated Mmax distribution is developed by increasing the lower bound Mmax of the South Coastal Margin source zone to m_b 5.5 while maintaining the original weights. The updated Mmax distribution is presented in Table 2.5.2-210.~~

2.5.2.4.2.2.2 ~~Mmax Update for Law Engineering New Mexico Texas Block~~

~~The Law Engineering New Mexico Texas Block (zone 124) is characterized by a Mmax distribution of m_b 4.9 (0.3), 5.5 (0.5), and 5.8 (0.2) with weights shown in parentheses (Table 2.5.2-210). On January 2, 1992, an earthquake with an Emb magnitude of 5.0 occurred in the southeast corner of New Mexico. This event is located well within the boundaries of the Law Engineering New Mexico Texas Block (zone 124) (Figure 2.5.2-201 and Figure 2.5.2-205). Because the Emb magnitude of this event is greater than the lower bound Mmax for this zone, the Mmax distribution needs to be revised.~~

~~The Law Engineering methodology for developing the New Mexico Texas Block Mmax distribution is not explicitly stated within the EPRI SOG study documentation (References 2.5-369 and 2.5-335). However, the 1986 volume for Law Engineering (Reference 2.5-369) does indicate that the 5.8 upper bound Mmax is based on observations of seismicity within the zone, and that the lower bound 4.9 is the maximum observed earthquake magnitude within the zone (EPRI, 1986). Based on these statements, the Mmax distribution is updated by increasing the lower bound Mmax value to 5.0 and maintaining the remaining Mmax values and original weights. A summary of the updated New Mexico Texas Block is shown in Table 2.5.2-210.~~

CTS-01521

~~Law Engineering assigned Mmax values of 4.6 and 4.9 to the South Coastal Block Source Zone (Zone 126) (Table 2.5.2-210). The 2006 Emb 5.5 and Emb 6.1 earthquakes within the Gulf of Mexico (see Subsection 2.5.2.1.3.1) are 39 mi (63 km) and 97.6 mi (157 km) outside this zone, respectively. The Emb 6.1 earthquake was well recorded and clearly lies outside the source zone (Reference 2.5-478). The Emb 5.5 earthquake was not well recorded and attempts at relocating the event using proprietary data from ocean bottom seismographs have resulted in significant (10s of kilometers) variation in the position of the earthquake epicenter (Reference 2.5-479). Although current published locations of the Emb 5.5 earthquake locate it outside the source zone boundaries, the uncertainty in the epicentral location of the earthquake is such that it could have occurred within the source zone. The earthquake is conservatively assumed to have occurred within the South Coastal Block Zone. Because the Emb 5.5 earthquake is larger than the lower bound Mmax value of the South Coastal Block Source Zone, the Mmax distribution has been revised accordingly.~~

~~The updated Mmax values of 5.5 and 5.7 adopted here (Table 2.5.2-210) are derived using Law Engineering's methodology for developing Mmax distributions as follows (Reference 2.5-369):~~

- ~~The lower bound Mmax is the magnitude of the maximum observed earthquake in the zone~~

- ~~The upper bound Mmax magnitude defined by Law Engineering for regions with earthquakes occurring within 6.2 mi (10 km) of the surface is mb 5.7~~

~~Weights for the original Mmax distribution (0.9 on the lower bound Mmax and 0.1 on the upper bound Mmax) are retained in the updated Mmax distribution (Table 2.5.2-210).~~

2.5.2.4.2.2.3 ~~Mmax Update for Bechtel Gulf Coast~~

~~The Bechtel Group assigned Mmax values of 5.4, 5.7, 6.0, and 6.6 to the Gulf Coast source zone (zone BZ1) (Table 2.5.2-210). Because the 2006 Emb 5.5 and Emb 6.1 earthquakes in the Gulf of Mexico occur well within this zone (Figure 2.5.2-204), and because these magnitudes are greater than the lower bound Mmax values for the source zone, the Mmax distribution for this source zone has been updated.~~

~~The Bechtel Group's methodology for defining Mmax distributions is described within their EST volume (Reference 2.5-369) and can be applied to Zone BZ1 as follows (Table 2.5.2-210):~~

- ~~The lower bound magnitude of the distribution is defined as the greater of the largest observed earthquake within the zone or m_b 5.4. For Zone BZ1, this lower bound Mmax value is m_b 6.1 with a weight of 0.1.~~

- The next higher magnitude is 0.3 magnitude units greater than the minimum and is given a weight of 0.4. For Zone BZ1, this results in a Mmax value of m_b 6.4 with a weight of 0.4.

- The third magnitude is mb 6.6, interpreted by the Bechtel EST as the largest intraplate earthquake in the CEUS with specific exceptions, and is given a weight of 0.1.

- The fourth magnitude is 0.6 magnitude units above the minimum and is given a weight of 0.4. For Zone BZ1, this results in a Mmax value of mb 6.7 with a weight of 0.4.

CTS-01521

2.5.2.4.2.2.4 Mmax Update for Rondout Gulf Coast to Bahamas Fracture Zone

Rondout Associates assigned Mmax values of 4.8, 5.5, and 5.8 to the Gulf Coast to Bahamas Fracture Zone source zone (zone 51) (Table 2.5.2-210). Because both the 2006 Emb 5.5 and Emb 6.1 earthquakes in the Gulf of Mexico occur within this zone, and because these magnitudes are greater than the lowest Mmax values for the source zone, the Mmax distribution for this source zone has been updated.

The updated Mmax values of 6.1, 6.3, and 6.5 with weightings of 0.3, 0.55, and 0.15, respectively, used here (Table 2.5.2-210) follow from reclassifying the source zone as one capable of producing moderate earthquakes instead of the original classification of the source zone as one only capable of producing smaller than moderate earthquakes (Reference 2.5.2-369). The original Rondout Mmax distribution for moderate earthquake source zones is 5.2, 6.3, and 6.5 with weightings of 0.3, 0.55, and 0.15, respectively. The updated Mmax distribution follows this distribution with the exception of an increase in the lower bound of the distribution to 6.1 to account for the observed Emb 6.1 earthquake within this zone.

2.5.2.4.2.2.5 Mmax Update for Weston Gulf Coast

Weston Geophysical Corporation assigned Mmax values of 5.4 and 6.0 to the Gulf Coast source zone (zone 107) (Table 2.5.2-210). Both the 2006 Emb 5.5 and Emb 6.1 earthquakes in the Gulf of Mexico occur within this zone. Because these magnitudes are greater than the original Mmax values for the source zone, the Mmax distribution for this source zone has been revised.

Weston Geophysical Corporation's (Reference 2.5.2-369) methodology for defining Mmax is based on developing discrete distributions for the probability of Mmax being a particular value. For the Gulf Coast source zone, these Mmax values and probabilities determined by the Weston Geophysical Corporation EST are: 3.6 (0.04628), 4.2 (0.11982), 4.8 (0.27542), 5.4 (0.34415), 6.0 (0.16169), 6.6 (0.04461), and 7.2 (0.00553) (Reference 2.5.2-369). Conservatively applying the Weston Geophysical Corporation's methodology, this discrete probability

distribution is truncated at the magnitude that is closest to, yet greater than, the maximum observed earthquake within the source zone. For this study the distribution is truncated at 6.6 because the Emb 6.1 earthquake occurred within the source zone, and the next highest discrete magnitude in the distribution is 6.6. The truncated distribution is then renormalized so that the sum of all the probabilities is 1.0. The final Mmax values are the truncated distribution, and the weights are the renormalized probabilities.

CTS-01521

2.5.2.4.2.3 New Seismic Source Characterizations

Geologic, geophysical, and seismological information developed since the EPRI SOG study (Reference 2.5-369) was reviewed to identify seismic sources not included in the original EPRI SOG screening study for CPNPP Units 1 and 2 that should be evaluated to determine their potential contribution to seismic hazard at CPNPP Units 3 and 4. New seismic source characterizations are developed for four tectonic features thought to have the potential to impact seismic hazard at CPNPP Units 3 and 4. These features are the New Madrid Seismic Zone (NMSZ), the Meers fault, the Rio Grande Rift (RGR), and the Cheraw fault (Figure 2.5.2-212). The development of seismic source characterizations for these features is described in Subsection 2.5.2.4.2.3.1 through Subsection 2.5.2.4.2.3.4 based on the post-EPRI SOG information summarized in Subsection 2.5.1.1.4.3.6. Source characterizations developed since the EPRI SOG study commonly use moment magnitude (Mw) to describe earthquake magnitude, whereas the EPRI SOG study used body wave magnitude (m_b). To allow comparisons between these magnitudes, both m_b and Mw magnitudes are reported below. To convert between the two magnitude scales, the arithmetic mean of the magnitude conversions reported in Atkinson and Boore (Reference 2.5-386), Frankel, et al. (Reference 2.5-339), and EPRI (Reference 2.5-387) are used.

2.5.2.4.2.3.1 New Madrid Seismic Zone

The NMSZ extends from southeastern Missouri to southwestern Tennessee and is located approximately 500 mi northeast of CPNPP Units 3 and 4 (Figure 2.5.2-212). The NMSZ produced a series of large magnitude earthquakes between December 1811 and February 1812 (Reference 2.5-328). Subsection 2.5.1.1.4.3.7.3 presents a detailed discussion of the NMSZ. In brief, several post-EPRI SOG studies demonstrate that the source parameters for geometry, Mmax, and recurrence of Mmax in the New Madrid region need to be updated to capture the current understanding of this seismic source (References 2.5-321, 2.5-328, 2.5-329, 2.5-330, 2.5-336, and 2.5-393).

The original EPRI SOG screening study for CPNPP Units 1 and 2 did not show any New Madrid source zones from the EPRI SOG ESTs as contributing to 99% of the hazard (Reference 2.5-370). However, with the updated geometry, Mmax values and recurrence intervals for the New Madrid source and updated ground motion attenuation relations developed for the CEUS require reevaluation of the NMSZ as a potential contributor to seismic hazard at CPNPP Units 3 and 4.

CTS-01521

~~The updated New Madrid seismic source model described in the Early Site Permit (ESP) application for the Exelon Generation Company ESP site near Clinton, Illinois (Reference 2.5-395) (Figure 2.5.2-213 and Figure 2.5.2-214) and as modified for the Tennessee Valley Authority Bellefonte Nuclear Site COLA (Reference 2.5-402) is the basis for the NMSZ source model used here for CPNPP Units 3 and 4. This source model accounts for new information on recurrence intervals for large earthquakes in the New Madrid area, for recent estimates of possible earthquake sizes on each of the active faults, and for the possibility of multiple earthquake occurrences within a short period of time (earthquake clusters).~~

~~The time-dependent treatment of the NMSZ is the same as the treatment used in the Bellefonte FSAR, which used a combination of the Poisson model and a Brownian passage time (BPT) model. The Bellefonte FSAR used a cluster model for earthquake occurrences, and gave Cluster Model A a weight of 1.0 and Cluster Model B a weight of 0.0, and this interpretation is followed for the Comanche Peak FSAR.~~

~~Within this model, three faults are identified in the NMSZ, each with two alternative geometries, as follows (Figure 2.5.2-212):~~

~~Fault~~	~~Geometry~~
~~Blytheville~~	~~Blytheville arch/Bootheel lineament~~
	~~Blytheville arch/Blytheville fault zone~~
~~Northern~~	~~New Madrid north~~
	~~New Madrid north with extension~~
~~Reelfoot~~	~~Reelfoot central section~~
	~~Reelfoot full length~~

~~Also, earthquakes are treated as characteristic events in terms of magnitudes, with the following sets of magnitudes modeled for each fault (Reference 2.5-395):~~

~~Blytheville~~		~~Reelfoot~~		~~Northern~~		~~Weight~~
~~Mw~~	~~m_b~~	~~Mw~~	~~m_b~~	~~Mw~~	~~m_b~~	
~~7.3~~	~~7.1~~	~~7.5~~	~~7.2~~	~~7.0~~	~~6.9~~	~~0.1667~~
~~7.2~~	~~7.0~~	~~7.4~~	~~7.2~~	~~7.0~~	~~6.9~~	~~0.1667~~
~~7.2~~	~~7.0~~	~~7.4~~	~~7.2~~	~~7.2~~	~~7.0~~	~~0.0833~~
~~7.6~~	~~7.3~~	~~7.8~~	~~7.4~~	~~7.5~~	~~7.2~~	~~0.25~~
~~7.9~~	~~7.4~~	~~7.8~~	~~7.4~~	~~7.6~~	~~7.3~~	~~0.1667~~
~~7.8~~	~~7.4~~	~~7.7~~	~~7.3~~	~~7.5~~	~~7.2~~	~~0.1667~~

~~The above magnitudes represent the centers of characteristic magnitude ranges that extend ± 0.25 moment magnitude units above and below the indicated magnitude.~~ CTS-01521

~~Seismic hazard is calculated considering the possibility of clustered earthquake occurrences. The modeling of earthquake clusters in the NMSZ has undergone considerable study, and this model will continue to evolve as further field evidence on paleo-earthquakes is found and analyzed. In the Exelon cluster model for multiple earthquake occurrences, the possibility of three clustered earthquakes is taken into account, as is the possibility of clustered earthquakes on two of the faults (but not the third), or the possibility of two faults generating a characteristic earthquake magnitude and the third fault generating a smaller magnitude. The cluster model used for CPNPP Units 3 and 4 is a conservative simplification of the Exelon model (Reference 2.5-395) in that hazard is computed assuming that all clustered events generate earthquakes on each of the three faults and that the magnitudes of those events correspond to the characteristic magnitude distribution.~~

~~Consistent with the Exelon model (Reference 2.5-395), the NMSZ faults used for CPNPP Units 3 and 4 are assumed to be vertical and to extend from the surface to 12 mi (20 km) depth, and a finite rupture model is used to represent an extended rupture on all faults. An additional simplification was made in that only the preferred geometry of each fault is used. This is justified because of the large distance between CPNPP Units 3 and 4 and NMSZ (approximately 500 mi) and the small differences between the preferred and alternative geometries. This simplification allows efficiency in calculations while providing an accurate estimate of seismic hazard. The final model used here for the NMSZ is the same in all important aspects affecting hazard to the model used in the Tennessee Valley Authority Bellefonte Nuclear Site COLA (Reference 2.5-402).~~

2.5.2.4.2.3.2 ~~Meers Fault~~

~~The Meers fault, the southern boundary of the Frontal Wichita fault system in southern Oklahoma, is approximately 180 mi from CPNPP Units 3 and 4. Two surface-rupturing earthquakes along the fault have occurred in the Holocene (Reference 2.5-278), making the Meers fault the only recognized capable fault within the Frontal Wichita fault system. The potential for Quaternary events on the Meers fault, and in particular these two Holocene events, was identified in research (see summary in Subsection 2.5.1.1.4.3.6.1.1) (References 2.5-389, 2.5-284, 2.5-296, and 2.5-293) that post-dated the development of the EPRI-SOG source models (Reference 2.5-369), and thus this Holocene activity was not taken into account in the EPRI-SOG source models or hazard calculations for CPNPP Units 1 and 2. For CPNPP Units 3 and 4 it is necessary to develop an updated source characterization of the Meers fault.~~

~~Following the guidance of RG 1.208, a seismic source characterization of the Meers fault is developed for CPNPP Units 3 and 4 using the SSHAC guidelines for a Level 2 study described in NUREG/CR-6372. The characterization of the~~

Meers fault used for CPNPP Units 3 and 4 is developed from a thorough review of existing literature and consultation with experts familiar with the Meers fault so that the new characterization represents the legitimate range of technically supportable interpretations of the seismic capability of the Meers fault among the informed technical community. A summary of the current state of knowledge regarding the tectonics and seismic capability of the Meers fault, as determined through the literature review and elicitation of expert opinion, is presented in Subsection 2.5.1.1.4.3.6.1.1, and the source model developed from this information is presented below. CTS-01521

As discussed in Subsection 2.5.2.2.2.6, the USGS has developed a seismic source characterization of the Meers fault for use in the USGS National Seismic Hazard Maps. As stated in that subsection, the USGS does not use a formal expert elicitation process and does not explicitly attempt to represent the full uncertainty of source characterizations. However, the source models are developed from the range of published literature and source characterizations are discussed in regional working groups, and as such the USGS source model for the Meers fault is deemed a good base model that is modified to create the updated Meers fault characterization for CPNPP Units 3 and 4.

The USGS characterization of the Meers fault for the 2002 National Seismic Hazard Maps (Reference 2.5-321) is summarized in Table 2.5.2-206. Preliminary documentation for the 2007 National Seismic Hazard Maps (Reference 2.5-392) has the same characterization for the fault. The USGS characterization of the Meers fault is a reasonable representation of the modern state of knowledge regarding the seismic capability of the fault as described in Subsection 2.5.2.2.2.6. However, there is no epistemic uncertainty built into the USGS characterization. In particular, there is considerable uncertainty in the characteristic magnitude, characteristic return period, and fault length that is not included in the USGS source model, so these characteristics are updated for the CPNPP Units 3 and 4 source model. Any uncertainty that exists in the other fault characteristics (e.g., dip, dip direction, sense of slip) does not have a significant impact on hazard at CPNPP Units 3 and 4 due to the considerable distance between the fault and site. The updated Meers fault source model for CPNPP Units 3 and 4 is presented in Table 2.5.2-213.

2.5.2.4.2.3.2.1 Fault Location and Length

The surface trace of the Meers fault used in the updated source model is based on a simplified version of the USGS source model trace that is itself a discretized version of the fault trace from the USGS Quaternary Fault and Fold Database (Reference 2.5-278). The simplification used here (Table 2.5.2-213) uses the two endpoints of the USGS source model (Table 2.5.2-212). The additional fault trace detail provided by the two additional points in the USGS model is insignificant to calculating seismic hazard at CPNPP Units 3 and 4 given the distance between the site and fault.

~~The distance between the two endpoints of the fault trace is approximately 23 mi (37 km), representing the maximum expected length of the Meers fault Holocene rupture. As discussed in Subsection 2.5.1.1.4.3.6.1.1, the western 16 mi (26 km) of the fault is positively associated with the Holocene rupture, given the mapping of the trace on aerial photographs, the continuous nature of the fault scarp over those 16 mi (26 km), and the trenching studies at different locations along the fault (Figure 2.5.1-211) (References 2.5-289, 2.5-284, 2.5-278, 2.5-281, and NUREG/CR-4852). The easternmost portion of the fault scarp that extends the possible length of the Holocene scarp to 23 mi (37 km) was identified in low-sun-angle aerial photography (Figure 2.5.1-211) and is more subtle and discontinuous (NUREG/CR-4852; Reference 2.5-281). Field investigations of this easternmost extent of the scarp have not been conducted to determine if it is from the same Holocene events as is the western extent of the scarp because the area is within the U.S. Army's Fort Sill artillery range. To account for this uncertainty in the length of the Holocene surface ruptures, characteristic magnitudes for the fault are calculated using both 16 and 23 mi (26 and 37 km) as discussed in Subsection 2.5.4.2.3.2.3. However, to simplify the updated Meers fault source model, the location of the fault trace does not include this uncertainty. Not allowing for variations in the extent of fault trace in the source model is a conservative simplification because it allows short rupture scenarios (i.e., 16 mi fault length scenarios) to occur closer to CPNPP Units 3 and 4 than if the fault trace also included the uncertainty (Figure 2.5.1-211).~~ CTS-01521

~~It should be noted that one researcher (Reference 2.5-289) suggests that Quaternary activity on the Meers fault extends 30 km to the northwest of the westernmost extent of the scarp shown in Figure 2.5.1-211. Cetin (Reference 2.5-289) proposes this extension based on "displaced terrace deposits of Pleistocene age, displaced, buried and/or overthickened soil horizons, fault-related colluvium deposits (colluvial wedges) found near and only on the downthrown side of the fault, active seepage near the fault, deflection of stream alignments and the land use pattern along the fault." However, as is summarized by Wheeler and Crone (Reference 2.5-397), the evidence presented by Cetin (Reference 2.5-289) for Quaternary faulting is inconclusive, has not been confirmed by other researchers who have attempted to visit the same field sites as Cetin (Reference 2.5-289), and has never been presented as peer-reviewed research. As such, this potential northwest extension of the capable Meers fault is not considered to be within the legitimate range of technically supportable interpretations.~~

2.5.2.4.2.3.2.2 ~~Characteristic Magnitude~~

~~Previous studies summarized in Subsection 2.5.1.1.4.3.6.1.1 and Subsection 2.5.2.2.2 have characterized the Holocene events on the Meers fault with Mmax on the order of Mw 7.0 (m_b 6.9). Characteristic magnitudes for the updated Meers fault source model are based on using the Holocene events identified on the Meers fault as proxies for the fault's characteristic magnitude. Magnitudes for the Holocene events are estimated using the empirical relationships of Wells and Coppersmith (Reference 2.5-398) between observed earthquake magnitude and characteristics of the earthquake rupture (e.g., surface rupture length, rupture~~

area, maximum surface displacement). For each of the empirical relationships discussed below, the "all faults" regressions of Wells and Coppersmith (Reference 2.5-398) are used to estimate characteristic magnitudes. CTS-01521

Magnitude from Surface Rupture Length

As discussed in Subsection 2.5.1.1.4.3.6.1.1, mapping of the Meers fault scarp on aerial photographs by Ramelli, et al. (NUREG/CR-4852) and other researchers (Reference 2.5-278) indicates that the scarp associated with the Holocene events is between 16 and 23 mi (26 and 37 km) long (Figure 2.5.2-202). Because of this uncertainty in the length of the Holocene surface rupture, both 16 and 23 mi (26 and 37 km) are used with the regressions of Wells and Coppersmith (Reference 2.5-398) to estimate magnitude. Using the regression between rupture length and moment magnitude for all faults, estimated characteristic event magnitudes are:

- Mw 6.7 (m_b 6.7) for a 16-mi (26-km) long rupture; and
- Mw 6.9 (m_b 6.9) for a 23-mi (37-km) long rupture.

Magnitude from Rupture Area

Rupture area for the Holocene ruptures of the Meers fault is estimated using the length of the scarp and the downdip width of the rupture, itself a function of the fault dip and depth of rupture bottom. The lengths of 16 and 23 mi (26 and 37 km) from above are used for rupture length. The dip of the Meers fault is taken from USGS source model, with an 89° dip to the southwest (Reference 2.5-321). The near-vertical orientation of the fault is supported by exposures of the fault in trenches, but the dip of the fault at depth is poorly constrained (Reference 2.5-280). The depth of the rupture bottom is taken as 9 to 12 mi (15 to 20 km) based on NUREG/CR-6034 that reports there is no indication of earthquakes occurring within Oklahoma at greater depths. Using the regressions of Wells and Coppersmith (Reference 2.5-398) between rupture area and moment magnitude for all faults results in the following values:

- Mw 6.6 (m_b 6.7) for the minimum rupture area of 9 mi x 16 mi = 144 mi^2 (15 km x 26 km = 390 km^2); and
- Mw 6.9 (m_b 6.9) for the maximum rupture area of 12 mi x 23 mi = 276 mi^2 (20 km x 37 km = 740 km^2).

Magnitude from Maximum Surface Displacement

The best estimates of surface displacement per event on the Meers fault come from the study of Swan, et al. (Reference 2.5-389) reviewed in Subsection 2.5.1.1.4.3.6.1, and these estimates are used with the regressions of Wells and Coppersmith (Reference 2.5-398) to estimate characteristic magnitudes. The

CTS-01521

~~regressions of Wells and Coppersmith (Reference 2.5-398) were determined using net surface displacements, and because the Meers fault exhibits oblique slip there is only one combined observation of vertical and lateral displacement with which net displacement can be determined (7.5 ft or 2.29 m per event). However, Swan, et al. (Reference 2.5-389) report a best estimate of vertical displacement at a different location that is greater than this net displacement (8.5 ft or 2.6 m per event). Both of these displacement values are used to estimate characteristic magnitudes for the Meers fault.~~

~~The regression on maximum surface displacement, and not the regression for the average surface displacement, of Wells and Coppersmith (Reference 2.5-398) is used to estimate magnitude because the average surface displacement regression is not appropriate for the displacement data available for the Meers fault. Wells and Coppersmith (Reference 2.5-398) explicitly state that the regression for maximum displacement was determined using the maximum reported displacement for an event, while the regressions for average displacement were done on faults where an average displacement was calculated from either an extensive study of the entire surface rupture or a minimum of 10 displacement measurements. The data available for the Meers fault is a maximum reported displacement and not an along-fault average.~~

~~Using the displacements described above results in the following magnitude estimates:~~

- ~~Mw 7.0 (m_b 6.9) from a maximum vertical displacement of 8.5 ft (2.6 m); and~~
- ~~Mw 7.0 (m_b 6.9) from a maximum net displacement of 7.5 ft (2.29 m).~~

~~Final Magnitude Distribution~~

~~The final characteristic magnitude distribution used for the Meers fault is: Mw 6.7 (m_b 6.7), Mw 6.85 (m_b 6.82), and Mw 7.0 (m_b 6.9) with weights 0.2, 0.6, and 0.2, respectively (Figure 2.5.2-259). Mw 6.7 (m_b 6.7) is chosen as the lower bound instead of Mw 6.6 (m_b 6.7) because it is not considered likely that only the 26 km of the Meers fault scarp is related to the Holocene ruptures. Mw 7.0 (m_b 6.9) is chosen as the maximum bound because it is the maximum estimated magnitude of any regression and it is roughly equivalent to other estimates of characteristic earthquake magnitude for the fault (References 2.5-389 and 2.5-321). The weighting of the distribution reflects the opinion that the best estimates of magnitude come from regressions on surface rupture length and rupture area.~~

2.5.2.4.2.3.2.3 ~~Characteristic Return Period~~

~~Epistemic uncertainty in return periods for characteristic earthquakes on the Meers fault is implemented through return period branches on a logic tree (Figure 2.5.2-259). The data presented by Swan, et al. (Reference 2.5-389) on the timing~~

CTS-01521

~~of Meers earthquakes suggests that there have been two Holocene events preceded by a long period (greater than 200,000 years) of inactivity, indicating that the Meers fault exhibits clustered earthquake behavior. The initial branch of the logic tree represents uncertainty in whether or not the Meers fault is in an earthquake cluster.~~

~~Weightings of 0.9 and 0.1 are used for the logic tree branches describing the Meers fault as in an earthquake cluster or in between earthquake clusters, respectively. High weighting on the "in earthquake cluster" conservatively reflects the observation that there is no information to suggest that the Meers fault is not in a cluster; insufficient time has elapsed since the most recent event to conclude that there is a moderate possibility that the period of increased Holocene activity has passed. Return periods for the inter cluster branch are based on the work of Swan, et al. (Reference 2.5-389) that estimates a minimum period of inactivity prior to the Holocene ruptures of 200,000 to 500,000 years. Based on this observation, return period branches of 500,000, 350,000, and 200,000 years with weights of 0.2, 0.6, and 0.2, respectively, are used for the inter cluster branch (Figure 2.5.2-259).~~

~~Return periods for the intra cluster branch are based on the elapsed time since the oldest Holocene event and the observation of two earthquakes during that time span. Assuming that the Meers fault is currently in an earthquake cluster, this method results in a reasonable estimate of the intra cluster return period. Swan, et al. (Reference 2.5-389) report two dates to constrain the maximum age of the oldest Holocene rupture: sample PITT-0477 with a calibrated age of 3397 years B.P. and sample PITT-0373 with a calibrated age of 2918 years B.P. The mean of these two ages is taken as the most probable maximum age of the event, and half that age (1580 years) is taken as the most probable maximum return period for intra cluster events. Swan, et al. (Reference 2.5-389) also report four ages that they believe best constrain the minimum age of the oldest Holocene event: PITT-0370 with a calibrated age of 1942 years B.P., PITT-0369 with a calibrated age of 1610 years B.P., PITT-0378 with a calibrated age of 1912 years B.P., and PITT-0478 with a calibrated age of 2093 years B.P. The mean of these four ages is taken as the most probable minimum age of the event, and half the age (950 years) is taken as the most probable minimum return period for intra cluster events.~~

~~A direct inter event return period for the two Holocene events can also be determined from ages reported by Swan, et al. (Reference 2.5-389) as constraining the bounds of the oldest and youngest Holocene events. The return period determined using the time elapsed between the mean upper bound age of the oldest Holocene event and the mean lower bound age of the youngest Holocene event is 2000 years. The return period determined using the time elapsed between the mean lower bound age of the oldest Holocene event and the mean upper bound age of the youngest Holocene event is 300 years. The large range in return period determined using this methodology is due to the compounded uncertainty from using the dates constraining both Holocene events as opposed to just the time elapsed since the oldest event. The 300 year lower~~

CTS-01521

bound return period is unrealistic since it would imply significantly more events between the oldest Holocene event and the present time than the two observed. For this reason, and because the plausible range of return periods determined from the inter-event period is captured in the return periods previously described, the inter-event period is not used to estimate return periods.

The most probable minimum and maximum return periods are both given equal weight of 0.2 in the logic tree for the return period of intra-cluster events. The remaining 0.6 weight is given to the median of the most probable minimum and maximum return periods (1265 years) (Figure 2.5.2-259). This weighting reflects the belief that it is most likely for the intra-cluster return period to be somewhere between the minimum and maximum bounds.

2.5.2.4.2.3.2.4 PSHA Implementation of Updated Meers Fault Source

The updated source characterization for the Meers fault developed for CPNPP Units 3 and 4 is shown in Table 2.5.2-213, Figure 2.5.2-211, and Figure 2.5.2-259. This characterization is implemented in the CPNPP Units 3 and 4 PSHA model as a line source extending to 9.3 mi (15 km) depth. The possibility of ruptures extending to 20 km depth is taken into account in estimating characteristic earthquake magnitudes, but ruptures in the PSHA do not extend to 20 km. This potential discrepancy does not affect the ground motion estimates at CPNPP Units 3 and 4 given the large distance between the Meers fault and the site.

2.5.2.4.2.3.3 Rio Grande Rift

The RGR is a north-south trending continental rift system recognized to extend from central Colorado through New Mexico, Texas, and into northern Mexico (References 2.5-297, 2.5-298, 2.5-299, and 2.5-300). The RGR is generally characterized by north- to north-northwest trending grabens centered on a broad topographic high, a well-defined gravity high, elevated heat flow, and a tensile stress regime (References 2.5-300, 2.5-313, 2.5-310, and 2.5-296) (see discussion in Subsection 2.5.1.1.4.3.7.1). At the time of the EPRI-SOG study, relatively little was known about the seismogenic potential of faults within the RGR, and only the Weston EST explicitly included the RGR as a seismic source zone. Other ESTs either (1) did not extend their source model boundaries to include the RGR, or (2 included the RGR in large background source zones (Reference 2.5-369). Research post-dating the EPRI study has documented previously unrecognized late Quaternary fault activity within parts of the RGR (References 2.5-303, 2.5-309, 2.5-302, 2.5-304, 2.5-305, 2.5-306, and 2.5-307), as well as evidence that the RGR extends into southwestern Texas and northern Mexico (References 2.5-296 and 2.5-301). These post-EPRI-SOG studies indicate that the RGR is a zone of distinct and elevated tectonic activity relative to other regions at a similar distance from CPNPP Units 3 and 4. Therefore, despite the greater than 400-mi distance between the RGR and CPNPP Units 3 and 4 (Figure 2.5.2-213), RGR sources should be included in a screening study to determine their potential contribution to hazard at CPNPP Units 3 and 4.

CTS-01521

~~Two independent and complementary seismic characterizations of the RGR are developed to characterize the potential contribution to hazard at CPNPP Units 3 and 4. Because of the great distance between the RGR and CPNPP Units 3 and 4 and the intent of using these sources in a screening study for CPNPP Units 3 and 4, these characterizations are simple in comparison to the source model developed for the Meers fault. The first model of the RGR represents discrete faults within the RGR that have been characterized within the USGS National Seismic Hazard Map program (Reference 2.5-321). The second model of the RGR is a point source that generates earthquakes with the bulk characteristics of fully characterized capable faults within the RGR (e.g., magnitude, recurrence rate) at the closest position of the RGR to the CPNPP Units 3 and 4 site.~~

2.5.2.4.2.3.3.1 ~~RGR Fault Source Characterization~~

~~The fault source characterization of the RGR is based on a conservative simplification of the USGS representation of RGR faults in the National Seismic Hazard Maps (Reference 2.5-321). For the National Seismic Hazard Maps, the USGS characterizes the seismic behavior of 41 RGR faults (Table) (Figure 2.5.2-213). These characterizations are based on the USGS compilation of Quaternary folds and faults within the U.S. (Reference 2.5-399). As with all USGS source characterizations, a formal expert opinion elicitation process is not followed and the characterization is not designed to represent the full uncertainty of source characterizations. However, the source models are developed from published literature, and source characterizations are discussed in regional working groups. As such, the USGS source models are a good characterization of the RGR faults for the CPNPP Units 3 and 4 screening study. It should be noted that the preliminary documentation of the 2007 update to the USGS National Seismic Hazard Maps (Reference 2.5-392) does not indicate any changes to the characterization of these faults that would significantly affect seismic hazard at CPNPP Units 3 and 4.~~

~~The USGS characterization includes alternative models of fault recurrence behavior including truncated Gutenberg-Richter and characteristic earthquake relationships. For CPNPP Units 3 and 4, the USGS characterization is simplified by assuming only a characteristic earthquake recurrence relationship parameterized by the characteristic recurrence rate and characteristic earthquake magnitude taken from the USGS parameterization of the faults (Reference 2.5-321). Uncertainty is added to the characteristic magnitudes using a magnitude distribution of ± 0.2 magnitude units about the USGS-reported magnitude with weightings of 0.2, 0.6, and 0.2 for the lowest to highest magnitudes. The surface trace of each fault is simplified from the USGS description by using only the endpoints of the fault trace (Table). Table summarizes this model. These characterizations are implemented into the CPNPP Units 3 and 4 PSHA model as vertical line sources extending to 15 km depth. Given the large distance between the RGR faults and CPNPP Units 3 and 4, details of the geometry do not have a significant impact on ground motions at the site.~~

2.5.2.4.2.3.3.2 ~~RGR Point Source Simplification~~

CTS-01521

~~The fault source characterization of the RGR captures the potential seismic hazard at CPNPP Units 3 and 4 from only faults within the RGR that have been identified as active within the Quaternary and that have been studied in enough detail to develop a seismic source characterization of the fault. As discussed in Subsection 2.5.1.1.4.3.7.1, in addition to these faults the RGR is characterized by a larger scale lithospheric expression (elevated topography, long wavelength gravity anomaly, elevated heat flow, tensile stress regime, region of thinned crust and elevated mantle) (References 2.5.300, 2.5.313, 2.5.310, 2.5.296, 2.5.314, 2.5.315, 2.5.241, and 2.5.245). The observation of the extended area of the lithospheric scale structure of the RGR compared to the surficial expression of RGR faults suggests that the processes driving Quaternary faulting and seismic activity may extend beyond, and in particular to the east of, the observed faults (Reference 2.5.316). This interpretation is supported by the April 14, 1995, earthquake (see discussion in Subsection 2.5.1.1.4.3.7.1 and Subsection 2.5.2.1.3.1).~~

~~Any potentially capable faults within this larger region of the RGR are at a minimum between approximately 300 and 400 miles (480 and 640 km) from the CPNPP Units 3 and 4 site, and are located within the southern portion of the Big Bend region of Texas. Some faults within this region have been hypothesized to have had Quaternary activity based on limited reconnaissance level studies (e.g., mapping from aerial photos); however, there has been little to no work conducted to either confirm initial observations or develop source characterizations for the faults (e.g., recurrence rates, probability of activity, characteristic magnitudes) (References 2.5.301, 2.5.440, 2.5.441, 2.5.442, 2.5.443, 2.5.444 and 2.5.446). Given the great distance between the site and these potentially capable, yet unconfirmed and uncharacterized, faults, the point source model was developed to determine whether a fault with the bulk characteristics of the identified, capable RGR faults at the closest distance possible to the site has any significant impact on the site hazard. If there is a significant contribution from this point source characterization, further investigations of potentially capable RGR faults would be required. However, as discussed in Subsection 2.5.2.4.4, none of the RGR faults or the point source contributes to the site hazard, so no additional studies were conducted.~~

~~The closest extent of the RGR to CPNPP Units 3 and 4 is determined by defining the probable easternmost extent of the lithospheric scale structure of the rift, and then determining the closest point of that line to CPNPP Units 3 and 4 (Figure 2.5.2-213). The position of the line is based on the extent of thinned crust related to the RGR (Reference 2.5.314), the relationship between topography and gravitational potential energy thought to drive RGR related deformation (References 2.5.245, 2.5.320, 2.5.311, and 2.5.316), the extent of the region of tensile stress (References 2.5.241 and 2.5.245), and the location of RGR related earthquakes (References 2.5.289 and 2.5.319). Essentially, the easternmost extent of each of these features roughly correlates to the distinct decrease in topography from the RGR to the Great Plains. The closest point on this line to CPNPP Units 3 and 4 is located in the Big Bend region of western Texas over 300 mi from CPNPP Units 3 and 4 (Figure 2.5.2-201).~~

CTS-01521

~~The source characterization of the RGR point source is based on the bulk characteristics of RGR related faults within the USGS National Seismic Hazard Map database from 2002 (Reference 2.5.321). Preliminary documentation for the 2007 update to that database does not include any changes that would significantly affect seismic hazard at CPNPP Units 3 and 4 (Reference 2.5.392). The magnitude and return period distributions for the RGR point source model are developed by assuming the 41 characteristic magnitudes and return periods defined by the USGS for the RGR faults represent the distribution of characteristic earthquake magnitudes and return period for the RGR. As such, the observed distributions are used to derive simplified representative distributions for use in the updated characterization.~~

~~The observed characteristic magnitudes for RGR faults are shown in Table 2.5.2-214 and vary between Mw 6.1 (m_b 6.3) and Mw 7.5 (m_b 7.2), with a mean magnitude of Mw 6.9 (m_b 6.9). Approximately 10% of observed magnitudes are between Mw 6.1 and 6.5 (m_b 6.3 and 6.6), 30% are between Mw 6.5 and 6.8 (m_b 6.6 and 6.8), 40% are between Mw 6.8 and 7.1 (m_b 6.8 and 7.0), and 20% are between Mw 7.1 and 7.5 (m_b 7.0 and 7.2). The model distribution uses the midpoints of these magnitude ranges as the magnitude and the respective percentage as the weighting. This procedure results in a model magnitude distribution of Mw 6.3 (m_b 6.5), 6.65 (m_b 6.7), 6.95 (m_b 6.88), and 7.3 (m_b 7.1) with weights of 0.1, 0.3, 0.4, and 0.2, respectively (Table 2.5.2-217).~~

~~The observed characteristic return periods for RGR faults are simply the reciprocal of the recurrence rates shown in Table 2.5.2-214 and vary between 4000 years and 188,000 years, with a mean return period of 36,000 years. Approximately 40% of the observed return periods are between 4000 and 188,000 years, 40% are between 25,000 and 50,000 years, and 20% are between 119,000 and 188,000 years. The model return period distribution is based on using the midpoints of these return period ranges as the return period and the respective percentage as the weighting. This procedure results in model return period distributions of 14,500 years, 37,500 years, and 119,000 years with weights of 0.4, 0.4, and 0.2, respectively. The model distribution does not contain the minimum return period observed in the data of approximately 4000 years. This exclusion was intentional because the 4000-year return period represents only 2.5% of the data, and including these shorter return periods with an appropriately low weighting would have little effect on seismic hazard at CPNPP Units 3 and 4.~~

~~A summary of the seismic source characterization for the RGR point source is shown in Table 2.5.2-217. Given the large distance between the RGR faults and CPNPP Units 3 and 4, details of the geometry do not have a significant impact on ground motions at the site.~~

2.5.2.4.2.3.4 ~~Cheraw Fault~~

~~The Cheraw fault, located in southeastern Colorado over 500 mi from CPNPP Units 3 and 4 (Figure 2.5.2-213), has been reported as having three~~

CTS-01521

surface-rupturing earthquakes within the past 25,000 years (see discussion in Subsection 2.5.1.1.4.3.7.2) (References 2.5-323 and 2.5-326). While the potential for Quaternary activity on the Meers fault was identified prior to the EPRI SOG study (Reference 2.5-322), the identification of the Cheraw fault as a capable fault did not occur until after the EPRI SOG study (References 2.5-323 and 2.5-326). As such, none of the EPRI SOG ESTs identified the Cheraw fault as a tectonic feature or seismogenic source. Despite the considerable distance between CPNPP Units 3 and 4 and the fault, the Cheraw fault is included in a screening study for CPNPP Units 3 and 4 because it was not included in the EPRI SOG model and because the low level of seismicity surrounding CPNPP Units 3 and 4 may allow for earthquakes on the Cheraw fault to contribute to hazard at CPNPP Units 3 and 4.

The seismic source characterization of the Cheraw fault used here is a conservative simplification of the Cheraw fault in the 2002 USGS National Seismic Hazard Maps (Reference 2.5-321). As discussed in Subsection 2.5.2.2.2.6, the USGS seismic source characterizations do not undergo a formal expert elicitation process and do not explicitly attempt to represent the full uncertainty of source characterizations. However, the source models are developed from the range of published literature, and source characterizations are discussed in regional working groups. As such, the USGS source model for the Cheraw fault is deemed a good representation of the potential seismic hazard contributed by the Cheraw fault.

The USGS characterization of the Cheraw fault includes alternative models of fault recurrence behavior including truncated Gutenberg-Richter and characteristic earthquake relationships. For CPNPP Units 3 and 4, the USGS characterization is simplified by assuming only a characteristic earthquake recurrence relationship parameterized by the characteristic recurrence rate and characteristic earthquake magnitude taken from the USGS parameterization of the fault (Reference 2.5-321). Uncertainty is added to the characteristic magnitude (Mw 7.0 or m_b 6.9) using a magnitude distribution of ± 0.2 Mw units about the USGS-reported magnitude with weightings of 0.2, 0.6, and 0.2 for the lowest to highest magnitude. The characteristic recurrence rate of 1.148×10^{-4} earthquakes per year (return period of 8711 years) is taken directly from the USGS model (Reference 2.5-321). The surface trace of the Cheraw fault is simplified from the USGS description of the fault by using only the endpoints of the fault trace, and the fault dip is assumed to be 90° instead of the 60° to the northwest used in the 2002 USGS hazard maps (Reference 2.5-321). These simplifications will not affect the hazard at CPNPP Units 3 and 4, given the large distance between the fault and site. Finally, a probability of activity of 1.0 is used in the characterization for CPNPP Units 3 and 4 instead of the 0.5 used in the USGS model (Reference 2.5-321) because there is conclusive evidence of Holocene fault rupture.

A summary of the seismic source characterization for the Cheraw fault is shown in Table 2.5.2-218. This characterization is implemented into the CPNPP Units 3 and 4 PSHA model as a line source extending to 15 km depth.

2.5.2.4.3 ~~New~~EPRI Ground Motion Models

CTS-01521

~~Ground motion models for the central and eastern US (CEUS) have evolved since the EPRI SOG (Reference 2.5-370) study. An EPRI project was conducted to summarize knowledge about CEUS ground motions, and results were published in an EPRI report (Reference 2.5-401).~~The EPRI ground-motion characterization (GMC) model (Reference 2.5-401) is the most current and applicable ground-motion model for the CEUS SSC (Reference 2.5-486) and is currently in use for ground motion analyses for COL applications. These ~~updated~~ equations estimate median spectral acceleration and its uncertainty as a function of earthquake magnitude and distance. Epistemic uncertainty is modeled using multiple ground motion equations with weights, and multiple estimate of aleatory uncertainty, also with weights. Different sets of equations are recommended for seismic sources that represent rifted vs. non-rifted regions of the earth's crust. Separate equations are recommended for attenuation in the stable continental region of the CEUS and for the Gulf Coast region. Equations are available for spectral frequencies at hard rock sites of 100 Hz (which is equivalent to peak ground acceleration, PGA), 25 Hz, 10 Hz, 5 Hz, 2.5 Hz, 1 Hz, and 0.5 Hz. All ground motion estimates are for spectral response with 5% of critical damping.

CTS-01521

The aleatory uncertainties published in ~~the~~ EPRI GMC ground motion model (Reference 2.5-401) were re-examined by Abrahamson and Bommer (Reference 2.5-403), because it was thought that the aleatory uncertainties in the ~~2004 EPRI report~~EPRI GMC (Reference 2.5-401) were too large, resulting in over-estimates of seismic hazard. The EPRI (Reference 2.5-403) study recommends a revised set of aleatory uncertainties and weights that can be used to replace the original EPRI (Reference 2.5-401) aleatory uncertainties. The EPRI study (Reference 2.5-403) is used in the CEUS SSC report (Reference 2.5-486).

CTS-01521

CTS-01521

A minimum moment magnitude (Mmin) of 5.0 was used per Reference 2.5-489 instead of using the modified Cumulative Absolute Velocity (CAV) model revised from Hardy et al. (Reference 2.5-404).

~~To correctly model the damageability of small magnitude earthquakes to engineered facilities, the Cumulative Absolute Velocity (CAV) model of Hardy, et al. (Reference 2.5-404) was used. The CAV model in effect filters out the fraction of small magnitude earthquakes that will not cause damage and includes in the hazard calculations only those ground motions with CAV values greater than 0.16 g-sec. The filter that is used is based on empirical ground motion records and depends on ground motion amplitude, earthquake magnitude, duration of motion (which in turn depends on earthquake magnitude), and shear wave velocity in the top 30 m at the site. The ground motions for frequencies other than 100 Hz are assumed to be correlated with the ground motions at 100 Hz, so that the filtering is consistent from frequency to frequency.~~

In summary the ground motion model used in the seismic hazard calculations for CPNPP Units 3 and 4 consisted of the median equations from EPRI GMC (Reference 2.5-401) combined with the updated aleatory uncertainties of the

CTS-01521

EPRI study (Reference 2.5-404). ~~The~~No CAV filter (Reference 2.5-404) was applied. ~~to account for the damageability of small magnitude earthquake ground motions.~~Instead an Mmin of 5.0 was applied per Reference 2.5-489. CTS-01521

2.5.2.4.4 Updated Probabilistic Seismic Hazard Analysis and Deaggregation

~~The seismic hazard at the CPNPP Units 3 and 4 site was investigated with the changes described in Subsections 2.5.2.4.2 through 2.5.2.4.3 to seismic sources, seismicity parameters, maximum magnitudes, and ground motion equations. The initial investigation was made for hard rock conditions, followed by the incorporation of site specific conditions at the CPNPP Units 3 and 4 site.~~The seismic hazard at the CPNPP Units 3 and 4 site was evaluated using the CEUS SSC (Reference 2.5-486) for the full CEUS Study Region with no refinements as discussed in Subsection 2.5.2.4.2 and the EPRI GMC model described in Subsection 2.5.2.4.3. The initial investigation was made for hard rock conditions, followed by the incorporation of site-specific conditions at the CPNPP Units 3 and 4 site. CTS-01521

A ~~probabilistic seismic hazard analysis (~~PSHA~~)~~ consists of calculating annual frequencies of exceeding various ground motion amplitudes for all possible earthquakes that are hypothesized in a region. The seismic sources specify the rates of occurrence of earthquakes as a function of magnitude and location, and the ground motion model estimates the distribution of ground motions at the site for each event. ~~Multiple weighted hypotheses on seismic sources, earthquake rates of occurrence, and ground motions (characterized by the median ground motion amplitude and its uncertainty) result in multiple weighted seismic hazard curves. The calculation is made separately for each of the six EPRI teams (as described in Subsection 2.5.2.4.1), and the seismic hazard distributions for the teams are combined, weighting each team equally. This combination gives the overall mean and distribution of rock seismic hazard at the site.~~The calculation is made for the all background and RLME sources in the CEUS SSC summarized in Subsection 2.5.2.2.1. The recurrence rates for the Charleston and NMFS RLME sources were updated for the seismic hazard calculations, based on the plant start date for the CPNPP Units 3 and 4 site. The seismic hazard distributions are combined for the overall mean and fractiles of the rock seismic hazard at the site. CTS-01521 CTS-01521
The effects of local site conditions on seismic ground motions are taken into account as described below.

~~A preliminary calculation of rock seismic hazard was made with the EPRI SOG sources plus the Meers fault and New Madrid faults, using the EPRI ground motion equations (Reference 2.5-401) with the EPRI aleatory uncertainties (Reference 2.5-403) and no CAV filter. Sensitivity studies indicated that of the faults identified in Subsection 2.5.2.4.2.3, only the New Madrid and Meers faults contributed significantly to the hazard. The other faults discussed in Subsection 2.5.2.4.2.3 (the Rio Grande Rift faults and the Cheraw fault) did not contribute 1% of the total hazard for 10 Hz and 1 Hz spectral acceleration. The preliminary calculation of hazard was done for the purpose of deaggregating the hazard. The~~ CTS-01521

CTS-01521

~~CAV filter was not used for this analysis because the CAV filter depends on site amplitude and shear wave velocity in the top 30 meters from the surface. The reason was that incoming seismic waves that might produce low amplitude rock motions and be removed by the CAV filter, might also be amplified by local soil conditions, producing higher amplitudes on soil that would not be removed by the CAV filter.~~The calculation of the rock seismic hazard was performed for the purpose of determining the uniform hazard response spectra (UHRS) for the 10^{-4}, 10^{-5}, and 10^{-6} mean hazard levels using the EPRI GMC ground motion model (Reference 2.5-401) with the EPRI aleatory uncertainties (Reference 2.5-403) and without applying a CAV filter using a minimum moment magnitude (Mmin) of 5.0 (Reference 2.5-489).

~~Figures 2.5.2-215 through 2.5.2-221 show total rock hazard as the mean, 15th, 50th, and 85th fractile curves for the EPRI SOG sources plus the Meers fault and New Madrid faults, using the EPRI ground motion equations (Reference 2.5-401) with the EPRI aleatory uncertainties (Reference 2.5-403) and no CAV filter. The total mean and fractile rock hazard curves are shown for all sources. In addition, the mean hazard from the New Madrid faults is shown (this is included in the total curves). The Meers fault and New Madrid faults dominate the hazard for frequencies of 5 Hz and lower, and contribute a significant part of the hazard for 10 Hz amplitudes and higher. One of the characteristics of the hazard curves at low spectral frequencies (2.5 Hz and lower) is that the mean rock hazard curves exceeded the 85th fractile at high ground motion amplitudes. This exceedance occurs because the New Madrid seismic source dominates the hazard, and is caused by a few EPRI ground motion equations (Reference 2.5-401) indicating relatively high hazards for the large distance between the New Madrid seismic source and the CPNPP Units 3 and 4 site.~~Figures 2.5.2-210 though 2.5.2-216 show the contribution to total mean hazard at the CPNPP Units 3 and4 site of each seismic source for the seven spectral frequencies of 0.5 Hz, 1 Hz, 2.5 Hz, 5 Hz, 10 Hz, 25 Hz, and 100 Hz (PGA). Figures 2.5.2-217 through 2.5.2-223 show the total mean, median (50th fractile), and selected fractile curves (5th, 16th, 84th, and 95th fractiles) for the seven spectral frequencies for all seismic sources at the CPNPP Units 3 and 4 site. The background sources, NMFS, and Meers fault provide significant contribution to the hazard at all frequencies, with contributions from NMFS and Meers increasing at the lower frequencies (2.5 Hz and lower). The NMFS is the most significant contributor at 0.5 Hz. One of the characteristics of the hazard curves at low spectral frequencies (2.5 Hz and lower) is that the mean rock hazard curves exceeded the 85th fractile at high ground motion amplitudes. This exceedance occurs because NMFS dominates the hazard, and is caused by a few EPRI ground motion equations (Reference 2.5-401) indicating that relatively high hazards for the large distance between NMFS and the CPNPP Units 3 and 4 site.

Figure 2.5.2-224 shows the mean and median 10^{-4}, 10^{-5}, and 10^{-6} UHRS for hard rock conditions, based on the seven ground motion frequencies for which ground motion estimates are available. Numerical values of the mean and median UHRS are presented in Table 2.5.2-204.

The rock seismic hazard was deaggregated following the guidelines of Regulatory Guide 1.208 (2007). Mean contributions to the seismic hazard were deaggregated for magnitude and distance as recommended in Regulatory Guide 1.206 (2007). Deaggregations for 5 and 10 Hz were combined, as well as for 1 and 2.5 Hz. Figures 2.5.2-225 through 2.5.2-230 show the combined deaggregations of the mean hazard for the 10^{-4}, 10^{-5}, and 10^{-6} hard rock ground motions. The contribution of the NMFS, located at approximately 540 mi (870 km) from the site, is evidenced in the deaggregation figures in the last distance intervals, which represent 186+ mi (300+ km). CTS-01521

~~Figure 2.5.2-222 shows the mean and median 10^{-4} and 10^{-5} UHRS for hard rock conditions, based on the seven ground motion frequencies for which ground motion estimates are available. Numerical values for the mean UHRS are shown in Table 2.5.2-219.~~

~~The seismic hazard was deaggregated following the guidelines of Regulatory Guide 1.208 (USNRC, 2007). Specifically, the mean contributions to seismic hazard for 5 Hz and 10 Hz hazards were deaggregated by magnitude and distance for the mean 10^{-4} ground motions at 5 Hz and 10 Hz, and these deaggregations were combined. Figure 2.5.2-223 shows this combined deaggregation. Similar deaggregations of the mean hazard were performed for 1 and 2.5 Hz spectral accelerations (Figure 2.5.2-224). Deaggregations of the mean hazard for 10^{-5} and 10^{-6} ground motions are shown in Figures 2.5.2-225 through 2.5.2-228. Deaggregation of the mean seismic hazard is recommended in Regulatory Guide 1.206 (USNRC, 2007). The contribution of the New Madrid source to seismic hazard is plotted in the deaggregation figures in the last distance interval, which represents 400+ km; the New Madrid source is actually about 870 km from the Comanche Peak site.~~

Figures 2.5.2-22~~3~~5 through 2.5.2-2~~28~~30 include the contribution to hazard by epsilon, which is the number of logarithmic standard deviations that the applicable ground motion (10^{-4}, 10^{-5}, or 10^{-6}) is above the logarithmic mean. ~~These figures indicate that the largest contribution to hazard for 10^{-4} and 10^{-5} ground motions comes from values between 0 and 2 standard deviations above the mean, which is a common result.~~These figures indicate that the largest contribution to hazard for 10^{-4} and 10^{-5} ground motions comes from values between 0 and 2 standard deviations, which is a common result.

The deaggregation plots in Figures 2.5.2-225 through 2.5.2-228 for 10^{-4} and 10^{-5} ground motions indicate that the Meers fault and NMFS are major contributors to seismic hazard at the Comanche Peak site. For the 10^{-4} and 10^{-5} annual frequency, these sources are the largest contributors to seismic hazard for both 5 and 10 Hz (Figures 2.5.2-225 and 2.5.2-227) and 1 and 2.5 Hz (Figures 2.5.2-226 and 2.5.2-228). For the annual frequency of 10-6, most of the hazard at high frequencies comes from local sources (Figure 2.5.2-229), while low frequencies are still dominated by the NMFS (Figure2.5.2-230). All of these observations are

consistent with Figures 2.5.2-211 through 2.5.2-216, when observing the contribution to hazard from the Meers fault and the NMFS. CTS-01521

~~The deaggregation plots in Figures 2.5.2-223 through 2.5.2-228 for 10^{-4} and 10^{-5} ground motions indicate that the Meers fault and New Madrid faults have major contributions to seismic hazard at the Comanche Peak site. For 10^{-4} annual frequency of exceedance, these sources are the largest contributors to seismic hazard for both 5 and 10 Hz (Figure 2.5.2-223) and 1 and 2.5 Hz (Figure 2.5.2-224). For an annual frequency of 10^{-5}, the Meers fault and New Madrid faults are also dominant contributors to seismic hazard, even for high frequencies (Figures 2.5.2-225 and 2.5.2-226). For an annual frequency of 10^{-6}, most of the hazard at high frequencies comes from local sources (Figure 2.5.2-227), while low frequencies still have a dominant contributions from the New Madrid faults (Figure 2.5.2-228). All of these observations are confirmed qualitatively in Figures 2.5.2-217 through 2.5.2-220, which compare the hazard from the Meers fault and the New Madrid faults to the hazard from all sources for 10, 5, 2.5, and 1 Hz.~~

~~Table 2.5.2-220~~Table 2.5.2-205 summarizes the mean magnitude and distance resulting from these deaggregations, for all contributions to hazard and for contributions with distances exceeding 100 km. For the 1 and 2.5 Hz results, contributions from events with R>100 km exceed 5% of the total hazard. As a result, following the guidance of RG1.208, the controlling earthquake for low-frequency ground motions was selected from the R>100 km calculation, and the controlling earthquake for high-frequency ground motions was selected from the overall calculation. The values of Mw and R selected in this way are shown in shaded cells in ~~Table 2.5.2-220~~Table 2.5.2-205. CTS-01521

~~Tables 2.5.2-221~~Tables 2.5.2-206 through ~~2.5.2-226~~2.5.2-211 document the deaggregation of seismic hazard for the following deaggregations: 10^{-4} high frequencies, 10^{-4} low frequencies, 10^{-5} high frequencies, 10^{-5} low frequencies, 10^{-6} high frequencies, and 10^{-6} low frequencies.

Smooth rock UHRS were developed from the UHRS amplitudes in ~~Table 2.5.2-219~~Table 2.5.2-204, using controlling earthquake Mw and R values shown in ~~Table 2.5.2-220~~Table 2.5.2-205 and using the hard rock spectral shapes for CEUS earthquake ground motions recommended in NUREG/CR-6728. Separate spectral shapes were developed for high frequencies (HF) and low frequencies (LF). In order to accurately reflect the UHRS values calculated by the PSHA as shown in ~~Table 2.5.2-220~~Table 2.5.2-205, the HF spectral shape was anchored to the UHRS values from ~~Table 2.5.2-220~~Table 2.5.2-205 at 100 Hz, 25 Hz, 10 Hz, and 5 Hz. In between these frequencies, the spectrum was calculated using shapes anchored to the next higher and lower frequency and weighting those shapes. The weighting was based on the inverse logarithmic difference between the intermediate frequency and the next higher or lower frequency. This technique provided a smooth, realistic spectral shape at these intermediate frequencies. Below 5 Hz, the HF shape was extrapolated from 5 Hz. CTS-01521 CTS-01521 CTS-01521

For the LF spectral shape a similar procedure was used except that the LF spectral shape was anchored to the UHRS values at all seven ground motion frequencies for which hazard calculations were made (100 Hz, 25 Hz, 10 Hz, 5 Hz, 2.5 Hz, 1 Hz, and 0.5 Hz). Anchoring the LF spectral shape to all frequencies was necessary because otherwise the LF spectral shape exceeded the HF spectral shape at high frequencies. The use of a LF shape with amplitudes higher than the HF UHRS amplitudes would not be appropriate because this would overdrive the soil column. Anchoring the LF spectrum to the UHRS amplitudes at all frequencies ensures that appropriate ground motions are represented. The lack of fit of the LF spectral shape to the HF UHRS amplitudes results from distant, large earthquakes that contribute to seismic hazard at this site, with ground motion ε values greater than unity. In these cases, the spectral shapes of NUREG/CR-6728 are not appropriate and the LF spectrum needs to be anchored to the HF UHRS amplitudes.

Figures 2.5.2-~~229~~231 through 2.5.2-~~231~~233 show the smooth horizontal HF and LF UHRS calculated in this way for 10^{-4}, 10^{-5}, and 10^{-6} annual frequencies of exceedance, respectively. As mentioned previously, these spectra accurately reflect the UHRS amplitudes in Table 2.5.2-219 that were calculated for the seven spectral frequencies at which PSHA calculations were done. Because the HF and LF spectra were scaled to the same high-frequency amplitudes, they are very similar at high frequencies and differ only for frequencies below 5 Hz. As a result of these similarities, a broad-banded spectrum was used as input to site response calculations, using the envelope of the HF and LF spectra shown in Figures 2.5.2-~~229~~231 through 2.5.2-~~231~~233. CTS-01521

CTS-01521

2.5.2.5 Seismic Wave Transmission Characteristics of the Site

CP COL 2.5(1) ~~Replace the content of~~Add the following at the end of DCD Subsection 2.5.2.5 with the following. CTS-01521

The subsurface conditions necessary to predict and model the seismic wave transmission characteristics for CPNPP Units 3 and 4 were determined from both site-specific and regional data. These data included both stratigraphic and representative shear and compressional wave measurements that were used to develop the site profile and are summarized in ~~Table 2.5.2-227~~Table 2.5.2-212. A detailed discussion of the data and methodology for developing the stratigraphy and corresponding dynamic properties used to define the dynamic profile for the site is provided in Subsection 2.5.4.4.2.2. CTS-01521

The profile is divided into the shallow profile (surface to about 500 ft) and the deep profile (about 500 ft to “basement”). The shallow profile represents depth to which extensive characterization has been performed. The lateral and vertical control on the subsurface strata (layering) was defined primarily on lithology and material properties. The velocity measurements in the shallow profile have been developed from 15 suspension logs from borings drilled as part of the foundation exploration described in Subsection 2.5.4.4.2.1.

The foundation basemats of all seismic Catergory I structures will be founded on or embedded in a limestone unit (denoted as Layer C in Subsection 2.5.4). Excavation to Layer C will remove the shallower units (layers A, B1, and B2) and, where the top of Layer C is below the bottom of the elevation, fill concrete will be placed to achieve the bottom of basemat elevation. The average thickness of Layer C is greater than 60 ft and dips less than 1°. The average shear wave velocity of Layer C is greater than 5800 ft/sec, as determined from the 15 suspension log borings. Profiles for development of the GMRS and FIRS are detailed in Subsection 2.5.2.6 and provide the criteria for exclusion or inclusion of specific layers including fill concrete and compacted fill. CTS-01521

The deep profile was characterized from regional wells and maps. Strata that define the deep profile are based primarily on lithology and stratigraphic surfaces projected to the CPNPP site to estimate the elevation. Velocity data for the deep profile was limited to only a few wells and consisted primarily of compressional wave velocities except where shear wave velocity data was available from a single well as discussed in the following section on uncertainties. Basement was defined as the depth at which a shear wave velocity of 9,200 ft/sec and greater was achieved. Basement was therefore defined as the top of the Ellenburger limestone located at a depth of about 5,300 ft at the site. The Ellenburger is a regionally extensive unit with an estimated shear wave velocity of nearly 11,000 ft/sec. CTS-01521 CTS-01521

2.5.2.5.1 Aleatory and Epistemic Uncertainty

The shallow profile has been extensively characterized from over 150 geotechnical borings and geologic mapping of the area. The profile has been stratified based on vertical changes in lithology that can be mapped laterally from boring to boring. Standard deviations for the top of each shallow profile layer are less than 2 ft for the upper 200 ft of the profile. The standard deviation for the layers defining the shallow profile from about 200 ft to about 500 ft range from about 1 to 5 ft. Velocity data for the shallow profile acquired from 15 suspension borings demonstrated a strong correlation between the layering and places where simulated down-hole travel time gradient “breaks” occurred.

The deep profile was developed from regional wells and results in a higher uncertainty in both the layering (stratigraphy) and velocity measurements. Shear wave velocity measurements were available from a single well located about 6 mi from the site and were limited to the Barnett Shale (a shale unit at a depth of about 5,000 ft) for a total depth interval of about 4,000 ft (about 5,000 ft depth to about 9,000 ft depth). This data was used to develop a linear extrapolation to estimate shear wave velocity from available pressure wave velocities from other wells to complete the deep profile. Thus, the epistemic uncertainty for the deep profile is much greater than for the shallow profile. See Subsection 2.5.4.4.2.2 for detailed discussion. CTS-01521

The deep profile lacks a statistical basis for estimating a robust standard deviation for all layer velocities. The coefficient of variation (CoV=standard deviation/mean)

calculated as 31% for the Atoka formation demonstrated the highest CoV for all deep profile layers. Therefore, the variability in velocity was calculated at 31% for all deep profile layers. The velocity range for the shallow profile was defined as 25% of the mean velocity of each layer. Subsection 2.5.4.4.2.2 provides a detailed discussion of the data and methodology for development of the dynamic profile.

~~Table 2.5.2-227~~Table 2.5.2-212 summarizes the layer properties including depth, thickness, velocities and assigned variabilities based on the aleatory and epistemic uncertainties discussed. CTS-01521

2.5.2.5.2 Description of Site Response Analysis

The site response analysis was conducted in three steps that are common to analyses of this type. First, the site geology and geotechnical properties were reviewed and used to generate multiple synthetic profiles of site characteristics. Second, sets of rock spectra were selected to represent rock ground motions corresponding to mean annual exceedence frequencies of 10^{-4}, 10^{-5}, and 10^{-6}. Finally, site response was calculated using an equivalent-linear technique, using the multiple synthetic profile and the sets of rock spectra representing input motions. These three steps are described in detail in the following sections.

2.5.2.5.2.1 Generation of Synthetic Profiles

To account for the epistemic and aleatory uncertainties in the site's dynamic properties, 60 synthetic profiles were generated using the stochastic model developed by Toro (Reference 2.5-432), with some modifications to account for the conditions at the Comanche Peak site. These synthetic profiles represent the site column from the top of the bedrock to the ~~elevations where the GMRS and the various FIRS are defined (see Subsection 2.5.2.6)~~ground surface. Bedrock is defined as having a shear-wave velocity of 9,200 fps, in order to achieve consistency with the 2004 EPRI ~~attenuation equations~~GMC model used for the rock hazard calculations (Reference 2.5-401). For each site column, this stochastic model uses as inputs the following quantities: (1) the median shear-wave velocity profile, which is equal to the base-case profile given in ~~Table 2.5.2-227~~Table 2.5.2-212; (2) the standard deviation of ln(Vs) (the natural logarithm of the shear-wave velocity) as a function of depth, which is calculated from the values in ~~Table 2.5.2-227~~Table 2.5.2-212; (3) the correlation coefficient between ln(Vs) in adjacent layers, which is taken from generic results for rock in Toro (Reference 2.5-432). Layer thickness was not randomized because the site's stratigraphy is very uniform. CTS-01521 CTS-01521 CTS-01521 CTS-01521

The correlation coefficient between ln(Vs) in adjacent layers is estimated using the inter-layer correlation model from Toro (Reference 2.5-432) for USGS category A. In the log-normal randomization model used to calculate the synthetic Vs for each layer, it is possible for the synthetic Vs in the deeper formations to be greater than 9,200 fps. When this happens for a certain synthetic profile, the randomization scheme sets that Vs to 9,200 fps and defines the corresponding depth to be the depth to bedrock for that synthetic profile.

~~Figure 2.5.2-240 illustrates the Vs value for the first 10 synthetic profiles for the GMRS/FIRS1 site column. Figure 2.5.2-241 compares the median of these 60 Vs profiles to the Vs ±1 sigma Variability values given in Table 2.5.2-227, indicating excellent agreement. The difference in the mean +sigma values below 800 m is a consequence of imposing the 9200 fps upper bound dictated by the bedrock Vs(see above). Figures 2.5.2-242 and 2.5.2-243 show analogous results for top portion the FIRS4 site column.~~Figure 2.5.2-234 illustrates the Vs value for the first ten synthetic profiles for the FIRS3 site column (which is the Performance Based Surface Response Spectrum PBSRS site column for GMRS/FIRS1/FIRS2). Figure 2.5.2-235 compares the logarithmic mean of the sixty Vs profiles for FIRS3 to the logarithmic (mean ±1 sigma) variability values given in Table 2.5.2-212, indicating excellent agreement. The calculated mean+sigma from the artificial profiles (black line) is lower than the target mean+sigma at depths greater than 2,600 ft because of imposing the 9,200 fps upper bound dictated by the bedrock as implicit in the EPRI GMC model (Reference 2.5-401). The differences between 430 and 2,600 ft depth are a consequence of statistical variations (sample size of 60) and are not a cause for concern. Figures 2.5.2-236 through 2.5.2-239 show analogous results for top portion the FIRS3_COV50 and FIRS4_SCSR(which is the PBSRS site column corresponding to FIRS4) site columns. CTS-01521

The best-estimate values for the damping ratio and for the stiffness degradation (G/Gmax) are given in ~~Table 2.5.2-227~~Table 2.5.2-212. ~~Except for the fill at the top of the FIRS4 soil column, materials are assumed to behave linearly (strain-independent), with constant damping and G/Gmax=1.~~ The uncertainty in damping is specified as 35%, (following the generic values in EPRI, Reference 2.5-387) and the uncertainty in G/Gmax for fill is specified as 15% at $3x10^{-3}$% strain (following the generic values given by Costantino, Reference 2.5-433). The correlation coefficient between ln(G/Gmax) and ln(damping) of the fill is specified as -0.75. This implies that in synthetic profiles where the fill has higher than average G/Gmax, the fill tends to have lower than average damping. The degradation and damping properties are treated as fully correlated among layers in the same geological unit, but independent between different units. ~~Figure 2.5.2-244 shows the damping ratios for the Strawn formation in the 60 synthetic profiles corresponding to FIRS1. Similarly, Figure 2.5.2-245 shows the G/Gmax and damping ratios for the 60 synthetic profiles corresponding to FIRS4. A sensitivity study that evaluates the effect of using strain dependent shear modulus degradation (G/Gmax) and damping ratio, instead of using constant shear modulus degradation (G/Gmax =1) and constant damping ratio. Results from this study indicate that the spectra at the top of the profile obtained with the constant material properties are slightly higher than those obtained with strain dependent properties. The profile with constant material properties was used to develop all FIRS (GMRS/FIRS1, FIRS2, FIRS2, FIRS4, and FIRS4_CoV50), as presented in Subsection 2.5.2.6, and to develop the inputs for the SSI analysis in Subsection 3.7.2.4.1.~~Figure 2.5.2-240 shows the G/Gmax and damping ratio curves for the rock materials in the sixty synthetic profiles. Similarly, Figure 2.5.2-241 shows the G/Gmax and damping ratio curves for the granular fill. Strain-dependent properties were used to develop all FIRS (GMRS/FIRS1/FIRS2, FIRS1_COV50/FIRS2_COV50, and FIRS4) and all corresponding PBSRS (FIRS3 CTS-01521 CTS-01521

and FIRS4_SCSR), as presented in Subsection 2.5.2.6. These profiles were then used as the basis for development of the strain compatible profiles for the site-specific SSI analyses in Subsection 3.7.1.3. The control motion time histories used as input for the embedded foundation SSI analyses are developed in Subsection 3.7.1 per the NEI guidelines in Reference 2.5-490. CTS-01521

Each set of ~~60~~sixty synthetic profiles, consisting of Vs and unit weight vs. depth, depth to bedrock, stiffness, and damping curves, is used to calculate and quantify site response and its uncertainty, as described below.

2.5.2.5.2.2 Selection of Rock Input Motions

Rock input motions were selected for input to the site response calculations using the seismic hazard results presented in Subsection 2.5.2. Uniform hazard response spectra (UHRS) for rock conditions corresponding to mean annual exceedence frequencies of 10^{-4}, 10^{-5}, and 10^{-6} were used. The base spectrum for each mean annual exceedence frequency was a broad-banded (BB) spectrum, because deaggregation and fitting of high-and low-frequency (HF and LF) spectra indicated the same high-frequency amplitudes. These spectra are plotted in Figures 2.5.2-~~229~~231 through 2.5.2-~~231~~233 and are given in tabular form in ~~Table 2.5.2-219~~Table 2.5.2-204. The development of these spectra is documented in Subsection 2.5.2.4.4. ~~The effect of choosing a broad-banded spectrum was investigated by also computing response to the 10^{-4} HF spectrum, and comparing that response to the 10^{-4} BB spectrum, as described in the next subsection.~~The effect of choosing a broad-banded (BB) spectrum was investigated by also computing response to the 10^{-4}, 10^{-5}, and 10^{-6} HF spectra, and comparing those to the 10^{-4}, 10^{-5}, and 10^{-6} BB spectra, as described in the next subsection. CTS-01521

2.5.2.5.2.3 Site Response Calculations

The site response calculations for Comanche Peak were performed using the Random Vibration Theory (RVT) approach. In many respects, the inputs and assumptions are the same for an RVT analysis and for a time-history based analysis (e.g., an analysis with the program SHAKE, Reference 2.5-434). Both the RVT and time-history (SHAKE, Reference 2.5-434) procedures use a horizontally-layered half-space representation of the site and use an equivalent-linear representation of dynamic response to vertically propagating shear waves. Starting from the same inputs (in the form of response spectra), both procedures will lead to similar estimates of site response (see, for example, Rathje and Ozbey, Reference 2.5-435). The main advantage of the RVT approach is that it does not require the spectral matching of multiple time histories to a given rock response spectrum. Instead, the RVT approach uses a probabilistic representation of the ensemble of all input motions corresponding to that given response spectrum and then calculates the response spectrum of the ensemble of dynamic responses.

~~Site response calculations were performed for the three broad banded (BB) bedrock motions, and for the 10^{-4} HF motion,as described in the previous section.~~Site response calculations were performed for 10^{-4}, 10^{-5}, and 10^{-6} BB bedrock motions (5% damping) with sensitivity analyses performed for the 10^{-4}, 10^{-5}, and 10^{-6} HF bedrock motions (5% damping), as described in the previous section. CTS-01521

In addition to the rock response spectra, the RVT site-response calculations require the following inputs: (1) the strong-motion duration associated with each rock spectrum; and (2) the equivalent-strain ratio to use in the equivalent-linear calculations (this input is required for both the time-history and RVT approaches) and depends on magnitude. The duration is calculated from the de-aggregation results in Subsection 2.5.2.4.4 (~~Table 2.5.2-220~~Table 2.5.2-205), using standard seismological relations between magnitude, seismic moment, corner frequency, and duration (see, for example, Rathje and Ozboy, Reference 2.5-435) and using stress-drop and crustal Vs values typical of the eastern United States. The effective strain ratio is calculated using the expression (M-1)/10 (Reference 2.5-434). Values smaller than 0.5 or greater than 0.65 were brought into the 0.5-0.65 range, which is the range recommended by Kramer (Reference 2.5-436). The calculated values of duration and effective strain ratio are given in ~~Table 2.5.2-230~~Table 2.5.2-213. CTS-01521 CTS-01521

For each site column and each rock-motion input, separate site response calculations were performed for the corresponding 60 synthetic profiles. These results for each combination of input motion and site column were then used to calculate the logarithmic mean and standard deviation of the amplification factor.

~~Results for the various site columns, and for the 10^{-4}, 10^{-5}, and 10^{-6} BB inputs, are given in Figures 2.5.2-233 and 2.5.2-235 through 2.5.2-238. Tabular results are provided in Tables 2.5.2-231 through 2.5.2-235.~~ CTS-01521

~~Figure 2.5.2-253 and Figure 2.5.2-254 present the peak strain in the upper 500 ft of the GMRS/FIRS1 soil column for the $1x10^{-4}$ and $1x10^{-5}$ broad band (BB) spectra, respectively. The maximum value of the logarithmic mean strain (over the 60 synthetic profiles) in the entire GMRS/FIRS1 profile for the $1x10^{-4}$ spectrum is approximately 0.0035% ad occurs at a depth of approximately 390 ft in the profile. The maximum value of the logarithmic mean strain in the entire GMRS/FIRS1 profile for the $1x10^{-5}$ spectrum is approximately 0.0075% and also occurs at a depth of approximately 390 ft in the profile.~~

~~Figure 2.5.2-255 and Figure 2.5.2-256 present the peak strain in the upper 50 ft of the FIRS4 soil column for the $1x10^{-4}$ broad band (BB) spectra, respectively. As described in FSAR Subsection 2.5.2.6, the FIRS4 site profile consists of compacted fill overlying the stiff limestone that is the outcrop of the GMRS/FIRS1 profile. As such, the peak strains within most of the FIRS4 profile are similar to the peak strains within the GMRS/FIRS1 profile with the exception of peak strains within the fill (i.e., the upper 40 ft).~~

CTS-01521

~~Therefore, Figure 2.5.2-255 and Figure 2.5.2-256 only show the peak strains within the upper 50 ft of the FIRS4 profile. The maximum value of the logarithmic mean strain in the FIRS4 profile for the $1x10^{-4}$ spectrum is approximately 0.006% and occurs at depths of approximately 17 and 37 ft in the profile. The maximum value of the logarithmic mean strain in the FIRS4 profile for the $1x10^{-5}$ spectrum is approximately 0.016% and also occurs at depths of approximately 17 and 37 ft in the profile.~~

~~The logarithmic mean value of the peak strain in the fill is approximately 0.03% for the 10^{-6} inputs.~~

~~In addition, Figure 2.5.2-246 compares the median amplification factors obtained for GMRS/FIRS1 site column using the 10^{-4} HF and BB rock inputs. Although Figure 2.5.2-246 shows that the BB spectrum gives larger amplification factors for frequencies above 3 Hz, the effect of this difference on the 10^{-4} site hazard will be negligible because most of the 10^{-4} hazard at all frequencies comes from distant events (see Figures 2.5.2-223 and 2.5.2-224). These distant events will generate a BB rock spectrum. The effect of a difference in amplification factors at 10^{-5} would be somewhat larger (and would result in lower mean site spectra) because roughly 40% of the 10^{-5} hazard comes from local, small magnitude events (see Figures 2.5.2-225 and 2.5.2-226). As a result, use of the BB amplification factors for all magnitude-distance combinations in the soil hazard calculations (Subsection 2.5.2.6.1.1) yields slightly conservative hazard results at 10^{-5}, resulting in slightly conservative estimates of the design spectrum.~~Site response calculations using FIRS3 site column were used to generate the median amplification factors and logarithmic sigmas for GMRS/FIRS1 (equivalent to FIRS2). FIRS3 itself is the Performance Based Surface Response Spectrum (PBSRS) for GMRS/FIRS1 and FIRS2. Equivalently, FIRS3_COV50 site column was used for FIRS1_COV50 and FIRS2_COV50. Calculations using FIRS4_SCSR (PBSRS for FIRS4) site column were used to generate the median amplification factors and logarithmic sigmas for FIRS4.

Figures 2.5.2-242 and 2.5.2-243 provide the GMRS/FIRS1 profile (equivalent to FIRS2) and FIRS3 (PBSRS for GMRS/FIRS1 and FIRS2) profile median amplification factors and logarithmic sigmas, respectively, using the BB bedrock inputs in graphical form comparing between the two cases where the Vs of the granular fill material (included in the full soil column analysis for GMRS/FIRS and FIRS2) had a coefficient of variation (CoV) of 30% and 50% (designated as _COV50). The median amplification factors is the same for the cases where the granular fill material has a CoV of 30% compared to the 50%. The differences in logarithmic sigmas are minor and generally in the mid-frequency range (2.5 Hz to 15 Hz). Figures 2.5.2-244 and 2.5.2-245 present the amplification factors and logarithmic sigmas for FIRS4 and FIRS4_SCSR (PBSRS for FIRS4) profiles, respectively. Tabular results are provided in Tables 2.5.2-214 through 2.5.2-219 for each profile.

Figures 2.5.2-246 through 2.5.2-254 present the maximum shear strain profiles in the upper 500 feet of all the FIRS profiles and for the 10^{-4}, 10^{-5}, and 10^{-6} BB spectra. The maximum logarithmic mean shear strain (over the sixty synthetic profiles) for the FIRS3 site column (full site column for GMRS/FIRS1 and FIRS2), shown in Figures 2.5.2-246 through 2.5.2-248, has a peak value of about 0.06%. For the FIRS3_COV50 site column (full site column for FIRS1_COV50and FIRS2_COV50), shown in Figures 2.5.2-249 through 2.5.2-251, the maximum logarithmic mean shear strain value also has a peak value of 0.06%. For the FIRS4_SCSR site column (full site column for FIRS4), shown in Figures 2.5.2-252 through 2.5.2-254, the maximum logarithmic mean shear strain has a peak value of 0.05%. For all the FIRS profiles, the maximum shear strain occurs within the granular fill material in the upper 40 feet of the soil column. CTS-01521

In addition, Figures 2.5.2-255 through 2.5.2-260 present the comparison of the median amplification factors obtained for all the FIRS(GMRS/FIRS/FIRS2, FIRS1_COV50/FIRS2_COV50, FIRS3, FIRS3_COV50, FIRS4, and FIRS4_SCSR) using the 10^{-4}, 10^{-5}, and 10^{-6} HF and BB rock inputs. The HF rock input median amplification factors are either lower than or equal to the BB rock input median amplification factors in all the cases. There is little high-frequency energy in the soil motion (as indicated by the relatively flat character of the HF spectra above about 3 Hz). This is particularly true for the 10^{-4} results since the most of the hazard at all frequencies comes from distant events, as summarized in Table 2.5.2-213. Additionally, Table 2.5.2-213 indicates that the 10^{-5} and 10^{-6} hazards come from more local, smaller magnitude events. Use of the BB amplification factors for all magnitude-distance combinations yield conservative hazard results at 10^{-5} and 10^{-6}.

2.5.2.6 Ground Motion and Site Response Analysis

CP COL 2.5(1) Replace the content of DCD Subsection 2.5.2.6 with the following.

Four FIRS have been identified for the CPNPP Units 3 and 4 and are calculated for both the Safe Shutdown Earthquake (SSE) and Operating Basis Earthquake (OBE) where OBE=(1/3)SSE. The SSE is the envelope of the GMRS and the minimum earthquake requirements of 10 CFR 50 Appendix S, based on the shape of the Certified Site Design Response Spectra (CSDRS) scaled down to a PGA of 0.1 g. The CSDRS is itself a modified RG 1.60 shape formed by shifting the control points at 9 Hz and 33 Hz to 12 Hz and 50 Hz, respectively.

2.5.2.6.1 Ground Motion Response Spectrum (GMRS)

All category 1 structures as well as the Turbine Building Pedestal will be founded directly on or embedded in a stiff limestone (Layer C) at, or slightly above or below elevation 782 ft. Thus the GMRS/FIRS1 (referred to hereafter as GMRS) represents the top of stiff limestone (Layer C) at, or slightly above or below, foundation basemat elevation for the following safety-related ~~and seismic Category II~~ structures: CTS-01521

- Reactor Building Complex
- Ultimate Heat Sink Related Structures
- Turbine Building Pedestal
- ~~Auxiliary Building~~
- Essential Service Water Pipe Tunnel
- Essential Service Water Pipe Tunnel integrated to the Reactor Building Complex and also known as the Essential Service Water Pipe Chase
- Essential Service Water Pipe Tunnel integrated to the UHSRS
- East and West Power Source Fuel Storage Vaults
- East and West Power Source Buildings

CTS-01521

CTS-01521

In some cases, slight amounts of over-excavation will be required below the planned foundation subgrade elevations to reach the stiff limestone (Layer C). In these cases, a relatively thin layer of fill concrete will be placed on the cleaned limestone sub-excavation and extended to the foundation subgrade elevation. The thickness of the fill concrete will potentially range from about 0 ft to less than ~~2~~4 ft.

CTS-01521

Ground motion response spectra (GMRS) were calculated for horizontal and vertical motion by the methods discussed below.

2.5.2.6.1.1 Horizontal GMRS Spectrum

A seismic hazard calculation was made using the site amplification factors for the GMRS elevation, which is elevation 782 ft (top of Layer C). Figure 2.5.2-~~233~~242 shows the median amplification factor (AF) and logarithmic standard deviation of AF for this elevation, using broad-banded input motions (the envelope of the spectra in Figures 2.5.2-~~229~~231 through 2.5.2-~~231~~233). This calculation was made at the seven spectral frequencies at which ground motion equations were available from the 2004 EPRI study (Reference 2.5-401) (100 Hz, 25 Hz, 5 Hz, 2.5 Hz, 1 Hz, and 0.5 Hz).

CTS-01521

CTS-01521

The seismic hazard for horizontal motion was calculated by integrating the horizontal amplification factors shown in Figure 2.5.2-~~233~~242 with the rock hazard ~~and applying the CAV filter~~and using a minimum moment magnitude (Mmin) of 5.0 (Reference 2.5-489). This corresponds to Approach 3 in NUREG/CR-6769.

CTS-01521

The horizontal GMRS was developed from the horizontal UHRS using the approach described in ASCE/SEI Standard 43-05 (Reference 2.5-371) and Regulatory Guide 1.208. The ASCE/SEI Standard 43-05 (Reference 2.5-371)

approach defines the GMRS using the site-specific UHRS, which is defined for Seismic Design Category SDC-5 at a mean 10^{-4} annual frequency of exceedance. The procedure for computing the GMRS is as follows.

For each spectral frequency at which the UHRS is defined, a slope factor A_R is determined from:

$$A_R = SA(10^{-5})/SA(10^{-4}) \qquad \text{(Equation 5)}$$

where $SA(10^{-4})$ is the spectral acceleration SA at a mean UHRS exceedance frequency of 10^{-4}/yr (and similarly for $SA(10^{-5})$). A design factor (DF) is defined based on A_R, which reflects the slope of the mean hazard curve between 10^{-4} and 10^{-5} mean annual frequencies of exceedance. The DF at each spectral frequency is given by:

$$DF = 0.6(A_R)^{0.80} \qquad \text{(Equation 6)}$$

and

$$GMRS = \max[SA(10^{-4}) \times \max(1, DF), 0.45 \times SA(10^{-5})] \qquad \text{(Equation 7)}$$

The derivation of DF is described in detail in the Commentary to ASCE/SEI Standard 43-05 and in Regulatory Guide 1.208.

~~For the CPNPP Units 3 and 4 site, the horizontal hazard curves for GMRS elevation roll over at low amplitudes to an annual frequency of exceedance less than 10^{-4}. This means that the frequency of damaging ground motions is less than 10^{-4}. Under these conditions, the GMRS is calculated from Equation 7 above as 0.45 x $SA(10^{-5})$. Table 2.5.2-228~~Table 2.5.2-220 shows the 10^{-4} and 10^{-5} ground motion at the seven spectral frequencies for which ground motion equations are available, and shows the GMRS ~~calculated as 0.45 x $SA(10^{-5})$~~.

CTS-01521

CTS-01521

~~Figure 2.5.2-234 shows the horizontal GMRS spectrum taken from Table 2.5.2-228, plotted with the horizontal DCD spectrum.~~Figure 2.5.2-261 shows the horizontal GMRS spectrum taken from Table 2.5.2-220, plotted with the minimum horizontal DCD spectrum as discussed in Section 3.7.1. This figure shows that the GMRS at the seven spectral frequencies at which ground motion equations were available from the ~~2004~~ EPRI GMC ground motion study (Reference 2.5-401) is enveloped by the DCD spectrum.

CTS-01521

~~The horizontal 10^{-5} and GMRS spectra were calculated at 39 frequencies between 0.1 Hz and 100 Hz for the GMRS elevation. This spectral frequency range encompasses all the energy of the rock ground motions for earthquakes in the Central and Eastern United States and meets the requirements in Subsection 3.4 "Hazard Assessment" in item C "Regulatory Position" of Regulatory Guide~~

CTS-01521

~~1.208. The natural frequency of the GMRS soil column is 0.29 Hz. Because of the very flat appearance of the spectra at the seven spectral frequencies at which hazard calculations were made, log-log interpolation between available hazard values was used, with the exception of the following frequency ranges.~~ CTS-01521

~~1 Hz to 5Hz: Within this frequency range, a peak in site spectra occurs at 2.5 Hz, reflecting a site amplification at about 2 Hz. To reflect this amplification, the 10^{-5} spectral amplitude at 2.5 Hz was broadened using rock spectral shapes from NUREG/CR-6728 and using the broad-banded values of M=7.5 and R=650 km for 10^{-5} (on which the site amplification calculations were based). This is an acceptable approximation given that the rock spectrum is decreasing between 2.5 and 1 Hz.~~

~~0.5 Hz to 0.1 Hz: Below 0.5 Hz, the site-specific spectral shape determined during site amplification calculations was used to extrapolate to 0.1 Hz. This spectral shape was determined from the 10^{-5} surface spectrum at the GMRS elevation, using the 10^{-5} rock input motion. This spectral shape between 0.5 Hz and 0.1 Hz was used to extrapolate the GMRS from 0.5 Hz to 0.1 Hz. The GMRS shape at long periods is thereby consistent with the site-specific amplification calculation for the GMRS elevation.~~

~~The horizontal GMRS and 10^{-5} spectra are plotted in Figure 2.5.2-247, and the numerical values of the spectra are shown in Table 2.5.2-236.~~

~~The smooth horizontal GMRS spectrum is plotted in Figure 2.5.2-257 along with the respective DCD spectrum. This figure shows that the GMRS spectrum is enveloped by the DCD.~~The smoothing of the GMRS spectra is performed by calculating the horizontal GMRS/FIRS at 335 spectral frequencies between 0.1 Hz and 100 Hz. The spectral frequency range encompasses all the energy of the rock ground motions for earthquakes in the Central and Eastern US and meets the requirements in Subsection 3.4 "Hazard Assessment" in item C "Regulatory Position" of the Regulatory Guide 1.208. The natural frequency of the GMRS soil column is 0.28 Hz.

A log-log interpolation is used to fit the site-specific soil spectral shapes obtained from the site response calculations in Subsection 2.5.2.5.2.3 between the seven computed spectral amplitudes from 100 Hz to 0.5 Hz. Below 0.5 Hz, the site-specific soil spectral shapes were used to extrapolate to 0.1 Hz, by anchoring the extrapolated tail to the computed GMRS spectral acceleration at 0.5 Hz. The GMRS shape at long periods is thereby consistent with the site amplification calculation for the GMRS elevation. The smooth horizontal GMRS spectrum is plotted in Figure 2.5.2-262 along with the minimum horizontal DCD spectrum, the horizontal DCD acceleration time histories scaled by one third. Figure 2.5.2-262 and Subsection 3.7.1.1 show that the computed GMRS spectrum is below the minimum earthquake. The numerical values of the GMRS spectrum sampled at 38 frequencies between 0.1 and 100 Hz are presented in Table 2.5.2-221.

2.5.2.6.1.2 Vertical GMRS Spectrum

Vertical motions at the CPNPP Units 3 and 4 site are addressed by reviewing results in NUREG/CR-6728 for V/H ratios at deep soil sites, for both the western US (WUS) and the CEUS. Example results presented in the NUREG/CR-6728 indicate that for earthquakes >40 km from a deep soil site, V/H ratios are expected to be less than unity for all frequencies (Figures J-31 and J-32 in Appendix J of the NUREG/CR-6728). For the 10^{-5}~~4~~ ground motion, expected distances from deaggregation are greater than 100 km (~~Table 2.5.2-220~~Table 2.5.2-205). Any exceedance of unity occurs for high frequencies (>10 Hz) for short source-to-site distances. Also, for ground motions with peak horizontal accelerations <0.2g, the recommended V/H ratios for hard rock conditions are less than unity; see Table 4-5 of the NUREG/CR-6728. The conclusion is that V/H ratios for the CPNPP Units 3 and 4 site will be less than or equal to unity for all spectral frequencies. Therefore, the vertical GMRS will be below the horizontal GMRS shown in Figure 2.5.2-~~234~~261. CTS-01521 CTS-01521 CTS-01521

Figure 2.5.2-~~234~~261 shows that the horizontal DCD spectrum exceeds the horizontal GMRS. The vertical DCD spectrum equals or does not exceed the horizontal DCD spectrum for frequencies above 3.5 Hz. The conclusion is that the vertical DCD spectrum will also exceed the vertical GMRS. Under this condition, the DCD minimum vertical design motion will govern the vertical response, just as the DCD minimum horizontal design motion will govern the horizontal response.

Vertical GMRS and FIRS spectra were developed using vertical-to-horizontal (V/H) ratios. NUREG/CR-6728 and RG 1.60 indicate proposed V/H ratios for design spectra for nuclear facilities, and these V/H ratios are plotted in Figure 2.5.2-~~252~~263. The V/H ratios in Figure 2.5.2-~~252~~263 taken from NUGREG/CR-6728 (the blue curve) are recommended for hard sites in the CEUS. The Comanche Peak site is a deep, soft-rock site with shale and limestone near the surface having shear-wave velocities of about 2,600 fps, and the V/H ratios for this site condition will be similar to those for hard rock sites. CTS-01521 CTS-01521

Based on these comparisons, it is concluded that the applicable V/H ratios at the Comanche Peak site will be ≤ 1.0 at all spectral frequencies between 100 Hz and 0.1 Hz. As a conservative assumption, the V /H ratio is assumed to be equal to the V/H ratio from RG 1.60. This assumption is also plotted in Figure 2.5.2-~~252~~263. The vertical GMRS spectrum resulting from this assumption is presented in ~~Table 2.5.2-236~~Table 2.5.2-221. CTS-01521

~~The smooth vertical GMRS spectrum is plotted in Figure 2.5.2-258 along with the respective DCD spectrum.~~The smooth vertical GMRS spectrum is plotted in Figure 2.5.2-265 along with the minimum DCD spectrum and the vertical DCD acceleration time history scaled by one third. This figure and Subsection 3.7.1.1 show~~s~~ that the GMRS spectrum is enveloped by the DCD. CTS-01521

2.5.2.6.2 Foundation Input Response Spectrum

CTS-01521

~~Site response analyses were conducted for an additional four cases (FIRS 2, FIRS 3, FIRS 4_CoV30, and FIRS 4_CoV50) to consider foundation input response spectra for specific conditions different from the GMRS elevation. These four cases are as follows:~~Site response analyses were conducted for three different site columns: FIRS3, FIRS3_COV50, and FIRS4_SCSR. FIRS3 is the full site column profile for the GMRS, FIRS1 and FIRS2. FIRS3_COV50 (full site column profile for FIRS1_COV50 and FIRS2_COV50) is similar to FIRS3 with the granular fill Vs modeled as having a Coefficient of variation (CoV) of 50% compared to 30% in the base case. FIRS4_SCSR (Soil Column Surface Response) is the full site column profile for FIRS4. FIRS3, FIRS3_COV50, and FIRS4_SCSR do not correspond to an actual FIRS, but are computed and designated as such as they represent the Performance Based Seismic Response Spectra (PBSRS) for use in Subsection 2.5.2.6.3 when performing the NEI check for embedded foundation analyses for SSI (Reference 2.5-490). The FIRS are defined as follows:

~~**FIRS 2** – Set at elevation 787 ft.~~

~~This FIRS represents generic site response conditions for structures resting on fill concrete layer in which the fill concrete thickness and horizontal extent away from the edge of the foundation is significant and thus modeled as a horizontally infinite layer.~~

- ~~FIRS 2 analysis demonstrates that the response at the top of the fill concrete remains well below the minimum earthquake and does not apply to any specific structure.~~

~~The FIRS 2 profile consists of 5 ft of fill concrete placed over a sub-excavated stiff limestone (Layer C) surface at elevation 782 ft. Fill concrete with compressive strength ranging from 2,500 psi to 4,400 psi is considered by using a mean shear wave velocity of 6800 fps with a range of +/- 500 fps. See Table 2.5.2-227 for properties used for FIRS 2 analysis. Note that the site-specific soil-structure interaction analyses described in Subsection 3.7.2 model the fill concrete under the category 1 foundations as part of the structural model.~~

~~**FIRS 3** – Set at Plant Grade elevation 822 ft.~~

~~The FIRS 3 profile considers the ground surface seismic response in areas of the site where cutting of the native soil is required to reach final Plant Grade elevation 822 ft.~~

- ~~FIRS 3 analysis demonstrates that the response at Plant Grade elevation in regions of the site with native soil remains below the minimum earthquake. It does not represent the foundation subgrade elevation for any safety-related facilities identified, but could accommodate possible future shallow (at-grade) facilities.~~

~~The profile consists of stiff limestone at elevation 782 ft and overlying shale (Glen Rose Layer B1 and B2) and interbedded limestone/shale (Glen Rose Layer A) to Plant Grade elevation 822 ft. See Table 2.5.2-227 for properties used for FIRS 2 analysis.~~ CTS-01521

~~**FIRS 4** Set at Plant Grade elevation 822 ft:~~

- ~~FIRS 4 analysis demonstrates that the response of engineered compacted backfill at Plant Grade elevation remains below the minimum earthquake.~~

~~The elevations of FIRS 4 and FIRS 3 are identical, but this profile consists of sub-excavation to stiff limestone at elevation 782 ft, and backfilling to Plant Grade with cohesionless engineered fill to Plant Grade elevation 822 ft. Assumed shear-wave velocity and shear modulus/damping properties for the fill are estimated based on a specified range of cohesionless fill materials, and reported properties for similar compacted fill materials. Ranges of values representing best estimates, and lower and upper bounding values, are provided in Table 2.5.2-227. Degradation curves are provided in Figure 2.5.2-232. FIRS 4 consists of two different cases (FIRS 4_CoV30 and FIRS4_CoV50) to provide a wide variability on shear wave velocities estimated for the cohesionless compacted fill.~~

~~FIRS4_CoV30: elevation 822 ft. The elevation for FIRS 4 is the same as for FIRS 3, but the profile consists of sub-excavation to stiff limestone at elevation 782 ft, and backfilling to plant grade with cohesionless engineered compacted fill.~~

~~FIRS4_CoV50: elevation 822 ft. This profile is the same as for FIRS 4 except it uses a coefficient of variation (CoV) of 50% (instead of 30%) for the Vs of the fill material.~~

FIRS1 (this is the Ground Motion Response Spectrum - GMRS). Set at elevation 782 feet (top of Glen Rose Limestone Layer C). This FIRS represents the top of stiff limestone and the bottom of the foundation mat for the Power Source Fuel Storage Vaults (PSFSVs) or slightly below the control elevation (786 ft) for the bottom of the foundation mat for the Ultimate Heat Sink Related Structures (UHSRS). FIRS1 is initially considered as the Soil Column Outcrop Response (SCOR) of FIRS3 described below. This was compared against the Performance Based Surface Response Spectra (PBSRS) in Subsection 2.5.2.6.3, which uses the full site column and is equivalent to FIRS3. This check is consistent with NEI guidelines for embedded foundation SSI analyses (Reference 2.5-490).

FIRS2. Set at elevation 779.75 feet (near the top of Glen Rose Limestone Layer C). This FIRS is equivalent to FIRS1 above as it lies in the same layer and is only 2.25 feet below the FIRS1 control elevation. This elevation represents the bottom of the foundation mat for the Reactor Building Complex (R/B Complex) and for the segment of the Essential Service Water Pipe Tunnel (ESWPT) that is integrated with the R/B Complex.

FIRS3. Set at Plant Grade elevation of 822 feet. This is the full site column developed for FIRS1 and FIRS2. The profile for this FIRS consists of sub-excavation to stiff limestone at Elevation 782 feet and backfilling to Plant Grade elevation of 822 feet with sandy engineered compacted fill. The Soil Column Surface Response (SCSR) spectrum generated for this scenario as FIRS3 is equivalent to the PBSRS for which GMRS/FIRS1/FIRS2 was checked in Subsection 2.5.2.6.3 per NEI guidelines for embedded foundation SSI analyses (Reference 2.5-490) in Subsection 2.5.2.6.3. CTS-01521

FIRS4. Set at elevation 791.08 feet. The profile for this FIRS incorporated 9.08 feet of fill concrete placed over a sub-excavated stiff limestone surface at elevation 782 feet. FIRS4 profile was developed by modeling a full site column profile where sandy engineered compacted fill is backfilled above the fill concrete to Plant Grade elevation 822 feet. The FIRS4 Soil Column Surface Response (SCSR) is also developed as it will be the PBSRS against which the FIRS4 was checked per NEI guidelines for embedded foundation SSI analyses (Reference 2.5-490) in Subsection 2.5.2.6.3.

For sensitivity purposes, an additional set of randomized profiles were also considered as follows:

FIRS1, FIRS2, FIRS3 (all COV50) using a CoV of 50% (instead of the base case of 30%) for the Vs of the granular fill material (denoted FIRS1_COV50, FIRS2_COV50, and FIRS3_COV50). FIRS2_COV50 is equivalent to FIRS1_COV50, since it is only 2.25 below the control elevation of FIRS1_COV50 and lies in the same formation with the same material properties.

Figures 2.5.2-~~235~~242 through 2.5.2-~~238~~245 show median amplification factors and logarithmic standard deviations for these ~~four~~ FIRS ~~cases~~, for the 10^{-4}, 10^{-5}, and 10^{-6} broadband input motions.

The seismic hazard for each FIRS case was calculated by integrating the horizontal amplification factors shown in Figures 2.5.2-~~235~~242 through 2.5.2-~~238~~245 with the rock hazard ~~and applying the CAV filter~~and using a minimum moment magnitude (Mmin) of 5.0 (Reference 2.5-489). This is an analogous calculation to the calculation of hazard for the GMRS elevation. ~~For all FIRS cases the hazard curves at low amplitudes rolled over to an annual frequency of exceedance that was less than 10^{-4}. As was the case for the GMRS, the FIRS spectra were calculated using the 10^{-5} UHRS and applying the factor from Eq. 2.5.2-3; i.e., FIRS = 0.45 × SA(10^{-5}).~~The FIRS is calculated in the same manner as the GMRS in Subsection 2.5.2.6.1.1. CTS-01521

~~Figure 2.5.2-239 plots the four horizontal FIRS and compares them to the horizontal minimum DCD spectrum.~~Figure 2.5.2-261 plots the horizontal FIRS spectra along with the GMRS/FIRS1/FIRS2 spectrum described in Subsection 2.5.2.6.1.1, and compares them with the horizontal minimum DCD spectrum. The minimum DCD spectrum envelops all ~~four~~ FIRS, down to frequencies of 0.5 Hz.

Values of the horizontal ~~10^{-5} UHRS and~~ FIRS are shown in ~~Table 2.5.2-229~~Table 2.5.2-221 and Table 2.5.2-222 for the seven spectral frequencies. CTS-01521

~~Smooth horizontal spectra for the four FIRS conditions (FIRS2, FIRS3, FIRS4, and FIRS4-CoV50) were calculated in a manner similar to the way in which the smooth GMRS was calculated, as described in Section 2.5.2.6.1.1. Note that the FIRS3 spectra have peaks at about 2.5 Hz and 10 Hz, and that the FIRS4 and FIRS4-CoV50 spectra have peaks at about 1.5 Hz and 5 Hz. These peaks were broadened in an approximate way similar to the procedure used for the GMRS.~~Smooth horizontal spectra for the FIRS weredeveloped.The smoothing was performed similar to the procedure used for the GMRS in Subsection 2.5.2.6.1.1.

The smooth horizontal FIRS spectra are plotted in Figure 2.5.2-262 along with the minimum horizontal DCD spectrum, the horizontal DCD acceleration time histories scaled by one third, and the computed GMRS/FIRS1/FIRS2 spectra (see Subsection 2.5.2.6.1.1). Figure 2.5.2-262 also shows that the computed FIRS spectra are below the minimum DCD spectrum.

For vertical FIRS motions, the same considerations used for the GMRS were used for the FIRS. That is, as a conservative assumption the V/H ratio for the FIRS spectra is assumed to be equal to the V/H ratio from RG 1.60. The smooth vertical FIRS spectra are plotted in Figure 2.5.2-265 along with the minimum vertical DCD spectrum and vertical DCD acceleration time histories scaled by one third. The figure shows that the FIRS spectra are enveloped by the minimum DCD spectrum.

The horizontal and vertical numerical values for FIRS1_COV50 (equivalent to FIRS2_COV50) and FIRS4 spectra, sampled at 38 frequencies between 0.1 and 100 Hz (PGA), are presented in Table 2.5.2-223, while the numerical values for GMRS/FIRS1/FIRS2 are presented in Table 2.5.2-221.

~~The horizontal 10^{-5} and FIRS spectra are plotted in Figures 2.5.2-248 through 2.5.2-251. Table 2.5.2-237 shows the numerical values for the 10^{-5} and FIRS spectra.~~

~~For vertical FIRS motions, the same considerations used for the GMRS were used for the FIRS. That is, as a conservative assumption the V/H ratio for the FIRS spectra is assumed to be equal to the V/H ratio from RG 1.60.~~

~~The smooth horizontal and vertical FIRS spectra are plotted in Figures 2.5.2-257 and 2.5.2-258, respectively, along with the respective DCD spectrum. These figures show that the FIRS spectra are enveloped by the DCD.~~

2.5.2.6.3 Consistent Site Response Soil-Structure Interaction Analysis and Evaluation Check

CTS-01521

To ensure that the site response motion developed above for the GMRS and FIRS are consistent with its application to SSI analysis and evaluation, the NEI guidelines for embedded foundations modeled as embedded is followed (Reference 2.5-490). The NEI check is performed using the full site column lower bound (LB), best estimate (BE), and upper bound (UB) strain compatible profiles developed from the median profiles plus/minus one standard deviation maintaining the minimum variation of 1.5 x Gbest and Gbest/1.5 to define the range as required in SRP 3.7.2. The strain compatible profiles were generated from the site response analyses in Subsection 2.5.2.5.2.3, corresponding to the 10^{-4} broad-band bedrock motions. For backfill, an additional high bound (HB) profile is also used together with the UB subgrade profile in Section 3.7 to account for expected uncertainty in the backfill properties.

Since the horizontal and vertical GMRS and FIRS were all enveloped by the minimum DCD spectra, the minimum earthquake is what governs and the DCD acceleration time histories scaled by one third are the outcrop time histories for use with the GMRS and all FIRS. Site response analyses were performed using the Random Vibration Theory (RVT) approach using the LB, BE, and UB strain compatible profiles, truncated at the corresponding GMRS and FIRS control elevations. The Soil Column Surface Response (SCSR) obtained from the site response analyses are then compared to the Performance-Based Surface Response Spectra (PBSRS) computed in Subsection 2.5.2.6.2. In other words, the LB, BE, and UB strain compatible profiles developed for the full site column FIRS3 are truncated from the ground surface to the GMRS/FIRS1 (equivalent to FIRS2) control elevation of 782 feet and the one third scaled DCD acceleration time histories applied as an outcrop motion at the base of the profile. Similarly, the same is performed for FIRS3_COV50. Finally, the LB, BE, and UB strain compatible profiles developed for the full site column FIRS4_SCSR is truncated from the ground surface to the FIRS4 control elevation of 791.08 feet and the one third scaled DCD acceleration time histories applied as an outcrop motion at the base of the profile. The SCSR generated from these analyses is then compared to the PBSRS from Subsection 2.5.2.6.

The compression wave velocity (Vp) profiles above the nominal ground water level (GWL) and for the rock layers below the nominal GWL were obtained from the corresponding shear wave velocity (Vs) profiles using the base case (unsaturated) Poisson's ratio for each layer. For saturated granular fill below the groundwater level, Vp for the best estimate soil profile should initially be set to 5,000 fps and Poisson's ratio calculated for the layer using the corresponding Vs for each layer. An upper limit on Poisson's ratio of 0.48 was set for the best estimate case to ensure numerical convergence in SSI analyses and to account for the material properties anticipated for the saturated granular fill. If the calculated Poisson's ratio is higher than 0.48, a Poisson's ratio of 0.48 would be set as the Poisson's ratio for the saturated granular fill layer, and the corresponding strain compatible Vp would be calculated for the value of 0.48. The

final Poisson's ratio obtained for the saturated granular fill for the BE cases will then be used for the other cases (LB and UB) to maintain the variability between the LB and UB profiles per SRP 3.7.2. For all conditions, the strain compatible compression wave damping will be considered equal to the strain compatible shear wave damping per the recommendation in Reference 2.5-490. CTS-01521

The PBSRS calculated was less than the envelope of the SCSR from the three profiles (LB, BE, and UB) as shown in Figures 2.5.2-266 to 2.5.2-277. As a result, the strain compatible profiles developed through the site response analyses discussed in Subsection 2.5.2.5.2.3 are appropriate for use along with the one third scaled DCD outcrop time histories for SSI analyses.

2.5.3 Surface Faulting

CP COL 2.5(1) Replace the content of DCD Subsection 2.5.3 with the following.

This subsection evaluates the potential for tectonic and non-tectonic surface deformation at the CPNPP Units 3 and 4 site (CPNPP Units 3 and 4). Information contained in Subsection 2.5.3 was developed in accordance with Regulatory Guide (RG) 1.165, and is intended to demonstrate compliance with 10 CFR 100.23. RG 1.165 contains guidance on characterizing seismic sources, and defines a "capable tectonic source" as a tectonic structure that can generate both vibratory ground motion and tectonic surface deformation, such as faulting or folding at or near the earth's surface, in the present seismotectonic regime.

This subsection contains information on:

- Potential surface deformation associated with capable tectonic sources
- Potential surface deformation associated with non-tectonic processes, such as collapse structures (karst collapse), subsurface salt migration (salt domes), volcanism, and man-induced deformation (e.g., mining collapse and subsidence due to fluid withdrawal)

There are no capable faults and there is no potential for non-tectonic fault rupture within the 25-mi-radius CPNPP Units 3 and 4 site vicinity. Similarly, there is no potential for tectonic or non-tectonic deformation in the 5-mi-radius site area or the 0.6-mi-radius site. The following subsections contain the data, observations, and references to support these conclusions.

2.5.3.1 Geological, Seismological, and Geophysical Investigations

An extensive body of information regarding the potential for surface faulting is available for the CPNPP Units 3 and 4 site and is documented in several primary sources:

- Geologic mapping published by the U.S. Geological Survey (USGS), the state of Texas, and other researchers (Reference 2.5-228)
- Articles published by various researchers in refereed journals and field trip guidebooks
- Seismicity data compiled and analyzed in published journal articles, ~~EPRI's seismic hazard methodology (Reference 2.5-369), and the updated~~CEUS SSC (Reference 2.5-486) seismicity catalog (Subsection 2.5.2) CTS-01521
- Previous site investigations performed for the final safety analysis for CPNPP Units 1 and 2 (Reference 2.5-201)

In addition to reviewing this existing information, the following investigations were performed to assess the potential for tectonic and non-tectonic deformation within the 5-mi-radius CPNPP Units 3 and 4 site area:

- Compilation and review of existing data and literature, with emphasis on reports published since the CPNPP Units 1 and 2 FSAR (Reference 2.5-201) and ~~EPRI studies (Reference 2.5-369)~~and CEUS SSC (Reference 2.5-486) CTS-01521
- Interpretation of aerial photography and remote sensing imagery
- Field and aerial reconnaissance
- Review of pre- and post-~~EPRI SOG~~CEUS SSC seismicity CTS-01521

2.5.3.1.1 Previous Site Investigations

The results of previous geology and seismology investigations at CPNPP are summarized in Subsection 2.5.3 of the CPNPP Units 1 and 2 FSAR (Reference 2.5-201) with the simple statement:

> "No evidence of surface faulting was found within five miles of the site."

In Subsection 2.5.1, it is indicated that no faults, shear zones, or anomalies were found within 5 miles of the site.

2.5.3.1.2 Regional and Local Geological Studies

The USGS has compiled information related to all known Quaternary faults, liquefaction features, and possible tectonic features in the CEUS (References 2.5-236 and 2.5-405). These compilations do not show any Quaternary tectonic faults or tectonic features within a 25-mi or 5-mi radius of the CPNPP Units 3 and 4 site. Additionally, compilation of local mapping does not show any surface faults within the 25-mi radius (Figure 2.5.1-216; Reference 2.5-406).

2.5.3.2 Geological Evidence, or Absence of Evidence, for Surface Deformation

As shown on Figure 2.5.1-216, no surface bedrock faults have been mapped within the 25-mi-radius CPNPP Units 3 and 4 site vicinity. Almost the entire site vicinity is located in the Grand Prairie physiographic province, a tectonically stable region underlain by thick continental crust (Figure 2.5.1-201). This region is characterized by low rates of seismicity, and ~~no~~sparse seismicity in the updated catalog has been found ~~greater than~~within 50 mi from the site (Subsection 2.5.2.1.3). For example, review of the updated seismicity catalog covering the period between January 1, 2009 and December 31, 2011 shows five earthquakes occurred within the 50-mile radius surrounding Units 3 and 4. Of these five earthquakes, the maximum Mw was 3.1. A single earthquake of Mw 3.0 occurred CTS-01521

within 25 miles of the site. None of these events correspond to a mapped fault or fold. The only structures at the surface within the 25-, 5-, and 0.6-mi radii are sedimentary in nature (i.e., unconformities). Bedding is nearly horizontal (dips <1°) at the 25-, 5- and 0.6-mi radii scale (Figures 2.5.1-214, 2.5.1-215, 2.5.1-216, 2.5.1-222, and 2.5.1-223; see discussion in Subsection 2.5.4.4). Two exceptions to this are seen within the 5-mi radius, where bedding locally exhibits a ~5° dip (Figures 2.5.1-226b and 2.5.1-227). However, these features are minimal in extent, and while their cause is unresolved, no evidence indicates that these outcrop-scale, sedimentary thickness variations signal any sort of hazard for CPNPP Units 3 and 4. CTS-01521

Initial inspections of stereo-pair black and white, ~1:20,000 scale, aerial photographs from the 1940s yielded linear features or lineaments to be investigated in the field (Figure 2.5.3-201). These features were classified as vegetation, stream, tonal, and topographic. The mapped linear features are randomly distributed and variably oriented within the 5-mi radius of the site (Figure 2.5.3-201). The accessible features within the site area were investigated, and most of these lineaments were not identifiable in the modern landscape. Occasionally, a linear feature could be identified as a fence line or an outcrop of bedrock along a paleo-drainage. None of the lineaments investigated indicated any tectonic or geologic disruptions. A discussion of the lineament analysis is provided in the following subsection.

2.5.3.2.1 Lineament Analysis and Ground Surveys

An evaluation of the presence of geologic structures (i.e., faults and folds) expressed at the ground surface within the 5-mi radius of the CPNPP site was performed using aerial photography, satellite imagery and ground surveys (i.e, field reconnaissance). Results of this evaluation were used to focus further field reconnaissance and mapping activities. Satellite imagery of the area surrounding the site indicated that much of the surface has been modified by residential development, agricultural and ranching activities. Thus historical black and white aerial photography was assembled including USGS 1958 1:62,500 obliques and, 1948 and 1949 1:20,000 stereo pairs from the Texas Natural Resources Information System (TNRIS) covering the 5-mi area surrounding the site. The 1948 and 1949 photos were noted to be of good quality and minimal distortion and indicated less surface modification from anthropogenic activities compared to the 1958 photos which provided much less contrast. The 1948 and 1949 photo set was used for a detailed evaluation of surface lineaments.

The photographs were analyzed to identify surface features of linear to sub-linear expression of possible fault off-sets or fold hinge-lines or limbs manifested topographically as ridge lines or stream segments. The stereo pairs were indexed and tiled according to the master index file provided by the TNRIS. For the analysis, the photographs were evaluated for the following feature classifications and were cataloged for mapping and further evaluation through field reconnaissance:

This was concluded from the lateral continuity of bedding that could mapped on the aerial photography as well as field observations of outcrops along the Brazos River that indicated undeformed, horizontal bedding.

2.5.3.3 Correlation of Earthquakes with Capable Tectonic Sources

~~There is no seismicity within the 25-mi-radius site vicinity and therefore there is no spatial correlation of earthquake epicenters with known or postulated faults, other tectonic features, or other geomorphic features (Figure 2.5.2-201).~~A single seismic event of Mw 3.0 was recorded on June 2, 2009 within the 25-mile radius of the site vicinity, but there is no spatial correlation of the earthquake epicenter with known or postulated faults, other tectonic features, or other geomorphic features (Figure 2.5.2-201). As part of this COL application, the ~~EPRI~~CEUS SSC earthquake catalog was updated to incorporate southern United States earthquakes that occurred between ~~1985~~1568 and 200~~6~~8 (see Subsection 2.5.2.1.2. The updated earthquake catalog contains ~~no~~five earthquakes with ~~body-wave magnitude (m_b) ≥3.0 with~~Mw > 2.9 more than 50 mi ~~of~~from the CPNPP Units 3 and 4 site. There is no spatial correlation of the earthquake epicenters with known or postulated faults, other tectonic features, or other geomorphic features (Figure 2.5.2-201). CTS-01521 CTS-01521

2.5.3.4 Ages of Most Recent Deformation

No faults or tectonic deformation has been identified at the surface within 25 mi of the CPNPP Units 3 and 4 site. The region in fact has experienced only sedimentation and erosion since the Permian Period, the last time of faulting or uplift in the area. The only disruptions to completely planar bedding are the two localized, probably sedimentary, features described in Subsection 2.5.1.2.4.1 and Subsection 2.5.1.2.4.2. These features were most likely developed in the Cretaceous Period.

2.5.3.5 Relationship of Tectonic Structures in the Site Area to Regional Tectonic Sources

There are no tectonic bedrock faults within the 5-mi-radius site area. Consequently, it is concluded that there is no correlation of geologic structures in the site area to regional, capable tectonic sources.

2.5.3.6 Characterization of Capable Tectonic Sources

On the basis of data presented in Subsection 2.5.1 and previous discussions in Subsection 2.5.3.4, there are no capable tectonic sources within 5 mi of the CPNPP Units 3 and 4 site.

2.5-287 Madole, R.F., *The Meers Fault—Quaternary stratigraphy and evidence for late Holocene movement,* in *Oklahoma Geologic Survey Guidebook 24.* 1986.

2.5-288 Burrell, R., *Characteristics and ground acceleration associated with recent movement along the Meers Fault.* 1997.

2.5-289 Cetin, H., *Comment on "Known and suggested Quaternary faulting in the midcontinent United States" by Russell L. Wheeler and Anthony Crone.* Engineering Geology, 2003. 69: p. 193-210.

2.5-290 Luza, K.V., R.F. Madole, and A.J. Crone, *Investigation of the Meers fault in southwestern Oklahoma.* US Nuclear Regulatory Commission: NUREG/CR-4937, 1987. p. 67.

2.5-291 NRC, *Revised Livermore Seismic Hazard Estimates for Sixty-Nine Nuclear Power Plant Sites East of the Rocky Mountains.* 1994, US Nuclear Regulatory Commission, NUREG-1488: Washington, D.C. p. 95.

2.5-292 Budnitz, R.J., et al., *Recommendations for Probabilistic Seismic Hazard Analysis: Guidance on Uncertainty and Use of Experts* 1997, U.S. Nuclear Regulatory Commission: NUREG/CR-6372. CTS-01521

2.5-293 Gilbert, M.C., *The Meers fault of southwestern Oklahoma: evidence for possible strong seismicity.* EOS Trans Am Geophysical Union, 1983.

2.5-294 Williamson, S.C., *Observations on the capability of the Criner Fault, southern Oklahoma.* 1996, Texas A&M University: College Station, Texas.

2.5-295 Hanson, K., et al., *Quaternary deformation along the Criner fault, Oklahoma: A case study for evaluating tectonic versus landslide faulting.* AGU, 1997 Spring Meeting, 1997.

2.5-296 Keller, G.R., et al., *Preliminary investigations of the extent of the Rio Grande Rift in the northern portion of the state of Chihuahua. Geofisica* Internacional, 1989. 28: p. 1043–1049.

2.5-297 Tweto, O., *The Rio Grande Rift system in Colorado, in Rio Grande rift in southern New Mexico, west Texas, and Northern Chihuahua,* R.E. Riecker, Editor. 1979, American Geophysical Union: Washington, D.C. p. 33-56.

2.5-298 Seager, W.R. and P. Morgan, *Rio Grande rift in southern New Mexico, west Texas, and northern Chihuahua, in Rio Grande Rift:*

2.5-333 Van Arsdale, R.B., *Displacement history and slip rate on the Reelfoot fault of the New Madrid seismic zone.* Engineering Geology, 2000. 55: p. 219-226.

2.5-334 Van Arsdale, R.B., K.I. Kelson, and C.H. Lurnsden, *Northern extension of the Tennessee Reelfoot scarp into Kentucky and Missouri.* Seismological Res. Lett., 1995. 66: p. 57-62.

2.5-335 EPRI, *EQHAZARD Primer (NP-6452-D).* 1989, Electric Power Research Institute (EPRI), prepared by Risk Engineering for Seismicity Owners Group and EPRI. p. 226.

2.5-336 Tuttle, M.P., et al., *The Earthquake Potential of the New Madrid seismic zone.* Bulletin of the Seismological Society of America, 2002. 92: p. 2080–2089.

2.5-337 Guccione, M.J., *Late Pleistocene and Holocene paleoseismology of an intraplate seismic zone in a large alluvial valley, the New Madrid seismic zone, central USA.* Tectonophysics, 2005. 408: p. 237-264.

2.5-338 Tuttle, M.P., et al., *Evidence for New Madrid earthquakes in A. D. 300 and 2350 B. C.* Seismological Res. Lett., 2005. 76: p. 489-501.

2.5-339 Frankel, A., et al., *National Seismic-Hazard Maps: Documentation, June 1996.* 1996, Denver, CA: U.S. Geological Survey Open-File Report 96-532. 41.

2.5-340 ~~EPRI, *Seismic Hazard Methodology for the Central and Eastern United States, V.1, Part 2: Methodology (NP-4726-A).* 1988, Electric Power Research Institute.~~Removed CTS-01521

2.5-341 Bell, W.C. and V.E. Barnes, *Cambrian History, Llano Region Geology of the Llano Region and Austin Area,* in *Geology of the Llano Region and Austin Area,* V.E. Barnes, et al., Editors. 1972, The University of Texas at Austin, Bureau of Economic Geology: Austin, Texas. p. 24–29.

2.5-342 Barnes, V.E. and P.E.J. Cloud, *Ordovician to earliest Mississippian rocks, Llano region,* in *Ordovician to earliest Mississippian rocks, Llano region,* V.E. Barnes, et al., Editors. 1972, The University of Texas at Austin, Bureau of Economic Geology: Austin, Texas. p. 30–37.

2.5-343 Montgomery, S.L., et al., *Mississippian Barnett Shale, Fort Worth basin, north-central Texas: Gas-shale play with multi-trillion cubic foot potential.* AAPG Bulletin, 2005. 89(2): p. 155–175.

2.5-365 Grasso, J. and G. Wittlinger, *Ten years of seismic monitoring over a gas field.* Bulletin of the Seismological Society of America; April 1990; v. 80; no. 2; p. 450-473, 1990. 80(2): p. 450–473.

2.5-366 Maury, V., J. Grasso, and G. Wittlinger, *Monitoring of subsidence and induced seismicity in the Lacq gas field (France): The Consequences on.* Engineering Geology, 1992.

2.5-367 Davis, S.D., P.A. Nyffenegger, and C. Frohlich, *The 9 April 1993 earthquake in south-central Texas: Was it induced by fluid withdrawal?* Bulletin of the Seismological Society of America, 1995. 85(6): p. 1888–1895.

2.5-368 Hsieh, P.A. and J.D. Bredehoeft, *Reservoir analysis of the Denver earthquakes: A case of induced seismicity.* J. Geophys. Res. , 1981. 86(B2): p. 903–920.

2.5-369 Electric Power Research Institute, Seismic Hazard Methodology for the Central and Eastern United States (NP-4726), Vol. 1, 3, and 5–10. Electric Power Research Institute: Palo Alto, CA, 1986–1989.

2.5-370 Electric Power Research Institute, Probabilistic Seismic Hazard Evaluations at Nuclear Plant Sites in the Central and Eastern United States: Resolution of the Charleston Earthquake Issue (NP-6395-D). Electric Power Research Institute: Palo Alto, CA, 1989.

2.5-371 American Society of Civil Engineers, Seismic Design Criteria for Structures, Systems, and Components in Nuclear Facilities. 2005, ASCE Standard, ASCE/SEI 43-05.

2.5-372 ANSS, ANSS Catalog Search Output. 20~~06~~12, Advanced National Seismic System (ANSS). CTS-01521

2.5-373 NEIC, NEIC Catalog Search Output. 20~~06~~12, National Earthquake Information Center Preliminary Determination of Epicenters. CTS-01521

2.5-374 OGS, Oklahoma Geological Survey Earthquake Catalog, ~~1895~~2009–20~~06~~11~~. 2006~~2, Oklahoma Geologic Survey (OGS). CTS-01521

2.5-375 Sanford, A.R., et al., Earthquake catalogs for New Mexico and bordering areas: 2010–2011~~1869–1998. 2002, Socorro, NM: New Mexico Bureau of Geology and Mineral Resources, data files stored as NMT_catalog_1962_1995.pdf. 15~~. CTS-01521

2.5-376 CERI, CERI Earthquake Catalog Search Output. 20~~07~~12, Center for Earthquake Research and Information (CERI).

2.5-377 ~~NEIC, NEIC PDE-W earthquake summary for 10 February 2006 041717 event. 2007, USGS.~~Removed CTS-01521

2.5-378 Frohlich, C. and S.D. Davis, Texas Earthquakes. 2002, Austin: University of Texas Press. 275.

2.5-379 Sanford, A.R., et al., Location and Fault Mechanism of the 2 January 1992 Rattlesnake Canyon Earthquake in Southeastern New Mexico. 1993, Geophysical Research Center and Geoscience Department, New Mexico Institue of Mining and Technology: Socorros, NM. p. 11.

2.5-380 Doser, D.I., et al., The not so simple relationship between seismicity and oil production in the Permian Basin, West Texas. Pure and Applied Geophys., 1992. 139: 481–506.

2.5-381 ~~NEIC, NEIC Monthly Earthquake Data Report file for event 200602104011. 2007, US Geological Survey.~~Removed CTS-01521

2.5-382 Nettles, M. Analysis of the 10 February 2006: Gulf of Mexico earthquake from global and regional seismic data. in 2007 Offshore Technology Conference. 2007. Houston, TX.

2.5-383 Dellinger, J.A., et al., Relocating and characterizing the 10 Feb 2006 "Green Canyon" Gulf of Mexico earthquake using oil-industry data. Eos Trans. AGU, 2007. 88(52), Fall Meet. Suppl., Abstract S13F-01.

2.5-384 Carlson, S., Investigations of Recent and Historical Seismicity in East Texas. 1984, Univ. Texas, Austin: Austin, TX. p. 197.

2.5-385 Collins, E., Fault number 918c, West Lobo Valley fault zone, Mayfield section, in Quaternary fault and fold database of the United States. 1993, USGS.

2.5-386 ~~Atkinson, G.M. and D.M. Boore, Ground motion relations for eastern North America. Bulletin of the Seismological Society of America, 1995. 85(1): 17–30.~~Removed CTS-01521

2.5-387 Electric Power Research Institute (1993). Guidelines for Determining Design Basis Ground Motions, EPRI Report TR-102293, Palo Alto, CA, November.

2.5-388 ~~Geomatrix Consultants, Draft Report: Seismotectonic Evaluation, Wichita Uplift Region Southern Oklahoma and Northern Texas. 1990, prepared by Geomatrix Consultants for US Bureau of Reclamation: San Francisco, CA. p. 108.~~Removed CTS-01521

2.5-389 ~~Swan, F.H., et al., Draft Report: Investigation of the Quaternary Structural and Tectonic Character of the Meers Fault (Southwestern Oklahoma). 1993, Geomatrix Consultants, Inc.: San Francisco, CA. p. 104 plus appendices.~~Removed CTS-01521

2.5-390 ~~LaForge, R.C., Seismic Hazard and Ground Motion Analysis for Altus, Arbuckle, Fort Cobb, Foss, McGee Creek, Mountain Park, and Norman Dams, Oklahoma. 1997, Department of Interior, Bureau of Reclamation, Seismotectonic report 97-1: Denver, CO. p. 19.~~Removed

2.5-391 ~~Savy, J.B., W. Foxall, and D.L. Bernreuter, Probabilistic seismic hazard characterization and design parameters for the Pantex plant. 1998, Hazards Mitigation Center, Lawrence Livermore National Laboratory, prepared for Mason and Hanger Corporation, UCRL-CR-132282. p. 93.~~Removed

2.5-392 ~~USGS, Preliminary Documentation for the 2007 Update of the United States National Seismic Hazard Maps. 2007, USGS: Reston, Virginia. p. 93.~~Removed

2.5-393 ~~Cramer, C.H., A seismic hazard uncertainty analysis for the New Madrid Seismic Zone. Engineering Geology, 2001. 62 (1-3): 251-266.~~Removed

2.5-394 Removed

2.5-395 ~~EGC, Exelon Generation Company (EGC) Early Site Permit (ESP) Application for the EGC ESP Site. 2006, April 4, 2006, NRC Docket No. 52-007.~~Removed CTS-01521

2.5-396 Gilbert, M.C., The Meers fault: Unusual aspects and possible tectonic consequences. Abstracts with Programs, GSA South Central Section Annual Meeting, 1983. 15, abstract no. 17428: p. 12,903.

2.5-397 ~~Wheeler, R.L. and A.J. Crone, Reply to comment on evaluation of Meers fault, Oklahoma in "Known and suggested Quaternary faulting in the midcontinent United States" by Russell L. Wheeler and Anthony J. Crone. Engineering Geology, 2003. 69 (1-2): 211-215.~~Removed CTS-01521

2.5-398 ~~Wells, D.L. and K.J. Coppersmith, New empirical relationships among magnitude, rupture length, rupture width, rupture area, and surface displacement. Bulletin of the Seismological Society of America,1994. 84 (4): 974-1002.~~Removed

2.5-399 ~~Machette, N.M., K. Haller, and L. Wald, Quaternary Fault and Fold Database for the Nation. 2004, USGS, Fact Sheet 2004-3033: Denver, CO. 2.~~Removed CTS-01521

2.5-400 Removed

2.5-401 EPRI, CEUS Ground Motion Project, Model Development and Results. Report No. 1008910. Electric Power Research Institute: Palo Alto, CA, 2004.

2.5-402 ~~TVA, Tennessee Valley Authority (TVA) COL Application for Bellefonte Nuclear Site, Units 3 and 4, Rev. 0. October 30, 2007, NRC Docket Nos. 52-014 and 52-015.~~Removed CTS-01521

2.5-403 EPRI, Program on Technology Innovation: Truncation of the Lognormal Distribution and Value of the Standard Deviation for Ground Motion Models in the Central and Eastern United States. Report No. 1014381. Electric Power Research Institute: Palo Alto, CA, 2006.

2.5-404 ~~EPRI, Program on Technology Innovation: Use of Cumulative Absolute Velocity (CAV) in Determining Effects of Small Magnitude Earthquakes on Seismic Hazard Analyses. Report No. 1014099. Electric Power Research Institute: Palo Alto, CA, 2006.~~Removed CTS-01521

2.5-405 Wheeler, R.L., Known or suggested Quaternary tectonic faulting, central and eastern United States—new and updated assessments for 2005. 2005, U.S. Geological Survey Open-File Report 2005-1336. p. 40.

2.5-406 TCEQ, Geologic Atlas of Texas. 2002, Bureau of Economic Geology. Texas Commission on Environmental Quality: Austin, TX.

2.5-407 Deere, D.U. (1964), Technical Description of Rock Cores for Engineering Purposes, Rock Mechanics and Engineering Geology, Vol. 1, No. 1, pages 17-22. (Copyrighted Material)

2.5-408 Gamble, J.C. (1971), Durability-plasticity classification of shales and other argillaceous rocks, Ph.D. thesis, University of Illinois. (Copyrighted Material)

2.5-409 Hoek, E. (2007), Practical Rock Engineering, notes from Rock Engineering Course, on-line webpage document at www.rocscience.com, latest revision date April 2007. (Copyrighted Material)

Submitted to Brookhaven National Laboratory, Associated Universities, Inc. Upton, New York 11973, Contract No. 770573.

2.5-434 Idriss, I.M., and Sun, J. I. (1992). SHAKE91: A Computer Program for Conducting Equivalent Linear Seismic Response Analyses of Horizontally layered Soil Deposits, Dept. of Civil and Environmental Engineering, Center for Geotechnical Modeling, Univ. of California, Davis, Calif.

2.5-435 Rathje, E.M., and M.C. Ozbey (2006). Site-Specific Validation of Random Vibration Theory-Based Seismic Site Response Analysis. Journal of Geotechnical and Geoenviromnental Engineering, ASCE, Vol 132, No.7, July.

2.5-436 Kramer, Steven L. (1996). Geotechnical Earthquake Engineering. Prentice-Hall.

2.5-437 Perloff, W.H., Baron, W. (1976), Soil Mechanics Principles and Applications, The Ronald Press Company, N.Y.

2.5-438 Taylor, D.W. (1948), Fundamentals of Soil Mechanics, John Wiley and Sons, Inc., New York.

2.5-439 Poulos, H.G., and Davis, E.H. (1974), Elastic Solutions for Soil and Rock Mechanics, Wiley and Sons, New York.

2.5-440 American Concrete Institute, ACI 349-01, Code Requirements for Nuclear Safety Related Concrete Structures.

2.5-441 2.5-441United States Nuclear Regulatory Commission, Information Notice 97-11, Cement Erosion From Containment Subfoundations At Nuclear Power Plants, March 21, 1997.

2.5-442 ~~Collins, E.E., 1994a, Fault number 921, Unnamed fault east of Ruidosa, in Quaternary fault and fold database of the United States, USGS. Available at: http://earthquakes.usgs.gov/regional/qfaults, accessed on 7-17-2009.~~Removed CTS-01521

2.5-443 ~~Collins, E.E. 1994b, Fault number 922, Unnamed fault southeast of Ruidosa, in Quaternary fault and fold database of the United States, USGS. Available at: http://earthquakes.usgs.gov/regional/qfaults, accessed on 7-17-2009.~~Removed

2.5-444 ~~Collins, E.E., 1995a, Fault number 917, Unnamed fault east of Santiago Peak, in Quaternary fault and fold database of the United States, USGS. Available at: http://earthquakes.usgs.gov/regional/qfaults, accessed on 7-17-2009.~~Removed

2.5-445 ~~Collins, E.E. 1995b, Fault number 923, Dugout Wells fault, in Quaternary fault and fold database of the United States, USGS. Available at: http://earthquakes.usgs.gov/regional/qfaults, accessed on 7-17-2009.~~Removed CTS-01521

2.5-446 ~~Collins, E.W., and Raney, J.A., 1994, Tertiary and Quaternary tectonics of the Hueco bolson, Trans-Pecos Texas and Chihuahua, Mexico, in Keller, G.R., and Cather, S.M., eds., Basins of the Rio Grande Rift: Structure, Stratigraphy, and Tectonic Setting: Boulder, CO, Geological Society of America, Special Paper 291, p. 265-282.~~Removed

2.5-447 Collins, E.W., and Raney, J.A., 1997, Quaternary Faults within Intermontane Basins of Northwest Trans-Pecos Texas and Chihuahua: Austin, TX, Bureau of Economic Geology, Report of Investigations No. 245, 59 p.

2.5-448 Muehlberger, W.R., Belcher, R.C., and Goetz, L.K., 1978, Quaternary faulting in Trans-Pecos Texas: Geology, v. 6, p. 337-340.

2.5-449 King, P.B. and Beikman H.M., *Geologic Map of the United States (Exclusive of Alaska and Hawaii)*, U.S. Geological Survey, 3 sheets, 1:250,000 scale, 1974. (Digitized by Schruben, P.G., Arndt, R.E., Bawiec, W.J., King, P.B., and Beikman, H.M., *Geology of the Conterminous United States at 1:2,500,000 Scale - a Digital Representation of the 1974 P.B. King and H.M. Beikman Map*, U.S. Geological Survey Digital Data Series DDS-11, 1994.)

2.5-450 Abdulah, K.C., Anderson, J. B., Snow, J. N., Holdford-Jack, L. (2004) “The late Quaternary Brazos and Colorado deltas, offshore Texas, U. S. A. – Their evolution and the factors that controlled their deposition”. In Late Quaternary Stratigraphic Evolution of the Northern Gulf of Mexico Margin, SEPM Special Publication No. 79, p.237-269.

2.5-451 Anderson, J. B., Rodriguez, A., Abdulah, K. C., Fillon, R. H., Banfield, L. A., McKeown, H. A., Wellner, J. S. (2004) “Late Quaternary stratigraphic evolution of the northern Gulf of Mexico margin: A synthesis”. In Late Quaternary Stratigraphic Evolution of the Northern Gulf of Mexico Margin, SEPM Special Publication No. 79, p.1-23.

2.5-452 Baker, V. R., Penteado-Orellana, M. (1978) “Fluvial sedimentation conditioned by Quaternary climatic change in central Texas”. Journal of Sedimentary Petrology, v.48, no.2, p.433-451.

2.5-474 Westaway, R. (2007) “Late Cenozoic uplift of the eastern United States revealed by fluvial sequences of the Susquehanna and Ohio systems: coupling between surface processes and lower-crustal flow”. Quaternary Science Reviews, v.26, p.2823-2843.

2.5-475 Zachos, J. C., Quinn, T. M., Salamy, K. A. (1996) “High resolution (104 years) deep-sea foraminiferal stable isotope records of the Eocene-Oligocene climate transition”. Paleoceanography, v.11, no.3, p.251-266.

2.5-476 Davis, D.M., Pennington, W., and Carlson, S., 1985, Historical seismicity of the state of Texas: a summary: Gulf Coast Association of Geological Societies Transactions, v. 35, p. 39-44.

2.5-477 Luza, K.V., and Lawson, J.E., 1993, Oklahoma Seismic Network: Washington, D.C., US Nuclear Regulatory Commission, NUREG/CR-6034, p. 33.

2.5-478 USGS, 2006, M5.8 Gulf of Mexico earthquake of 10 September 2006, U.S. Geological survey, Earthquake Summary MAP, p. 1: 4,500,000. Map released 9/18/2006.

2.5-479 ~~Dewey, J.A., and J.A. Dellinger (2008). Location of Green Canyon (Offshore Souther Lousiana) Seismic Event of February 10, 2006, US Geological Survey Open File Rept. 2008-1184.~~Removed CTS-01521

2.5-480 ASTM International, ASTM C94, Standard Specification for Ready-Mixed Concrete.

2.5-481 ASTM International, ASTM C39, Standard Test Method for Compressive Strength of Cylindrical Concrete Specimens.

2.5-482 ASTM International, ASTM C150, Standard Specification for Portland Cement.

2.5-483 ASTM International, ASTM C31/C31-08a, Standard Practice for Making and Curing Concrete Test Speciments in the Field.

2.5-484 ASTM International, ASTM D1557, Standard Test Methods for Laboratory Compaction Characteristics of Soil Using Modified Effort.

2.5-485 ASTM International, ASTM D422, Standard Test Method for Particle-Size Analysis of Soils.

2.5-486 NRC, U.S. Nuclear Regulatory Commission, Office of Nuclear Regulatory Research. 2012: Technical Report: Central and Eastern CTS-01521

United States Seismic Source Characterization for Nuclear Facilities, Washington DC, NUREG-2115. CTS-01521

2.5-487 Gardner J.K and Knopoff (1974). Is the Sequence of Earthquakes in Southern California, with Aftershocks Removed, Poissonian? Bulletin of the Seismological Society of America, Vol 64, No. 5.

2.5-488 Northrop S.A. and Sanford A.R. Earthquakes of Northeastern New Mexico and the Texas Panhandle.

2.5-489 NRC, U.S. Nuclear Regulatory Commission. 2012, Request for Information Pursuant to Title 10 of the Code of Federal Regulations 50.54(f) Regarding Recommendations 2.1, 2.3, and 9.3, of the Near-Term Task Force Review of Insights from the Fukushima Dai-ichi Accident, ADAMS Accession No. ML12053A340.

2.5-490 Nuclear Engineering Institute (2009). Consistent Site-Response/ Soil-Structure Interaction Analysis and Evaluation, NEI White Paper, ADAMS Accession No. ML091680715.

CTS-01521

CP COL 2.5(1)

Table 2.5.2-201 (Sheet 1 of 6)

Updated Seismicity Catalog for CPNPP 3 & 4 With Time of Event, Location of Event, Best Estimate Body-wave Magnitude (Emb), Estimate of Standard Deviation of Magnitude (Smb), Uniform Magnitude (Rmb), and Source Catalog

Year	Mon	Day	Hr	Min	Sec	Lat	Lon	Emb	Smb	Rmb	Cat
1985	2	10	14	15	52.21	36.4330	-98.4120	3.00	0.10	3.01	OGS
1985	5	5	1	39	30.78	34.6640	-97.5290	3.00	0.10	3.01	OGS
1985	9	6	22	17	2.86	35.81	-93.12	3.80	0.10	3.81	PDE
1985	9	18	15	54	4.64	33.55	-97.05	3.30	0.10	3.31	PDE
1985	9	23	1	3	44.10	34.7250	-95.0590	3.30	0.10	3.31	OGS
1985	12	31	18	27	26.12	34.7030	-97.4590	3.00	0.10	3.01	OGS
1986	1	30	22	26	37.07	32.07	-100.69	3.30	0.10	3.31	PDE
1986	3	3	11	45	17.48	35.31	-102.51	3.10	0.10	3.11	PDE
1986	10	20	4	32	49.00	37.92	-101.37	3.00	0.10	3.01	PDE
1987	1	24	16	8	17.01	35.8280	-98.0970	3.40	0.10	3.41	OGS
1987	12	6	17	43	48.18	34.6640	-97.3940	3.00	0.10	3.01	OGS
1987	12	8	1	42	40.28	36.0550	-98.0240	3.70	0.10	3.71	OGS
1989	7	20	6	7	51.54	36.3820	-98.8180	3.10	0.10	3.11	OGS
1990	7	28	7	53	33.75	34.6000	-93.3760	3.01	0.41	3.20	ANSS
1990	08	03	15	31	40.32	32.2050	-100.6925	3.35	0.30	3.45	NMT
1990	9	16	21	13	33.38	34.8550	-95.5770	3.20	0.10	3.21	OGS
1990	10	11	11	7	22.14	34.7770	-97.5030	3.60	0.10	3.61	OGS
1990	11	15	11	44	41.63	34.7610	-97.5500	4.00	0.10	4.01	OGS

CTS-01521

CP COL 2.5(1)

Table 2.5.2-201 (Sheet 2 of 6)

Updated Seismicity Catalog for CPNPP 3 & 4 With Time of Event, Location of Event, Best Estimate Body wave Magnitude (Emb), Estimate of Standard Deviation of Magnitude (Smb), Uniform Magnitude (Rmb), and Source Catalog

Year	Mon	Day	Hr	Min	Sec	Lat	Lon	Emb	Smb	Rmb	Cat
1990	11	15	11	45	35.06	35.6030	-93.0420	3.50	0.41	3.69	ANSS
1991	1	24	5	0	26.90	36.38	-97.30	3.00	0.10	3.01	PDE
1991	7	20	23	38	19.21	28.91	-98.04	3.60	0.10	3.61	PDE
1992	1	2	11	45	35.61	32.33	-103.10	5.00	0.10	5.01	PDE
1992	08	26	03	24	51.16	32.2093	-102.5920	3.15	0.30	3.25	NMT
1992	12	17	7	18	5.65	34.7300	-97.5410	3.80	0.10	3.81	OGS
1993	1	14	17	6	10.45	35.5950	-98.2750	3.20	0.10	3.21	OGS
1993	4	9	12	29	19.17	28.81	-98.12	4.30	0.10	4.31	PDE
1993	5	7	17	50	37.70	34.7380	-97.5410	3.10	0.10	3.11	OGS
1993	5	16	15	30	19.39	28.81	-98.17	3.00	0.10	3.01	PDE
1993	9	29	2	1	19.06	35.87	-102.98	3.30	0.10	3.31	PDE
1993	10	19	16	59	52.41	36.5460	-98.1730	3.10	0.10	3.11	OGS
1993	11	30	03	07	36.28	35.8088	-103.1567	3.26	0.30	3.37	NMT
1993	12	05	00	58	24.06	27.9877	-102.0607	4.03	0.30	4.13	NMT
1993	12	05	03	35	14.14	27.8975	-102.0582	3.43	0.30	3.53	NMT
1994	4	16	7	20	29.99	34.6630	-97.7130	3.10	0.10	3.11	OGS
1994	4	29	3	28	58.68	36.25	-98.09	3.00	0.10	3.01	PDE
1995	1	18	15	51	39.90	34.7120	-97.5420	4.20	0.10	4.21	OGS
1995	4	5	5	31	16.23	35.20	-99.03	3.00	0.10	3.01	PDE

CTS-01521

CP COL 2.5(1)

Table 2.5.2-201 (Sheet 3 of 6)

Updated Seismicity Catalog for CPNPP 3 & 4 With Time of Event, Location of Event, Best Estimate Body wave Magnitude (Emb), Estimate of Standard Deviation of Magnitude (Smb), Uniform Magnitude (Rmb), and Source Catalog

Year	Mon	Day	Hr	Min	Sec	Lat	Lon	Emb	Smb	Rmb	Cat
1995	4	14	0	32	56.17	30.28	-103.35	5.71	0.10	5.71	PDE
1995	4	14	2	19	38.50	30.30	-103.35	3.30	0.10	3.31	PDE
1995	4	15	14	33	29.51	30.27	-103.32	4.00	0.10	4.01	PDE
1995	6	1	1	6	15.70	30.30	-103.35	3.50	0.10	3.51	PDE
1995	6	1	4	49	27.70	34.1340	-96.6830	3.30	0.10	3.31	OGS
1995	9	15	0	31	33.26	36.87	-98.69	4.10	0.10	4.11	PDE
1995	11	12	17	45	59.40	30.30	-103.35	3.60	0.10	3.61	PDE
1995	12	1	14	37	43.00	35.1550	-98.8970	3.00	0.10	3.01	OGS
1996	3	25	6	43	46.86	35.61	-102.60	3.50	0.10	3.51	PDE
1996	11	23	10	54	18.50	35.0400	-100.5040	3.09	0.41	3.28	ANSS
1997	2	12	23	53	10.77	34.9470	-100.8900	3.09	0.41	3.28	ANSS
1997	2	15	9	8	55.46	34.9730	-100.5690	3.25	0.41	3.45	ANSS
1997	3	16	19	7	28.00	34.2700	-93.4900	3.42	0.41	3.61	ANSS
1997	5	31	3	26	41.34	33.1820	-95.9660	3.42	0.41	3.61	ANSS
1997	9	6	23	38	0.91	34.66	-96.43	4.50	0.10	4.51	PDE
1997	9	6	23	38	1.99	34.6760	-96.4990	4.40	0.10	4.41	OGS
1997	10	19	11	12	09.74	32.3347	-103.9360	3.11	0.30	3.21	NMT
1998	1	2	15	47	16.43	37.8280	-103.4080	3.42	0.41	3.61	ANSS
1998	4	15	10	33	42.42	30.19	-103.30	3.60	0.10	3.61	PDE

CTS-01521

CP COL 2.5(1)

Table 2.5.2-201 (Sheet 4 of 6)
Updated Seismicity Catalog for CPNPP 3 & 4 With Time of Event, Location of Event, Best Estimate Body wave Magnitude (Emb), Estimate of Standard Deviation of Magnitude (Smb), Uniform Magnitude (Rmb), and Source Catalog

Year	Mon	Day	Hr	Min	Sec	Lat	Lon	Emb	Smb	Rmb	Cat
1998	4	27	15	22	46.25	35.4530	-102.3830	3.25	0.41	3.45	ANSS
1998	4	28	14	13	1.27	34.7550	-98.4470	4.20	0.10	4.21	OGS
1998	7	7	18	44	44.46	34.7190	-97.5890	3.25	0.41	3.45	ANSS
1998	7	14	5	38	48.75	35.3440	-103.4730	3.01	0.41	3.20	ANSS
1998	10	30	17	41	21.42	36.7710	-97.6230	3.50	0.10	3.51	OGS
1998	10	30	17	41	22.20	36.8000	-97.6000	3.50	0.41	3.69	ANSS
1999	10	25	23	19	51.68	36.9462	-100.0700	3.00	0.10	3.01	OGS
1999	10	25	23	19	58.37	36.8460	-99.6590	3.09	0.41	3.28	ANSS
2000	1	14	10	39	34.94	34.6735	-95.0949	3.00	0.10	3.01	OGS
2000	8	7	17	19	8.00	35.3920	-101.8120	3.33	0.41	3.53	ANSS
2000	8	7	18	34	9.00	35.3920	-101.8120	3.09	0.41	3.28	ANSS
2000	8	7	21	36	21.00	35.3920	-101.8120	3.09	0.41	3.28	ANSS
2000	8	10	13	39	50.00	35.3920	-101.8120	3.09	0.41	3.28	ANSS
2000	8	17	1	8	5.45	35.39	-101.81	3.90	0.10	3.91	PDE
2000	12	16	22	8	54.00	35.40	-101.80	3.90	0.10	3.91	PDE
2001	3	30	17	13	55.60	37.9330	-93.3270	3.17	0.41	3.37	ANSS
2001	6	2	1	55	53.72	32.3340	-103.1410	3.33	0.41	3.53	ANSS
2001	7	24	14	2	35.00	37.7000	-97.0000	3.09	0.41	3.28	ANSS
2001	8	4	1	13	28.00	34.4200	-93.2300	3.25	0.41	3.45	ANSS

CTS-01521

CP COL 2.5(1)

Table 2.5.2-201 (Sheet 5 of 6)
Updated Seismicity Catalog for CPNPP 3 & 4 With Time of Event, Location of Event, Best Estimate Body wave Magnitude (Emb), Estimate of Standard Deviation of Magnitude (Smb), Uniform Magnitude (Rmb), and Source Catalog

Year	Mon	Day	Hr	Min	Sec	Lat	Lon	Emb	Smb	Rmb	Cat
2001	11	22	0	7	8.02	31.7860	-102.6310	3.17	0.41	3.37	ANSS
2002	2	8	16	7	13.84	34.6514	-98.3021	3.80	0.10	3.81	OGS
2002	5	31	9	57	9.87	34.9997	-97.6228	3.00	0.10	3.01	OGS
2002	5	31	9	57	10.02	34.0250	-97.6190	3.33	0.41	3.53	ANSS
2002	6	19	12	14	20.30	36.57	-103.03	3.70	0.10	3.71	PDE
2002	10	20	2	18	14.06	34.2140	-96.1810	3.60	0.10	3.61	OGS
2003	4	7	10	2	12.51	33.8920	-97.6950	3.01	0.41	3.20	ANSS
2003	9	24	15	2	9.09	35.2770	-101.7420	3.33	0.41	3.53	ANSS
2004	4	22	16	13	2.25	34.8040	-97.6770	3.01	0.41	3.20	ANSS
2004	6	8	0	15	8.38	34.0410	-97.3070	3.70	0.10	3.71	OGS
2004	6	8	0	15	9.99	34.23	-97.25	3.50	0.10	3.51	PDE
2004	6	10	12	30	9.86	34.2360	-97.2670	3.01	0.41	3.20	ANSS
2004	11	22	23	42	13.45	34.8640	-97.6720	3.09	0.41	3.28	ANSS
2004	11	30	23	59	34.00	36.9400	-93.8900	3.01	0.41	3.20	ANSS
2005	2	6	15	59	14.48	34.2380	-95.2380	3.50	0.10	3.51	OGS
2005	4	3	14	39	16.97	28.3930	-100.3050	3.50	0.41	3.69	ANSS
2005	4	22	5	17	4.09	34.1790	-95.1920	3.09	0.41	3.28	ANSS
2006	2	18	5	49	41.45	35.6720	-101.7940	3.50	0.41	3.69	ANSS
2006	3	28	23	55	11.49	35.3630	-101.8710	3.09	0.41	3.28	ANSS

CTS-01521

CP COL 2.5(1)

Table 2.5.2-201 (Sheet 6 of 6)
Updated Seismicity Catalog for CPNPP 3 & 4 With Time of Event, Location of Event, Best Estimate Body-wave Magnitude (Emb), Estimate of Standard Deviation of Magnitude (Smb), Uniform Magnitude (Rmb), and Source Catalog

Year	Mon	Day	Hr	Min	Sec	Lat	Lon	Emb	Smb	Rmb	Cat
2006	4	5	18	46	23.14	34.0690	-97.3140	3.09	0.41	3.28	ANSS
2006	4	8	18	8	35.23	31.9540	-101.4190	3.01	0.41	3.20	ANSS
2006	10	6	22	13	16.78	34.12	-97.62	3.50	0.10	3.51	PDEW

CP COL 2.5(1)

CTS-01521

Table 2.5.2-201 (Sheet 1 of 4)
Regional Seismicity Catalog Update

Year	Month	Day	Hour	Min	Sec	Lat	Lon	Depth	Mw	Catalog
2009	01	28	11	19	09.47	35.1600	-97.8700	5	3.08	NEIC
2009	02	03	10	23	10.01	34.5890	-96.3400	5	3.23	ANSS
2009	02	22	09	43	06.75	36.3690	-98.0870	5	3.31	ANSS
2009	02	25	04	14	15.33	34.7400	-96.0400	5	2.98	NEIC
2009	03	17	17	41	37.00	35.4460	-97.4560	5	3.10	OGS+LGO
2009	04	11	22	14	20.12	28.8760	-98.5260	5	3.00	ANSS
2009	05	16	16	24	06.57	32.7900	-97.0200	8	2.98	NEIC
2009	06	02	20	06	45.38	32.3520	-97.4030	5	3.00	ANSS
2009	06	14	21	31	09.02	35.6600	-96.8500	5	3.08	NEIC
2009	06	16	16	32	46.00	35.8900	-96.8730	5	3.00	ANSS
2009	06	26	21	23	13.75	36.3600	-97.4700	5	3.38	NEIC
2009	07	01	17	14	48.24	35.5500	-97.1700	5	3.08	NEIC
2009	07	22	02	25	59.80	35.7400	-96.9400	5	2.98	NEIC
2009	08	27	08	22	14.53	34.9400	-96.6200	5	3.08	NEIC
2009	08	28	02	09	06.00	35.5600	-97.2900	5	3.18	NEIC
2009	10	23	03	56	29.73	35.8040	-97.0290	5	3.16	ANSS
2009	11	02	18	27	05.86	35.4320	-96.5500	5	2.93	ANSS

CP COL 2.5(1)

CTS-01521

Table 2.5.2-201 (Sheet 2 of 4)
Regional Seismicity Catalog Update

Year	Month	Day	Hour	Min	Sec	Lat	Lon	Depth	Mw	Catalog
2009	11	14	11	13	01.34	35.4940	-97.2040	5	3.23	ANSS
2009	11	17	04	00	17.77	34.4620	-97.5320	5	3.23	ANSS
2009	12	05	05	30	11.84	32.4120	-97.0040	5	3.08	ANSS
2009	12	11	14	00	42.00	35.5800	-97.3200	5	3.38	OGS+LGO
2010	02	04	09	41	28.12	35.4900	-102.620	2	3.30	NEIC
2010	02	27	22	22	27.31	35.5500	-96.7500	5	4.10	NEIC
2010	03	08	23	47	28.12	28.9460	-98.0390	5	3.16	ANSS
2010	03	11	08	11	01.90	35.3800	-98.0500	5	3.16	NEIC
2010	03	28	15	29	56.00	35.5436	-97.2419	5	3.38	OGS+LGO
2010	04	12	09	40	10.00	34.6300	-96.3200	0	3.00	NEIC
2010	05	07	12	44	57.00	35.5300	-97.3000	5	3.08	NEIC
2010	05	21	00	01	52.81	36.4060	-94.2980	6	2.93	ANSS
2010	06	02	23	24	19.00	36.7309	-95.3909	5	2.93	OGS+LGO
2010	06	12	04	29	53.00	35.6300	-97.2000	5	2.93	NEIC
2010	06	14	21	33	56.50	34.8700	-97.6800	5	3.23	NEIC
2010	06	19	02	14	32.00	35.0100	-97.4200	5	2.93	NEIC
2010	06	22	23	27	37.50	35.5300	-97.2900	4	2.93	NEIC
2010	06	30	16	19	00.00	35.5220	-96.7702	5	2.93	OGS+LGO
2010	06	30	23	34	51.00	34.2700	-97.4800	3	2.93	NEIC

CP COL 2.5(1)

CTS-01521

Table 2.5.2-201 (Sheet 3 of 4)
Regional Seismicity Catalog Update

Year	Month	Day	Hour	Min	Sec	Lat	Lon	Depth	Mw	Catalog
2010	07	14	13	24	06.00	36.8510	-98.2220	5	2.93	ANSS
2010	07	26	09	56	43.00	35.5462	-97.2621	5	3.46	OGS+LGO
2010	08	07	14	24	03.00	34.6668	-96.0950	5	3.08	OGS+LGO
2010	08	08	00	50	38.00	35.8477	-96.8093	5	3.08	NMT
2010	08	08	01	12	33.00	33.1730	-100.7610	5	2.97	OGS+LGO
2010	08	08	01	12	38.07	32.9000	-100.8500	5	3.40	NEIC
2010	08	25	09	48	34.00	35.5413	-96.7617	5	3.54	OGS+LGO
2010	09	25	12	19	26.00	34.1100	-96.7100	5	2.98	NEIC
2010	10	01	22	39	14.00	34.8610	-96.0290	5	3.23	ANSS
2010	10	11	03	37	07.00	35.6209	-97.2485	5	3.69	OGS+LGO
2010	10	13	14	06	30.00	35.1900	-97.3200	13	4.40	NEIC
2010	10	13	23	21	38.00	35.0798	-95.6202	5	3.00	OGS+LGO
2010	10	25	20	53	13.00	34.8740	-97.7410	5	3.31	ANSS
2010	11	16	00	46	06.00	34.7175	-97.3941	5	2.93	OGS+LGO
2010	12	21	13	53	18.04	28.6420	-98.0390	5	3.16	ANSS
2010	12	24	10	49	07.00	34.6900	-96.3600	5	3.16	NEIC
2010	12	28	01	49	23.00	34.7202	-95.9107	0	3.23	OGS+LGO
2011	01	10	05	35	50.00	34.7800	-96.6700	5	2.93	NEIC
2011	01	18	03	40	06.00	34.5700	-97.4300	0	3.00	NEIC

CP COL 2.5(1)

CTS-01521

Table 2.5.2-201 (Sheet 4 of 4)
Regional Seismicity Catalog Update

Year	Month	Day	Hour	Min	Sec	Lat	Lon	Depth	Mw	Catalog
2011	01	24	17	33	09.00	36.6723	-94.8312	0	3.00	OGS+LGO
2011	02	04	02	06	29.00	35.4801	-97.4018	5	2.93	OGS+LGO
2011	02	19	05	39	56.00	35.7500	-99.6700	5	2.93	NEIC
2011	03	13	20	16	20.62	32.9900	-100.770	5	3.80	NEIC
2011	03	17	01	27	23.00	34.8636	-97.7521	3	2.93	OGS+LGO
2011	05	28	07	32	51.00	34.5173	-96.4959	3	3.08	OGS+LGO
2011	06	07	22	59	56.00	35.8323	-98.3980	3	3.00	OGS+LGO
2011	06	12	16	51	48.06	32.2360	-97.0020	5	2.93	ANSS
2011	07	17	06	58	0.040	32.4240	-97.0840	5	3.15	ANSS
2011	08	18	16	50	52.00	34.8800	-97.7400	5	3.15	NEIC
2011	09	11	12	27	44.32	32.8500	-100.770	5	4.30	NEIC
2011	10	20	12	24	41.60	28.8600	-98.0800	5	4.80	NEIC
2011	11	06	03	53	10.00	35.5300	-96.7600	5	5.60	NEIC
2011	11	07	01	26	31.00	35.5180	-96.7860	3	3.38	ANSS
2011	11	09	15	21	2.00	35.5100	-97.3900	3	3.15	NEIC
2011	11	29	15	03	14.00	34.9200	-96.0000	0	2.93	NEIC
2011	12	07	22	54	19.15	32.4180	-97.1060	5	2.93	ANSS
2011	12	09	18	47	33.24	32.9400	-100.860	5	3.18	NEIC

CP COL 2.5(1)

CTS-01521

Table 2.5.2-202 (Sheet 1 of 2)
Summary of Bechtel Group Seismic Source Zones

Source	Description	Distance[a] (km)	Distance[a] (mi)	Pa[b]	M_{max} (m_b) and Wts.[c]	Smoothing Options and Wts.[d]	Contributes to 99% of Hazard[e]
39	Oklahoma Aulacogen	143	89	0.20	5.4 [0.1] 5.7 [0.4] 6.0 [0.4] 6.6 [0.1]	1 [0.33] 2 [0.34] 3 [0.33]	Yes
BZ2	Texas Platform	0	0	1.0	5.4 [0.1] 5.7 [0.4] 6.0 [0.4] 6.6 [0.1]	1 [0.33] 2 [0.34] 3 [0.33]	Yes
38	Ouachita	205	125	0.25	5.4 [0.1] 5.7 [0.4] 6.0 [0.4] 6.6 [0.1]	1 [0.33] 2 [0.34] 4 [0.33]	Yes
BZ3	North Great Plains	143	89	1.0	5.4 [0.1] 5.7 [0.4] 6.0 [0.4] 6.6 [0.1]	1 [0.33] 2 [0.34] 3 [0.33]	Yes
C04	Combination Zone	143	89	NA	5.4 [0.1] 5.7 [0.4] 6.0 [0.4] 6.6 [0.1]	1 [0.33] 2 [0.34] 4 [0.33]	Yes
40	Meers Fault	268	166	0.70	5.4 [0.1] 6.0 [0.4] 6.6 [0.4] 7.5 [0.1]	1 [0.33] 2 [0.34] 4 [0.33]	NA - replaced

CP COL 2.5(1)

CTS-01521

Table 2.5.2-202 (Sheet 2 of 2)
Summary of Bechtel Group Seismic Source Zones

Source	Description	Distance[a] (km)	Distance[a] (mi)	Pa[b]	M_{max} (m_b) and Wts.[c]	Smoothing Options and Wts.[d]	Contributes to 99% of Hazard[e]
65	El Reno	315	196	0.35	5.4 [0.1] 5.7 [0.4] 6.0 [0.4] 6.6 [0.1]	1 [0.33] 2 [0.34] 4 [0.33]	No
BZ1	Gulf Coast	219	136	1.0	5.4 [0.1] 5.7 [0.4] 6.0 [0.4] 6.6 [0.1]	1 [0.33] 2 [0.34] 3 [0.33]	No
55	S.E. Oklahoma	235	146	0.15	5.4 [0.1] 5.7 [0.4] 6.0 [0.4] 6.6 [0.1]	1 [0.33] 2 [0.34] 4 [0.33]	No

a) Shortest distance between CPNPP 3 & 4 and source zone.

b) Probability of activity (EPRI, 1989a).

c) Maximum earthquake magnitude (M_{max}) in body wave magnitude (m_b) and weighting (Wts.) (EPRI, 1989a).

d) Smoothing options (EPRI, 1989a):
1 = constant a, constant b, no b prior;
2 = low smoothing on a, high smoothing on b, no b prior;
3 = low smoothing on a, low smoothing on b, no b prior;
4 = low smoothing on a, low smoothing on b, weak b prior of 1.05;
Weights on magnitude intervals are [1.0, 1.0, 1.0, 1.0, 1.0, 1.0, 1.0].

e) Whether or not the source contributes to 99% of the hazard at CPNPP Units 3 and 4.

CP COL 2.5(1)

CTS-01521

Table 2.5.2-202 (Sheet 1 of 2)
CEUS SSC Seismic Sources

Source		Name
Background	Mmax	CEUS SSC Study Region (STUDY-R)
		Mesozoic-and-Younger Extended - Narrow (MESE-N)
		Mesozoic-and-Younger Extended - Wide (MESE-W)
		Non-Mesozoic-and-Younger Extended - Narrow (NMESE-N)
		Non-Mesozoic-and-Younger Extended - Wide (NMESE-W)
	Seismotectonic	Atlantic Highly Extended Crust (AHEX)
		Extended Continental Crust - Atlantic Margin (ECC-AM)
		Extended Continental Crust - Gulf Coast (ECC-GC)
		Gulf Highly Extend Crust (GHEX)
		Great Meteor Hotspot (GMH)
		Illinois Basin Extended Basement (IBEB)
		Midcontinent-Craton alternative (MIDC-A, MIDC-B, MIDC-C, and MIDC-D)
		Northern Appalachians (NAP)
		Oklahoma Aulacogen (OKA)
		Paleozoic Extended Crust - Narrow (PEZ-N)
		Paleozoic Extended Crust - Wide (PEZ-W)
		Reelfoot Rift (RR)
		Reelfoot Rift including Rough Creek Graben (RR-RCG)
		St. Lawrence Rift, including the Ottawa and Saguenay Grabens (SLR)

CP COL 2.5(1)

Table 2.5.2-202 (Sheet 2 of 2)
CEUS SSC Seismic Sources

CTS-01521

Source	Name
RLME	Charleston (CHARLESTON)
	Charlevoix (CHARLEVOIX)
	Cheraw
	Reelfoot Rift - Commerce (COMMERCE)
	Reelfoot Rift - Eastern Rift Margin (ERM-N and ERM-S)
	Reelfoot Rift - Marianna (MARIANNA)
	Meers (MEERS)
	Reelfoot Rift - Central Fault System (NMFS) – New Madrid Fault System
	Wabash Valley (WABASH_VALLEY)

CP COL 2.5(1)

CTS-01521

Table 2.5.2-203 (Sheet 1 of 2)
Summary of Dames & Moore Seismic Source Zones

Source	Description	Distance[a] (km)	Distance[a] (mi)	Pa[b]	M_{max} (m_b) and Wts.[c]	Smoothing Options and Wts.[d]	Contributes to 99% of Hazard[e]
20	Southern Coastal Margin	134	83	1.0	5.3 [0.8] 7.2 [0.2]	1 [0.75] 2 [0.25]	Yes
25	Ouachitas Fold Belt	42	26	0.35	5.5 [0.8] 7.2 [0.2]	1 [0.75] 2 [0.25]	Yes
25a	Kink in Ouachita Fold Belt	121	75	0.65	5.7 [0.75] 7.2 [0.25]	3 [0.75] 4 [0.25]	Yes
28	S. Oklahoma Aulacogen	147	91	0.44	6.0 [0.75] 7.2 [0.25]	3 [0.75] 4 [0.25]	Yes
28b	Default for S. Oklahoma Aulacogen	113	70	0.56	5.0 [0.8] 7.2 [0.2]	1 [0.75] 2 [0.25]	Yes
67	New Mexico	0	0	1.0	5.5 [0.8] 7.2 [0.2]	1 [0.75] 2 [0.25]	Yes
C08	Combination Zone	42	26	NA	5.5 [0.8] 7.2 [0.2]	1 [0.75] 2 [0.25]	Yes
29	B-W-M Fault	160	100	0.31	6.0 [0.75] 7.2 [0.25]	3 [0.75] 4 [0.25]	No
30	A/W Uplift	170	110	0.42	6.0 [0.75] 7.2 [0.25]	3 [0.75] 4 [0.25]	No

CP COL 2.5(1)

CTS-01521

Table 2.5.2-203 (Sheet 2 of 2)
Summary of Dames & Moore Seismic Source Zones

Source	Description	Distance[a] (km)	Distance[a] (mi)	Pa[b]	M_{max} (m_b) and Wts.[c]	Smoothing Options and Wts.[d]	Contributes to 99% of Hazard[e]
32	Ardmore Basin	230	140	0.51	6.0 [0.75] 7.2 [0.25]	3 [0.75] 4 [0.25]	No
33	Anadarko Basin	266	165	1.0	5.8 [0.75] 7.2 [0.25]	1 [0.34] 2 [0.11] 3 [0.41] 4 [0.14]	No
31	Mt. View/Meers	210	130	0.45	6.0 [0.75] 7.2 [0.25]	3 [0.75] 4 [0.25]	NA - replaced

a) Shortest distance between CPNPP 3 & 4 and source zone.

b) Probability of activity (EPRI, 1989a).

c) Maximum earthquake magnitude (M_{max}) in body wave magnitude (m_b) and weighting (Wts.) (EPRI 1989a).

d) Smoothing options (EPRI, 1989a):

1 = no smoothing on a, no smoothing on b, strong b prior of 1.04:

2 = no smoothing on a, no smoothing on b, weak b prior of 1.04;

3 = constant a, constant b, strong b prior of 1.04;

4 = constant a, constant b, weak b prior of 1.04;

Weights on magnitude intervals are [0.1, 0.2, 0.4, 1.0, 1.0, 1.0, 1.0].

e) Whether or not the source contributes to 99% of the hazard at CPNPP Units 3 and 4.

CP COL 2.5(1)

CTS-01521

Table 2.5.2-203 (Sheet 1 of 2)
Comparison of Lowest Mmax in the CEUS SSC Mmax Distribution of each Backgound Zone with the Mmax of each zone based on the CEUS SSC Seismicity Catalog Update

M_{max} and Seismotectonic (Background) Zones	Lowest Mmax in CEUS SSC Mmax Distribution	Mmax for CEUS SSC Catalog Update
Study Region	6.5	5.80
MESE_N	6.4	5.80
NMESE_N	6.4	5.60
MESE_W	6.5	5.80
NMESE_W	5.7	5.60
AHEX	6.0	< 2.9
ECC_AM	6.0	5.80
ECC_GC	6.0	4.80
GHEX	6.0	3.58
GMH	6.0	5.20
IBEB	6.5	2.93
MID_A	5.6	5.60
MID_B	5.6	5.60

CP COL 2.5(1)

CTS-01521

Table 2.5.2-203 (Sheet 2 of 2)
Comparison of Lowest Mmax in the CEUS SSC Mmax Distribution of each Backgound Zone with the Mmax of each zone based on the CEUS SSC Seismicity Catalog Update

M_{max} and Seismotectonic (Background) Zones	Lowest Mmax in CEUS SSC Mmax Distribution	Mmax for CEUS SSC Catalog Update
MID_C	5.6	5.60
MID_D	5.6	5.60
NAP	6.1	3.17
OKA	5.8	3.23
PEZ_N	5.9	3.40
PEZ_W	5.9	3.40
RR	6.2	3.40
RR_RCG	6.1	3.69
SLR	6.2	3.67

CP COL 2.5(1)

CTS-01521

Table 2.5.2-204
Summary of Law Engineering Seismic Source Zones

Source	Description	Distance[a] (km)	Distance[a] (mi)	Pa[b]	M_{max} (m_b) and Wts.[c]	Smoothing Options and Wts.[d]	Contributes to 99% of Hazard[e]
124	New Mexico–Texas Block	0	0	1.0	4.9 [0.3] 5.5 [0.5] 5.8 [0.2]	1a [1.0]	Yes
26	Oklahoma Aulacogen-Arbuckle Wichita Rift	150	93	0.6	5.0 [0.2] 5.2 [0.5 6.8 [0.3]	1a [1.0]	Yes
119	Eastern Mid-Continent	151	94	1.0	4.6 [0.3] 5.0 [0.3] 5.5 [0.4]	1a [1.0]	No
120	Western Mid-Continent	300	190	1.0	4.9 [0.5] 5.5 [0.5]	3a [1.0]	No
126	South Coastal Block	148	92	1.0	4.6 [0.9] 4.9 [0.1]	1a [1.0]	No

a) Shortest distance between CPNPP 3 & 4 and source zone.

b) Probability of activity (EPRI, 1989a).

c) Maximum earthquake magnitude (M_{max}) in body wave magnitude (m_b) and weighting (Wts.) (EPRI, 1989a).

d) Smoothing options (EPRI, 1989a):

1a = high smoothing on a, constant b, strong b prior of 1.05;

Weights on magnitude intervals are all 1.0.

e) Whether or not the source contributes to 99% of the hazard at CPNPP Units 3 and 4.

CTS-01521

CP COL 2.5(1)

Table 2.5.2-204

Values of Mean and Median UHRS Rock Seismic Hazard (in g) for 10^{-4}, 10^{-5}, and 10^{-6}

Frequency	10^{-4} Mean UHRS	10^{-5} Mean UHRS	10^{-6} Mean UHRS	10^{-4} Median UHRS	10^{-5} Median UHRS	10^{-6} Median UHRS
0.5	0.0413	0.121	0.255	0.0137	0.0282	0.0565
1	0.0533	0.131	0.264	0.0244	0.0528	0.109
2.5	0.0831	0.198	0.416	0.0480	0.111	0.240
5	0.107	0.268	0.652	0.0682	0.164	0.395
10	0.124	0.334	0.948	0.0796	0.205	0.556
25	0.158	0.477	1.440	0.0783	0.235	0.752
100	0.0609	0.164	0.512	0.0354	0.0931	0.281

CP COL 2.5(1)

CTS-01521

Table 2.5.2-205
Summary of Rondout Associates Seismic Source Zones

Source	Description	Distance[a] (km)	Distance[a] (mi)	Pa[b]	M_{max} (m_b) and Wts.[c]	Smoothing Options and Wts.[d]	Contributes to 99% of Hazard[e]
16	S. Oklahoma Aulacogen Ouachita Mts.	129	80	1.0	5.8 [0.15] 6.5 [0.60] 6.8 [0.25]	1 [1.0]	Yes
C02	Grenville Crust	0	0	NA	4.8 [0.2] 5.5 [0.6] 5.8 [0.2]	3 [1.0]	Yes
23	Nemaha Anadark	230	140	1.0	6.6 [0.2] 6.8 [0.6] 7.0 [0.2]	1 [1.0]	Yes
51	Gulf Coast to Bahamas Fracture Zone	92	57	1.0	4.8 [0.2] 5.5 [0.6] 5.8 [0.2]	3 [1.0]	Yes
52	Pre-Grenville Precambrian Craton	290	180	1.0	4.8 [0.2] 5.5 [0.6] 5.8 [0.2]	3 [1.0]	No

a) Shortest distance between CPNPP 3 & 4 and source zone.

b) Probability of activity (EPRI, 1989a).

c) Maximum earthquake magnitude (M_{max}) in body wave magnitude (m_b) and weighting (Wts.) (EPRI, 1989a).

d) Smoothing options (EPRI, 1989a):

1 = constant a of -1.590, constant b of 1.020

2 = constant a of -1.350, constant b of 0.960

3 = low smoothing on a, constant b, strong b prior of 1.0.

e) Whether or not the source contributes to 99% of the hazard at CPNPP Units 3 and 4.

CP COL 2.5(1)

CTS-01521

Table 2.5.2-205
Mean Magnitudes and Distances from Deaggregation

Hazard	All *R*		*R*< 100 km		*R*> 100 km	
	Magnitude	Distance	Magnitude	Distance	Magnitude	Distance
Mean 10^{-4} HF (5+10 Hz)	7.0	220	6.0	23	7.2	360
Mean 10^{-4} LF (1+2.5 Hz)	7.5	410	7.0	9	7.6	600
Mean 10^{-5} HF (5+10 Hz)	6.7	97	5.9	18	7.4	360
Mean 10^{-5} LF (1+2.5 Hz)	7.6	420	6.8	13	7.7	640
Mean 10^{-6} HF (5+10 Hz)	6.2	20	6.0	12	7.5	310
Mean 10^{-6} LF (1+2.5 Hz)	7.6	290	6.7	14	7.8	640

Note: Light-gray cells indicate High Frequency (HF) controlling earthquakes and dark-gray cells indicate Low Frequency (LF) controlling earthquakes

CTS-01521

CP COL 2.5(1)

Table 2.5.2-206
Summary of Weston Geophysical Corporation Seismic Source Zones

Source	Description	Distance[a] (km)	Distance[a] (mi)	P*[b]	M_{max} (Em_b) and Wts.[c]	Smoothing Options and Wts.[d]	Contributes to 99% of Hazard[e]
109	Southwest	0	0	1.0	5.4 [0.33] 6.0 [0.49] 6.6 [0.18]	1a [0.2] 2a [0.8]	Yes
C31	Combination Zone	0	0	NA	5.4 [0.33] 6.0 [0.49] 6.6 [0.18]	1a [0.7] 2a [0.3]	Yes
36	Ancestral Rockies	137	85	1.0	5.4 [0.43] 6.0 [0.41] 6.6 [0.16]	1b [0.3] 2b [0.7]	Yes
107	Gulf Coast	128	79	1.0	5.4 [0.71] 6.0 [0.29]	1a [0.2] 2a [0.8]	Yes
37	Delaware Basin	230	140	0.81	5.4 [0.33] 6.0 [0.49] 6.6 [0.18]	1b [0.3] 2b [0.7]	No

a) Shortest distance between CPNPP 3 & 4 and source zone.

b) Probability of activity for earthquakes with magnitudes greater than the minimum magnitude of mb 5.0 (EPRI, 1989a).

c) Maximum earthquake magnitude (M_{max}) in body wave magnitude (m_b) and weighting (Wts.) (EPRI, 1989a).

d) Smoothing options (EPRI, 1989a):

1a = constant a, constant b, medium b prior of 1.0;

1b = constant a, constant b, medium b prior of 0.9;

2a = medium smoothing on a, medium smoothing on b, medium b prior of 1.0.

2b = medium smoothing on a, medium smoothing on b, medium b prior of 0.9.

e) Whether or not the source contributes to 99% of the hazard at CPNPP Units 3 and 4.

CP COL 2.5(1)

CTS-01521

Table 2.5.2-206

Deaggregation of the 10^{-4} High Frequencies

Distance Bin (km)	Magnitude Bin 5.25	5.75	6.25	6.75	7.25	7.75	8.25	8.75
0-20	2.6%	1.0%	0.3%	0.9%	1.2%	1.1%	<< 0.1%	<< 0.1%
20-40	2.2%	1.8%	0.7%	0.2%	< 0.1%	<< 0.1%	<< 0.1%	<< 0.1%
40-60	1.4%	1.0%	0.7%	0.2%	< 0.1%	<< 0.1%	<< 0.1%	<< 0.1%
60-80	0.3%	0.4%	0.3%	0.3%	< 0.1%	< 0.1%	<< 0.1%	<< 0.1%
80-100	0.3%	0.4%	0.6%	0.3%	0.1%	< 0.1%	<< 0.1%	<< 0.1%
100-200	1.0%	2.2%	2.8%	2.1%	0.9%	0.2%	< 0.1%	<< 0.1%
200-300	0.2%	0.7%	1.5%	17.0%	17.2%	6.2%	< 0.1%	<< 0.1%
> 300	< 0.1%	0.2%	0.8%	1.6%	3.6%	17.5%	5.5%	<< 0.1%

CP COL 2.5(1)

CTS-01521

Table 2.5.2-207 (Sheet 1 of 2)
Summary of Woodward-Clyde Consultants Seismic Source Zones

Source	Description	Distance[a] (km)	Distance[a] (mi)	P*[b]	M_{max} (m_b) and Wts.[c]	Smoothing Options and Wts.[d]	Contributes to 99% of Hazard[e]
BG44	Central US Backgrounds	0	0	NA	4.9 [0.17] 5.4 [0.28] 5.8 [0.27] 6.5 [0.28]	1 [0.25] 6 [0.25] 7 [0.25] 8 [0.25]	Yes
46	S. Oklahoma Aulacogen	161	100	0.084	5.7 [0.33] 6.8 [0.34] 7.2 [0.33]	3 [0.33] 4 [0.34] 5 [0.33]	Yes
46a	S. Oklahoma Aulacogen	161	100	0.083	5.7 [0.33] 6.8 [0.34] 7.2 [0.33]	3 [0.33] 4 [0.34] 5 [0.33]	Yes
49	Meers Fault	262	163	0.85	6.8 [0.33] 7.3 [0.34] 7.5 [0.33]	2^+ [1.0]	NA - replaced
52	E. Oklahoma Seismic Zone	238	148	0.4	5.4 [0.33] 6.0 [0.34] 6.5 [0.33]	3 [0.33] 4 [0.34] 5 [0.33]	No

CP COL 2.5(1)

CTS-01521

Table 2.5.2-207 (Sheet 2 of 2)
Summary of Woodward-Clyde Consultants Seismic Source Zones

Source	Description	Distance[a] (km)	Distance[a] (mi)	P*[b]	M_{max} (m_b) and Wts.[c]	Smoothing Options and Wts.[d]	Contributes to 99% of Hazard[e]
48	S. Oklahoma Gravity Anomaly	211	131	0.263	5.7 [0.33] 6.5 [0.34] 7.1 [0.33]	3 [0.33] 4 [0.34] 5 [0.33]	Yes

a) Shortest distance between CPNPP 3 & 4 and source zone.

b) Probability of activity for earthquakes with magnitudes greater than the minimum magnitude of mb 5.0 (EPRI, 1989a).

c) Maximum earthquake magnitude (M_{max}) in body wave magnitude (m_b) and weighting (Wts.) (EPRI, 1989a).

d) Smoothing options (EPRI, 1989a):

1 = low smoothing on a, high smoothing on b, no b prior;

3 = high smoothing on a, high smoothing on b, moderate b prior of 1.0.

4 = high smoothing on a, high smoothing on b, moderate b prior of 0.9.

5 = high smoothing on a, high smoothing on b, moderate b prior of 0.8.

6 = low smoothing on a, high smoothing on b, moderate b prior of 1.0;

7 = low smoothing on a, high smoothing on b, moderate b prior of 0.9;

8 = low smoothing on a, high smoothing on b, moderate b prior of 0.8;

9 = use "a" and "b" from homogeneous solution for source zone 46 with smoothing option 4.

Weights on magnitude intervals are all 1.0.

e) Whether or not the source contributes to 99% of the hazard at CPNPP Units 3 and 4.

CTS-01521

CP COL 2.5(1)

Table 2.5.2-207

Deaggregation of the 10^{-4} Low Frequencies

Distance Bin (km)	Magnitude Bin 5.25	5.75	6.25	6.75	7.25	7.75	8.25	8.75
0-20	0.4%	0.4%	0.2%	0.5%	2.3%	2.9%	<< 0.1%	<< 0.1%
20-40	< 0.1%	0.3%	0.3%	0.1%	< 0.1%	<< 0.1%	<< 0.1%	<< 0.1%
40-60	< 0.1%	0.1%	0.2%	0.1%	< 0.1%	<< 0.1%	<< 0.1%	<< 0.1%
60-80	<< 0.1%	< 0.1%	< 0.1%	0.1%	< 0.1%	< 0.1%	<< 0.1%	<< 0.1%
80-100	<< 0.1%	< 0.1%	0.2%	0.1%	< 0.1%	< 0.1%	<< 0.1%	<< 0.1%
100-200	< 0.1%	0.2%	0.7%	0.9%	0.6%	0.2%	<< 0.1%	<< 0.1%
200-300	<< 0.1%	< 0.1%	0.4%	7.4%	9.6%	4.0%	<< 0.1%	<< 0.1%
> 300	<< 0.1%	< 0.1%	0.4%	2.0%	9.2%	43.4%	12.0%	<< 0.1%

CP COL 2.5(1)

CTS-01521

Table 2.5.2-208
Comparison of PGA Hazard Results

PGA comparison

Ampl. (cm/s^2)	Mean			Median			0.85 fractile		
	EPRI SOG	2007	% diff	EPRI SOG	2007	% diff	EPRI SOG	2007	% diff
50	4.26E-05	4.59E-05	7.7%	1.91E-05	2.40E-05	25.6%	8.71E-05	9.55E-05	9.6%
100	1.06E-05	1.16E-05	9.4%	4.62E-06	6.92E-06	49.7%	1.83E-05	2.09E-05	14.2%
250	1.23E-06	1.38E-06	12.4%	4.60E-07	7.08E-07	53.9%	2.02E-06	2.07E-06	2.2%
500	1.41E-07	1.64E-07	16.4%	3.17E-08	5.89E-08	85.7%	2.26E-07	2.34E-07	3.7%

CP COL 2.5(1)

CTS-01521

Table 2.5.2-208

Deaggregation of the 10^{-5} High Frequencies

Distance Bin (km)	Magnitude Bin							
	5.25	5.75	6.25	6.75	7.25	7.75	8.25	8.75
0-20	10.7%	6.1%	2.7%	1.5%	1.2%	1.0%	<< 0.1%	<< 0.1%
20-40	3.1%	4.4%	3.0%	1.2%	0.4%	< 0.1%	<< 0.1%	<< 0.1%
40-60	0.8%	1.1%	1.3%	0.8%	0.3%	< 0.1%	<< 0.1%	<< 0.1%
60-80	< 0.1%	0.3%	0.4%	0.6%	0.2%	< 0.1%	<< 0.1%	<< 0.1%
80-100	< 0.1%	0.2%	0.6%	0.5%	0.3%	0.1%	<< 0.1%	<< 0.1%
100-200	0.1%	0.7%	1.7%	2.2%	1.6%	0.6%	< 0.1%	<< 0.1%
200-300	< 0.1%	< 0.1%	0.5%	8.0%	14.1%	7.7%	< 0.1%	<< 0.1%
> 300	<< 0.1%	< 0.1%	0.2%	0.5%	1.3%	11.9%	5.5%	<< 0.1%

CP COL 2.5(1)

CTS-01521

Table 2.5.2-209
Comparison of 1 Hz SV Hazard Results

1 Hz SV comparison

Ampl. (cm/s)	Mean			Median			0.85 fractile		
	EPRI SOG	2007	% diff	EPRI SOG	2007	% diff	EPRI SOG	2007	% diff
1	2.50E-04	2.60E-04	4.0%	3.96E-05	5.31E-05	34.1%	4.53E-04	3.43E-04	-24.3%
5	1.42E-05	1.56E-05	9.9%	4.15E-07	9.02E-07	117.3%	1.15E-05	1.16E-05	1.0%
10	3.08E-06	3.50E-06	13.5%	3.86E-08	1.26E-07	226.2%	2.27E-06	3.02E-06	33.0%
20	5.74E-07	6.66E-07	16.0%	9.08E-10	7.16E-09	688.7%	4.15E-07	5.37E-07	29.4%

CTS-01521

CP COL 2.5(1)

Table 2.5.2-209

Deaggregation of the 10^{-5} Low Frequencies

Distance Bin (km)	Magnitude Bin 5.25	5.75	6.25	6.75	7.25	7.75	8.25	8.75
0-20	1.1%	1.1%	0.8%	1.3%	2.3%	<< 0.1%	<< 0.1%	1.1%
20-40	0.3%	0.7%	0.5%	0.2%	< 0.1%	<< 0.1%	<< 0.1%	0.3%
40-60	< 0.1%	0.3%	0.3%	0.2%	< 0.1%	<< 0.1%	<< 0.1%	< 0.1%
60-80	< 0.1%	< 0.1%	0.2%	0.1%	< 0.1%	<< 0.1%	<< 0.1%	< 0.1%
80-100	< 0.1%	0.1%	0.2%	0.2%	< 0.1%	<< 0.1%	<< 0.1%	< 0.1%
100-200	< 0.1%	0.3%	0.8%	0.9%	0.4%	< 0.1%	<< 0.1%	< 0.1%
200-300	<< 0.1%	0.1%	3.8%	8.2%	4.7%	< 0.1%	<< 0.1%	<< 0.1%
> 300	<< 0.1%	< 0.1%	0.6%	5.0%	46.6%	17.6%	<< 0.1%	<< 0.1%

CP-COL 2.5(1)

CTS-01521

Table 2.5.2-210
Mmax Update for EPRI Team Sources

Team	Source Zone	Original Mmax Distribution and Weights (EPRI, 1989)	Updated Mmax Distribution and Weights
Bechtel	Background (BZI)	5.4 [0.1] 5.7 [0.4] 6.0 [0.4] 6.6 [0.1]	6.1 [0.1] 6.4 [0.4] 6.6 [0.1] 6.7 [0.4]
Dames & Moore	South Coastal Margin (zone 20)	5.3 [0.8] 7.2 [0.2]	5.5 [0.8] 7.2 [0.2]
Law Engineering	New Mexico Texas Block (zone 124)	4.9 [0.3] 5.5 [0.5] 5.8 [0.2]	5.0 [0.3] 5.5 [0.5] 5.8 [0.2]
Law Engineering	South Coastal Block (zone 126)	4.6 [0.9] 4.9 [0.1]	5.5 [0.9] 5.7 [0.1]
Rondout	Gulf Coast to Bahamas Fracture zone (zone 51)	4.8 [0.2] 5.5 [0.6] 5.8 [0.2]	6.1 [0.3] 6.3 [0.55] 6.5 [0.15]
Weston	Gulf Coast (zone 107)	5.4 [0.71] 6.0 [0.29]	6.6 [0.89] 7.2 [0.11]

CTS-01521

CP COL 2.5(1)

Table 2.5.2-210

Deaggregation of the 10^{-6} High Frequencies

Distance Bin (km)	Magnitude Bin							
	5.25	5.75	6.25	6.75	7.25	7.75	8.25	8.75
0-20	21.5%	19.4%	12.4%	5.5%	2.0%	0.7%	<< 0.1%	<< 0.1%
20-40	1.5%	4.1%	5.1%	3.6%	1.5%	0.4%	<< 0.1%	<< 0.1%
40-60	0.2%	0.4%	0.9%	1.2%	0.8%	0.3%	<< 0.1%	<< 0.1%
60-80	<< 0.1%	< 0.1%	0.2%	0.5%	0.3%	0.2%	< 0.1%	<< 0.1%
80-100	<< 0.1%	< 0.1%	0.2%	0.3%	0.3%	0.2%	< 0.1%	<< 0.1%
100-200	<< 0.1%	< 0.1%	0.3%	0.8%	1.1%	0.8%	< 0.1%	<< 0.1%
200-300	<< 0.1%	<< 0.1%	< 0.1%	1.3%	4.1%	3.3%	< 0.1%	<< 0.1%
> 300	<< 0.1%	<< 0.1%	< 0.1%	< 0.1%	0.2%	2.3%	1.7%	<< 0.1%

CTS-01521

Table 2.5.2-211 ~~Deleted~~Deaggregation of the 10^{-6} Low Frequencies

Distance Bin (km)	5.25	5.75	6.25	6.75	7.25	7.75	8.25	8.75
0-20	0.5%	2.2%	3.7%	2.9%	1.8%	2.0%	<< 0.1%	<< 0.1%
20-40	< 0.1%	0.3%	1.2%	1.6%	1.0%	0.3%	<< 0.1%	<< 0.1%
40-60	<< 0.1%	< 0.1%	0.2%	0.6%	0.5%	0.2%	<< 0.1%	<< 0.1%
60-80	<< 0.1%	<< 0.1%	< 0.1%	0.3%	0.2%	0.2%	< 0.1%	<< 0.1%
80-100	<< 0.1%	<< 0.1%	< 0.1%	0.2%	0.3%	0.2%	< 0.1%	<< 0.1%
100-200	<< 0.1%	<< 0.1%	0.1%	0.6%	1.1%	0.8%	< 0.1%	<< 0.1%
200-300	<< 0.1%	<< 0.1%	< 0.1%	2.0%	6.7%	5.0%	< 0.1%	<< 0.1%
> 300	<< 0.1%	<< 0.1%	< 0.1%	0.2%	2.4%	39.7%	20.7%	<< 0.1%

CTS-01521

CP-COL 2.5(1)

Table 2.5.2-212

Moore Fault Characterization from 2002 USGS National Seismic Hazard Maps (Frankel et al., 2002)

Probability of Activity	1
Recurrence Model	Characteristic
Characteristic Magnitude	Mw 7.0
Characteristic Return Period	4545 years
Dip	89°
Dip Direction	SW
Sense of Slip	Strike-slip
Rupture Top	0 km
Rupture Bottom	15 km
Width	15 km
Length	35 km
Fault Trace Coordinates (Lat., Lon.)	(34.85°, -98.64°) (34.75°, -98.40°) (34.73°, -98.33°) (34.71°, -98.29°)

CP COL 2.5(1)

CTS-01521

Table 2.5.2-212 (Sheet 1 of 6)[14]
Dynamic Properties of Subsurface Rock Materials

			Stratigraphy			
			Top of Layer Depth from YG[3]	Mean Elv Top	Mean Elv Std Dev Top	Mean Thickness
	Unit	Lithology	(ft)	(MSL, ft)	(ft)	(ft)
	Fill Concrete	To be placed as needed from top of layer C	N/A	N/A	N/A	-
			0.0	822.0	N/A	3.0
		Fill for excavation	3.0	819.0	N/A	17.0
	Compacted Fill		20.0	802.0	N/A	20.0
	Fill/Residuum	Fill/Residuum/weathered limestone	-	847.0	N/A	-
Shallow Site Profile[1]	A	Limestone (will be removed)	-	834.0	12.1	36.0
	B1	Shale (will be removed)	24.0	798.0	1.8	8.0
	B2	Shale with limestone (will be removed)	32.0	790.0	1.8	8.0
	C	Limestone (foundation layer)	40.0	782.0	1.8	65.0
	D	Shale	105.0	717.0	1.5	3.0
	E1	Limestone	108.0	714.0	1.6	24.0
	E2	Limestone	132.0	690.0	1.0	34.0
	E3	Limestone	166.0	656.0	1.0	34.0
	F	Limestone with interbedded shales and sand	200.0	622.0	2.2	29.0
	G	Sandstone	229.0	593.0	4.0	80.0
	H	Shale	309.0	513.0	5.2	62.0
	I	Sandstone	371.0	451.0	3.3	63.0
	Strawn Group (MW)	Shales with sandstone and limestone beds	434.0	388.0	26.0	2202.0

Table 2.5.2-212 (Sheet 2 of 6)[14]

CTS-01521

CP COL 2.5(1)

Dynamic Properties of Subsurface Rock Materials

Deep Site Profile[2]	Atoka Sand	Sands and shales interbedded	2636.0	-1814.0	417.0	1995.0
	Smithwick	Shale	4631.0	-3809.0	34.0	123.0
	Big Saline	Conglomerate and sandstones	4754.0	-3932.0	122.0	41.0
	Marble Falls	Limestone	4795.0	-3973.0	37.0	223.0
	Barnett	Shale	5018.0	-4196.0	145.0	247.0
	Ellenburger	Limestone	5265.0	-4443.0	73.0	>3000

CTS-01521

CP COL 2.5(1)

Table 2.5.2-212 (Sheet 3 of 6)[14]

Dynamic Properties of Subsurface Rock Materials

		Velocity[4]						
		Vs			Vp			
	Unit	Mean Vs (ft/sec)	+Variability[4] (ft/sec)	-Variability[4] (ft/sec)	Mean Vp (ft/sec)	+Variability[4] (ft/sec)	-Variability[4] (ft/sec)	Poisson's Ratio[8]
	Fill Concrete	6800.0	7300.0	6300.0	-	-	-	0.20
		650.0	975.0	325.0	-	-	-	0.35
		800.0	1200.0	400.0	-	-	-	0.35
	Compacted Fill	1000.0	1500.0	500.0	-	-	-	0.35
	Fill/Residuum	-	-	-	-	-	-	-
Shallow Site Profile[1]	A	3548.0	4435.0	2661.0	8788.0	10985.0	6591.0	0.40
	B1	2609.0	3261.3	1956.8	6736.0	8420.0	5052.0	0.41
	B2	2716.0	3395.0	2037.0	7640.0	9550.0	5730.0	0.43
	C	5685.0	7106.3	4263.8	11324.0	14155.0	8493.0	0.33
	D	3019.0	3773.8	2264.3	8312.0	10390.0	6234.0	0.42
	E1	4943.0	6178.8	3707.3	10486.0	13107.5	7864.5	0.36
	E2	6880.0	8600.0	5160.0	13164.0	16455.0	9873.0	0.31
	E3	4042.0	5052.5	3031.5	9255.0	11568.8	6941.3	0.38
	F	3061.0	3826.3	2295.8	7927.0	9908.8	5945.3	0.41
	G	3290.0	4112.5	2467.5	7593.0	9491.3	5694.8	0.38
	H	3429.0	4286.3	2571.8	8188.0	10235.0	6141.0	0.39
	I	3092.0	3865.0	2319.0	7686.0	9607.5	5764.5	0.40
	Strawn Group (MW)	5546.0	6932.5	4159.5	10627.0	13283.8	7970.3	0.32

CTS-01521

CP COL 2.5(1)

Table 2.5.2-212 (Sheet 4 of 6)[14]

Dynamic Properties of Subsurface Rock Materials

Deep Site Profile[2]	Atoka Sand	7642.0	10011.0	5273.0	13921.0	18236.5	9605.5	0.28
	Smithwick	5557.0	7279.7	3834.3	10894.0	14271.1	7516.9	0.32
	Big Saline	10247.0	13423.6	7070.4	18004.0	23585.2	12422.8	0.26
	Marble Falls	10520.0	13781.2	7258.8	19740.0	25859.4	13620.6	0.30
	Barnett	7783.0	10195.7	5370.3	12858.0	16844.0	8872.0	0.21
	Ellenburger	10906.0	14286.9	7525.1	20382.0	26700.4	14063.6	0.30

CTS-01521

CP COL 2.5(1)

Table 2.5.2-212 (Sheet 5 of 6)[14]
Dynamic Properties of Subsurface Rock Materials

		Unit Weight[9]		Shear Modulus[10]	Minimum C_v for Shear Modulus[12]		G_{max} Variation		Variation with Strain Relation
							LB	UB	
	Unit	(pcf)	(pcf)	(ksi)	LB	UB	$[G_{max}/(1+C_v)]$ (ksi)	$[G_{max}x(1+C_v)]$ (ksi)	-
	Fill Concrete	150.0	140.0	1495.9	-	-	-	-	N/A
		125.0	-	11.4	-	-	-	-	Fig. 2.5.2-241[13]
		125.0	-	17.3	-	-	-	-	Fig. 2.5.2-241[13]
	Compacted Fill	125.0	-	27.0	-	-	-	-	Fig. 2.5.2-241[13]
	Fill/Residuum	-	-		-	-	-	-	-
Shallow Site Profile[1]	A	145.0	135.0	393.7	0.8	0.6	218.7	629.9	Fig. 2.5.2-240[13]
	B1	135.0	117.0	198.2	0.8	0.6	110.1	317.1	Fig. 2.5.2-240[13]
	B2	135.0	117.0	214.8	0.8	0.6	119.3	343.7	Fig. 2.5.2-240[13]
	C	155.0	148.0	1080.4	0.8	0.6	600.2	1728.6	Fig. 2.5.2-240[13]
	D	135.0	117.0	265.4	0.8	0.6	147.4	424.6	Fig. 2.5.2-240[13]
	E1	155.0	149.0	816.8	0.8	0.6	453.8	1306.9	Fig. 2.5.2-240[13]
	E2	155.0	149.0	1582.3	0.8	0.6	879.1	2531.7	Fig. 2.5.2-240[13]
	E3	150.0	142.0	528.5	0.8	0.6	293.6	845.6	Fig. 2.5.2-240[13]
	F	130.0	112.0	262.7	0.8	0.6	145.9	420.3	Fig. 2.5.2-240[13]
	G	135.0	120.0	315.1	0.8	0.6	175.1	504.2	Fig. 2.5.2-240[13]
	H	140.0	130.0	355.0	0.8	0.6	197.2	568.0	Fig. 2.5.2-240[13]
	I	145.0	132.0	299.0	0.8	0.6	166.1	478.4	Fig. 2.5.2-240[13]
	Strawn Group (MW)	150.0	-	995.0	0.8	0.6	552.8	1592.0	Fig. 2.5.2-240[13]

CP COL 2.5(1)

CTS-01521

Table 2.5.2-212 (Sheet 6 of 6)[14]
Dynamic Properties of Subsurface Rock Materials

Deep Site Profile[2]	Atoka Sand	150.0	-	1890.0	1.0	1.0	945.0	3780.0	Fig. 2.5.2-240[13]
	Smithwick	150.0	-	1000.0	1.0	1.0	500.0	2000.0	Fig. 2.5.2-240[13]
	Big Saline[11]	150.0	-	3400.0	1.0	1.0	1700.0	6800.0	Fig. 2.5.2-240[13]
	Marble Falls	150.0	-	3580.0	1.0	1.0	1790.0	7160.0	Fig. 2.5.2-240[13]
	Barnett	150.0	-	1960.0	1.0	1.0	980.0	3920.0	Fig. 2.5.2-240[13]
	Ellenburger	150.0	-	3850.0	1.0	1.0	1925.0	7700.0	Fig. 2.5.2-240[13]

Notes:

1 Shallow Site Profile derived from site specific data.

2 Deep Velocity Profile derived from regional wells.

3 Depth calculated from the difference between Yard Grade (822 ft MSL (Mean Sea Level)) and the average elevation of top of layer.

4 The selected Variability for Velocity is +/-25% for shallow profile, +/-50% for the compacted fill, +/-31% for deep profile, and +/-500 fps for fill concrete.

5 Yard Grade is the elevation to which the site will be cut = 822 ft MSL.

6 Foundation Unit is the top of Layer C on which all critical structures will be founded (either directly or backfilled with concrete).

7 Max and Min elevation tops not available for deep site profile, which yielded only one estimate for the top each horizon.

8 Poisson's Ratio for Shallow Site Profile calculated from Vs and Vp suspension measurements. Deep Site Profile values estimated from deep regional well Vp data.

9 Unit weight values for Layers A through G estimated based on results of the laboratory tests. Values for Layers H, I and Strawn (MW) estimated from FSAR Table 2.5.4-5G and based on lithology.

10 G_{max} calculated based on suspension Vs or estimated Vs for Deep Site Profile Materials.

11 Standard deviation in elevation of the top of Big Saline and top Atoka estimated from average standard deviation for other layer elevations.

12 Recommended minimum C_V (shear modulus variation factor) values are based on +/-25% variation in V_S or Min values recommended by DCD (0.5 if test data are available or 1.0 if test data are not available), whichever is higher. This is consistent with the minimum shear modulus variation factor of 0.5 defined in DCD Section 3.7.2.

13 EPRI Curves shown on FSAR Figure 2.5.2-241 were used for non-linear response of the compacted fill layers. Curves shown in FSAR Figure 2.5.2-240 were used for non-linear response of all other layers/

14 The soil properties presented in Table 2.5.2-212 are site-specific for developing the site GMRS and FIRS for comparison to the CSDRS. The soil properties and variations for SSI analysis are discussed in FSAR Chapter 3 Appendix 3NN.

CTS-01521

CP-COL 2.5(1)

Table 2.5.2-213

Updated Seismic Source Characterization of the Moore Fault

Probability of Activity	1
Recurrence Model	Characteristic
Characteristic Magnitude	6.7 [0.2][a], 6.85 [0.6][a], 7.0 [0.2][a]
Characteristic Return Period	See logic tree in Figure 4 of TXUT-001-PR-003
Dip	89°
Dip Direction	SW
Rupture Top	0 km
Rupture Bottom	15 to 20 km
Width	15 to 20 km
Length	26 to 37 km
Fault Trace Coordinates (Lat., Lon.)	(34.85°, -98.64°) (34.71°, -98.29°)

a) [ ] = percentage % of 100 for each magnitude weighted in the model

CP COL 2.5(1)

CTS-01521

Table 2.5.2-213
Calculation of Strong-Motion Durations and Effective Strain Ratios

Case	Magnitude M	Distance R (km)	Seismic Moment Mo (dyn-cm)	Corner Frequency fc (Hz)	Duration T (sec)	Effective Strain Ratio (-)
10^{-4} HF	7	220	3.55E+26	0.12	19.37	0.60
10^{-4} BB	7.6	600	2.82E+27	0.06	46.70	0.65
10^{-5} HF	6.7	97	1.26E+26	0.17	10.77	0.57
10^{-5} BB	7.7	640	3.98E+27	0.05	50.74	0.65
10^{-6} HF	6.2	20	2.24E+25	0.30	4.33	0.52
10^{-6} BB	7.8	640	5.62E+27	0.05	53.02	0.65

CTS-01521

CP-COL-2.5(1)

Table 2.5.2-214 (Sheet 1 of 2)
Rio Grande Rift Faults Modeled as Discrete Fault Sources

Fault Name	Recurrence Rate (EQs/yr)	Magnitude (Mw)
Puye fault	4.0140E-05	6.6
Sawyer Canyon fault	5.4280E-05	6.2
La Canada del Amagre fault zone	9.5530E-05	6.5
Embudo fault	3.7700E-05	7.2
Lobato Mesa fault zone	6.3390E-05	6.6
Canones fault	2.0724E-05	6.8
Black Mesa fault zone	3.4270E-05	6.5
Gallina fault	1.8790E-05	6.9
Southern Sangre de Cristo fault	5.7220E-05	7.4
Northern Sangre de Cristo fault	1.0040E-04	7.5
Southern Sawatch fault	4.6820E-05	7.0
West Lobo Valley fault zone	1.7700E-05	7.2
West Indio Mountains fault	4.8600E-05	6.7
Caballo fault	7.8790E-05	7.0
West Eagle Mountains-Red Hills fault	1.5140E-05	6.7
Amargosa fault	6.5170E-05	7.2
East Baylor Mountain – Carizzo Mountain fault	5.3200E-06	7.0
Arroyo Diablo fault	2.4520E-05	6.4
East Sierra Diablo fault	1.6510E-05	6.9
Campo Grande fault	3.6540E-05	7.0
Acala fault	2.4770E-04	6.1
West Delaware Mountains fault zone	2.8590E-05	6.7
East Franklin Mountains fault	8.1530E-05	7.0
Organ Mountains fault	1.4976E-04	6.8
San Andres Mountains fault	3.9120E-05	7.5
Alamogordo fault	3.9970E-05	7.5
Caballo fault	3.7440E-05	6.6
La Jencia fault	2.3120E-05	6.8
Hubbell Springs fault	5.3650E-05	7.0
Tijeras-Canoncito fault	3.2820E-05	7.3
County Dump fault	3.3260E-05	6.9
Zia fault	4.2010E-05	6.8

CP COL 2.5(1)

CTS-01521

Table 2.5.2-214 (Sheet 2 of 2)
Rio Grande Rift Faults Modeled as Discrete Fault Sources

Fault Name	Recurrence Rate (EQs/yr)	Magnitude (Mw)
San Francisco fault	6.6380E-05	6.8
San Felipe fault zone	3.1180E-05	7.0
La Bajada fault	4.9530E-05	7.0
Jemez-San Ysidro fault	1.2850E-05	7.1
Picuris-Pecos fault	2.1030E-05	7.4
Nacimiento fault	9.9400E-06	7.3
Nambe fault	1.6790E-05	7.0
Pajarito fault	5.7380E-05	7.0
Pojoaque fault	1.6260E-05	7.0

CP COL 2.5(1)

CTS-01521

Table 2.5.2-214 (Sheet 1 of 2)
Amplification Factors for the GMRS/FIRS1 (Equivalent to FIRS2) Profile

Freq. (Hz)	Amplification Factor for 10^{-4}		Amplification Factor for 10^{-5}		Amplification Factor for 10^{-6}	
	Median	Logarithmic Sigma	Median	Logarithmic Sigma	Median	Logarithmic Sigma
0.1	1.12	0.05	1.12	0.05	1.12	0.05
0.125	1.16	0.07	1.17	0.07	1.17	0.08
0.15	1.22	0.10	1.23	0.10	1.23	0.10
0.2	1.36	0.14	1.36	0.15	1.38	0.15
0.3	1.51	0.15	1.51	0.15	1.51	0.15
0.4	1.40	0.16	1.39	0.16	1.38	0.16
0.5	1.29	0.17	1.28	0.17	1.27	0.17
0.6	1.28	0.16	1.27	0.16	1.27	0.17
0.7	1.35	0.15	1.35	0.16	1.35	0.16
0.8	1.42	0.14	1.41	0.14	1.42	0.15
0.9	1.43	0.13	1.43	0.14	1.43	0.15
1	1.43	0.15	1.43	0.16	1.43	0.17
1.25	1.62	0.20	1.61	0.19	1.55	0.18
1.5	1.60	0.17	1.54	0.16	1.45	0.16
2	1.38	0.14	1.29	0.16	1.17	0.19
2.5	1.04	0.18	0.97	0.18	0.87	0.20
3	0.81	0.17	0.76	0.18	0.69	0.20
4	0.64	0.17	0.61	0.18	0.53	0.19
5	0.60	0.20	0.56	0.19	0.48	0.21
6	0.58	0.19	0.53	0.20	0.43	0.23
7	0.52	0.19	0.47	0.19	0.37	0.23
8	0.46	0.18	0.41	0.18	0.32	0.23
9	0.42	0.17	0.38	0.17	0.29	0.22
10	0.40	0.17	0.35	0.17	0.27	0.22
12.5	0.37	0.19	0.32	0.19	0.23	0.24
15	0.34	0.20	0.28	0.20	0.20	0.25
20	0.28	0.15	0.23	0.15	0.16	0.18
25	0.26	0.13	0.20	0.12	0.14	0.15
30	0.25	0.12	0.20	0.12	0.13	0.13
35	0.25	0.11	0.21	0.11	0.14	0.13

CP COL 2.5(1)

CTS-01521

Table 2.5.2-214 (Sheet 2 of 2)
Amplification Factors for the GMRS/FIRS1 (Equivalent to FIRS2) Profile

Freq. (Hz)	Amplification Factor for 10^{-4}		Amplification Factor for 10^{-5}		Amplification Factor for 10^{-6}	
	Median	Logarithmic Sigma	Median	Logarithmic Sigma	Median	Logarithmic Sigma
40	0.26	0.11	0.21	0.10	0.14	0.12
45	0.27	0.10	0.23	0.10	0.15	0.12
50	0.29	0.10	0.24	0.10	0.16	0.11
60	0.34	0.10	0.29	0.10	0.19	0.11
70	0.41	0.10	0.35	0.10	0.23	0.11
80	0.49	0.10	0.43	0.09	0.28	0.11
90	0.56	0.10	0.50	0.09	0.33	0.11
100	0.62	0.10	0.56	0.09	0.36	0.11

CP COL 2.5(1)

CTS-01521

Table 2.5.2-215 (Sheet 1 of 2)
Surface Trace Coordinates of Rio Grande Rift Faults

Fault Name	Longitude 1	Latitude 1	Longitude 2	Latitude 2
Puye fault	-106.158	35.893	-106.154	36.064
Sawyer Canyon fault	-106.254	35.908	-106.281	35.979
La Canada del Amagre fault zone	-106.242	36.023	-106.211	36.170
Embudo fault	-105.599	36.329	-106.224	36.035
Lobato Mesa fault zone	-106.276	36.207	-106.300	36.041
Canones fault	-106.529	36.081	-106.319	36.284
Black Mesa fault zone	-105.963	36.220	-106.121	36.125
Gallina fault	-106.901	36.220	-106.791	36.525
Southern Sangre de Cristo fault	-105.503	37.178	-105.597	36.328
Northern Sangre de Cristo fault	-105.994	38.393	-105.369	37.006
Southern Sawatch fault	-106.245	38.563	-106.211	38.930
West Lobo Valley fault zone	-104.604	30.466	-104.807	30.939
West Indio Mountains fault	-105.029	30.667	-105.136	30.838
Caballo fault	-105.527	31.095	-105.284	30.779
West Eagle Mountains-Red Hills fault	-105.269	31.003	-105.085	30.857
Amargosa fault	-105.555	30.874	-106.047	31.314
East Baylor Mountain - Carizzo Mountain fault	-104.905	30.952	-104.723	31.285
Arroyo Diablo fault	-105.720	31.306	-105.637	31.202
East Sierra Diablo fault	-104.873	31.224	-104.871	31.517
Campo Grande fault	-106.033	31.495	-105.629	31.292
Acala fault	-105.938	31.411	-105.888	31.360

CP COL 2.5(1)

CTS-01521

Table 2.5.2-215 (Sheet 2 of 2)

Surface Trace Coordinates of Rio Grande Rift Faults

Fault Name	Longitude 1	Latitude 1	Longitude 2	Latitude 2
West Delaware Mountains fault zone	-104.819	31.669	-104.716	31.467
East Franklin Mountains fault	-106.487	31.605	-106.447	32.011
Organ Mountains fault	-106.490	32.191	-106.486	32.417
San Andres Mountains fault	-106.486	32.417	-106.412	33.437
Alamogordo fault	-106.120	33.493	-105.924	32.520
Caballo fault	-107.266	33.114	-107.253	32.923
La Jencia fault	-107.074	34.011	-107.166	34.263
Hubbell Springs fault	-106.509	34.998	-106.563	34.616
Tijeras-Canoncito fault	-105.881	35.479	-106.507	34.987
County Dump fault	-106.775	35.008	-106.749	35.326
Zia fault	-106.843	35.189	-106.748	35.471
San Francisco fault	-106.321	35.488	-106.470	35.292
San Felipe fault zone	-106.607	35.312	-106.584	35.683
La Bajada fault	-106.302	35.702	-106.214	35.346
Jemez-San Ysidro fault	-106.788	35.420	-106.634	35.833
Picuris-Pecos fault	-105.609	36.329	-105.879	35.479
Nacimiento fault	-106.857	35.485	-106.901	36.220
Nambe fault	-105.883	36.021	-105.852	35.591
Pajarito fault	-106.297	35.646	-106.225	36.034
Pojoaque fault	-106.004	36.088	-106.062	35.671

CP COL 2.5(1)

CTS-01521

Table 2.5.2-215 (Sheet 1 of 2)
Amplification Factors for the FIRS1_COV50 (Equivalent to FIRS2_COV50) Profile

Freq. (Hz)	Amplification Factor for 10^{-4}		Amplification Factor for 10^{-5}		Amplification Factor for 10^{-6}	
	Median	Logarithmic Sigma	Median	Logarithmic Sigma	Median	Logarithmic Sigma
0.1	1.11	0.05	1.11	0.06	1.11	0.06
0.125	1.15	0.08	1.15	0.08	1.16	0.09
0.15	1.21	0.10	1.21	0.11	1.22	0.12
0.2	1.33	0.15	1.33	0.15	1.35	0.16
0.3	1.49	0.15	1.48	0.15	1.48	0.16
0.4	1.42	0.16	1.41	0.16	1.40	0.17
0.5	1.33	0.17	1.32	0.18	1.31	0.18
0.6	1.30	0.16	1.30	0.16	1.29	0.16
0.7	1.34	0.13	1.34	0.13	1.34	0.14
0.8	1.39	0.11	1.40	0.12	1.40	0.13
0.9	1.44	0.13	1.44	0.14	1.44	0.16
1	1.47	0.15	1.46	0.16	1.45	0.17
1.25	1.63	0.18	1.61	0.19	1.58	0.19
1.5	1.67	0.18	1.61	0.17	1.53	0.17
2	1.43	0.15	1.35	0.17	1.24	0.20
2.5	1.08	0.19	1.02	0.20	0.92	0.24
3	0.87	0.20	0.81	0.20	0.73	0.22
4	0.67	0.17	0.64	0.17	0.57	0.19
5	0.64	0.18	0.60	0.18	0.51	0.21
6	0.62	0.21	0.56	0.21	0.47	0.25
7	0.55	0.22	0.50	0.22	0.40	0.27
8	0.49	0.22	0.44	0.22	0.35	0.26
9	0.45	0.21	0.41	0.22	0.32	0.27
10	0.44	0.21	S0.39	0.21	0.30	0.26
12.5	0.41	0.23	0.35	0.24	0.26	0.30
15	0.37	0.25	0.31	0.25	0.22	0.30
20	0.30	0.18	0.24	0.18	0.17	0.21
25	0.27	0.15	0.22	0.15	0.15	0.18
30	0.27	0.14	0.21	0.13	0.14	0.16
35	0.27	0.13	0.22	0.13	0.14	0.15

CP COL 2.5(1)

CTS-01521

Table 2.5.2-215 (Sheet 2 of 2)
Amplification Factors for the FIRS1_COV50 (Equivalent to FIRS2_COV50) Profile

Freq. (Hz)	Amplification Factor for 10^{-4}		Amplification Factor for 10^{-5}		Amplification Factor for 10^{-6}	
	Median	Logarithmic Sigma	Median	Logarithmic Sigma	Median	Logarithmic Sigma
40	0.27	0.12	0.22	0.12	0.15	0.14
45	0.28	0.12	0.24	0.12	0.16	0.14
50	0.30	0.12	0.25	0.11	0.17	0.13
60	0.35	0.11	0.30	0.11	0.20	0.13
70	0.43	0.11	0.37	0.11	0.24	0.13
80	0.51	0.11	0.45	0.11	0.30	0.13
90	0.59	0.11	0.52	0.11	0.34	0.13
100	0.65	0.11	0.58	0.11	0.38	0.13

CTS-01521

CP-COL 2.5(1)

Table 2.5.2-216
Summary of Rio Grand Rift Fault Source Characterization

Trace Coordinates	Table 2.5.2-215
Dip, Dip Direction	90°, NA
Recurrence Model	Characteristic Earthquake
Recurrence Rate (EQs/yr)	Table 2.5.2-CF12
Magnitude (Mw) and weights	Take magnitude from Table 2.5.2-214 and use Mw −0.2 [0.2][(a)], Mw [0.6][(a)], Mw +0.2 [0.2][(a)] with weights in parentheses
Probability of Activity	1.0

a) [ ] = percentage % of 100 for each magnitude weighted in the model

CP COL 2.5(1)

CTS-01521

Table 2.5.2-216 (Sheet 1 of 2)
Amplification Factors for the FIRS3 Profile
(PBSRS for GMRS/FIRS1 and FIRS2)

Freq. (Hz)	Amplification Factor for 10^{-4}		Amplification Factor for 10^{-5}		Amplification Factor for 10^{-6}	
	Median	Logarithmic Sigma	Median	Logarithmic Sigma	Median	Logarithmic Sigma
0.1	1.12	0.05	1.12	0.05	1.13	0.05
0.125	1.17	0.07	1.17	0.07	1.18	0.08
0.15	1.23	0.10	1.23	0.10	1.24	0.10
0.2	1.36	0.14	1.37	0.14	1.39	0.15
0.3	1.52	0.15	1.52	0.15	1.53	0.15
0.4	1.41	0.16	1.41	0.16	1.41	0.17
0.5	1.31	0.17	1.30	0.17	1.32	0.19
0.6	1.30	0.16	1.30	0.16	1.34	0.19
0.7	1.38	0.15	1.39	0.16	1.46	0.20
0.8	1.46	0.14	1.48	0.15	1.56	0.22
0.9	1.49	0.13	1.51	0.15	1.61	0.25
1	1.51	0.16	1.53	0.17	1.65	0.28
1.25	1.76	0.21	1.78	0.22	1.90	0.30
1.5	1.79	0.20	1.79	0.20	1.87	0.29
2	1.68	0.19	1.66	0.23	1.67	0.34
2.5	1.42	0.25	1.42	0.31	1.37	0.40
3	1.28	0.33	1.31	0.40	1.17	0.43
4	1.49	0.57	1.30	0.47	1.02	0.44
5	1.60	0.46	1.32	0.45	0.94	0.47
6	1.56	0.45	1.18	0.46	0.78	0.45
7	1.21	0.39	0.92	0.39	0.62	0.39
8	0.97	0.34	0.76	0.33	0.51	0.33
9	0.82	0.26	0.66	0.26	0.43	0.26
10	0.76	0.25	0.60	0.23	0.39	0.24
12.5	0.65	0.26	0.49	0.23	0.32	0.25
15	0.58	0.27	0.43	0.25	0.28	0.25
20	0.48	0.25	0.35	0.22	0.22	0.21
25	0.42	0.22	0.31	0.19	0.20	0.19
30	0.41	0.21	0.31	0.19	0.20	0.18
35	0.42	0.21	0.31	0.18	0.20	0.18

CP COL 2.5(1)

CTS-01521

Table 2.5.2-216 (Sheet 2 of 2)
Amplification Factors for the FIRS3 Profile
(PBSRS for GMRS/FIRS1 and FIRS2)

Freq. (Hz)	Amplification Factor for 10^{-4}		Amplification Factor for 10^{-5}		Amplification Factor for 10^{-6}	
	Median	Logarithmic Sigma	Median	Logarithmic Sigma	Median	Logarithmic Sigma
40	0.43	0.20	0.33	0.18	0.21	0.18
45	0.44	0.20	0.34	0.18	0.22	0.18
50	0.47	0.20	0.37	0.18	0.23	0.18
60	0.55	0.20	0.44	0.18	0.28	0.18
70	0.67	0.20	0.54	0.18	0.34	0.18
80	0.80	0.20	0.65	0.18	0.41	0.18
90	0.92	0.20	0.76	0.18	0.48	0.18
100	1.01	0.20	0.85	0.18	0.53	0.18

CTS-01521

CP-COL-2.5(1)

Table 2.5.2-217

Rio Grande Rift Point Source Characterization

Point location (Lon., Lat.)	(-102.671°, 29.796°)
Recurrence Model	Characteristic Earthquake
Return Period (yrs) and weights	14,500 [0.4][(a)], 37,500 [0.4][(a)], 119,000 [0.2][(a)]
Magnitude (Mw) and weights	6.3 [0.1][(a)], 6.65 [0.3][(a)], 6.95 [0.4][(a)], 7.3 [0.2][(a)]
Probability of Activity	1.0

a) [ ] = percentage % of 100 for each magnitude or period weighted in the model

CP COL 2.5(1)

CTS-01521

Table 2.5.2-217 (Sheet 1 of 2)
Amplification Factors for the FIRS3_COV50 Profile (PBSRS for FIRS1_COV50 and FIRS2_COV50)

Freq. (Hz)	Amplification Factor for 10^{-4}		Amplification Factor for 10^{-5}		Amplification Factor for 10^{-6}	
	Median	Logarithmic Sigma	Median	Logarithmic Sigma	Median	Logarithmic Sigma
0.1	1.12	0.05	1.12	0.06	1.14	0.07
0.125	1.16	0.08	1.17	0.08	1.19	0.10
0.15	1.21	0.10	1.23	0.11	1.25	0.13
0.2	1.34	0.15	1.36	0.16	1.40	0.18
0.3	1.50	0.15	1.54	0.20	1.58	0.20
0.4	1.45	0.17	1.49	0.22	1.53	0.24
0.5	1.37	0.19	1.40	0.21	1.48	0.30
0.6	1.36	0.19	1.40	0.21	1.51	0.34
0.7	1.43	0.18	1.49	0.23	1.62	0.36
0.8	1.52	0.18	1.60	0.27	1.73	0.36
0.9	1.59	0.20	1.70	0.31	1.82	0.37
1	1.65	0.21	1.75	0.32	1.85	0.36
1.25	1.94	0.27	2.00	0.32	2.02	0.38
1.5	2.11	0.33	2.04	0.33	1.92	0.37
2	1.96	0.37	1.74	0.35	1.53	0.38
2.5	1.62	0.46	1.37	0.38	1.19	0.42
3	1.39	0.47	1.17	0.39	1.01	0.46
4	1.28	0.49	1.10	0.53	0.80	0.43
5	1.32	0.52	1.00	0.44	0.73	0.50
6	1.21	0.45	0.93	0.49	0.66	0.57
7	1.07	0.48	0.81	0.51	0.56	0.55
8	0.93	0.44	0.71	0.46	0.48	0.50
9	0.84	0.40	0.65	0.42	0.44	0.49
10	0.79	0.37	0.61	0.40	0.41	0.47
12.5	0.70	0.32	0.51	0.32	0.33	0.38
15	0.61	0.29	0.44	0.30	0.28	0.35
20	0.49	0.27	0.35	0.26	0.22	0.28
25	0.44	0.25	0.31	0.23	0.20	0.26
30	0.43	0.24	0.31	0.21	0.20	0.24
35	0.43	0.23	0.32	0.21	0.20	0.23

CP COL 2.5(1)

CTS-01521

Table 2.5.2-217 (Sheet 2 of 2)
Amplification Factors for the FIRS3_COV50 Profile
(PBSRS for FIRS1_COV50 and FIRS2_COV50)

Freq. (Hz)	Amplification Factor for 10^{-4}		Amplification Factor for 10^{-5}		Amplification Factor for 10^{-6}	
	Median	Logarithmic Sigma	Median	Logarithmic Sigma	Median	Logarithmic Sigma
40	0.44	0.23	0.33	0.20	0.21	0.23
45	0.46	0.23	0.34	0.20	0.22	0.23
50	0.49	0.23	0.37	0.20	0.23	0.23
60	0.57	0.23	0.44	0.20	0.27	0.22
70	0.69	0.23	0.54	0.20	0.34	0.22
80	0.83	0.23	0.65	0.20	0.41	0.22
90	0.95	0.23	0.76	0.20	0.48	0.22
100	1.05	0.23	0.85	0.20	0.53	0.22

CTS-01521

CP-COL 2.5(1)

Table 2.5.2-218
Choraw Fault Source Characterization

Trace Coordinates (Lon., Lat.)	(-103.22°, 38.43°), (-103.59°, 38.15°)
Dip, Dip Direction	90°, NA
Recurrence Model	Characteristic Earthquake
Recurrence Rate	1.148e-4 per year
Magnitude (Mw) and weights	6.8 [0.2][a], 7.0 [0.6][a], 7.2 [0.2][a]
Probability of Activity	1.0

a) [ ] = percentage % of 100 for each magnitude weighted in the model

CP COL 2.5(1)

CTS-01521

Table 2.5.2-218 (Sheet 1 of 2)
Amplification Factors for the FIRS4 Profile

Freq. (Hz)	Amplification Factor for 10^{-4}		Amplification Factor for 10^{-5}		Amplification Factor for 10^{-6}	
	Median	Logarithmic Sigma	Median	Logarithmic Sigma	Median	Logarithmic Sigma
0.1	1.12	0.06	1.13	0.06	1.13	0.07
0.125	1.18	0.09	1.18	0.09	1.19	0.09
0.15	1.24	0.12	1.25	0.12	1.26	0.13
0.2	1.39	0.17	1.40	0.17	1.41	0.18
0.3	1.54	0.17	1.54	0.17	1.53	0.17
0.4	1.41	0.16	1.40	0.16	1.38	0.17
0.5	1.29	0.18	1.28	0.18	1.27	0.19
0.6	1.27	0.18	1.27	0.18	1.27	0.19
0.7	1.33	0.17	1.33	0.17	1.34	0.18
0.8	1.40	0.17	1.40	0.17	1.42	0.19
0.9	1.44	0.17	1.44	0.17	1.45	0.19
1	1.44	0.17	1.44	0.18	1.43	0.19
1.25	1.57	0.21	1.56	0.20	1.54	0.19
1.5	1.61	0.18	1.55	0.17	1.46	0.17
2	1.36	0.16	1.28	0.18	1.16	0.22
2.5	1.06	0.20	0.98	0.21	0.87	0.24
3	0.84	0.19	0.78	0.20	0.69	0.22
4	0.64	0.15	0.60	0.16	0.53	0.19
5	0.59	0.18	0.55	0.19	0.48	0.22
6	0.56	0.20	0.52	0.20	0.43	0.24
7	0.52	0.20	0.48	0.21	0.39	0.26
8	0.48	0.21	0.44	0.21	0.34	0.26
9	0.45	0.19	0.40	0.20	0.30	0.26
10	0.42	0.20	0.37	0.20	0.28	0.27
12.5	0.39	0.24	0.34	0.24	0.24	0.29
15	0.35	0.21	0.29	0.21	0.21	0.25
20	0.29	0.18	0.23	0.18	0.16	0.22
25	0.26	0.14	0.21	0.14	0.14	0.16
30	0.26	0.13	0.21	0.13	0.14	0.15
35	0.26	0.12	0.21	0.12	0.14	0.14
40	0.26	0.12	0.22	0.11	0.14	0.13

CP COL 2.5(1)

CTS-01521

Table 2.5.2-218 (Sheet 2 of 2)
Amplification Factors for the FIRS4 Profile

Freq. (Hz)	Amplification Factor for 10^{-4}		Amplification Factor for 10^{-5}		Amplification Factor for 10^{-6}	
	Median	Logarithmic Sigma	Median	Logarithmic Sigma	Median	Logarithmic Sigma
45	0.27	0.11	0.23	0.11	0.15	0.13
50	0.29	0.11	0.24	0.11	0.16	0.13
60	0.34	0.11	0.29	0.10	0.19	0.12
70	0.41	0.10	0.36	0.10	0.23	0.12
80	0.49	0.10	0.43	0.10	0.28	0.12
90	0.57	0.10	0.51	0.10	0.33	0.12
100	0.63	0.10	0.56	0.10	0.37	0.12

CTS-01521

CP COL 2.5(1)

Table 2.5.2-219

Values of Mean and Median Rock UHRS (in g) for 10^{-4} and 10^{-5}

freq	10^{-4} mean UHRS	10^{-4} median UHRS	10^{-5} mean UHRS	10^{-5} median UHRS
100	0.0516	0.0353	0.127	0.0815
25	0.0127	0.0728	0.370	0.193
10	0.105	0.0810	0.263	0.187
5	0.0944	0.0743	0.222	0.163
2.5	0.0761	0.0543	0.173	0.113
1	0.0500	0.0277	0.123	0.0554
0.5	0.0380	0.0155	0.116	0.0301

CP COL 2.5(1)

CTS-01521

Table 2.5.2-219 (Sheet 1 of 2)
Amplification Factors for the FIRS4_SCSR Profile (PBSRS for FIRS4)

Freq. (Hz)	Amplification Factor for 10^{-4}		Amplification Factor for 10^{-5}		Amplification Factor for 10^{-6}	
	Median	Logarithmic Sigma	Median	Logarithmic Sigma	Median	Logarithmic Sigma
0.1	1.13	0.06	1.13	0.06	1.13	0.06
0.125	1.18	0.09	1.18	0.09	1.19	0.09
0.15	1.24	0.12	1.25	0.12	1.26	0.13
0.2	1.39	0.17	1.40	0.17	1.41	0.18
0.3	1.55	0.17	1.54	0.17	1.54	0.17
0.4	1.42	0.16	1.41	0.16	1.40	0.17
0.5	1.30	0.18	1.29	0.19	1.29	0.20
0.6	1.29	0.18	1.29	0.18	1.30	0.19
0.7	1.35	0.17	1.35	0.17	1.38	0.19
0.8	1.43	0.17	1.44	0.17	1.47	0.19
0.9	1.48	0.17	1.49	0.17	1.52	0.19
1	1.49	0.17	1.49	0.18	1.52	0.21
1.25	1.66	0.21	1.66	0.21	1.70	0.25
1.5	1.73	0.19	1.69	0.19	1.66	0.25
2	1.54	0.18	1.49	0.22	1.42	0.29
2.5	1.28	0.24	1.23	0.29	1.17	0.36
3	1.10	0.25	1.08	0.30	1.04	0.39
4	1.10	0.40	1.09	0.42	1.00	0.41
5	1.39	0.49	1.28	0.45	1.03	0.44
6	1.60	0.49	1.32	0.46	0.91	0.45
7	1.50	0.44	1.15	0.42	0.75	0.43
8	1.29	0.39	0.96	0.39	0.61	0.41
9	1.03	0.35	0.77	0.34	0.49	0.36
10	0.84	0.29	0.65	0.29	0.43	0.33
12.5	0.67	0.31	0.52	0.31	0.35	0.34
15	0.59	0.31	0.45	0.29	0.29	0.31
20	0.49	0.29	0.36	0.26	0.23	0.26
25	0.43	0.24	0.31	0.22	0.20	0.23
30	0.41	0.23	0.31	0.20	0.20	0.21
35	0.41	0.22	0.31	0.20	0.20	0.21

CP COL 2.5(1)

CTS-01521

Table 2.5.2-219 (Sheet 2 of 2)
Amplification Factors for the FIRS4_SCSR Profile (PBSRS for FIRS4)

Freq. (Hz)	Amplification Factor for 10^{-4}		Amplification Factor for 10^{-5}		Amplification Factor for 10^{-6}	
	Median	Logarithmic Sigma	Median	Logarithmic Sigma	Median	Logarithmic Sigma
40	0.42	0.21	0.32	0.19	0.21	0.20
45	0.44	0.21	0.34	0.19	0.22	0.20
50	0.46	0.21	0.36	0.19	0.23	0.20
60	0.54	0.21	0.43	0.19	0.27	0.20
70	0.65	0.21	0.53	0.19	0.34	0.20
80	0.78	0.21	0.64	0.19	0.41	0.20
90	0.90	0.20	0.75	0.19	0.47	0.20
100	0.99	0.20	0.83	0.19	0.52	0.20

CTS-01521

CP COL 2.5(1)

~~**Table 2.5.2-220**~~
~~**Mean Magnitudes and Distances from Deaggregation**~~

	~~1E-4, 5 and 10 Hz~~	~~1E-4, 1 and 2.5 Hz~~	~~1E-5, 5 and 10 Hz~~	~~1E-5, 1 and 2.5 Hz~~	~~1E-6, 5 and 10 Hz~~	~~1E-6, 1 and 2.5 Hz~~
~~M~~	~~6.9~~	~~7.3~~	~~6.7~~	~~7.4~~	~~6.1~~	~~7.4~~
~~R~~	~~300~~	~~540~~	~~180~~	~~550~~	~~46~~	~~470~~
~~M (r >100 km)~~	~~7.0~~	~~7.3~~	~~7.1~~	~~7.5~~	~~7.2~~	~~7.6~~
~~R (r >100 km)~~	~~400~~	~~570~~	~~430~~	~~630~~	~~440~~	~~680~~

CP COL 2.5(1)

Table 2.5.2-220
Horizontal UHRS and GMRS Values with the Site Amplification

Frequency (Hz)	10^{-4} Mean UHRS (g)	10^{-5} Mean UHRS (g)	GMRS FIRS1/FIRS2 (g)
0.5	0.0548	0.161	0.0778
1	0.0781	0.194	0.0972
2.5	0.0883	0.204	0.1036
5	0.0659	0.160	0.0803
10	0.0504	0.125	0.0624
25	0.0396	0.101	0.0504
100 (PGA)	0.0373	0.091	0.0458

CTS-01521

CP COL 2.5(1)

Table 2.5.2-221

Deaggregation of 10^{-4} High Frequencies

Percent contribution by M-R bin

	5.25	5.75	6.25	6.75	7.25	7.75	8.25	8.75
0-20 km	3.3	0.2	0.1	0.0	0.0	0.0	0.0	0.0
20-40 km	3.1	0.3	0.1	0.0	0.0	0.0	0.0	0.0
40-60 km	1.4	0.3	0.1	0.0	0.0	0.0	0.0	0.0
60-80 km	0.6	0.2	0.1	0.0	0.0	0.0	0.0	0.0
80-100 km	0.4	0.2	0.1	0.0	0.0	0.0	0.0	0.0
100-200 km	1.3	1.0	1.0	0.3	0.2	0.0	0.0	0.0
200-300 km	0.3	0.4	0.7	51.0	0.2	0.0	0.0	0.0
>300 km	0.0	0.1	0.2	0.3	6.4	24.3	1.6	0.0

CP COL 2.5(1)

CTS-01521

Table 2.5.2-221 (Sheet 1 of 2)
Horizontal and Vertical GMRS/FIRS1 (Equivalent to FIRS2) Amplitudes

Frequency	Horizontal GMRS (g)	Vertical GMRS (g)
100 (PGA)	4.58E-02	4.58E-02
90	4.59E-02	4.59E-02
80	4.60E-02	4.60E-02
75.9	4.61E-02	4.61E-02
70	4.62E-02	4.62E-02
60	4.64E-02	4.64E-02
50	4.68E-02	4.68E-02
40	4.74E-02	4.74E-02
30	4.88E-02	4.88E-02
25	5.04E-02	5.04E-02
20	5.43E-02	5.43E-02
15	6.08E-02	6.08E-02
12.5	6.22E-02	6.22E-02
10	6.24E-02	6.24E-02
9	6.46E-02	6.46E-02
8	6.96E-02	6.96E-02
7.4	7.31E-02	7.30E-02
7	7.62E-02	7.62E-02
6	8.22E-02	8.22E-02
5	8.03E-02	8.02E-02
4	7.99E-02	7.98E-02
3	8.86E-02	7.60E-02
2.5	1.04E-01	7.41E-02
2	1.27E-01	9.04E-02
1.8	1.34E-01	9.46E-02
1.5	1.32E-01	9.27E-02
1.25	1.23E-01	8.64E-02
1	9.72E-02	6.77E-02
0.9	9.57E-02	6.64E-02
0.8	9.33E-02	6.45E-02

CP COL 2.5(1)

CTS-01521

Table 2.5.2-221 (Sheet 2 of 2)
Horizontal and Vertical GMRS/FIRS1 (Equivalent to FIRS2) Amplitudes

Frequency	Horizontal GMRS (g)	Vertical GMRS (g)
0.7	8.71E-02	6.00E-02
0.6	8.02E-02	5.50E-02
0.5	7.78E-02	5.31E-02
0.4	6.34E-02	4.30E-02
0.3	4.67E-02	3.14E-02
0.2	2.33E-02	1.56E-02
0.15	1.32E-02	8.82E-03
0.125	9.21E-03	6.16E-03
0.1	5.88E-03	3.93E-03

CTS-01521

CP COL 2.5(1)

~~**Table 2.5.2-222**~~

~~**Deaggregation of 10^{-4} Low Frequencies**~~

~~Percent contribution by M-R bin~~

	~~5.25~~	~~5.75~~	~~6.25~~	~~6.75~~	~~7.25~~	~~7.75~~	~~8.25~~	~~8.75~~
~~0-20 km~~	~~0.8~~	~~0.1~~	~~0.0~~	~~0.0~~	~~0.0~~	~~0.0~~	~~0.0~~	~~0.0~~
~~20-40 km~~	~~0.3~~	~~0.1~~	~~0.1~~	~~0.0~~	~~0.0~~	~~0.0~~	~~0.0~~	~~0.0~~
~~40-60 km~~	~~0.1~~	~~0.1~~	~~0.1~~	~~0.0~~	~~0.0~~	~~0.0~~	~~0.0~~	~~0.0~~
~~60-80 km~~	~~0.0~~	~~0.0~~	~~0.0~~	~~0.0~~	~~0.0~~	~~0.0~~	~~0.0~~	~~0.0~~
~~80-100 km~~	~~0.0~~	~~0.0~~	~~0.0~~	~~0.0~~	~~0.0~~	~~0.0~~	~~0.0~~	~~0.0~~
~~100-200 km~~	~~0.0~~	~~0.1~~	~~0.3~~	~~0.2~~	~~0.1~~	~~0.0~~	~~0.0~~	~~0.0~~
~~200-300 km~~	~~0.0~~	~~0.1~~	~~0.2~~	~~32.4~~	~~0.1~~	~~0.0~~	~~0.0~~	~~0.0~~
~~>300 km~~	~~0.0~~	~~0.0~~	~~0.1~~	~~0.5~~	~~13.4~~	~~47.7~~	~~2.8~~	~~0.0~~

CP COL 2.5(1)

Table 2.5.2-222

Horizontal FIRS Values (g) including Site Amplification

Frequency (Hz)	FIRS1_COV50/ FIRS2_COV50 (g)	FIRS3 (g)	FIRS3_COV50 (g)	FIRS4 (g)	FIRS4_SCSR (g)
0.5	0.0803	0.0792	0.0857	0.0784	0.0792
1	0.0996	0.104	0.121	0.0987	0.102
2.5	0.109	0.154	0.194	0.107	0.135
5	0.0853	0.252	0.214	0.0787	0.236
10	0.0699	0.115	0.132	0.0662	0.130
25	0.0539	0.0819	0.0859	0.0515	0.0841
100 (PGA)	0.0480	0.0745	0.0768	0.0463	0.0734

CTS-01521

CP COL 2.5(1)

Table 2.5.2-223

Deaggregation of 10^{-5} High Frequencies

Percent contribution by M-R bin

	5.25	5.75	6.25	6.75	7.25	7.75	8.25	8.75
0-20 km	15.0	1.3	0.5	0.0	0.0	0.0	0.0	0.0
20-40 km	5.0	1.2	0.6	0.1	0.0	0.0	0.0	0.0
40-60 km	0.9	0.4	0.4	0.1	0.1	0.0	0.0	0.0
60-80 km	0.2	0.2	0.2	0.1	0.1	0.0	0.0	0.0
80-100 km	0.1	0.1	0.2	0.1	0.1	0.0	0.0	0.0
100-200 km	0.3	0.4	0.8	0.4	0.4	0.1	0.0	0.0
200-300 km	0.1	0.1	0.3	39.2	0.3	0.0	0.0	0.0
>300 km	0.0	0.0	0.1	0.1	3.4	24.7	2.3	0.0

CP COL 2.5(1)

CTS-01521

Table 2.5.2-223 (Sheet 1 of 2)
Horizontal and Vertical FIRS Amplitudes

Frequency	FIRS1_COV50/FIRS2_COV50		FIRS4	
	Horizontal (g)	Vertical (g)	Horizontal (g)	Vertical (g)
100	4.80E-02	4.80E-02	4.63E-02	4.63E-02
90	4.81E-02	4.81E-02	4.65E-02	4.65E-02
80	4.83E-02	4.83E-02	4.66E-02	4.66E-02
75.9	4.84E-02	4.84E-02	4.67E-02	4.67E-02
70	4.85E-02	4.85E-02	4.68E-02	4.68E-02
60	4.88E-02	4.88E-02	4.71E-02	4.71E-02
50	4.93E-02	4.93E-02	4.75E-02	4.75E-02
40	5.02E-02	5.02E-02	4.83E-02	4.83E-02
30	5.19E-02	5.19E-02	4.99E-02	4.99E-02
25	5.39E-02	5.39E-02	5.15E-02	5.15E-02
20	5.80E-02	5.80E-02	5.55E-02	5.55E-02
15	6.81E-02	6.81E-02	6.36E-02	6.36E-02
12.5	7.03E-02	7.03E-02	6.73E-02	6.73E-02
10	6.99E-02	6.99E-02	6.62E-02	6.62E-02
9	7.07E-02	7.07E-02	6.93E-02	6.93E-02
8	7.46E-02	7.46E-02	7.36E-02	7.35E-02
7.4	7.87E-02	7.87E-02	7.56E-02	7.56E-02
7	8.18E-02	8.18E-02	7.69E-02	7.69E-02
6	8.70E-02	8.69E-02	7.96E-02	7.95E-02
5	8.53E-02	8.52E-02	7.87E-02	7.87E-02
4	8.31E-02	8.30E-02	7.94E-02	7.93E-02
3	9.58E-02	8.21E-02	9.27E-02	7.95E-02
2.5	1.09E-01	7.78E-02	1.07E-01	7.63E-02
2	1.33E-01	9.45E-02	1.27E-01	9.01E-02
1.8	1.37E-01	9.67E-02	1.30E-01	9.21E-02
1.5	1.39E-01	9.77E-02	1.34E-01	9.42E-02
1.25	1.25E-01	8.72E-02	1.21E-01	8.46E-02
1	9.96E-02	6.93E-02	9.87E-02	6.87E-02
0.9	9.66E-02	6.70E-02	9.72E-02	6.75E-02
0.8	9.21E-02	6.37E-02	9.31E-02	6.44E-02

CP COL 2.5(1)

CTS-01521

Table 2.5.2-223 (Sheet 2 of 2)
Horizontal and Vertical FIRS Amplitudes

Frequency	FIRS1_COV50/FIRS2_COV50		FIRS4	
	Horizontal (g)	Vertical (g)	Horizontal (g)	Vertical (g)
0.7	8.65E-02	5.96E-02	8.63E-02	5.94E-02
0.6	8.17E-02	5.60E-02	8.03E-02	5.50E-02
0.5	8.03E-02	5.48E-02	7.84E-02	5.35E-02
0.4	6.45E-02	4.37E-02	6.41E-02	4.34E-02
0.3	4.59E-02	3.08E-02	4.77E-02	3.21E-02
0.2	2.29E-02	1.53E-02	2.40E-02	1.60E-02
0.15	1.30E-02	8.72E-03	1.35E-02	9.00E-03
0.125	9.13E-03	6.11E-03	9.36E-03	6.25E-03
0.1	5.86E-03	3.91E-03	5.96E-03	3.98E-03

CTS-01521

CP COL 2.5(1)

Table 2.5.2-224

Deaggregation of 10^{-5} Low Frequencies

	Percent contribution by M-R bin							
	5.25	5.75	6.25	6.75	7.25	7.75	8.25	8.75
0-20 km	1.8	0.5	0.3	0.0	0.0	0.0	0.0	0.0
20-40 km	0.2	0.2	0.2	0.0	0.0	0.0	0.0	0.0
40-60 km	0.0	0.1	0.1	0.0	0.0	0.0	0.0	0.0
60-80 km	0.0	0.0	0.0	0.0	0.0	0.0	0.0	0.0
80-100 km	0.0	0.0	0.0	0.0	0.0	0.0	0.0	0.0
100-200 km	0.0	0.0	0.2	0.2	0.2	0.1	0.0	0.0
200-300 km	0.0	0.0	0.1	23.9	0.2	0.0	0.0	0.0
>300 km	0.0	0.0	0.0	0.2	9.3	57.5	4.3	0.0

CTS-01521

CP COL 2.5(1)

Table 2.5.2-225

Deaggregation of 10^{-6} High Frequencies

	Percent contribution by M-R bin							
	5.25	5.75	6.25	6.75	7.25	7.75	8.25	8.75
0-20 km	42.6	6.5	3.1	0.3	0.1	0.0	0.0	0.0
20-40 km	4.0	2.1	1.7	0.3	0.2	0.0	0.0	0.0
40-60 km	0.3	0.3	0.5	0.2	0.2	0.0	0.0	0.0
60-80 km	0.0	0.1	0.2	0.1	0.2	0.0	0.0	0.0
80-100 km	0.0	0.0	0.1	0.1	0.1	0.0	0.0	0.0
100-200 km	0.0	0.1	0.4	0.3	0.6	0.2	0.0	0.0
200-300 km	0.0	0.0	0.1	18.5	0.2	0.0	0.0	0.0
>300 km	0.0	0.0	0.0	0.0	1.0	13.3	1.9	0.0

CTS-01521

CP COL 2.5(1)

Table 2.5.2-226

Deaggregation of 10^{-6} Low Frequencies

	Percent contribution by M-R bin							
	5.25	5.75	6.25	6.75	7.25	7.75	8.25	8.75
0-20 km	3.8	1.7	1.4	0.2	0.1	0.0	0.0	0.0
20-40 km	0.2	0.3	0.5	0.1	0.1	0.0	0.0	0.0
40-60 km	0.0	0.0	0.2	0.1	0.1	0.0	0.0	0.0
60-80 km	0.0	0.0	0.0	0.0	0.1	0.0	0.0	0.0
80-100 km	0.0	0.0	0.0	0.0	0.1	0.0	0.0	0.0
100-200 km	0.0	0.0	0.1	0.2	0.4	0.1	0.0	0.0
200-300 km	0.0	0.0	0.0	17.1	0.2	0.0	0.0	0.0
>300 km	0.0	0.0	0.0	0.1	5.7	60.5	6.2	0.0

CP COL 2.5(1)

CTS-01521

Table 2.5.2-227 (Sheet 1 of 6)[16]
Dynamic Properties of Subsurface Rock Materials

			Stratigraphy			
			Top of Layer Depth from YG[3]	Mean Elv Top	Mean Elv Std Dev Top	Mean Thickness
	Unit	Lithology	(ft)	(MSL, ft)	(ft)	(ft)
	Fill Concrete	To be placed as needed from top of layer C	N/A	N/A	N/A	-
			0.0	822.0	N/A	3.0
		Fill for excavation	3.0	819.0	N/A	17.0
	Compacted Fill		20.0	802.0	N/A	20.0
	Fill/Residuum	Fill/Residuum/weathered limestone	-	847.0	N/A	-
Shallow Site Profile[4]	A	Limestone (will be removed)	-	834.0	12.1	36.0
	B1	Shale (will be removed)	24.0	798.0	1.8	8.0
	B2	Shale with limestone (will be removed)	32.0	790.0	1.8	8.0
	C	Limestone (foundation layer)	40.0	782.0	1.8	65.0
	D	Shale	105.0	717.0	1.5	3.0
	E1	Limestone	108.0	714.0	1.6	24.0
	E2	Limestone	132.0	690.0	1.0	34.0
	E3	Limestone	166.0	656.0	1.0	34.0
	F	Limestone with interbedded shales and sand	200.0	622.0	2.2	29.0
	G	Sandstone	229.0	593.0	4.0	80.0
	H	Shale	309.0	513.0	5.2	62.0
	I	Sandstone	371.0	451.0	3.3	63.0
	Strawn Group (MW)	Shales with sandstone and limestone beds	434.0	388.0	26.0	2202.0

CP COL 2.5(1)

CTS-01521

Table 2.5.2-227 (Sheet 2 of 6)[16]
Dynamic Properties of Subsurface Rock Materials

Deep Site Profile[2]	Atoka Sand	Sands and shales interbedded	2636.0	-1814.0	417.0	1995.0
	Smithwick	Shale	4631.0	-3809.0	34.0	123.0
	Big Saline	Conglomerate and sandstones	4754.0	-3932.0	122.0	41.0
	Marble Falls	Limestone	4795.0	-3973.0	37.0	223.0
	Barnett	Shale	5018.0	-4196.0	145.0	247.0
	Ellenburger	Limestone	5265.0	-4443.0	73.0	>3000

CP COL 2.5(1)

CTS-01521

Table 2.5.2-227 (Sheet 3 of 6)[16]
Dynamic Properties of Subsurface Rock Materials

		Velocity[4]						
		Vs			Vp			
		Mean Vs	+Variability[4]	-Variability[4]	Mean Vp	+Variability[4]	-Variability[4]	Poisson's Ratio[8]
	Unit	(ft/sec)	(ft/sec)	(ft/sec)	(ft/sec)	(ft/sec)	(ft/sec)	
	Fill Concrete	6800.0	7300.0	6300.0	-	-	-	0.20
		650.0	975.0	325.0	-	-	-	0.35
		800.0	1200.0	400.0	-	-	-	0.35
	Compacted Fill	1000.0	1500.0	500.0	-	-	-	0.35
	Fill/Residuum	-	-	-	-	-	-	-
Shallow Site Profile[4]	A	3548.0	4435.0	2661.0	8788.0	10985.0	6591.0	0.40
	B1	2609.0	3261.3	1956.8	6736.0	8420.0	5052.0	0.41
	B2	2716.0	3395.0	2037.0	7640.0	9550.0	5730.0	0.43
	C	5685.0	7106.3	4263.8	11324.0	14155.0	8493.0	0.33
	D	3019.0	3773.8	2264.3	8312.0	10390.0	6234.0	0.42
	E1	4943.0	6178.8	3707.3	10486.0	13107.5	7864.5	0.36
	E2	6880.0	8600.0	5160.0	13164.0	16455.0	9873.0	0.31
	E3	4042.0	5052.5	3031.5	9255.0	11568.8	6941.3	0.38
	F	3061.0	3826.3	2295.8	7927.0	9908.8	5945.3	0.41
	G	3290.0	4112.5	2467.5	7593.0	9491.3	5694.8	0.38
	H	3429.0	4286.3	2571.8	8188.0	10235.0	6141.0	0.39
	I	3092.0	3865.0	2319.0	7686.0	9607.5	5764.5	0.40
	Strawn Group (MW)	5546.0	6932.5	4159.5	10627.0	13283.8	7970.3	0.32

CP COL 2.5(1)

CTS-01521

Table 2.5.2-227 (Sheet 4 of 6)[16]
Dynamic Properties of Subsurface Rock Materials

Deep Site Profile[2]	Atoka Sand	7642.0	10011.0	5273.0	13921.0	18236.5	9605.5	0.28
	Smithwick	5557.0	7279.7	3834.3	10894.0	14271.1	7516.9	0.32
	Big Saline	10247.0	13423.6	7070.4	18004.0	23585.2	12422.8	0.26
	Marble Falls	10520.0	13781.2	7258.8	19740.0	25859.4	13620.6	0.30
	Barnett	7783.0	10195.7	5370.3	12858.0	16844.0	8872.0	0.21
	Ellenburger	10906.0	14286.9	7525.1	20382.0	26700.4	14063.6	0.30

CP COL 2.5(1)

CTS-01521

Table 2.5.2-227 (Sheet 5 of 6)[16]
Dynamic Properties of Subsurface Rock Materials

	Unit	Unit Weight[9] Wet (pcf)	Unit Weight[9] Dry (pcf)	Shear Modulus[10] Mean (ksi)	Minimum C_v for Shear Modulus[14] LB	Minimum C_v for Shear Modulus[14] UB	G_{max} Variation LB $[G_{max}/(1+C_v)]$ (ksi)	G_{max} Variation UB $[G_{max}x(1+C_v)]$ (ksi)	Low Strain D_s Damping[11] (%)	Variation with Strain Relation -	Low Strain D_e Damping[13] (%)
	Fill Concrete	150.0	140.0	1495.9	-	-	-	-	-	N/A	-
		125.0	-	11.4	-	-	-	-	1.5	Fig. 2.5.2-232[15]	0.8
		125.0	-	17.3	-	-	-	-	1.5	Fig. 2.5.2-232[15]	0.8
	Compacted Fill	125.0	-	27.0	-	-	-	-	1.1	Fig. 2.5.2-232[15]	0.6
	Fill/Residuum	-	-		-	-	-	-	-	-	-
Shallow Site Profile[4]	A	145.0	135.0	393.7	0.8	0.6	218.7	629.9	1.8	-	0.9
	B1	135.0	117.0	198.2	0.8	0.6	110.1	317.1	2.0	-	1.0
	B2	135.0	117.0	214.8	0.8	0.6	119.3	343.7	2.0	-	1.0
	C	155.0	148.0	1080.4	0.8	0.6	600.2	1728.6	1.8	-	0.9
	D	135.0	117.0	265.4	0.8	0.6	147.4	424.6	2.0	-	1.0
	E1	155.0	149.0	816.8	0.8	0.6	453.8	1306.9	1.8	-	0.9
	E2	155.0	149.0	1582.3	0.8	0.6	879.1	2531.7	1.8	-	0.9
	E3	150.0	142.0	528.5	0.8	0.6	293.6	845.6	1.8	-	0.9
	F	130.0	112.0	262.7	0.8	0.6	145.9	420.3	2.0	-	1.0
	G	135.0	120.0	315.1	0.8	0.6	175.1	504.2	2.0	-	1.0
	H	140.0	130.0	355.0	0.8	0.6	197.2	568.0	2.0	-	1.0
	I	145.0	132.0	299.0	0.8	0.6	166.1	478.4	2.0	-	1.0
	Strawn Group (MW)	150.0	-	995.0	0.8	0.6	552.8	1592.0	1.8	-	0.9

CP-COL-2.5(1)

CTS-01521

Table 2.5.2-227 (Sheet 6 of 6)[16]
Dynamic Properties of Subsurface Rock Materials

Deep Site Profile[2]	Atoka Sand	150.0	-	1890.0	1.0	1.0	945.0	3780.0	1.0	-	0.5
	Smithwick	150.0	-	1000.0	1.0	1.0	500.0	2000.0	1.0	-	0.5
	Big Saline[12]	150.0	-	3400.0	1.0	1.0	1700.0	6800.0	1.0	-	0.5
	Marble Falls	150.0	-	3580.0	1.0	1.0	1790.0	7160.0	0.8	-	0.4
	Barnett	150.0	-	1960.0	1.0	1.0	980.0	3920.0	1.0	-	0.5
	Ellenburger	150.0	-	3850.0	1.0	1.0	1925.0	7700.0	0.8	-	0.4

Notes:

1 Shallow Site Profile derived from site specific data.

2 Deep Velocity Profile derived from regional wells.

3 Depth calculated from the difference between Yard Grade (822 ft MSL (Mean Sea Level)) and the average elevation of top of layer.

4 The selected Variability for Velocity is +/- 25% for shallow profile, +/- 50% for the compacted fill, +/- 31% for deep profile, and +/- 500 fps for fill concrete.

5 Yard Grade is the elevation to which the site will be cut = 822 ft MSL.

6 Foundation Unit is the top of Layer C on which all critical structures will be founded (either directly or backfilled with concrete).

7 Max and Min elevation tops not available for deep site profile, which yielded only one estimate for the top each horizon.

8 Poisson's Ratio for Shallow Site Profile calculated from Vs and Vp suspension measurements. Deep Site Profile values estimated from deep regional well Vp data.

9 Unit weight values for Layers A through G estimated based on results of the laboratory tests. Values for Layers H, I and Strawn (MW) estimated from FSAR Table 2.5.4-5G and based on lithology.

10 G_{max} calculated based on suspension Vs or estimated Vs for Deep Site Profile Materials.

11 Low Strain Damping Ratio in Shear estimated from lithology for Shallow Site Profile through discussion with Dr. Ken Stokoe. Deep Site Profile values based on comparison of Vs and lithology of shallow site layers.

12 Standard deviation in elevation of the top of Big Saline and top Atoka estimated from average standard deviation for other layer elevations.

13 Damping Ratio in unconstrained compression, D_c should be taken as $0.5D_c$ with a maximum value of 5%.

14 Recommended minimum C_v (shear modulus variation factor) values are based on +/- 25% variation in V_s or Min values recommended by DCD (0.5 if test data are available or 1.0 if test data are not available), whichever is higher.

15 EPRI Curves shown on FSAR Figure 2.5.2-232 were used for non-linear response of the compacted fill layers.

16 The soil properties presented in Table 2.5.2-227 are site-specific for developing the site GMRS and FIRS for comparison to the CSDRS.
The soil properties and variations for SSI analysis are discussed in FSAR Chapter 3 Appendix 3NN.

CTS-01521

CP COL 2.5(1)

Table 2.5.2-228

Values of Horizontal 10^{-5} UHRS and GMRS

Horizontal UHRS and GMRS values with site amplification (revised σ, CAV)

Freq	10^{-5}	GMRS
100	0.0826	0.0372
25	0.0928	0.0418
10	0.113	0.0509
5	0.121	0.0545
2.5	0.162	0.0729
1	0.100	0.0450
0.5	0.0789	0.0355

CP COL 2.5(1)

CTS-01521

Table 2.5.2-229

Values of Horizontal 10^{-5} UHRS and FIRS

Horizontal UHRS and FIRS values with site amplification (revised σ, CAV)

	FIRS2		FIRS3		FIRS4		FIRS4_CoV50	
Freq	10^{-5}	FIRS	10^{-5}	FIRS	10^{-5}	FIRS	10^{-5}	FIRS
100	0.0849	0.0382	0.101	0.0455	0.151	0.0680	0.148	0.0666
25	0.0980	0.0441	0.132	0.0594	0.194	0.873	0.190	0.0853
10	0.120	0.0540	0.208	0.0936	0.288	0.130	0.308	0.139
5	0.125	0.0563	0.149	0.0671	0.480	0.216	0.412	0.185
2.5	0.159	0.0716	0.177	0.0797	0.271	0.122	0.308	0.139
1	0.105	0.0473	0.118	0.0531	0.162	0.0729	0.170	0.0764
0.5	0.0830	0.0374	0.097	0.0437	0.132	0.0594	0.133	0.0597

CTS-01521

~~Table 2.5.2-230~~
~~Calculation of Duration and Effective Strain Ratio for Rock Input Motions Considered in Site Response Calculations~~

~~Case~~	~~Magnitude M~~	~~Distance R (km)~~	~~Seismic Moment Mo (dyn-cm)~~	~~Corner Frequency fc (Hz)~~	~~Duration T (sec)~~	~~Eff Strain Ratio~~
~~1E-4 HF~~	~~6.9~~	~~300~~	~~2.51E+26~~	~~0.13~~	~~22.46~~	~~0.59~~
~~1E-4 BB~~	~~7.3~~	~~570~~	~~1.00E+27~~	~~0.08~~	~~40.32~~	~~0.63~~
~~1E-5 BB~~	~~7.4~~	~~620~~	~~1.41E+27~~	~~0.08~~	~~44.26~~	~~0.64~~
~~1E-6 BB~~	~~7.5~~	~~660~~	~~2.00E+27~~	~~0.07~~	~~47.88~~	~~0.65~~

CTS-01521

Table 2.5.2-231
Amplification Factors for the GMRS/FIRS1 Site Column

-	Amplification Factor for 10^{-4}		Amplification Factor for 10^{-5}		Amplification Factor for 10^{-6}	
Freq (Hz)	Median	Logarithmic Std. Dev.	Median	Logarithmic Std. Dev.	Median	Logarithmic Std. Dev.
0.1	1.10	0.06	1.10	0.06	1.10	0.06
0.125	1.14	0.08	1.14	0.08	1.14	0.08
0.15	1.18	0.11	1.19	0.11	1.19	0.11
0.2	1.30	0.16	1.30	0.16	1.30	0.16
0.3	1.46	0.17	1.46	0.18	1.46	0.18
0.4	1.43	0.17	1.43	0.17	1.43	0.17
0.5	1.37	0.17	1.37	0.17	1.37	0.17
0.6	1.36	0.16	1.36	0.16	1.36	0.16
0.7	1.37	0.14	1.37	0.14	1.38	0.14
0.8	1.39	0.11	1.40	0.12	1.40	0.12
0.9	1.39	0.10	1.39	0.10	1.39	0.10
1	1.41	0.12	1.38	0.11	1.37	0.11
1.25	1.60	0.16	1.61	0.17	1.61	0.17
1.5	1.75	0.19	1.75	0.19	1.74	0.19
2	1.71	0.13	1.71	0.13	1.71	0.13
2.5	1.44	0.16	1.42	0.15	1.41	0.14
3	1.12	0.17	1.12	0.17	1.12	0.16
4	0.83	0.16	0.84	0.15	0.83	0.15
5	0.74	0.15	0.75	0.14	0.74	0.14
6	0.72	0.17	0.73	0.17	0.71	0.17
7	0.66	0.20	0.66	0.19	0.64	0.21
8	0.59	0.20	0.60	0.19	0.57	0.21
9	0.56	0.19	0.56	0.19	0.52	0.21
10	0.55	0.20	0.55	0.19	0.51	0.22
12.5	0.54	0.26	0.54	0.26	0.49	0.30
15	0.52	0.24	0.51	0.25	0.47	0.29
20	0.42	0.18	0.39	0.19	0.34	0.24
25	0.37	0.15	0.33	0.16	0.27	0.20
30	0.35	0.14	0.32	0.14	0.26	0.17
35	0.35	0.13	0.32	0.13	0.26	0.16
40	0.36	0.12	0.33	0.12	0.26	0.14
45	0.37	0.11	0.34	0.11	0.27	0.13
50	0.39	0.11	0.36	0.11	0.29	0.13
60	0.44	0.10	0.42	0.10	0.34	0.11
70	0.53	0.10	0.52	0.10	0.41	0.11
80	0.63	0.10	0.63	0.10	0.50	0.11
90	0.73	0.10	0.73	0.10	0.59	0.11
100	0.79	0.10	0.81	0.10	0.66	0.11

CTS-01521

Table 2.5.2-232
Amplification Factors for the FIRS2 Site Column

-	Amplification Factor for 10^{-4}		Amplification Factor for 10^{-5}		Amplification Factor for 10^{-6}	
Freq (Hz)	Median	Logarithmic Std. Dev.	Median	Logarithmic Std. Dev.	Median	Logarithmic Std. Dev.
0.1	1.09	0.05	1.09	0.05	1.09	0.06
0.125	1.12	0.08	1.12	0.08	1.12	0.08
0.15	1.16	0.10	1.16	0.10	1.16	0.11
0.2	1.26	0.16	1.26	0.16	1.26	0.16
0.3	1.42	0.18	1.42	0.18	1.43	0.18
0.4	1.44	0.17	1.44	0.17	1.44	0.17
0.5	1.40	0.18	1.40	0.18	1.40	0.18
0.6	1.37	0.15	1.37	0.15	1.38	0.15
0.7	1.37	0.13	1.37	0.13	1.37	0.13
0.8	1.39	0.10	1.39	0.10	1.39	0.10
0.9	1.41	0.11	1.41	0.11	1.40	0.11
1	1.45	0.14	1.41	0.13	1.41	0.13
1.25	1.64	0.19	1.65	0.19	1.65	0.19
1.5	1.83	0.18	1.83	0.18	1.83	0.18
2	1.72	0.14	1.72	0.13	1.72	0.13
2.5	1.38	0.17	1.36	0.16	1.36	0.15
3	1.07	0.18	1.08	0.18	1.08	0.17
4	0.80	0.16	0.81	0.15	0.81	0.15
5	0.75	0.17	0.76	0.17	0.74	0.17
6	0.73	0.20	0.74	0.19	0.72	0.20
7	0.66	0.24	0.67	0.23	0.64	0.24
8	0.59	0.25	0.60	0.25	0.57	0.27
9	0.56	0.26	0.56	0.25	0.53	0.28
10	0.56	0.26	0.56	0.25	0.52	0.29
12.5	0.57	0.32	0.57	0.32	0.53	0.36
15	0.54	0.30	0.52	0.31	0.48	0.36
20	0.42	0.22	0.39	0.23	0.34	0.28
25	0.37	0.19	0.34	0.21	0.28	0.25
30	0.36	0.20	0.33	0.21	0.27	0.25
35	0.36	0.19	0.33	0.20	0.27	0.25
40	0.37	0.17	0.34	0.17	0.27	0.20
45	0.37	0.15	0.35	0.15	0.28	0.18
50	0.39	0.14	0.37	0.15	0.29	0.17
60	0.45	0.13	0.43	0.13	0.34	0.15
70	0.54	0.13	0.53	0.12	0.42	0.14
80	0.64	0.12	0.64	0.12	0.51	0.14
90	0.74	0.12	0.74	0.12	0.60	0.14
100	0.80	0.12	0.82	0.12	0.67	0.14

CTS-01521

Table 2.5.2-233
Amplification Factors for the FIRS3 Site Column

	Amplification Factor for 10^{-4}		Amplification Factor for 10^{-5}		Amplification Factor for 10^{-6}	
Freq (Hz)	Median	Logarithmic Std. Dev.	Median	Logarithmic Std. Dev.	Median	Logarithmic Std. Dev.
0.1	1.09	0.07	1.09	0.07	1.09	0.07
0.125	1.13	0.10	1.13	0.10	1.13	0.10
0.15	1.17	0.14	1.17	0.14	1.17	0.14
0.2	1.26	0.19	1.26	0.19	1.26	0.19
0.3	1.39	0.19	1.39	0.19	1.39	0.19
0.4	1.39	0.16	1.39	0.16	1.39	0.16
0.5	1.37	0.17	1.36	0.17	1.36	0.17
0.6	1.35	0.16	1.35	0.16	1.35	0.16
0.7	1.35	0.13	1.35	0.13	1.36	0.13
0.8	1.40	0.11	1.40	0.11	1.40	0.11
0.9	1.44	0.12	1.43	0.12	1.43	0.12
1	1.46	0.14	1.41	0.13	1.41	0.13
1.25	1.60	0.20	1.61	0.20	1.60	0.20
1.5	1.78	0.18	1.78	0.18	1.77	0.18
2	1.65	0.15	1.66	0.15	1.66	0.1
2.5	1.35	0.23	1.34	0.21	1.34	0.20
3	1.10	0.22	1.11	0.21	1.10	0.21
4	0.84	0.18	0.85	0.17	0.85	0.17
5	0.80	0.21	0.81	0.20	0.80	0.20
6	0.79	0.23	0.80	0.22	0.79	0.23
7	0.77	0.29	0.77	0.28	0.76	0.29
8	0.74	0.33	0.75	0.32	0.72	0.34
9	0.76	0.37	0.77	0.37	0.74	0.39
10	0.81	0.38	0.82	0.38	0.79	0.40
12.5	0.88	0.35	0.88	0.35	0.86	0.37
15	0.74	0.36	0.72	0.37	0.69	0.41
20	0.57	0.33	0.55	0.35	0.51	0.40
25	0.46	0.26	0.42	0.28	0.37	0.33
30	0.41	0.22	0.37	0.23	0.32	0.27
35	0.40	0.21	0.37	0.22	0.31	0.25
40	0.41	0.20	0.38	0.21	0.31	0.24
45	0.42	0.20	0.39	0.20	0.32	0.23
50	0.44	0.19	0.41	0.19	0.34	0.22
60	0.50	0.18	0.48	0.17	0.40	0.20
70	0.60	0.17	0.59	0.17	0.49	0.19
80	0.71	0.17	0.71	0.16	0.59	0.19
90	0.82	0.16	0.83	0.16	0.69	0.19
100	0.89	0.16	0.92	0.16	0.77	0.19

CTS-01521

Table 2.5.2-234
Amplification Factors for the FIRS4 Site Column

-	Amplification Factor for 10^{-4}		Amplification Factor for 10^{-5}		Amplification Factor for 10^{-6}	
Freq (Hz)	Median	Logarithmic Std. Dev.	Median	Logarithmic Std. Dev.	Median	Logarithmic Std. Dev.
0.1	1.10	0.05	1.10	0.05	1.10	0.05
0.125	1.13	0.07	1.13	0.07	1.13	0.07
0.15	1.18	0.10	1.18	0.10	1.18	0.10
0.2	1.28	0.15	1.28	0.15	1.29	0.15
0.3	1.45	0.18	1.45	0.18	1.46	0.18
0.4	1.43	0.17	1.44	0.17	1.45	0.17
0.5	1.37	0.17	1.37	0.17	1.39	0.18
0.6	1.35	0.15	1.36	0.16	1.38	0.17
0.7	1.39	0.14	1.39	0.14	1.43	0.16
0.8	1.45	0.13	1.46	0.14	1.50	0.17
0.9	1.49	0.14	1.50	0.14	1.55	0.20
1	1.54	0.15	1.51	0.15	1.58	0.22
1.25	1.80	0.19	1.83	0.19	1.94	0.25
1.5	1.98	0.22	2.03	0.23	2.15	0.30
2	1.93	0.16	2.01	0.20	2.14	0.26
2.5	1.63	0.25	1.70	0.29	1.79	0.31
3	1.42	0.32	1.52	0.36	1.58	0.35
4	1.50	0.49	1.53	0.44	1.52	0.40
5	1.85	0.49	1.76	0.44	1.55	0.40
6	2.00	0.41	1.77	0.40	1.43	0.45
7	1.80	0.41	1.55	0.44	1.23	0.49
8	1.54	0.44	1.32	0.46	1.06	0.51
9	1.31	0.44	1.13	0.43	0.90	0.45
10	1.12	0.36	0.99	0.34	0.79	0.36
12.5	0.99	0.29	0.88	0.29	0.70	0.31
15	0.94	0.31	0.81	0.30	0.64	0.34
20	0.76	0.31	0.63	0.32	0.48	0.35
25	0.66	0.27	0.53	0.27	0.39	0.29
30	0.61	0.24	0.50	0.23	0.37	0.25
35	0.61	0.23	0.50	0.22	0.37	0.23
40	0.61	0.22	0.51	0.20	0.38	0.21
45	0.62	0.21	0.53	0.20	0.40	0.20
50	0.65	0.20	0.56	0.19	0.42	0.19
60	0.74	0.19	0.66	0.18	0.50	0.18
70	0.89	0.19	0.81	0.17	0.61	0.18
80	1.06	0.19	0.98	0.17	0.74	0.17
90	1.22	0.19	1.14	0.17	0.87	0.17
100	1.33	0.19	1.26	0.17	0.97	0.17

CTS-01521

Table 2.5.2-235
Amplification Factors for the FIRS4_CoV50 Site Column

-	Amplification Factor for 10^{-4}		Amplification Factor for 10^{-5}		Amplification Factor for 10^{-6}	
Freq (Hz)	Median	Logarithmic Std. Dev.	Median	Logarithmic Std. Dev.	Median	Logarithmic Std. Dev.
0.1	1.10	0.05	1.10	0.05	1.11	0.05
0.125	1.13	0.07	1.13	0.07	1.14	0.07
0.15	1.18	0.10	1.18	0.10	1.19	0.10
0.2	1.28	0.15	1.29	0.15	1.30	0.15
0.3	1.45	0.18	1.46	0.18	1.48	0.19
0.4	1.44	0.17	1.45	0.17	1.48	0.20
0.5	1.38	0.18	1.39	0.19	1.44	0.24
0.6	1.36	0.16	1.39	0.18	1.45	0.25
0.7	1.40	0.15	1.44	0.19	1.51	0.26
0.8	1.47	0.14	1.52	0.21	1.60	0.27
0.9	1.52	0.15	1.57	0.23	1.66	0.29
1	1.57	0.17	1.60	0.23	1.70	0.30
1.25	1.86	0.22	1.96	0.29	2.04	0.33
1.5	2.07	0.29	2.15	0.32	2.20	0.31
2	2.06	0.29	2.11	0.31	2.11	0.29
2.5	1.76	0.37	1.73	0.35	1.73	0.33
3	1.54	0.45	1.49	0.38	1.48	0.38
4	1.43	0.49	1.38	0.46	1.30	0.47
5	1.57	0.53	1.44	0.50	1.19	0.43
6	1.57	0.47	1.36	0.44	1.11	0.47
7	1.43	0.45	1.25	0.47	1.01	0.50
8	1.30	0.43	1.12	0.44	0.93	0.51
9	1.23	0.41	1.06	0.45	0.87	0.52
10	1.15	0.40	1.00	0.43	0.80	0.50
12.5	1.01	0.34	0.86	0.36	0.68	0.43
15	0.91	0.32	0.77	0.35	0.60	0.41
20	0.73	0.30	0.60	0.31	0.45	0.36
25	0.64	0.28	0.51	0.29	0.39	0.36
30	0.62	0.27	0.50	0.28	0.37	0.32
35	0.60	0.24	0.49	0.24	0.37	0.27
40	0.60	0.23	0.50	0.22	0.37	0.24
45	0.61	0.22	0.52	0.21	0.38	0.21
50	0.64	0.21	0.55	0.20	0.41	0.20
60	0.73	0.21	0.64	0.19	0.48	0.19
70	0.87	0.20	0.79	0.19	0.59	0.19
80	1.04	0.20	0.95	0.18	0.72	0.18
90	1.19	0.20	1.11	0.18	0.84	0.18
100	1.30	0.20	1.23	0.18	0.94	0.18

CTS-01521

~~Table 2.5.2-236~~
~~1E-5 and GMRS Amplitudes for GMRS Elevation, Horizontal and Vertical~~

~~Amplitudes for GMRS elevation~~			
~~Frequency (Hz)~~	~~Horizontal 1E-5 UHRS (g)~~	~~Hoizontal GMRS (g)~~	~~Vertical GMRS (g)~~
~~100~~	~~8.26E-02~~	~~3.72 E-02~~	~~3.72E-02~~
~~90~~	~~8.33E-02~~	~~3.75E-02~~	~~3.75E-02~~
~~80~~	~~8.42E-02~~	~~3.79E-02~~	~~3.79E-02~~
~~75~~	~~8.46E-02~~	~~3.81E-02~~	~~3.81E-02~~
~~70~~	~~8.51E-02~~	~~3.83E-02~~	~~3.83E-02~~
~~60~~	~~8.62E-02~~	~~3.88E-02~~	~~3.88E-02~~
~~50~~	~~8.76E-02~~	~~3.94E-02~~	~~3.94E-02~~
~~40~~	~~8.92E-02~~	~~4.01E-02~~	~~4.01E-02~~
~~30~~	~~9.14E-02~~	~~4.11E-02~~	~~4.11E-02~~
~~25~~	~~9.28E-02~~	~~4.18E-02~~	~~4.18E-02~~
~~20~~	~~9.74E-02~~	~~4.38E-02~~	~~4.38E-02~~
~~15~~	~~1.04-E01~~	~~4.66E-02~~	~~4.66E-02~~
~~12.5~~	~~1.08E-01~~	~~4.85E-02~~	~~4.85E-02~~
~~10~~	~~1.13E-01~~	~~5.09E-02~~	~~5.09E-02~~
~~9~~	~~1.14E-01~~	~~5.14E-02~~	~~5.14E-02~~
~~8~~	~~1.16E-01~~	~~5.20E-02~~	~~5.20E-02~~
~~7.5~~	~~1.16E-01~~	~~5.23E-02~~	~~5.23E-02~~
~~7~~	~~1.17E-01~~	~~5.27E-02~~	~~5.27E-02~~
~~6~~	~~1.19E-01~~	~~5.35E-02~~	~~5.34E-02~~
~~5~~	~~1.21E-01~~	~~5.45E-02~~	~~5.44E-02~~
~~4~~	~~1.42E-01~~	~~6.39E-02~~	~~6.38E-02~~
~~3~~	~~1.58E-01~~	~~7.13E-02~~	~~6.11E-02~~
~~2.5~~	~~1.62E-01~~	~~7.29E-02~~	~~5.21E-02~~
~~2~~	~~1.54E-01~~	~~6.94E-02~~	~~4.93E-02~~
~~1.8~~	~~1.50E-01~~	~~6.75E-02~~	~~4.78E-02~~
~~1.5~~	~~1.36E-01~~	~~6.14E-02~~	~~4.32E-02~~
~~1.25~~	~~1.20E-01~~	~~5.41E-02~~	~~3.79E-02~~
~~1~~	~~1.00E-01~~	~~4.50E-02~~	~~3.13E-02~~
~~0.9~~	~~9.65E-02~~	~~4.34E-02~~	~~3.01E-02~~
~~0.8~~	~~9.27E-02~~	~~4.17E-02~~	~~2.88E-02~~
~~0.7~~	~~8.85E-02~~	~~3.98E-02~~	~~2.74E-02~~
~~0.6~~	~~8.40E-02~~	~~3.78E-02~~	~~2.59E-02~~
~~0.5~~	~~7.89E-02~~	~~3.55E-02~~	~~2.42E-02~~
~~0.4~~	~~6.13E-02~~	~~2.76E-02~~	~~1.87E-02~~
~~0.3~~	~~4.19E-02~~	~~1.89E-02~~	~~1.27E-02~~
~~0.2~~	~~2.03E-02~~	~~9.12E-03~~	~~6.09E-03~~
~~0.15~~	~~1.14E-02~~	~~5.11E-03~~	~~3.42E-03~~
~~0.125~~	~~7.84E-03~~	~~3.53E-03~~	~~2.63E-03~~
~~0.1~~	~~4.95E-03~~	~~2.23E-03~~	~~1.49E-03~~

CTS-01521

~~Table 2.5.2-237 (Sheet 1 of 2)~~
~~1E-5 and FIRS Amplitudes for FIRS Elevations, Horizontal and Vertical~~

	~~FIRS2 (g)~~			~~FIRS3 (g)~~		
~~Frequency (Hz)~~	~~1E-5 UHRS~~	~~Horizontal FIRS2~~	~~Vertical FIRS2~~	~~1E-5 UHRS~~	~~Horizontal FIRS 3~~	~~Vertical FIRS3~~
~~100~~	~~8.49E-02~~	~~3.82E-02~~	~~3.82E-02~~	~~1.01E-01~~	~~4.55E-02~~	~~4.55E-02~~
~~90~~	~~8.58E-02~~	~~3.86E-02~~	~~3.86E-02~~	~~1.03E-01~~	~~4.64E-02~~	~~4.64E-02~~
~~80~~	~~8.69E-02~~	~~3.91E-02~~	~~3.91E-02~~	~~1.05E-01~~	~~4.75E-02~~	~~4.75E-02~~
~~75~~	~~8.75E-02~~	~~3.94E-02~~	~~3.94E-02~~	~~1.07E-01~~	~~4.80E-02~~	~~4.80E-02~~
~~70~~	~~8.81E-02~~	~~3.96E-02~~	~~3.96E-02~~	~~1.08E-01~~	~~4.87E-02~~	~~4.87E-02~~
~~60~~	~~8.95E-02~~	~~4.03E-02~~	~~4.03E-02~~	~~1.11E-01~~	~~5.02E-02~~	~~5.02E-02~~
~~50~~	~~9.12E-02~~	~~4.10E-02~~	~~4.10E-02~~	~~1.15E-01~~	~~5.20E-02~~	~~5.20E-02~~
~~40~~	~~9.33E-02~~	~~4.20E-02~~	~~4.20E-02~~	~~1.21E-01~~	~~5.42E-02~~	~~5.42E-02~~
~~30~~	~~9.62E-02~~	~~4.33E-02~~	~~4.33E-02~~	~~1.27E-01~~	~~5.73E-02~~	~~5.73E-02~~
~~25~~	~~9.80E-02~~	~~4.41E-02~~	~~4.41E-02~~	~~1.32E-01~~	~~5.94E-02~~	~~5.94E-02~~
~~20~~	~~1.03E-01~~	~~4.63E-02~~	~~4.63E-02~~	~~1.55E-01~~	~~6.96E-02~~	~~6.96E-02~~
~~15~~	~~1.10E-01~~	~~4.94E-02~~	~~4.94E-02~~	~~1.93E-01~~	~~8.67E-02~~	~~8.67E-02~~
~~12.5~~	~~1.14E-01~~	~~5.14E-02~~	~~5.14E-02~~	~~2.02E-01~~	~~9.10E-02~~	~~9.10E-02~~
~~10~~	~~1.20E-01~~	~~5.40E-02~~	~~5.40E-02~~	~~2.08E-01~~	~~9.36E-02~~	~~9.36E-02~~
~~9~~	~~1.21E-01~~	~~5.43E-02~~	~~5.43E-02~~	~~1.99E-01~~	~~8.97E-02~~	~~8.97E-02~~
~~8~~	~~1.22E-01~~	~~5.47E-02~~	~~5.47E-02~~	~~1.89E-01~~	~~8.52E-02~~	~~8.52E-02~~
~~7.5~~	~~1.22E-01~~	~~5.49E-02~~	~~5.49E-02~~	~~1.84E-01~~	~~8.27E-02~~	~~8.27E-02~~
~~7~~	~~1.23E-01~~	~~5.51E-02~~	~~5.51E-02~~	~~1.78E-01~~	~~8.01E-02~~	~~8.00E-02~~
~~6~~	~~1.24E-01~~	~~5.56E-02~~	~~5.56E-02~~	~~1.65E-01~~	~~7.41E-02~~	~~7.41E-02~~
~~5~~	~~1.25E-01~~	~~5.63E-02~~	~~5.62E-02~~	~~1.49E-01~~	~~6.71E-02~~	~~6.70E-02~~
~~4~~	~~1.43E-01~~	~~6.44E-02~~	~~6.44E-02~~	~~1.66E-01~~	~~7.45E-02~~	~~7.44E-02~~
~~3~~	~~1.57E-01~~	~~7.06E-02~~	~~6.05E-02~~	~~1.77E-01~~	~~7.95E-02~~	~~6.81E-02~~
~~2.5~~	~~1.59E-01~~	~~7.16E-02~~	~~5.12E-02~~	~~1.77E-01~~	~~7.97E-02~~	~~5.69E-02~~
~~2~~	~~1.55E-01~~	~~6.97E-02~~	~~4.95E-02~~	~~1.73E-01~~	~~7.79E-02~~	~~5.53E-02~~
~~1.8~~	~~1.52E-01~~	~~6.84E-02~~	~~4.85E-02~~	~~1.70E-01~~	~~7.65E-02~~	~~5.42E-02~~
~~1.5~~	~~1.40E-01~~	~~6.30E-02~~	~~4.44E-02~~	~~1.57E-01~~	~~7.06E-02~~	~~4.97E-02~~
~~1.25~~	~~1.25E-01~~	~~5.62E-02~~	~~3.93E-02~~	~~1.40E-01~~	~~6.30E-02~~	~~4.41E-02~~
~~1~~	~~1.05E-01~~	~~4.73E-02~~	~~3.29E-02~~	~~1.18E-01~~	~~5.31E-02~~	~~3.70E-02~~
~~0.9~~	~~1.01E-01~~	~~4.56E-02~~	~~3.16E-02~~	~~1.15E-01~~	~~5.16E-02~~	~~3.58E-02~~
~~0.8~~	~~9.73E-02~~	~~4.38E-02~~	~~3.03E-02~~	~~1.11E-01~~	~~4.99E-02~~	~~3.45E-02~~
~~0.7~~	~~9.30E-02~~	~~4.19E-02~~	~~2.88E-02~~	~~1.07E-01~~	~~4.81E-02~~	~~3.31E-02~~
~~0.6~~	~~8.83E-02~~	~~3.97E-02~~	~~2.72E-02~~	~~1.02E-01~~	~~4.60E-02~~	~~3.16E-02~~
~~0.5~~	~~8.30E-02~~	~~3.74E-02~~	~~2.55E-02~~	~~9.72E-02~~	~~4.37E-02~~	~~2.98E-02~~
~~0.4~~	~~6.35E-02~~	~~2.86E-02~~	~~1.94E-02~~	~~7.34E-02~~	~~7.34E-02~~	~~2.24E-02~~
~~0.3~~	~~4.23E-02~~	~~1.90E-02~~	~~1.28E-02~~	~~4.96E-02~~	~~4.96E-02~~	~~1.50E-02~~
~~0.2~~	~~2.03E-02~~	~~9.13E-03~~	~~6.10E-03~~	~~2.45E-02~~	~~2.45E-02~~	~~7.37E-03~~
~~0.15~~	~~1.15E-02~~	~~5.17E-03~~	~~3.46E-03~~	~~1.39E-02~~	~~1.39E-02~~	~~4.19E-03~~
~~0.125~~	~~7.97E-03~~	~~3.58E-03~~	~~2.40E-03~~	~~9.62E-03~~	~~9.62E-03~~	~~2.89E-03~~
~~0.1~~	~~5.05E-03~~	~~2.27E-03~~	~~1.52E-03~~	~~6.09E-03~~	~~6.09E-03~~	~~1.83E-03~~

CTS-01521

~~Table 2.5.2-237 (Sheet 2 of 2)~~
~~1E-5 and FIRS Amplitudes for FIRS Elevations, Horizontal and Vertical~~

	~~FIRS4 (g)~~			~~FIRS4-CoV50 (g)~~		
~~Frequency (Hz)~~	~~1E-5 UHRS~~	~~Horizontal FIRS4~~	~~Vertical FIRS4~~	~~1E-5 UHRS~~	~~Horizontal FIRS4-CoV50~~	~~Vertical FIRS4-CoV50~~
~~100~~	~~1.51E-01~~	~~6.80E-02~~	~~6.80E-02~~	~~1.48E-01~~	~~6.66E-02~~	~~6.66E-02~~
~~90~~	~~1.54E-01~~	~~6.93E-02~~	~~6.93E-02~~	~~1.51E-01~~	~~6.79E-02~~	~~6.79E-02~~
~~80~~	~~1.57E-01~~	~~7.07E-02~~	~~7.07E-02~~	~~1.54E-01~~	~~6.93E-02~~	~~6.93E-02~~
~~75~~	~~1.59E-01~~	~~7.16E-02~~	~~7.16E-02~~	~~1.56E-01~~	~~7.01E-02~~	~~7.01E-02~~
~~70~~	~~1.61E-01~~	~~7.25E-02~~	~~7.25E-02~~	~~1.58E-01~~	~~7.10E-02~~	~~7.10E-02~~
~~60~~	~~1.66E-01~~	~~7.45E-02~~	~~7.45E-02~~	~~1.62E-01~~	~~7.30E-02~~	~~7.30E-02~~
~~50~~	~~1.71E-01~~	~~7.70E-02~~	~~7.70E-02~~	~~1.67E-01~~	~~7.54E-02~~	~~7.54E-02~~
~~40~~	~~1.78E-01~~	~~8.02E-02~~	~~8.02E-02~~	~~1.74E-01~~	~~7.84E-02~~	~~7.84E-02~~
~~30~~	~~1.88E-01~~	~~8.45E-02~~	~~8.45E-02~~	~~1.83E-01~~	~~8.25E-02~~	~~8.25E-02~~
~~25~~	~~1.94E-01~~	~~8.73E-02~~	~~8.73E-02~~	~~1.90E-01~~	~~8.53E-02~~	~~8.53E-02~~
~~20~~	~~2.14E-01~~	~~9.61E-02~~	~~9.61E-02~~	~~2.13E-01~~	~~9.60E-02~~	~~9.60E-02~~
~~15~~	~~2.42E-01~~	~~1.09E-01~~	~~1.09E-01~~	~~2.49E-01~~	~~1.12E-01~~	~~1.12E-01~~
~~12.5~~	~~2.62E-01~~	~~1.18E-01~~	~~1.18E-01~~	~~2.74E-01~~	~~1.23E-01~~	~~1.23E-01~~
~~10~~	~~2.88E-01~~	~~1.30E-01~~	~~1.30E-01~~	~~3.08E-01~~	~~1.39E-01~~	~~1.39E-01~~
~~9~~	~~3.25E-01~~	~~1.46E-01~~	~~1.46E-01~~	~~3.30E-01~~	~~1.48E-01~~	~~1.48E-01~~
~~8~~	~~3.64E-01~~	~~1.64E-01~~	~~1.64E-01~~	~~3.52E-01~~	~~1.58E-01~~	~~1.58E-01~~
~~7.5~~	~~3.83E-01~~	~~1.73E-01~~	~~1.73E-01~~	~~3.62E-01~~	~~1.63E-01~~	~~1.63E-01~~
~~7~~	~~4.03E-01~~	~~1.81E-01~~	~~1.81E-01~~	~~3.73E-01~~	~~1.68E-01~~	~~1.68E-01~~
~~6~~	~~4.43E-01~~	~~1.99E-01~~	~~1.99E-01~~	~~3.94E-01~~	~~1.77E-01~~	~~1.77E-01~~
~~5~~	~~4.80E-01~~	~~2.16E-01~~	~~2.16E-01~~	~~4.12E-01~~	~~1.85E-01~~	~~1.85E-01~~
~~4~~	~~4.10E-01~~	~~1.84E-01~~	~~1.84E-01~~	~~3.83E-01~~	~~1.72E-01~~	~~1.72E-01~~
~~3~~	~~3.23E-01~~	~~1.45E-01~~	~~1.25E-01~~	~~3.40E-01~~	~~1.53E-01~~	~~1.31E-01~~
~~2.5~~	~~2.71E-01~~	~~1.22E-01~~	~~8.72E-02~~	~~3.08E-01~~	~~1.39E-01~~	~~9.91E-02~~
~~2~~	~~2.58E-01~~	~~1.16E-01~~	~~8.25E-02~~	~~2.86E-01~~	~~1.29E-01~~	~~9.14E-02~~
~~1.8~~	~~2.47E-01~~	~~1.11E-01~~	~~7.88E-02~~	~~2.71E-01~~	~~1.22E-01~~	~~8.64E-02~~
~~1.5~~	~~2.23E-01~~	~~1.01E-01~~	~~7.08E-02~~	~~2.41E-01~~	~~1.08E-01~~	~~7.64E-02~~
~~1.25~~	~~1.96E-01~~	~~8.81E-02~~	~~6.17E-02~~	~~2.08E-01~~	~~9.37E-02~~	~~6.57E-02~~
~~1~~	~~1.62E-01~~	~~7.29E-02~~	~~5.07E-02~~	~~1.70E-01~~	~~7.64E-02~~	~~5.32E-02~~
~~0.9~~	~~1.57E-01~~	~~7.07E-02~~	~~4.90E-02~~	~~1.64E-01~~	~~7.36E-02~~	~~5.11E-02~~
~~0.8~~	~~1.52E-01~~	~~6.82E-02~~	~~4.72E-02~~	~~1.57E-01~~	~~7.06E-02~~	~~4.88E-02~~
~~0.7~~	~~1.46E-01~~	~~6.56E-02~~	~~4.52E-02~~	~~1.50E-01~~	~~6.73E-02~~	~~4.64E-02~~
~~0.6~~	~~1.39E-01~~	~~6.27E-02~~	~~4.30E-02~~	~~1.42E-01~~	~~6.37E-02~~	~~4.37E-02~~
~~0.5~~	~~1.32E-01~~	~~5.94E-02~~	~~4.05E-02~~	~~1.33E-01~~	~~5.97E-02~~	~~4.07E-02~~
~~0.4~~	~~1.03E-01~~	~~4.62E-02~~	~~3.13E-02~~	~~1.03E-01~~	~~4.61E-02~~	~~3.13E-02~~
~~0.3~~	~~6.99E-02~~	~~3.15E-02~~	~~2.11E-02~~	~~6.95E-02~~	~~3.13E-02~~	~~2.10E-02~~
~~0.2~~	~~3.34E-02~~	~~1.50E-02~~	~~1.00E-02~~	~~3.31E-02~~	~~1.49E-02~~	~~9.94E-03~~
~~0.15~~	~~1.88E-02~~	~~8.47E-03~~	~~5.66E-03~~	~~1.86E-02~~	~~8.39E-03~~	~~5.61E-03~~
~~0.125~~	~~1.30E-02~~	~~5.85E-03~~	~~3.91E-03~~	~~1.29E-02~~	~~5.80E-03~~	~~3.88E-03~~
~~0.1~~	~~8.24E-03~~	~~3.71E-03~~	~~2.48E-03~~	~~8.17E-03~~	~~3.67E-03~~	~~2.46E-03~~

Chapter 3

Chapter 3 Tracking Report Revision List

Change ID No.	Section	FSAR Rev. 3 Page	Reason for change	Change Summary	Rev. of FSAR T/R
RCOL2_03.0 9.06-22 S01	3.9.6 3.9.10	3.9-2 [3.9-2, 3.9-3] 3.9-6	Supplemental Response to RAI No. 244 Luminant Letter no.TXNB-12021 Date 6/13/2012	Deleted references to NUREG-1482 Rev. 2.	-
RCOL2_14.03.07-38	3.8.4.1.3.2	3.8-6	Response to RAI No. 254 Luminant Letter no.TXNB-12022 Date 6/21/2012	Clarified design criteria.	-
RCOL2_09.02.05-25 S01	3.6.1.3 3.6.4 Table 3.6-201	3.6-1 3.6-2 3.6-3	Supplemental 01 Response to RAI No. 252 Luminant Letter no.TXNB-12031 Date 09/10/2012	Added Table for site-specific high and moderate energy fluid systems.	-
RCOL2_03.03.02-9	3.3 3.3.2.1 (New Subsection) 3.3.2.2.1 (New Subsection) 3.3.2.2.4 3.3.2.3 3.3.3 3.5.1.4 (New Subsection) 3.5.1.5 3.5.2 3.5.4 3.7.3.9 3.8.4.1.3.1	3.3-1 3.3-2, 3.3-3 3.3-3 [3.3-4] 3.5-3 3.5-3 [3.5-4] 3.5-5 [3.5-6] 3.7-11 3.8-4	Response to RAI No. 250 Luminant Letter no.TXNB-12032 Date 09/14/2012	Revised to incorporate RG 1.221.	-

Change ID No.	Section	FSAR Rev. 3 Page	Reason for change	Change Summary	Rev. of FSAR T/R
	3.8.4.1.3.2 3.8.4.4.3.2 Table 3.8-203 3.12.5.3.6 3.12.7 3LL.2	3.8-5 3.8-6 [3.8-5 through 3.8-7] 3.8-11 [3.8-11, 3.8-12] 3.8-21 3.12-1 3.12-2 3LL-1			
RCOL2_14.0 3.07-38 S01	Table 3.2-201 (Sheets 2, 3 of 3)	3.2-4 3.2-5	Supplemental Response to RAI No. 254 Luminant Letter no.TXNB-12034 Date 09/24/2012	Following SSCs for freeze protection are added to the table: - Drain lines from ESWS piping - ESW piping room unit heaters - UHS transfer piping room unit heaters	-
RCOL2_14.0 3.07-38 S01	Table 3D-201 (Sheets 4 through 11 of 11)	3D-5 through 3D-12	Supplemental Response to RAI No. 254 Luminant Letter no.TXNB-12034 Date 09/24/2012	Following SSCs for freeze protection are added to the table. - ESW piping room unit heaters - UHS transfer piping room unit heaters	-
RCOL2_03.06.01-1	3.6.1.3	3.6-1 [3.6-1 through 3.6-2]	Response to RAI No. 262 Luminant Letter no.TXNB-12035 Date 9/26/2012	Revised COL 3.6(1).	-

Change ID No.	Section	FSAR Rev. 3 Page	Reason for change	Change Summary	Rev. of FSAR T/R
RCOL2_03.06.01-1	3.6.2.1	3.6-2 [3.6-3]	Response to RAI No. 262 Luminant Letter no.TXNB-12035 Date 9/26/2012	Revised COL 3.6(4).	-
RCOL2_09.05.04-1	3.8.4.1.3.1	3.8-5	Response to RAI No. 265 Luminant Letter no.TXNB-12043 Date 12/18/2012	Description for environmental conditions of ESWPT and a temporary ventilation system are added.	-
CTS-01515	3.5.1.6	3.5-4 [3.5-5]	Consistency with DCD and site-specific changes as described in Letter. TXNB-12033 (ML12268A413)	Updated aircraft hazards evaluation to reflect changes in plant layout.	0
CTS-01512	Figure 3K-201 [Sheet 1, 2 of 2]	3K-2 [3K-3]	Consistency with DCD and site-specific changes as described in Letter. TXNB-12033 (ML12268A413)	Overall General Arrangement plan replaced with the updated version; and minor editorial correction.	0

*Page numbers for the attached marked-up pages may differ from the revision 3 page numbers due to text additions and deletions. When the page numbers for the attached pages do differ, the page number for the attached page is shown in brackets.

Chapter 4

Chapter 4 Tracking Report Revision List

Change ID No.	Section	FSAR Rev. 3 Page	Reason for change	Change Summary	Rev. of FSAR T/R

*Page numbers for the attached marked-up pages may differ from the revision 3 page numbers due to text additions and deletions. When the page numbers for the attached pages do differ, the page number for the attached page is shown in brackets.

Chapter 5

Chapter 5 Tracking Report Revision List

Change ID No.	Section	FSAR Rev. 3 Page	Reason for change	Change Summary	Rev. of FSAR T/R

*Page numbers for the attached marked-up pages may differ from the revision 3 page numbers due to text additions and deletions. When the page numbers for the attached pages do differ, the page number for the attached page is shown in brackets.

Chapter 6

Chapter 6 Tracking Report Revision List

Change ID No.	Section	FSAR Rev. 3 Page	Reason for change	Change Summary	Rev. of FSAR T/R
RCOL2_06.04-15	6.4.4.2	6.4-2 6.4-3	Supplemental 01 Response to RAI No. 240 Luminant Letter no.TXNB-12021 Date 6/13/2012	Figure 1 was added to the response due to inadvertently omitted in the original response. No changed in FSAR due to Supplemental Response to RAI No. 240.	-
RCOL2_06.02.02-5	6.2.2.3.2 6.2.8	6.2-2 6.2-2 [6.2-3]	Response to RAI No. 271 Luminant Letter no.TXNB-13001 Date 01/17/2013	Added discussion of administrative programs to maintain RMI, fiber insulation, and aluminum within design-basis limits.	-
RCOL2_06.02.02-6	Table 6.2.2-2R (Sheet 7 of 22)	6.2-4	Response to RAI No. 272 Luminant Letter no.TXNB-13005 Date 03/04/2013	COL Item 6.2(5) location made more specific (Section 6.2.2.3 to Section 6.2.2.3.2)	-
RCOL2_06.02.02-7	6.2.2.3.2	6.2-1	Response to RAI No. 272 Luminant Letter no.TXNB-13005 Date 03/04/2013	Changes are made to CP 3/4 latent debris sampling program. Sampling in accordance with NEI 04-07 with exceptions noted. Exceptions are based on CP 1/2 operating experience.	-
CTS-01522	6.4.4.2	6.4-2	To reflect the new seismic layout design change.	The MCR intake elevation is updated.	1

*Page numbers for the attached marked-up pages may differ from the revision 3 page numbers due to text additions and deletions. When the page numbers for the attached pages do differ, the page number for the attached page is shown in brackets.

requirements of RG 1.78. Chemicals, including chemicals in Comanche Peak Nuclear Power Plant (CPNPP) Units 1 and 2, are identified and screened as described in Subsection 2.2.3.1.3.

Several hazardous chemicals exceed the screening criteria provided in RG 1.78 and an analysis is required to determine control room concentrations. Toxic chemicals that do not meet RG 1.78 screening criteria are identified in Table 2.2-214, and calculated maximum control room concentrations of each chemical are also described in Table 2.2-214. Using conservative assumptions and input data for chemical source term, CPNPP Units 3 and 4 control room parameters, site characteristics, and meteorology inputs, postulated chemical releases are analyzed for maximum value concentration to the MCR using the HABIT code, version 1.1. RG 1.78 specifies the use of HABIT software for evaluating control room habitability. HABIT software includes modules that evaluate radiological and toxic chemical transport and exposure. For this analysis of chemical release concentrations, EXTRAN, and CHEM modules are utilized in the code. EXTRAN models toxic chemical transport from the selected release point to the HVAC intake for the MCR, considered at a bounding height of ~~14.3~~13.9 meters above an assumed ground level release (i.e., conservatively lower than the bottom elevation of the fresh air intake missile shield). CHEM is then applied by HABIT to model chemical exposure to control room personnel, based on EXTRAN output and MCR design parameters. CTS-01522

The meteorological conditions assumed for these cases were initially set at G stability and 2.5 m/s wind speed, which is more extreme than 95th percentile for the CPNPP site. The 2.5 m/s wind speed is higher than would be expected for G stability but is conservative in that it introduces the chemical gas into the intakes faster than at lower speeds. The analyses are thus bounding. Lower concentrations are calculated on average using F stability and results for a range of wind speeds and worst case conditions are also presented below as a sensitivity analysis.

The HABIT-based analysis determines the peak concentration in the MCR and compares this level to the RG 1.78 criterion, the specific chemical listed immediately dangerous to life and health (IDLH). In the cases that were analyzed, all postulated releases led to concentrations that are below the IDLH level. Values of IDLH for various chemicals are found in NUREG/CR-6624 (Reference 6.4-201).

The most limiting case, or the one that leads to the highest control room concentration relative to the IDLH, is the tanker truck release of chlorine on Highway FM 56, at a distance of closest approach to CPNPP Units 3 and 4 MCR intake of 1.4 miles. Chlorine is used for this case because it is one of the most hazardous Department of Transportation approved chemicals, and bounds other chemicals by toxicity, dispersibility, and quantity that may use public transportation such as Highway FM 56. Using the methodology prescribed by RG 1.78, as well as the heavy gas modeling in ALOHA, the analysis showed MCR concentration remains below 10 ppm throughout the evaluated transient under all conditions. The IDLH concentration for chlorine is 10 ppm.

Chapter 7

Chapter 7 Tracking Report Revision List

Change ID No.	Section	FSAR Rev. 3 Page	Reason for change	Change Summary	Rev. of FSAR T/R

*Page numbers for the attached marked-up pages may differ from the revision 3 page numbers due to text additions and deletions. When the page numbers for the attached pages do differ, the page number for the attached page is shown in brackets.

Chapter 8

Chapter 8 Tracking Report Revision List

Change ID No.	Section	FSAR Rev. 3 Page	Reason for change	Change Summary	Rev. of FSAR T/R
RCOL2_08.01-3	8.1.2.1	8.1-1	Response to RAI No. 249 Luminant Letter no.TXNB-12013 Date 05/16/2012	Subsection 8.1.2.1 was revised to state that the switching station equipment shared between Units 3 and 4 includes the circuit breakers, and that no important to safety SSCs are shared between Units 3 and 4, under any operating scenario (normal or emergency).	-
RCOL2_03.03.02-9	8.2.1.2.1.1	8.2-4	Response to RAI No. 250 Luminant Letter no.TXNB-12032 Date 9/14/2012	Revised to incorporate RG 1.221.	-
RCOL2_08.01-2 S03	8.1.2.1	8.1-1 [8.1-1 through 8.1-2]	3rd Supplemental Response to RAI No. 9 Luminant Letter No.TXNB-13007 Date 03/04/2013	Sentences of switching station moved to section 8.2.2.1 Applicable Criteria.	-
RCOL2_08.01-2 S03	8.2.2.1 (new section)	8.2-10 [8.2-10 through 8.2-11]	3rd Supplemental Response to RAI No. 9 Luminant Letter No.TXNB-13007 Date 03/04/2013	Compliance to GDC 5 of Switching Station added to 8.2.2.1 Applicable Criteria.	-
CTS-01508	Figure 8.3.1-201	8.3-21	Revised to reflect common foundation and the new plant layout	Figure was updated to reflect standard plant and site-specific layout changes.	0
CTS-01508	Figure 8.2-207	8.2-31	Turbine Building and Electrical Building layout change. Figure was updated to reflect standard plant and	The road surrounding the Unit 3 and Unit 4 switchyard are changed. Other non-technical editorial changes are made such as removal of dimension line of the building.	1

Change ID No.	Section	FSAR Rev. 3 Page	Reason for change	Change Summary	Rev. of FSAR T/R
			site-specific layout changes		
CTS-01508	Figure 8.2-208	8.2-32	Turbine Building and Electrical Building layout change. Figure was updated to reflect standard plant and site-specific layout changes	The road surrounding the Unit 3 and Unit 4 switchyard are changed. Other non-technical editorial changes are made such as removal of dimension line of the building.	1

*Page numbers for the attached marked-up pages may differ from the revision 3 page numbers due to text additions and deletions. When the page numbers for the attached pages do differ, the page number for the attached page is shown in brackets.

CTS-01508

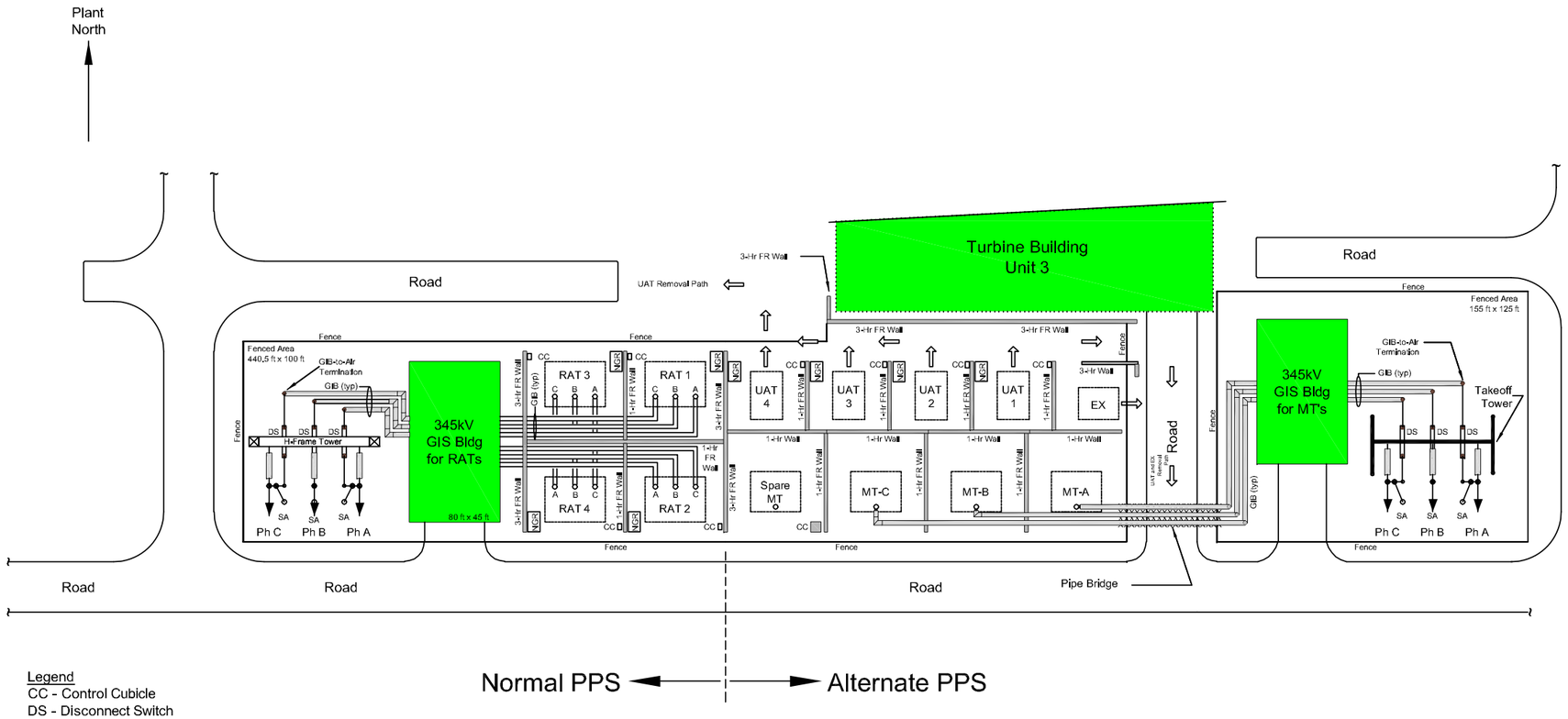

Legend
CC - Control Cubicle
DS - Disconnect Switch
EX - Excitation Transformer
FR - Fire-Rated
GIB - Gas-Insulated Bus
GIS - Gas-Insulated Switchgear
MT - Main Transformer
NGR - Neutral Grounding Resistor
PPS - Preferred Power Supply
RAT - Reserve Auxiliary Transformer
SA - Surge Arrester
T/B - Turbine Building
UAT - Unit Auxiliary Transformer

Note - Fire-rated walls between transformers and structures and between the transformers are in accordance with Reg Guide 1.189 and NFPA 804. Provisions for drainage and oil-spill containment are in accordance with NFPA 804 and IEEE 980.

CP COL 8.2(3)
CP COL 8.2(4)
CP COL 8.2(5)

Figure 8.2-207 Unit 3 Unit Switchyard Layout

CTS-01508

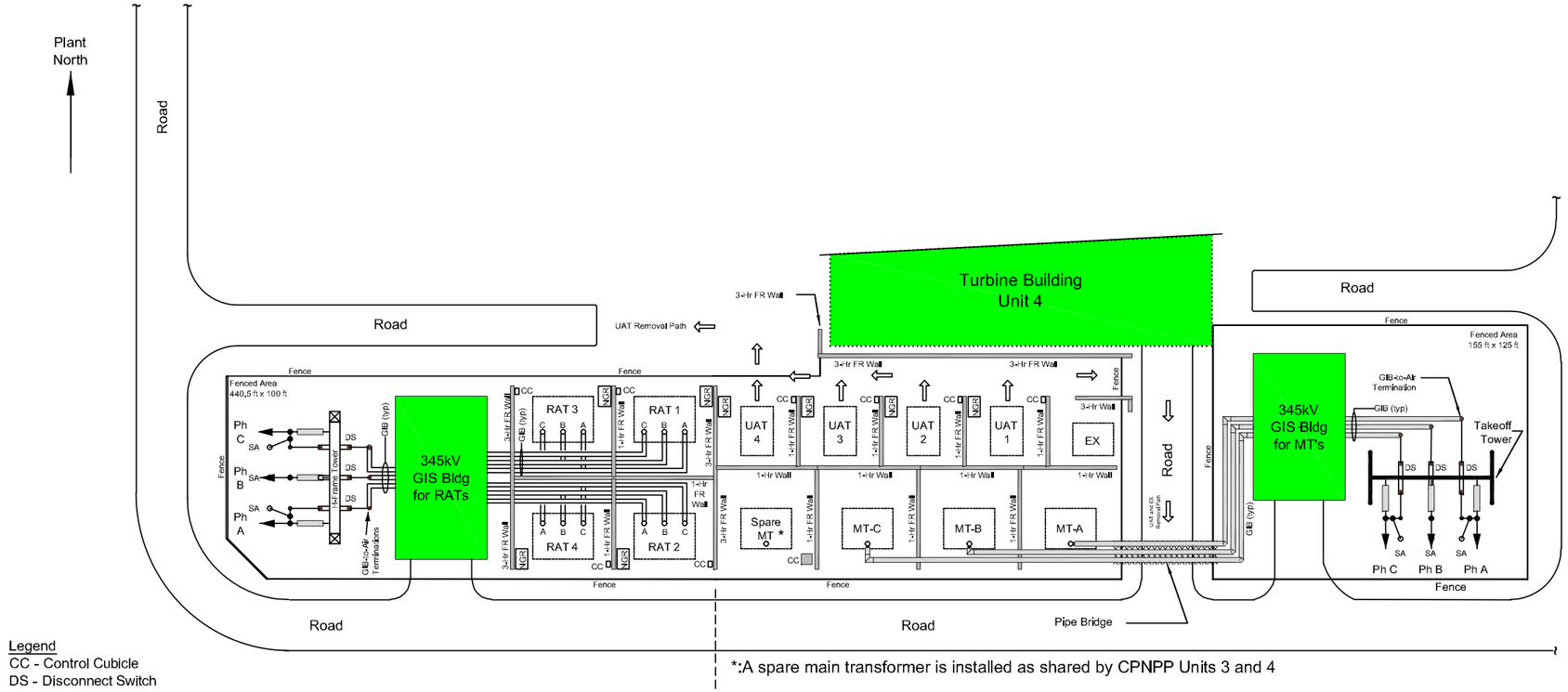

Legend
CC - Control Cubicle
DS - Disconnect Switch
EX - Excitation Transformer
FR - Fire-Rated
GIB - Gas-Insulated Bus
GIS - Gas-Insulated Switchgear
MT - Main Transformer
NGR - Neutral Grounding Resistor
PPS - Preferred Power Supply
RAT - Reserve Auxiliary Transformer
SA - Surge Arrester
T/B - Turbine Building
UAT - Unit Auxiliary Transformer

Note - Fire-rated walls between transformers and structures and between the transformers shall be in accordance with Reg Guide 1.189 and NFPA 804. Provisions for drainage and oil-spill containment shall be in accordance with NFPA 804 and IEEE 980.

CP COL 8.2(3)
CP COL 8.2(4)
CP COL 8.2(5)

Figure 8.2-208 Unit 4 Unit Switchyard Layout

Chapter 9

Chapter 9 Tracking Report Revision List

Change ID No.	Section	FSAR Rev. 3 Page	Reason for change	Change Summary	Rev. of FSAR T/R
RCOL2_09.02.01-7	9.2.1.3	9.2-5 [9.2-6]	Response to RAI No. 251 Luminant Letter no.TXNB-12016 Date 05/31/2012	Added discussion regarding CCW heat exchanger backflush procedure including valve alignment and identification as a maintenance outage train.	-
RCOL2_09.02.01-8	9.2.1.2.2.5	9.2-4	Response to RAI No. 251 Luminant Letter no.TXNB-12016 Date 05/31/2012	Revised to discuss the ESWS piping material and inspection.	-
RCOL2_09.02.01-9	9.2.5.5	9.2-21 [9.2-22 9.2-23]	Response to RAI No. 251 Luminant Letter no.TXNB-12016 Date 05/31/2012	Revised to clarify that level switches are utilized to prevent water hammer and are non safety-related.	
RCOL2_09.0 1.05-1 S01	9.1.5.3 9.1.5 (New Section) 9.1.5.1(New Subsection) 9.1.5.3 (New Subsection) 9.1.5.4 (New Subsection) 9.1.5.6 (New Subsection) 9.1.6	9.1-1 [9.1-1 through 9.1-5] 9.1-2 [9.1-5]	Supplemental 01 Response to RAI No. 52 Luminant Letter no.TXNB-12021 Date 6/13/2012	The heavy load handling program description is enhanced to satisfy the requirements of COL item 9.1 (6).	-
RCOL2_14.03.07-38	9.2.5.2.1 9.2.5.3	9.2-12 [9.2-13] 9.2-18 [9.2-20]	Response to RAI No. 254 Luminant Letter no.TXNB-12022 Date 6/21/2012	Added design criteria for cooling tower spray nozzle sizing. Clarified design criteria.	-
RCOL2_14.02-21	9.2.5.2.1 9.2.5.2.2	9.2-12 [9.2-13] 9.2-15	Response to RAI No. 257 Luminant Letter no.TXNB-12022 Date 6/21/2012	Added discussion about UHS fan speed and direction. Added discussion	-

Change ID No.	Section	FSAR Rev. 3 Page	Reason for change	Change Summary	Rev. of FSAR T/R
		[9.2-16]		about level switches.	
RCOL2_09.0 4.05-23 S01	9.4.5.3.6	9.4-6	Supplemental 01 RAI No. 243 Luminant Letter no.TXNB-12030 Date 08/29/2012	Added the design information about the wall separating the ESW pump room from the transfer pump room.	-
RCOL2_09.0 4.05-23 S01	Table 9.4-202	9.4-11	Supplemental 01 Response to RAI No. 243 Luminant Letter no.TXNB-12030 Date 08/29/2012	Changed the capacity of UHS ESW Pump House Ventilation System Equipment.	-
RCOL2_09.0 4.05-23 S01	9A.3.101 9A.3.102 9A.3.104 9A.3.105 9A.3.107 9A.3.108 9A.3.110 9A.3.111	9A-2 9A-3 9A-5 9A-6 9A-8 9A-9 9A-10 9A-12 9A-13	Supplemental 01 Response to RAI No. 243 Luminant Letter no.TXNB-12030 Date 08/29/2012	Changed or added fire protection design features for UHS basins, ESW pump rooms and transfer pump rooms.	-
RCOL2_09.02.01-9 S01	9.2.1.2.3.1 9.2.5.2.2 9.2.5.5	9.2-4 9.2-15 [9.2-17] 9.2-22 [9.2-25]	Supplemental 01 Response to RAI No. 251 Luminant Letter no.TXNB-12031 Date 9/10/2012	Removed description of level switches located in the UHS cooling tower riser piping.	-

Change ID No.	Section	FSAR Rev. 3 Page	Reason for change	Change Summary	Rev. of FSAR T/R
RCOL2_09.02.05-18 S01	9.2.5.2.1	9.2-12	Supplemental 01 Response to RAI No. 252 Luminant Letter no.TXNB-12031 Date 09/10/2012	Added description to discuss UHS cooling tower plume discharge.	-
RCOL2_03.03.02-9	9.2.5.2.1 9.2.5.2.2 9.4.5.3.6 9.4.5.4.6	9.2-12 [9.2-13] 9.2-15 [9.2-17] 9.4-7	Response to RAI No. 250 Luminant Letter no.TXNB-12032 Date 9/14/2012	Revised to incorporate RG 1.221.	-
RCOL2_14.0 3.07-38 S01	9.2.1.3 9.2.5.2.2 9.2.10	9.2-5 9.2-15 9.2-24	Supplemental Response to RAI No. 254 Luminant Letter no.TXNB-12034 Date 09/24/2012	Description is added regarding freeze protection of the UHS and ESWS. Table 9.2.5-201 is added for address of CP COL 9.2(19).	-
RCOL2_14.0 3.07-38 S01	Table 9.2.5-201 (New Table)	9.2-35	Supplemental Response to RAI No. 254 Luminant Letter no.TXNB-12034 Date 09/24/2012	New table is introduced to describe electric power division for clarification.	-
RCOL2_14.0 3.07-38 S01	Figure 9.2.5-1R (Sheets 1, 2 of 2)	9.2-38 9.2-39	Supplemental Response to RAI No. 254 Luminant Letter no.TXNB-12034 Date 09/24/2012	The figure is revised to show the newly introduced drain lines for freeze protection.	-

Change ID No.	Section	FSAR Rev. 3 Page	Reason for change	Change Summary	Rev. of FSAR T/R
RCOL2_14.0 3.07-38 S01	9.4.5.1.1.6 9.4.5.2.6	9.4-3 9.4-4 through 9.4-6	Supplemental Response to RAI No. 254 Luminant Letter no.TXNB-12034 Date 09/24/2012	Supply areas are added to the UHS ESW Pump House Ventilation System and to for freeze protection of the UHSS and ESWS.	-
RCOL2_14.0 3.07-38 S01	Table 9.4-202	9.4-11	Supplemental Response to RAI No. 254 Luminant Letter no.TXNB-12034 Date 09/24/2012	ESW piping room unit heaters and UHS transfer piping room unit heaters are added to the table.	-
RCOL2_14.0 3.07-38 S01	Table 9.4-203 (Sheet 3 of 6)	9.4-14	Supplemental Response to RAI No. 254 Luminant Letter no.TXNB-12034 Date 09/24/2012	ESW piping room unit heaters and UHS transfer piping room unit heaters are added to the table.	-
RCOL2_14.0 3.07-38 S01	Figure 9.4-201	9.4-18	Supplemental Response to RAI No. 254 Luminant Letter no.TXNB-12034 Date 09/24/2012	The figure is revised to add newly introduced dampers to inlets and exhausts of the ventilation system.	-
RCOL2_09.02.05-18 S02	9.2.5.2.1	9.2-12	Supplemental 02 Response to RAI No. 252 Luminant Letter no.TXNB-12036 Date 11/12/2012	Corrected vertical distance value for distance between UHS CT discharge and other intakes; Revised description to indicate pump house intakes on the south side take advantage of the prevailing wind direction.	-

Change ID No.	Section	FSAR Rev. 3 Page	Reason for change	Change Summary	Rev. of FSAR T/R
RCOL2_09.02.05-20 S02	9.2.5.2.2	9.2-15	Supplemental 02 Response to RAI No. 252 Luminant Letter no.TXNB-12036 Date 11/12/2012	Revised description to indicate that vortex is not a concern during simultaneous pump operation of ESWP and UHS Transfer Pump.	-
RCOL2_14.03.07-38 S02	9.2.1.3	9.2-5 [9.2-6]	Supplemental 02 Response to RAI No. 254 Luminant Letter no.TXNB-12036 Date 11/12/2012	Revised to include description that ESWPT is below grade and therefore freezing is not a concern.	-
RCOL2_09.02.01-9 S02	9.2.1.2.3.1 9.2.5.5 9.2.10	9.2-4 [9.2-4, 9.2-5] 9.2-21 [9.2-24] 9.2-25 [9.2-29]	Supplemental 02 Response to RAI No. 251 Luminant Letter no.TXNB-12041 Date 12/03/2012	Revise the location of the DCD reference location and add the evaluation of why void detection is not required. Change LMN from “STD COL 9.2(24) to STD COL 9.2(32)”. Delete “9.2.5.5” from 9.2(32) Void dection system.	-
RCOL2_12.03-12.04-11 S04	9.2.6.2 (New section)	9.2-22	Supplemental 04 Response to RAI No. 135 Luminant Letter no.TXNB-12042 Date 12/6/2012	Revised to state that the CST for CPNPP Unit 3 is located on west side of Unit 3 as depicted on Figure 12.3-201, while the CPNPP Unit 4 CST is located on the east side of Unit 4, as depicted on Figure 12.3-202.	-

Change ID No.	Section	FSAR Rev. 3 Page	Reason for change	Change Summary	Rev. of FSAR T/R
RCOL2_09.04.05-26	Table 9.4-201 (Sheet 1 of 2)	9.4-9 [9.4-10]	Response to RAI No. 266 Luminant Letter no.TXNB-12043 Date 12/18/2012	MCR/Class 1E Electrical HVAC Equipment Room In-duct Heater Capacity “Non-heating” is added for Train A and D.	-
RCOL2_09.04.05-27	9.4.3.2.2	9.4-2	Response to RAI No. 266 Luminant Letter no.TXNB-12043 Date 12/18/2012	The LMN “CP COL 9.4(4)” and description of supplemental heating is added.	-
RCOL2_09.05.04-1	9.5.4.2.2.1	9.5-21	Response to RAI No. 265 Luminant Letter no.TXNB-12043 Date 12/18/2012	Temperature condition of PSFSV is added.	-
RCOL2_09.04.05-23 S02	9.3.3.2.3 (new section)	9.3-2 [9.3-2 through 9.3-3]	Supplemental S02 Response to RAI No. 243 Luminant Letter no.TXNB-13006 Date 03/04/2013	Design description of floor drain system and liquid detection system were added.	-

Change ID No.	Section	FSAR Rev. 3 Page	Reason for change	Change Summary	Rev. of FSAR T/R
RCOL2_09.04.05-23 S02	9.4.5.1.1.6 9.4.5.2.6 9.4.5.3.6 9.4.7	9.4-3 9.4-4 [9.4-5] 9.4-7 9.4-8 [9.4-9]	Supplemental S02 Response to RAI No. 243 Luminant Letter no.TXNB-13006 Date 03/04/2013	Temperature range was deleted. A sentence describing the Table 9.4-202 was added. Table numbers were revised correspondence with a new table.	-
RCOL2_09.04.05-23 S02	Table 9.4-202 (replaced table) Table 9.4-203[204] (Sheets 1, 5[7] of 6[8])	9.4-11 [9.4-12] 9.4-12, 9.4-16 [9.4-14, 9.4-20]	Supplemental S02 Response to RAI No. 243 Luminant Letter no.TXNB-13006 Date 03/04/2013	New table was added as Table 9.4-202 and table numbers were revised correspondence with this new table.	-
CTS-01509	Table 9.4-201	9.4-9 9.4-10 [9.4-11]	To reflect impacts on heating and cooling capacity due to layout changes.	Heating and cooling capacity and in-duct heater capacity in Table 9.4-201 have been changed.	0
CTS-01517	Figure 9.5.1-202	9.5-148	Design change as described in Luminant ISCP Letter ML12268A413	Reflected new site plan.	0

Change ID No.	Section	FSAR Rev. 3 Page	Reason for change	Change Summary	Rev. of FSAR T/R
CTS-01516	9A.3	9A-1	Correction	Changed “Pumping Station” to “Pump House” in first bullet.	0
CTS-01518	9A.3	9A-1	Design change as described in Supplemental Response to RAI No. 254 (ML12334A026) and the ISCP (ML 12268A413).	Added bullets ESW-Piping Room and UHS-Transfer Piping Room.	0
CTS-01518	9A.3	9A-2	Design change as described in Supplemental Response to RAI No. 254 (ML12334A026) and the ISCP (ML 12268A413).	Changed the DCD Subsection to 9A.3.153.	0
CTS-01518	9A.3.101 [9A.3.201]	9A-2	Design change as described in Supplemental Response to RAI No. 254 (ML12334A026) and the ISCP (ML 12268A413).	Changed Section 9A.3.101 to 9A.3.201 and changed title to FA7-201-01.	0

Change ID No.	Section	FSAR Rev. 3 Page	Reason for change	Change Summary	Rev. of FSAR T/R
CTS-01516	9A.3.101 [9A.3.201]	9A-2	Correction	Changed “exceed” to “exceeding”	0
CTS-01516	9A.3.101 [9A.3.201]	9A-2	Correction	Added 3.2.1.j.	0
CTS-01518	9A.3.101 [9A.3.201]	9A-2 [9A-3]	Design change as described in Supplemental Response to RAI No. 254 (ML12334A026) and the ISCP (ML 12268A413).	Deleted “The electrical circuits from other safety trains in this area will be protected by a one-hour fire rated wrap.”	0
CTS-01518	9A.3.202 [New]	9A-3 and [9A-4]	Design change as described in Supplemental Response to RAI No. 254 (ML12334A026) and the ISCP (ML 12268A413).	Added new subsection 9A.3.202, FA7-201-02 A-ESW Piping Room	0

Change ID No.	Section	FSAR Rev. 3 Page	Reason for change	Change Summary	Rev. of FSAR T/R
CTS-01518	9A.3.102 [9A.3.203]	9A-3 [9A-5]	Design change as described in Supplemental Response to RAI No. 254 (ML12334A026) and the ISCP (ML 12268A413).	Changed Section 9A.3.102 to 9A.3.203 and changed fire area to FA7-202 to fire zone FA7-202-01.	0
CTS-01516	9A.3.102 [9A.3.203]	9A-3 [9A-5]	Correction	Changed “D” to “C or D.”	0
CTS-01516	9A.3.102 [9A.3.203]	9A-3 [9A-5]	Correction	Changed “exceed” to “exceeding”	0
CTS-01516	9A.3.102 [9A.3.203]	9A-3 [9A-5]	Correction	Added 3.2.1.j.	0

Change ID No.	Section	FSAR Rev. 3 Page	Reason for change	Change Summary	Rev. of FSAR T/R
CTS-01518	9A.3.204 [New]	9A-4 [9A-6, 9A-7]	Design change as described in Supplemental Response to RAI No. 254 (ML12334A026) and the ISCP (ML 12268A413).	Added new Subsection 9A.3.204, FA7-202-02 A-UHS Transfer Piping Room.	0
CTS-01518	9A.3.103 [9A.3.205]	9A-4 [9A-7]	Design change as described in Supplemental Response to RAI No. 254 (ML12334A026) and the ISCP (ML 12268A413).	Changed section from 9A.3.103 to 9A.3.205 and changed fire area from FA7-203 to fire zone FA7-203-01.	0
CTS-01518	9A.3.104 [9A.3.206]	9A-5 [9A-8]	Design change as described in Supplemental Response to RAI No. 254 (ML12334A026) and the ISCP (ML 12268A413).	Changed section from 9A.3.104 to 9A.3.206 and changed fire area from FA7-204 to fire zone FA7-204-01.	0
CTS-01516	9A.3.104 [9A.3.206]	9A-5 [9A-8]	Correction	Changed “exceed” to “exceeding”	0

Change ID No.	Section	FSAR Rev. 3 Page	Reason for change	Change Summary	Rev. of FSAR T/R
CTS-01516	9A.3.104 [9A.3.206]	9A-5 [9A-9]	Correction	Added 3.2.1.j.	0
CTS-01518	9A.3.104 [9A.3.206]	9A-6 [9A-9]	Design change as described in Supplemental Response to RAI No. 254 (ML12334A026) and the ISCP (ML 12268A413).	Deleted “The electrical circuits from other safety trains in this area will be protected by a one-hour fire rated wrap.”	0
CTS-01518	9A.3.207 [New]	9A-6 [9A-10, 9A-11]	Design change as described in Supplemental Response to RAI No. 254 (ML12334A026) and the ISCP (ML 12268A413).	Added new Subsection 9A.3.207, FA7-204-02 B-ESW Piping Room.	0
CTS-01518	9A.3.105 [9A.3.208]	9A-6 [9A-11]	Design change as described in Supplemental Response to RAI No. 254 (ML12334A026) and the ISCP (ML 12268A413).	Changed section from 9A.3.105 to 9A.3.208 and changed fire area from FA7-205 to fire zone FA7-205-01.	0

Change ID No.	Section	FSAR Rev. 3 Page	Reason for change	Change Summary	Rev. of FSAR T/R
CTS-01516	9A.3.105 [9A.3.208]	9A-6 [9A-11]	Correction	Changed “D” to “C or D.”	0
CTS-01516	9A.3.105 [9A.3.208]	9A-6 [9A-11]	Correction	Changed “exceed” to “exceeding”	0
CTS-01516	9A.3.105 [9A.3.208]	9A-6 [9A-12]	Correction	Added 3.2.1.j.	0
CTS-01518	9A.3.209 [New]	9A-7 [9A-13, 9A-14]	Design change as described in Supplemental Response to RAI No. 254 (ML12334A026) and the ISCP (ML 12268A413).	Added new Subsection 9A.3.209, FA7-205-02 B-UHS Transfer Piping Room.	0

Change ID No.	Section	FSAR Rev. 3 Page	Reason for change	Change Summary	Rev. of FSAR T/R
CTS-01518	9A.3.106 [9A.3.210]	9A-7 [9A-14]	Design change as described in Supplemental Response to RAI No. 254 (ML12334A026) and the ISCP (ML 12268A413).	Changed section from 9A.3.106 to 9A.3.210 and changed fire area from FA7-206 to fire zone FA7-206-01.	0
CTS-01518	9A.3.107 [9A.3.211]	9A-8 [9A-15]	Design change as described in Supplemental Response to RAI No. 254 (ML12334A026) and the ISCP (ML 12268A413).	Changed section from 9A.3.107 to 9A.3.211 and changed fire area from FA7-207 to fire zone FA7-207-01.	0
CTS-01516	9A.3.107 [9A.3.211]	9A-8 [9A-15]	Correction	Changed “exceed” to “exceeding”	0
CTS-01516	9A.3.107 [9A.3.211]	9A-9 [9A-15]	Correction	Added 3.2.1.j.	0

Change ID No.	Section	FSAR Rev. 3 Page	Reason for change	Change Summary	Rev. of FSAR T/R
CTS-01518	9A.3.107 [9A.3.211]	9A-9 [9A-16]	Design change as described in Supplemental Response to RAI No. 254 (ML12334A026) and the ISCP (ML 12268A413).	Deleted “The electrical circuits from other safety trains in this area will be protected by a one-hour fire rated wrap.”	0
CTS-01518	9A.3.212 [New]	9A-9 [9A-16, 9A-17, 9A-18]	Design change as described in Supplemental Response to RAI No. 254 (ML12334A026) and the ISCP (ML 12268A413).	Added new Subsection 9A.3.212, FA7-207-02 C-ESW Piping Room.	0
CTS-01518	9A.3.108 [9A.3.213]	9A-10 [9A-18]	Design change as described in Supplemental Response to RAI No. 254 (ML12334A026) and the ISCP (ML 12268A413).	Changed section from 9A.3.108 to 9A.3.213 and changed fire area from FA7-208 to fire zone FA7-208-01.	0
CTS-01516	9A.3.108 [9A.3.213]	9A-10 [9A-18]	Correction	Changed “A” to “A or B.”	0

Change ID No.	Section	FSAR Rev. 3 Page	Reason for change	Change Summary	Rev. of FSAR T/R
CTS-01516	9A.3.108 [9A.3.213]	9A-10 [9A-18]	Correction	Changed “exceed” to “exceeding”	0
CTS-01516	9A.3.108 [9A.3.213]	9A-10 [9A-18]	Correction	Added 3.2.1.j.	0
CTS-01518	9A.3.214 [New]	9A-11 [9A-19, 9A-20]	Design change as described in Supplemental Response to RAI No. 254 (ML12334A026) and the ISCP (ML 12268A413).	Added new Subsection 9A.3.214, FA7-208-02 C-UHS Transfer Piping Room.	0
CTS-01518	9A.3.109 [9A.3.215]	9A-11 [9A-20]	Design change as described in Supplemental Response to RAI No. 254 (ML12334A026) and the ISCP (ML 12268A413).	Changed section from 9A.3.109 to 9A.3.215 and changed fire area from FA7-209 to fire zone FA7-209-01.	0

Change ID No.	Section	FSAR Rev. 3 Page	Reason for change	Change Summary	Rev. of FSAR T/R
CTS-01518	9A.3.110 [9A.3.216]	9A-12 [9A-21]	Design change as described in Supplemental Response to RAI No. 254 (ML12334A026) and the ISCP (ML 12268A413).	Changed section from 9A.3.110 to 9A.3.216 and changed fire area from FA7-210 to fire zone FA7-210-01.	0
CTS-01516	9A.3.110 [9A.3.216]	9A-12 [9A-21]	Correction	Changed “exceed” to “exceeding”	0
CTS-01516	9A.3.110 [9A.3.216]	9A-12 [9A-22]	Correction	Added 3.2.1.j.	0
CTS-01518	9A.3.110 [9A.3.216]	9A-13 [9A-23]	Design change as described in Supplemental Response to RAI No. 254 (ML12334A026) and the ISCP (ML 12268A413).	Deleted “The electrical circuits from other safety trains in this area will be protected by a one-hour fire rated wrap.”	0

Change ID No.	Section	FSAR Rev. 3 Page	Reason for change	Change Summary	Rev. of FSAR T/R
CTS-01518	9A.3.217 [New]	9A-13 [9A-23, 9A-24]	Design change as described in Supplemental Response to RAI No. 254 (ML12334A026) and the ISCP (ML 12268A413).	Added new Subsection 9A.3.217, FA7-210-02 D-ESW Piping Room.	0
CTS-01516	9A.3.111 [9A.3.218]	9A-13 [9A-24]	Correction	Changed section from 9A.3.111 to 9A.3.218 and changed fire area from FA7-211 to fire zone FA7-211-01.	0
CTS-01516	9A.3.111 [9A.3.218]	9A-13 [9A-24]	Correction	Changed “A” to “A or B.”	0
CTS-01516	9A.3.111 [9A.3.218]	9A-13 [9A-24]	Correction	Changed “exceed” to “exceeding”	0

Change ID No.	Section	FSAR Rev. 3 Page	Reason for change	Change Summary	Rev. of FSAR T/R
CTS-01516	9A.3.111 [9A.3.218]	9A-13 [9A-25]	Correction	Added 3.2.1.j.	0
CTS-01518	9A.3.219 [New]	9A-14 [9A-26, 9A-27]	Design change as described in Supplemental Response to RAI No. 254 (ML12334A026) and the ISCP (ML 12268A413).	Added new Subsection 9A.3.219, FA7-211-02 D-UHS Transfer Piping Room.	0
CTS-01518	9A.3.112 [9A.3.220]	9A-14 [9A-27]	Design change as described in Supplemental Response to RAI No. 254 (ML12334A026) and the ISCP (ML 12268A413).	Changed section from 9A.3.112 to 9A.3.220 and changed fire area from FA7-212 to fire zone FA7-212-01.	0
CTS-01518	9A.3.113 [9A.3.221]	9A-15 [9A-28]	Design change as described in Supplemental Response to RAI No. 254 (ML12334A026) and the ISCP (ML 12268A413).	Changed subsection 9A.3.113 to 9A.3.221	0

Change ID No.	Section	FSAR Rev. 3 Page	Reason for change	Change Summary	Rev. of FSAR T/R
CTS-01518	9A.3.114 [9A.3.222]	9A-17 [9A-29]	Design change as described in Supplemental Response to RAI No. 254 (ML12334A026) and the ISCP (ML 12268A413).	Changed subsection 9A.3.114 to 9A.3.222	0
CTS-01518	Table 9A-201 [Sheet 1,2 of 2]	9A-19 [9A-31, 9A-32]	Design change as described in Supplemental Response to RAI No. 254 (ML12334A026) and the ISCP (ML 12268A413).	Revised table to include new fire zones.	0
CTS-01518	Table 9A-202 (Sheet 1 through 25 of 25 [Sheet 1 through 33 of 33])	9A-20 – 9A-44 [9A-33 through 9A-65]	Design change as described in Supplemental Response to RAI No. 254 (ML12334A026) and the ISCP (ML 12268A413).	Revised summary sheets associated with Fire Areas FA7-201 through 212 to reflect new fire zone information Revised summary sheets for Fire Zones FA7-301-01 through 13 to reflect revised FHA section.	0
CTS-01518	Table 9A-203 [Sheet 1,2 of 2]	9A-45 [9A-66, 9A-67]	Design change as described in Supplemental Response to RAI No. 254 (ML12334A026) and the ISCP (ML 12268A413).	Revised table to include new fire zones.	0

Change ID No.	Section	FSAR Rev. 3 Page	Reason for change	Change Summary	Rev. of FSAR T/R
CTS-01519	Figure 9A-201	9A-46 [9A-68]	Design change as described in Luminant ISCP Letter ML12268A413 and Supplemental Responses to RAIs No. 243 (ML12243A456) and No. 254 (ML12334A026)	Figure is revised to reflect: Integration of the north portions of the ESWPT into the south side of the UHSRS. Integration of adjacent UHSRS (C and D) and (A and B) on a single foundation. ESW Pump House layout changes described in responses to RAIs 243 S01 and 254 S03. New fire areas for ESW Piping Room and UHS Transfer Piping Room	0
CTS-01519	Figure 9A-202	9A-47 [9A-69]	Design change as described in Luminant ISCP Letter ML12268A413 and Supplemental Responses to RAIs No. 243 (ML12243A456) and No. 254 (ML12334A026)	Revised roadway north of Transformer Yard.	0

Change ID No.	Section	FSAR Rev. 3 Page	Reason for change	Change Summary	Rev. of FSAR T/R
MIC-03-09-00013	9.2.5.2.3	9.2-17 9.2-18 [9.2-20 9.2-21]	Consistency with DCD change	Updated heat loads to be consistent with associated DCD changes.	1
CTS-01529	9.2.5.3	9.2-18 [9.2-21]	Editorial correction	Replaced “type” with “types” in section 9.2.5.3.	1

*Page numbers for the attached marked-up pages may differ from the revision 3 page numbers due to text additions and deletions. When the page numbers for the attached pages do differ, the page number for the attached page is shown in brackets.

International Airport Station in accordance with RG 1.27. The worst 30 day period based on the above climatological data was between June 1, 1998 and June 30, 1998, with an average wet bulb temperature of 78.0°F. A 2°F recirculation penalty was added to the maximum average wet bulb temperature.

The 83° F wet bulb temperature as shown in the FSAR Table 2.0-1R corresponds to the 0% annual exceedance value (two consecutive hourly peak temperatures on July 12, 1995, at 1500 hours and 1600 hours) in accordance with SRP 2.3.1. The 0% exceedance criterion means that the wet bulb temperature does not exceed the 0% exceedance value for more than two consecutive data occurrences, namely two consecutive hours on data recorded hourly. The 83° F wet bulb temperature is used to establish the cooling tower basin water temperature surveillance requirements.

The UHS is analyzed using the heat loads provided in Table 9.2.5-2 for LOCA and safe shutdown conditions with LOOP and a maximum ESW supply temperature of 95°F. Per Subsection 9.2.1.2, each ESWP is designed to provide 13,000gpm flow. Since cooling water flow is inversely proportional to the cooling tower temperature range, for conservatism, a lower ESW flow of 12,000 gpm to each cooling tower is used in the analysis.

The required total water usage (due to cooling tower drift and evaporation) over the postulated 30 day period is determined using industry standard methodology as follows:

Total Evaporation (E) and Drift (D) rates were calculated using the ESW flow rate (GPM) of 12,000 gpm times the temperature rise (CR) and a conservative cooling tower factor of 0.0009, E (total) = GPM x CR x 0.0009.

a. The cooling tower factor of 0.0009 is considered conservative since it is based on standard cooling tower evaporation factor of 0.0008, and typical cooling tower drift rate of 0.0002 This is expressed as

   Total Evaporation (E) = GPM x CR x 0.0008 + GPM x 0.0002

b. The ESW temperature rise (CR) was based on heat rate equation of H as

   Heat Rate (H) = m x specific heat x CR,

   where, m = mass flow rate

c. Accumulative evaporation (gallons/cooling tower) is calculated by multiplying the evaporation rate (gpm) and its corresponding time interval.

d. The total water loss due to evaporation and drift for the 30 days period is calculated and is defined as the plant unit minimum required water capacity for the basin design in accordance with RG 1.27.

Based on the above analyses, the governing case for the maximum required 30 days cooling water capacity is two-train operation during ~~Safe Shutdown with~~

MIC-03-09-0
0013

~~LOOP~~LOCA condition, with a total required cooling water of approximately 8.40 million gallons. The total required 30 days cooling water capacity with two-train operation during ~~LOCA~~Safe Shutdown with LOOP condition is approximately 8.~~2~~30 million gallons. MIC-03-09-0 0013 MIC-03-09-0 0013

The safe shutdown conditions with LOOP for two-train operation, requires a peak heat load of 196 million Btu/hr to be dissipated. The LOCA case with two train operation peak heat load is ~~158~~160 million Btu/hr. Therefore safe shutdown with two train operation peak heat loads are used for cooling tower design. MIC-03-09-0 0013

9.2.5.3 Safety Evaluation

CP COL 9.2(22) Replace DCD Subsection 9.2.5.3 with the following.

The results of the UHS capability and safety evaluation are discussed in detail in Subsection 9.2.5.2.3 and in this Subsection. The UHS is capable of rejecting the heat under limiting conditions as discussed in Subsection 9.2.5.2.3.

The UHS is arranged to support separation of the four divisions of ESWS.

System functional capability is maintained assuming one division is unavailable due to on-line maintenance during a design basis accident with a single active failure, with or without a LOOP.

The failure modes and effects analysis for the UHS is included in Table 9.2.5-4R and demonstrates that the UHS satisfies the single failure criteria.

The safety-related SSCs of the UHS and the ESWS are classified as seismic Category I. The site-specific safety-related components are identified in FSAR Table 3.2-201. The non-seismic (NS) SSCs are segregated from the seismic Category I SSCs. Structural failure of the UHS non-safety related SSCs will not adversely impact the seismic category I SSCs. These non-safety SSCs are classified as non-seismic.

Leakage cracks and other types of pipe rupture are not postulated in the safety-related UHS piping because the UHS is a moderate energy fluid system and the piping is designed to comply with BTP 3-4 B(iii)(1)(c) and C as stated in DCD Subsection 3.6.2.1.2.2 and 3.6.2.1.3. RCOL2_09.02.05-25 CTS-01529

The ~~basin is~~UHS basins, cooling towers, fans, motors, and associated equipment are designed to withstand the effect of natural phenomena, such as earthquakes, tornadoes, hurricanes, and floods taken individually, without loss of capability to perform its safety function. RCOL2_14.03.07-38

The ~~basin~~basis for the structural adequacy of the UHSRS is provided in FSAR Sections 3.3, 3.4, 3.5, 3.7, and 3.8. RCOL2_14.03.07-38

Site-specific UHS design features to address limiting hydrology-related events are addressed in Subsection 2.4.8, 2.4.11, and 2.4.14.

Chapter 10

Chapter 10 Tracking Report Revision List

Change ID No.	Section	FSAR Rev. 3 Page	Reason for change	Change Summary	Rev. of FSAR T/R
RCOL2_12.03-12.04-11 S04	10.4.8.2.1	10.4-7 through 10.4-8	Supplemental 04 Response to RAI No. 135 Luminant Letter no. TXNB-12042 Date 12/6/2012	Revised to refer to Figures 12.3-201 and 12.3-202	-

*Page numbers for the attached marked-up pages may differ from the revision 3 page numbers due to text additions and deletions. When the page numbers for the attached pages do differ, the page number for the attached page is shown in brackets.

Chapter 11

Chapter 11 Tracking Report Revision List

Change ID No.	Section	FSAR Rev. 3 Page	Reason for change	Change Summary	Rev. of FSAR T/R
RCOL2_03.03.02-9	11.4.2.3	11.4-3	Response to RAI No. 250 Luminant Letter no.TXNB-12032 Date 9/14/2012	Revised to incorporate RG 1.221.	-
RCOL2_12.03-12.04-11 S04	11.2.3.4	11.2-8	Supplemental 04 Response to RAI No. 135 Luminant Letter no.TXNB-12042 Date 12/6/2012	Clarified the description of the piping run for Unit 3 and Unit 4.	-

*Page numbers for the attached marked-up pages may differ from the revision 3 page numbers due to text additions and deletions. When the page numbers for the attached pages do differ, the page number for the attached page is shown in brackets.

Chapter 12

Chapter 12 Tracking Report Revision List

Change ID No.	Section	FSAR Rev. 3 Page	Reason for change	Change Summary	Rev. of FSAR T/R
RCOL2_12.03-12.04-11 S04	12.3.6	12.3-4	Supplemental 04 Response to RAI No. 135 Luminant Letter no.TXNB-12042 Date 12/6/2012	Added Figure 12.3-202.	-
RCOL2_12.03-12.04-11 S04	Table 12.3-201 (Sheets 1, 4 of 5)	12.3-6, 12.3-9	Supplemental 04 Response to RAI No. 135 Luminant Letter no.TXNB-12042 Date 12/6/2012	Clarified the description of the piping run for Unit 3 and Unit 4.	-
RCOL2_12.03-12.04-11 S04	Figure 12.3-201	12.3-12	Supplemental 04 Response to RAI No. 135 Luminant Letter no.TXNB-12042 Date 12/6/2012	Clarified the description of the piping run from the T/B to the yard.	-
RCOL2_12.03-12.04-11 S04	Figure 12.3-202 (New Figure)	[12.3-13]	Supplemental 04 Response to RAI No. 135 Luminant Letter no.TXNB-12042 Date 12/6/2012	Revised figure to show that it is now only applicable to CPNPP Unit 3 and added new figure for CPNPP Unit 4 yard piping routing and building penetration schematic.	-
CTS-01510	Figure 12.3-1R (Sheet 1 of 34)	12.3-11	Consistency with DCD as described in Letter. TXNB-12033 (ML12268A413)	Figure was updated to reflect standard plant and site-specific layout changes.	0

*Page numbers for the attached marked-up pages may differ from the revision 3 page numbers due to text additions and deletions. When the page numbers for the attached pages do differ, the page number for the attached page is shown in brackets.

Chapter 13

Chapter 13 Tracking Report Revision List

Change ID No.	Section	FSAR Rev. 3 Page	Reason for change	Change Summary	Rev. of FSAR T/R
RCOL2_13.04-6	Table 13.4-201 (Sheet 6 of 11)	13.4-7	Response to RAI No. 255 Luminant Letter no.TXNB-12013 Date 05/31/2012	Deleted 10 CFR 52.78 has as a Program Source for Item 11, Program Title, “Non licensed Plant Staff Training Program” in FSAR Table 13.4-201.	-
RCOL2_01.05-3	13.3.2 13.3.5 (new section)	13.3-1 13.3-2	Response to RAI No. 261 Luminant Letter no.TXNB-12027 Date 7/24/2012	Added evaluation of emergency staffing in accordance with NEI 12-01 Added reference to the NEI 12-01	-

*Page numbers for the attached marked-up pages may differ from the revision 3 page numbers due to text additions and deletions. When the page numbers for the attached pages do differ, the page number for the attached page is shown in brackets.

Chapter 14

Chapter 14 Tracking Report Revision List

Change ID No.	Section	FSAR Rev. 3 Page	Reason for change	Change Summary	Rev. of FSAR T/R
RCOL2_09.02.01-6	14.2.12.1.113	14.2-5	Response to RAI No. 251 Luminant Letter no.TXNB-12016 Date 05/31/2012	Revised item A.2 to clarify that ESW pumps and UHS transfer pumps are demonstrated to have adequate NPSH and no vortex formation at minimum basin water level.	-
RCOL2_14.02-21	14.2.12.1.113	14.2-5 14.2-6 [14.2-7]	Response to RAI No. 257 Luminant Letter no.TXNB-12022 Date 6/21/2012	Clarified preoperational test objectives, methods, and acceptance criteria. Added preoperational test acceptance criteria for water hammer prevention.	-
RCOL2_14.02-20	14.2.12.1.113	14.2-5 through 14.2-6 [14.2-5 through 14.2-7]	Response to RAI No. 256 Luminant Letter no.TXNB-12026 Date 7/20/2012	An item is added to the UHSS preoperational test (14.2.12.1.113) to verify the ability of the UHS, in conjunction with the ESWS, CCWS, and RHRS, to cool down the RCS.	-
RCOL2_09.02.01-9 S01	14.2.12.1. 113	14.2-5 through 14.2-6 [14.2-5 through 14.2-7]	Supplemental 01 Response to RAI No. 251 Luminant Letter no.TXNB-12031 Date 9/10/2012	Removed description of level switches located in the UHS cooling tower riser piping.	-
RCOL2_14.02-21 S01	14.2.12.1.113	14.2-6	Supplemental Response to RAI No. 257 Luminant Letter no.TXNB-12034 Date 9/24/2012	An items is added to the UHSS preoperational test (14.2.12.1.113) to verify the function of the newly added drain valves for freeze protection.	-

Change ID No.	Section	FSAR Rev. 3 Page	Reason for change	Change Summary	Rev. of FSAR T/R
RCOL2_09.02.05-20 S02	14.2.12.1.113	14.2-5 14.2-6	Supplemental 02 Response to RAI No. 252 Luminant Letter no.TXNB-12036 Date 11/12/2012	Revised UHS Preoperational Test to include simultaneous operation of ESWP and UHS Transfer Pump with no interfering vortices.	-
RCOL2_14.02-21 S02	14.2.12.1.113	14.2-6 [14.2-7]	Supplemental 02 Response to RAI No. 257 Luminant Letter no.TXNB-12036 Date 11/12/2012	Corrected to remove reference to electrical heat tracing.	-
RCOL2_09.02.01-9 S02	14.2.12.1.113	14.2-5, 14.2-6 [14.2-5 through 14.2-7]	Supplemental 02 Response to RAI No. 251 Luminant Letter no.TXNB-12041 Date 12/03/2012	Revise the description about water hammer/ voids in the spray header or nozzles.	-

*Page numbers for the attached marked-up pages may differ from the revision 3 page numbers due to text additions and deletions. When the page numbers for the attached pages do differ, the page number for the attached page is shown in brackets.

Chapter 15

Chapter 15 Tracking Report Revision List

Change ID No.	Section	FSAR Rev. 3 Page	Reason for change	Change Summary	Rev. of FSAR T/R

*Page numbers for the attached marked-up pages may differ from the revision 3 page numbers due to text additions and deletions. When the page numbers for the attached pages do differ, the page number for the attached page is shown in brackets.

Chapter 16

Chapter 16 Tracking Report Revision List

Change ID No.	Section	FSAR Rev. 3 Page	Reason for change	Change Summary	Rev. of FSAR T/R

*Page numbers for the attached marked-up pages may differ from the revision 3 page numbers due to text additions and deletions. When the page numbers for the attached pages do differ, the page number for the attached page is shown in brackets.

Chapter 17

Chapter 17 Tracking Report Revision List

Change ID No.	Section	FSAR Rev. 3 Page	Reason for change	Change Summary	Rev. of FSAR T/R

*Page numbers for the attached marked-up pages may differ from the revision 3 page numbers due to text additions and deletions. When the page numbers for the attached pages do differ, the page number for the attached page is shown in brackets.

Chapter 18

Chapter 18 Tracking Report Revision List

Change ID No.	Section	FSAR Rev. 3 Page	Reason for change	Change Summary	Rev. of FSAR T/R

*Page numbers for the attached marked-up pages may differ from the revision 3 page numbers due to text additions and deletions. When the page numbers for the attached pages do differ, the page number for the attached page is shown in brackets.

Chapter 19

Chapter 19 Tracking Report Revision List

Change ID No.	Section	FSAR Rev. 3 Page	Reason for change	Change Summary	Rev. of FSAR T/R
RCOL2_19-19	19.1.5	19.1-9	Response to RAI No. 248 Luminant Letter no.TXNB-12016 Date 05/31/2012	Information for extreme wind bounding assessment added for LPSD and at power operation.	-
RCOL2_19-19	Table 19.1-205 (Sheets 24 through 25 of 35)	19.1-74 through 19.1-75	Response to RAI No. 248 Luminant Letter no.TXNB-12016 Date 05/31/2012	Information added to address risk from extreme winds.	-
RCOL2_03.03.02-9	19.1.5 Table 19.1-205 (Sheet 12, 16, 24 of 35) Table 19.1-206 (Sheet 2 of 2)	19.1-6 19.1-62 19.1-66 19.1-74 19.1-87	Response to RAI No. 250 Luminant Letter no.TXNB-12032 Date 9/14/2012	Revised to incorporate RG 1.221.	-
RCOL2_19-23	19.2.6.4 19.2.6.6	19.2-4	Response to RAI No. 267 Luminant Letter no.TXNB-12043 Date 12/18/2012	Updated values from using more recent dollar values in calculation.	-
RCOL2_19-21	19.1.5	19.1-9, 19.1-10	Response to RAI No. 264 Luminant Letter no.TXNB-12043 Date 12/18/2012	Clarified screening criteria used for external events and results of screening.	-

Change ID No.	Section	FSAR Rev. 3 Page	Reason for change	Change Summary	Rev. of FSAR T/R
RCOL2_19-21	Table 19.1-205 (Sheets 24 through 25 of 35)	19.1-74 through 19.1-75	Response to RAI No. 264 Luminant Letter no.TXNB-12043 Date 12/18/2012	Updated wording on extreme wind screening discussion.	-
RCOL2_19-22	19.1.5	19.1-5 through 19.1-6, 19.1-10	Response to RAI No. 264 Luminant Letter no.TXNB-12043 Date 12/18/2012	Clarified results of external flooding screening.	-
RCOL2_19-22	Table 19.1-205 (Sheets 27 through 31 of 35)	19.1-77 through 19.1-81	Response to RAI No. 264 Luminant Letter no.TXNB-12043 Date 12/18/2012	Updated wording on external flooding screening discussion.	-
RCOL2_19-24	19.1.2.3 (New Subsection)	19.1-2 [19.1-3]	Response to RAI No. 268 Luminant Letter no.TXNB-12043 Date 12/18/2012	Clarified expectations on requirements to demonstrate technical adequacy.	-
RCOL2_19-24	19.1.4.1.2	19.1-4 [19.1-5, 19.1-6]	Response to RAI No. 268 Luminant Letter no.TXNB-12043 Date 12/18/2012	Capture requirements to update PRA following construction to capture changes.	-

Change ID No.	Section	FSAR Rev. 3 Page	Reason for change	Change Summary	Rev. of FSAR T/R
RCOL2_19-24	19.3.3	19.3-1 [19.3-1, 19.3-2]	Response to RAI No. 268 Luminant Letter no.TXNB-12043 Date 12/18/2012	Update FSAR location references for PRA update requirements.	-
RCOL2_19-25	19.1 19.1.1.2.1 19.1.1.3.1 (New Subsection) 19.1.1.3.2 (New Subsection)	19.1-1 19.1-1 19.1-1 [19.1-2] 19.1-1 [19.1-2]	Response to RAI No. 268 Luminant Letter no.TXNB-12043 Date 12/18/2012	Updated and expanded FSAR section cross-references for risk informed applications.	-
RCOL2_19-25	19.1.7 (New Subsection)	19.1-13 [19.1-14, 19.1-15]	Response to RAI No. 268 Luminant Letter no.TXNB-12043 Date 12/18/2012	Updated and expanded FSAR section cross-references for risk informed applications.	-
RCOL2_19-25	Table 19.1-207 (Sheets 1, 2 of 2) (New Table)	19.1-89 [19.1-91, 19.1-92]	Response to RAI No. 268 Luminant Letter no.TXNB-12043 Date 12/18/2012	Updated and expanded FSAR section cross-references for risk informed applications.	-

Change ID No.	Section	FSAR Rev. 3 Page	Reason for change	Change Summary	Rev. of FSAR T/R
RCOL2_19-25	19.3.3	19.3-1	Response to RAI No. 268 Luminant Letter no.TXNB-12043 Date 12/18/2012	Updated and expanded FSAR section cross-references for risk informed applications.	-
DCD_16-117	Table 19.1-119R (Sheets 19, 34)	19.1-21 19.1-36	Response to RAI No. 161 MHI Letter No. UAP-HF-12022 Date 02/08/2012	Incorporated new key insights regarding administrative controls for AAC and demineralized water storage tank during atpower operation and SIS during LPSD operation	-
DCD_19-494	Table 19.1-119R (Sheet 34)	19.1-36	Response to RAI No. 669 MHI Letter No. UAP-HF-12023 Date 02/08/2012	Incorporated a new key insight regarding administrative controls for SIS during LPSD operation	-
CTS-01528	19.2.6.6 Table 19.2-9R	19.2-4 19.2-6	Consistency with RAI 267 Luminant Letter no.TXNB-12043 Date 12/18/2012	Maximum averted cost and SAMA benefit values at the corresponding discount rates were updated.	1

*Page numbers for the attached marked-up pages may differ from the revision 3 page numbers due to text additions and deletions. When the page numbers for the attached pages do differ, the page number for the attached page is shown in brackets.

19.2.6.4 Risk Reduction Potential of Design Improvements

CP COL 19.3(4) Replace the last sentence in DCD Subsection 19.2.6.4 with the following.

The maximum averted cost is ~~$305k~~approximately $400k. RCOL2_19-23

19.2.6.5 Cost Impacts of Candidate Design Improvements

STD COL 19.3(4) Replace the first sentence in the last paragraph in DCD Subsection 19.2.6.5 with the following.

SAMA cost evaluation results are described in Table 19.2-9R.

19.2.6.6 Cost-Benefit Comparison

CP COL 19.3(4) Replace the content of DCD Subsection 19.2.6.6 with the following.

The maximum averted cost-risk of ~~less than $305k~~approximately $400k for a single US-APWR unit at the CPNPP Unit 3 and 4 is so low that there are no design changes over those already incorporated into the US-APWR design that could be determined to be cost-effective. ~~Even with a conservative 3 percent discount rate, the valuation of the averted risk is less than $787k~~approximately ~~$1,055k.~~A sensitivity evaluation was performed with a conservative 3% discount rate and the valuation of the maximum averted cost is approximately $1,055K. The benefit of each SAMA at 3% and 7% discount rates was calculated and is presented in Table 19.2-9R. The cost of each SAMA exceeds the corresponding benefit. RCOL2_19-23 RCOL2_19-23 CTS-01528

Accordingly, further evaluation of design-related SAMAs is not warranted. Evaluation of administrative SAMAs would not be appropriate until the plant design is finalized, and plant administrative processes and procedures are developed. At that time, appropriate administrative controls on plant operations would be incorporated into the plant's management systems as part of its baseline.

19.2.7 References

CP COL 19.3(4)

Table 19.2-9R

SAMA Cost Evaluation Results

	Design Alternative	Cost Impact	Maximum Averted Cost	Sensitivity of each SAMA benefit	
				7% Discount rate (baseline)	3% Discount rate (Sensitivity)
1	Provide additional dc battery capacity.	$2,000k		$1~~22~~60k	$~~315~~422k
2	Provide an additional gas turbine generator.	$10,000k		$1~~22~~60k	$~~315~~422k
3	Install an additional, buried off-site power source.	$10,000k		$1~~25~~64k	$~~323~~433k
4	Provide an additional high-pressure injection pump with independent diesel.	$1,000k		$~~159~~208k	$~~409~~549k
5	Add a service water pump.	$5,900k		$~~76~~100k	$~~197~~264k
6	Install an independent reactor coolant pump seal injection system with dedicated diesel.	$3,800k	$~~305~~400k (Baseline) $1,055k (Sensitivity)	$1~~43~~88k	$~~370~~496k
7	Install an additional component cooling water pump.	$1,500k		$~~76~~100k	$~~197~~264k
8	Add a motor-driven feed-water pump.	$2,000k		$140~~7~~k	$~~275~~369k
9	Install a filtered containment vent to remove decay heat.	$3,000k		$~~183~~240k	$~~471~~632k
10	Install a redundant containment spray system.	$870k		$1~~4~~9k	$~~37~~50k

CTS-01528